

THE ROLE OF MACRO-ZOOPLANKTON IN THE GLOBAL CARBON CYCLE

BY

RÓISÍN MORIARTY

FOR THE DEGREE OF

DOCTOR OF PHILOSOPHY

THESIS PRESENTED TO THE

UNIVERSITY OF EAST ANGLIA,
SCHOOL OF ENVIRONMENTAL SCIENCES

SEPTEMBER 2009

THE ROLE OF MACRO-ZOOPLANKTON IN THE GLOBAL CARBON CYCLE

ABSTRACT

DOCTOR OF PHILOSOPHY

UNIVERSITY OF EAST ANGLIA, SCHOOL OF ENVIRONMENTAL SCIENCES

RÓISÍN MORIARTY

2009

Macro-zooplankton play a role in the removal of carbon from the sunlit surface waters of the world ocean and its transport to the deep sea. Their role in the export of large particulate organic carbon distinguishes them from other size classes of zooplankton. It is essential to investigate the effect of macro-zooplankton on the natural carbon cycle to assess their importance for ecosystem-climate feedbacks. This thesis presents (1) specially synthesised data sets for the parameterisation of growth, grazing, respiration and mortality rates (d^{-1}) of macro-zooplankton, (2) the inclusion of macro-zooplankton as a Plankton Functional Type (PFT) in the global biogeochemical model PlankTOM10 v1.0, (3) specially synthesised data sets for model evaluations, and (4) a comparison of macro-zooplankton with other heterotrophs. We used the PlankTOM10 model to investigate the role of macro-zooplankton in carbon export on a global scale. The model reproduced observations of biomass for both meso- ($0.4 \text{ Pg C} = 0.5 \mu\text{M C}$) and macro-zooplankton ($0.005 \text{ Pg C} = 0.006 \mu\text{M C}$ (the value in Pg C is the annual average of macro-zooplankton biomass in the top 200 m of the world ocean, the value in $\mu\text{M C}$ is the median concentration of macro-zooplankton biomass in one litre of sea water from the top 200 m of the world ocean)). Total carbon export from macro-zooplankton varied from 0.26 to 0.57 Pg C y^{-1} in the various model simulations. Export from macro-zooplankton had a turnover rate of $\sim 120 \text{ y}^{-1}$ (export/biomass), much higher than $\sim 18 \text{ y}^{-1}$ for meso-zooplankton. This suggests that small changes in macro-zooplankton can have disproportional effects on carbon export. However the model was unable to reproduce the very high biomass concentration ($\sim 1000 \mu\text{M C}$) that can be attained by macro-zooplankton and the mass sedimentation events associated with such patches. Until the processes involved in the dynamics of high macro-zooplankton biomass concentrations, patchy distribution and mass sedimentation can be reproduced by the model the full effect of macro-zooplankton on the global carbon cycle is likely to be underestimated.

TABLE OF CONTENTS

Table of Figures	ix
Table of Tables	xv
Table of Equations	xvii
Declaration of Authorship	xix
Acknowledgements	xxi
1 INTRODUCTION	1
1.1 Carbon and the Future - An Opening Statement	3
1.2 The Global Carbon Cycle	3
1.2.1 The Marine Carbon Cycle	4
1.2.2 Anthropogenic Climate Change	7
1.3 Plankton Functional Type Modelling and Macro-zooplankton	9
1.3.1 The Evolution of Plankton Functional Type Modelling	9
1.3.2 Macro-zooplankton	14
1.3.3 Macro-zooplankton as a PFT	22
1.3.4 Carbon Export by Macro-zooplankton	23
1.4 Thesis Outline	25
1.4.1 Thesis Objective	25
1.4.2 Thesis Structure	25
References	26
2 RESPIRATION RATES IN THE EPIPELAGIC MACRO-ZOOPLANKTON: RELATIONSHIP WITH BODY MASS & TEMPERATURE	33
2.1 Abstract	35
2.2 Introduction	35
2.3 Methods	39
2.4 Results	42
2.4.1 General patterns	42
2.4.2 Interspecific Respiration	45
2.4.3 Intra-group Respiration	47
2.4.4 Intraspecific Respiration	49
2.4.5 Comparison of Interspecific, Intra-group and Intraspecific Respiration	58

2.4.6	Intraspecific Respiration: Comparison with Glazier (2005)	59
2.5	Discussion	60
2.5.1	General Patterns	60
2.5.2	Interspecific Respiration	63
2.5.3	Intra-group Respiration	63
2.5.4	Intraspecific Respiration	64
2.5.5	Comparison of Interspecific, Intra-group and Intraspecific Respiration	65
2.5.6	Intraspecific Respiration: Comparison with Glazier (2005)	66
2.5.7	Metabolic Scaling in Epipelagic Macro-zooplankton	67
2.6	Conclusions	68
	References	70
3	MACRO-ZOOPLANKTON BIOMASS: A VALIDATION DATA SET	75
3.1	Abstract	77
3.2	Introduction	77
3.3	Methods	79
3.4	Results	81
3.5	Discussion	88
3.6	Conclusions	95
	References	96
4	MACRO-ZOOPLANKTON IN THE GLOBAL OCEAN BIOGEOCHEMICAL MODEL PLANKTOM10v1.0	99
4.1	Abstract	101
4.2	Introduction	101
4.3	Methods	104
4.3.1	Model	104
4.3.2	Macro-zooplankton Equations	105
4.3.3	Parameterisation	108
4.4	Results	115
4.4.1	Parameterisation	115
4.4.2	Model	121
4.5	Discussion	132

4.5.1	Macro-zooplankton Model Equations	132
4.5.2	Model Assumptions	132
4.5.3	Model	135
4.6	Conclusions	142
	References	143
5	THE EFFECT OF TEMPERATURE ON THE PHYSIOLOGICAL RATES OF HETEROTROPHIC ZOOPLANKTON: A SIZED BASED COMPARISON	149
5.1	Abstract	151
5.2	Introduction	152
5.3	Methods	154
5.4	Results	157
5.5	Discussion	163
5.6	Conclusions	168
	References	168
6	CONCLUSION	173
6.1	Introduction	175
6.2	Major Findings and Conclusions	176
6.2.1	Chapter 2	176
6.2.2	Chapter 3	177
6.2.3	Chapter 4	177
6.2.4	Chapter 5	179
6.2.5	Redefinition of Macro-zooplankton the PFT	179
6.3	Future Work	182
6.3.1	Respiration	183
6.3.2	Validation data	184
6.3.3	Characterisation of Physiological and Ecological Process Rates	185
6.3.4	Model Development and Future Use	187
6.4	General Review	188
6.5	Closing Statements	192
6.5.1	Marine Ecosystem - Climate Feedbacks	192
6.5.2	Change	192

TABLE OF FIGURES

Figure 1.1: The global carbon cycle: reservoirs (Pg C) and fluxes (Pg C y ⁻¹) of preindustrial estimate. Figure reproduced from Prentice et al. (2001).	4
Figure 1.2: Carbon cycling in the ocean: fluxes (Pg C y ⁻¹) estimated for the 1980s. Figure reproduced from Prentice et al. (2001).	6
Figure 1.3: Anthropogenic disturbance of the global carbon cycle: fluxes (Pg C y ⁻¹) estimated for 2000-2006. Figure reproduced from Prentice et al. (2001) with updated flux values from Canadell et al. (2007).	7
Figure 1.4: Concentrations of CO ₂ on different time scales. Top-left: concentrations of CO ₂ reconstructed from the Vostok Antarctic ice core over the last 420,000 years (Fischer et al. 1999, Petit et al. 1999). Top-right: CO ₂ concentrations in the Taylor Dome Antarctic ice core (Indermuhle et al. 1999) Bottom-left: Concentration of CO ₂ in Antarctic ice cores over the last thousand years (Siegenthaler et al. 1988, Barnola et al. 1993, Neftel et al. 1994, Etheridge et al. 1996, Keeling & Whorf 2000). Bottom-right: measurements of contemporary changes in atmospheric CO ₂ (Keeling & Whorf 2000). Figures reproduced from Prentice et al. (2001).	9
Figure 1.5: A simple NPZD model with carbon and nitrogen cycles. Figure reproduced from Anderson et al. (2007).	11
Figure 1.6: Ocean biogeochemical model with ecosystem composed of PFTs with a more sophisticated pelagic food web than that presented in Figure 1.4 and representations of nitrogen, phosphorus and silicate cycles. Figure reproduced from Allen et al. (2001).	12
Figure 2.1: Respiration rate (mg C ind ⁻¹ day ⁻¹) of marine epipelagic macro-zooplankton against body mass (mg ind ⁻¹): wet mass [top], dry mass [middle] and carbon mass [bottom]. Symbols: A is appendicularian spur (barely visible), B is the crustacean spur and C is the gelatinous spur. Temperature is corrected to 15°C using a Q ₁₀ of 2.14 see Table 2.1 for regression analysis.	44
Figure 2.2: Carbon-specific respiration (d ⁻¹) rates of different marine epipelagic macro-zooplankton against body mass (mg C ind ⁻¹). The data set was separated into four according to the mean carbon as a percentage dry mass in each group, see Table 1.3 Rates were corrected to 15°C using a Q ₁₀ of 2.14. Symbols: ctenophores (C), salps (S), scyphomedusae (Y), limnomedusae (L), trachymedusae (T), hydromedusae (H), siphonophores (Si), gastropod molluscs (G), heteropod molluscs (He), shelled pteropods (Ps), naked pteropods (Pn), polychaetes (P), chaetognaths (Ch), amphipods (A), stomatopoda (St), decapods (D), mysids (M), euphausiids (E), appendicularians (Ap).	45
Figure 2.3: Regression of interspecific respiration rate (mg C ind ⁻¹ d ⁻¹) against temperature (°C). A regression was fit to all data points, each originally calculated to represent an individual species. Symbols: data points calculated using regression and mid-point body mass to predict respiration (●) and data points calculated using within species mean body mass and mean within species respiration rate (○).	46
Figure 2.4: Regression of interspecific respiration rate (mg C ind ⁻¹ d ⁻¹) against temperature (°C). A regression was fit to all data points, each originally calculated to represent an individual species. Symbols: data points calculated using regression and mid-point temperature to predict respiration	

(●) and data points calculated using intraspecific mean temperature and mean intraspecific respiration rate (○). 46

Figure 2.5: Intraspecific and intra-group and interspecific respiration to body mass scaling exponents for marine epipelagic macro-zooplankton. Symbols: gelatinous (▲), semi-gelatinous (●), crustacean (■) and appendicularians (◆). For species id number see Table 2.5. Symbols in grey: ctenophores (C), salps (S), hydromedusae (H), siphonophores (Si), heteropod molluscs (He), shelled pteropods (Ps), polychaetes (P), chaetognaths (Ch), amphipods (A), decapods (D), mysids (M) and euphausiids (E) see Table 2.4. Interspecific metabolic scaling exponent is represented by All in red see Figure 2.3. Note: only scaling exponents significant at ($P \leq 0.025$, after application of Bonferonni correction) are shown. 50

Figure 2.6: Intraspecific metabolic scaling exponents expressed against sample size and \log_{10} body mass range (mg C) for marine epipelagic macro-zooplankton. Symbols: scaling exponents significant at $P \leq 0.025$ (after application of Bonferonni correction) (●) and non-significant scaling exponents (○). 50

Figure 2.7: Intraspecific and intra-group and interspecific respiration Q_{10} s for marine epipelagic macro-zooplankton. Symbols and notes: as in Figure 2.3. 50

Figure 2.8: Frequency of intraspecific and intra-group metabolic scaling exponents of marine epipelagic macro-zooplankton. Dashed line = interspecific metabolic scaling exponent, solid line = mean intraspecific metabolic scaling exponent, dotted line = mean intra-group metabolic scaling exponent. Whiskers are 95% confidence limits. 59

Figure 2.9: Comparison of metabolic scaling exponents from this study (top) and those presented in Glazier (2005). Whiskers are 95% confidence limits. 60

Figure 3.1: Body mass of COPEPOD groups and KRILLBASE species-specific conversions. Box plot shows median (black), mean (blue), upper and lower quartile (whiskers), upper and lower range of data (●) and species-specific conversion data (○). Data from Hirst & Bunker 2003 and Moriarty 2009. Euphausiid data excludes body mass data of *Euphausia superba*. 81

Figure 3.2: The annual average abundance (ind. L^{-1}) in the top 200 meters of the world ocean. Panels show the distribution of ctenophore [top row left], salp*, doliolid, and pyrosome [top row centre], cnidarians [top row right], scyphozoan [2nd row left], hydrazoan [2nd row centre], anthazoan [2nd row right], chaetognath [3rd row left], pelagic mollusc [3rd row centre], pelagic polychaete [3rd row right], decapods [4th row left], stomatopod [4th row centre], amphipod [4th row right], mysid [5th row left], euphausiid* [5th row centre] and appendicularian [5th row right]. All distribution data, unless otherwise stated, are from COPEPOD. *data from COPEPOD and KRILLBASE. White indicates no data. 83

Figure 3.3: The annual average of total abundance in the top 200 meters three areas of the world ocean. Panels show the frequency of macro-zooplankton abundance north of $30^{\circ}N$ [top], in the tropics [centre] and south of $30^{\circ}S$ [lower] in (ind. L^{-1}). Note: entire range of abundance is not shown at high latitudes. 84

Figure 3.4: The annual average distribution of macro-zooplankton in the top 200 meters of the world ocean. The panels show the total abundance (ind. L⁻¹) [top] and the total biomass (μM C) [bottom] in the top 200 meters of the world ocean. White indicates no data. 85

Figure 3.5: The annual average biomass (μM C) in the top 200 meters of the world ocean. Panels show the distribution of *Bolionopsis infundibulum* and *Pleurobrachia pileus* (ctenophores) [top row left], *Salpa thompsoni* and *Ihlea racovitzai* (salps) (KRILLBASE) [top row centre], *Cyaena capillata* (scyphozoan) [top row right], *Aglantha digitale*, *Eutonina indicans*, *Gonionemus vertens*, *Philalidium gregarium*, *Sarsia princeps*, *Sarsia tubulosa*, *Stomatoca atra* and *Agalma elegans* (hydrozoan) [2nd row left], *Clione limacine*, *Diacrea trispinosa* and *Limacina helicina* (pelagic molluscs) [2nd row centre], *Sagitta elegans* and *Sagitta enflata* (chaetognaths) [2nd row right], *Cyphocaris challengerii*, *Hyperia galba*, *Parathemisto japonica*, *Themisto libellula*, *Phronima sedentaria* and *Themisto pacifica* (amphipods) [3rd row left], *Acanthomysis pseudomacropsis* (mysid) [3rd row centre], *Euphausia superba*, *Euphausia pacifica*, *Meganyctiphanes norvegica*, *Thysanoessa inermis*, *Thysanoessa longipes*, *Thysanoessa raschi* and *Thysanoessa spinifera* (euphausiids) [3rd row right] and *Fritillaria borealis sargassi*, *Fritillaria haplostomai* and *Oikopleura dioica* [bottom row right]. All distribution data, unless otherwise stated, are from COPEPOD.* data from COPEPOD and KRILLBASE. White indicates no data. 86

Figure 3.6: The annual average of total biomass of in the top 200 meters of the world ocean. Panels show the frequency of macro-zooplankton [top], meso-zooplankton [centre] (Buitenhuis et al. 2006) and proto-zooplankton [lower] biomass (μM C) (Buitenhuis et al. 2009). White indicates no data. 87

Figure 3.7: The annual average distribution of total biomass of macro-zooplankton [top] (μM C), meso-zooplankton [centre] (μM C) (Buitenhuis et al. 2006) and proto-zooplankton [lower] (μM C) (Buitenhuis et al. 2009) in the top 200 meters of the world ocean. Note: not all abundance data shown. 88

Figure 3.8: Median and absolute deviation of heterotrophic phytoplankton (bacteria (Whitman et al. 1998), proto- (Buitenhuis et al. 2009), meso- (Buitenhuis et al. 2006) and macro-zooplankton) biomass relative to that of autotrophic (Conkright et al. 2002) biomass for the global ocean. Numbers are the relative median concentration (μM C) of each group ± the relative absolute deviation for the group. There is no data on the error associated with heterotrophic bacterial biomass as there was no information on the error of the original estimate. For phytoplankton chlorophyll concentration was converted to biomass using a C:Chl ratio of 50 (Uitz et al. 2006). 95

Figure 4.1: The relationship between mass-specific growth rate (d⁻¹) and temperature for macro-zooplankton [top] and four macro-zooplankton groups. Dashed line represents the normalised fit, the solid line represents the maximum growth rate with the temperature dependence of the original fit. Notes: gel = gelatinous, semi = semi-gelatinous, crust = crustacean and app = appendicularian. 116

Figure 4.2: The relationship between mass-specific routine respiration rate (d⁻¹) and temperature for macro-zooplankton [top] and four macro-zooplankton groups. Dashed line represents the normalised fit, the solid line represents the maximum growth rate with the temperature dependence of the

original fit. Notes: gel = gelatinous, semi = semi-gelatinous, crust = crustacean and app = appendicularian. 118

Figure 4.3: The relationship between mass-specific mortality rate (d^{-1}) and temperature for macro-zooplankton. The solid line represents the normalised mortality rate. White circles represent data excluded from the fit. 118

Figure 4.4: Export at 100m ($mol\ C\ m^{-2}\ y^{-1}$) for model simulations. Notes: exp = observations of export production at 100m (Schlitzer 2004), mac = macro-zooplankton, gel = gelatinous, semi = semi-gelatinous, crust = crustacean, app = appendicularian parameterisations. 122

Figure 4.5: Macro-zooplankton biomass ($\mu M\ C$) for model simulations. Notes: bio = observations of macro-zooplankton biomass (Chapter 3), others same as Figure 4.4. 122

Figure 4.6: Surface chlorophyll *a* ($\mu g\ L^{-1}$) for model simulations. Notes: chl *a* = surface chlorophyll *a* observations (SeaWIFS), others same as Figure 4.4. 124

Figure 4.7: Loss rates in model simulations with a calculated grazing threshold [left] and in model simulations with a grazing threshold of $7\ \mu M\ C$ [right]. Notes: from top to bottom: macro-zooplankton, gelatinous, semi-gelatinous, crustaceans and appendicularians. Black crosses = model loss rates, blue crosses = basal respiration (calculated from routine respiration observations), red crosses = mortality observations, blue line = maximum basal respiration, red line = fit to mortality data, blue crosses = maximum basal respiration, red crosses = mortality, both calculated from observations, black crosses = model loss rates. 126

Figure 4.8: Export at 100m ($mol\ C\ m^{-2}\ y^{-1}$) for standard and combined simulations. Observations (Schlitzer 2004) [top], standard run [centre] and combined run [bottom]. 129

Figure 4.9: Annual average macro-zooplankton grazing in the top 200m ($Pg\ C\ y^{-1}$) for six different temperature dependence (Q_{10}) simulations. $Q_{10} = 2.60$ [top left], $Q_{10} = 3.00$ [top right], standard crustacean run, $Q_{10} = 3.16$ [centre left], $Q_{10} = 3.20$ [centre right], $Q_{10} = 3.30$ [bottom left] and $Q_{10} = 3.60$ [bottom right]. 130

Figure 5.1: GGE (%) [left], grazing [middle] and respiration [right] rate (d^{-1}) as a function of temperature ($^{\circ}C$) for heterotrophic zooplankton. Relationship is only shown when significant and has predictive value. Where the temperature range was less than $20^{\circ}C$ no fit to grazing or respiration data was attempted. 158

Figure 5.2: Grazing rate (d^{-1}) calculated at $15^{\circ}C$ as a function of body mass ($\mu g\ C$) with standard deviation of the rate (whiskers) for heterotrophic plankton. Grazing rate is calculated at $15^{\circ}C$ for each group of heterotrophic zooplankton. Body mass for each group is a mean value for the group. Symbols: Flagellates (\blacktriangledown), dinoflagellates (\bullet), ciliates (\blacksquare), copepods (\blacklozenge), crustacean macro-zooplankton (\times), and gelatinous macro-zooplankton (\blacktriangle). 160

Figure 5.3: Q_{10} of grazing with standard deviation of Q_{10} (whiskers). Body mass for each group is a mean value for the group. Symbols as in Figure 5.2. Q_{10} values for copepods, crustacean macro-zooplankton and gelatinous macro-zooplankton (the three groups to the right of the figure) are a consequence of growth rate rather than grazing. 161

Figure 5.4: Respiration (d^{-1}) at 15°C as a function of body mass ($\mu\text{g C}$) with standard deviation (whiskers) for heterotrophic plankton. Symbols as in Figure 5.2, white symbols are flagellate and ciliate mean respiration at 25°C . There is no data on dinoflagellate respiration. 162

Figure 5.5: Q_{10} of respiration with standard deviation (whiskers). No data for temperature dependence of flagellate, dinoflagellate and ciliate respiration. Symbols as in Figure 5.2. 163

TABLE OF TABLES

Table 1.1: The number of species in holoplanktic and meroplanktic macro-zooplankton. Numbers in bold are rough estimates. Reproduced from Table 1.1 in Harris et al. (2000).	15
Table 1.2: Taxonomic classification of groups within the macro-zooplankton (classification is restricted to groups based on species data presented in Chapters 2, 3 and 4).	16
Table 1.3: Dry mass content (as % of wet mass) and carbon mass (as % of dry mass). Dry mass and polychaete data reproduced from Larson (1986 and references therein) and carbon data reproduced from Schneider (1989).	17
Table 1.4: Sinking rates of zooplankton faecal pellets, marine snow and phytoplankton detritus. Sinking rate is in meters per day. Reproduced from Turner (2002). Note: Macro-zooplankton groups are italicised.	24
Table 2.1: The relationship between respiration rate, body mass (BM, mg ind ⁻¹) and temperature (T, °C) presented for this study and Ikeda's (1985) study of epipelagic zooplankton. Note: the GLM used in this study was used on log ₁₀ transformed data whereas the regression analysis carried out in Ikeda (1985) used ln transformed data.	43
Table 2.2: Regression analysis of respiration rate (R, mg C ind ⁻¹ d ⁻¹) and body mass (BM, mg ind ⁻¹), the correlation coefficient (r ²) and minimum and maximum body mass for each mass type. Temperature is corrected to 15°C using a Q ₁₀ of 2.14	43
Table 2.3: Results of intra-group (interspecific) regressions using the species midpoint. n = number of species per group, P = significance, bold = significant at P ≤ 0.025 (after application of Bonferonni correction), r ² = the correlation coefficient, -- = no data, mass is measured in mg C ind ⁻¹ .	47
Table 2.4: Results of analysis of differences between the scaling exponent of respiration rate with mass and 0.66, 0.75, 0.90 and 1.0 for each of the groups where a linear regression through species mid-points was preformed. Notes: bold = <i>b</i> is significant at P ≤ 0.0125 (after application of the Bonferonni correction) and NS = difference from <i>b</i> is not significant.	48
Table 2.5: Results of regression analysis of relationship between respiration rate (mg C ind ⁻¹ d ⁻¹) and body mass (mg C ind ⁻¹) in 139 marine epipelagic macro-zooplankton species, where n < 4, n = number of species per group, bold = significant at P ≤ 0.05, r ² = the correlation coefficient, P = significance, NS = difference is not significant, -- = no data, mass is measured in mg C ind ⁻¹	52
Table 2.6: Results of analysis of differences between the scaling exponent of respiration rate with mass 0.66, 0.75 and 1 for each of the species where a linear regression was preformed. Notes: bold = <i>b</i> is significant at P ≤ 0.0125 (after application of Bonferonni correction), Stdev. = standard deviation and NS = difference from <i>b</i> is not significant.	58
Table 3.1: Mean body mass values used to convert COPEPOD species abundance data to biomass. N = number of data points, Stdev. = standard deviation, all units are μM C.	82
Table 4.1: Carbon composition of groups within the macro-zooplankton (see Table 2.3 for greater detail).	102
Table 4.2: A summary of macro-zooplankton grazing, respiration and mortality rates at 15°C, their temperature dependence and the breakdown of these rates between the umbrella groups that make	

up the macro-zooplankton. Notes: error was calculated for grazing rate and respiration in Equation 4.11 and for mortality in Equation 4.23, n = number of data points. For references see Table 4.4.	116
Table 4.3: The partitioning of grazing in macro-zooplankton and the different groups within the macro-zooplankton. Note: there was no data for appendicularians. There is no standard deviation for DOC and DIC as DOC has been recalculated as a fraction of grazing and DIC was calculated from GGE, POC and DOC. n = number of data points, -- = no data. For references see Table 4.4.	117
Table 4.4: Parameter values used in the standard model simulation. Note: * = only used to calculate grazing threshold	120
Table 4.5: Results of model simulations using macro-zooplankton and macro-zooplankton group parameterisations.	123
Table 4.6: Phytoplankton concentration results of model simulations using macro-zooplankton and macro-zooplankton group parameterisations.	123
Table 4.7: The contribution of various processes to the POC _i flux and to total particulate export production. All measurements in Pg C y ⁻¹ . Bold text identifies the parameterisation used in the standard run.	126
Table 4.8: Sensitivity analysis and evaluation of macro-zooplankton in the global biogeochemical model PlankTOM10. Bold text identifies the parameterisation used in the standard run.	128
Table 4.9: Sensitivity analysis of temperature dependence of macro-zooplankton grazing rate using the standard crustacean parameterisation in the global biogeochemical model PlankTOM10. All values are Pg C y ⁻¹ .	131
Table 5.1: Relationship between GGE (%) and temperature (°C) for heterotrophic plankton as calculated in Equation (5.2).	157
Table 5.2: Physiological rates for heterotrophic zooplankton. Notes: n = number of data points, d = day.	159
Table 5.3: Relationship between grazing (d ⁻¹) and temperature (°C) for heterotrophic plankton calculated with Equation 5.5.	160
Table 5.4: Relationship between respiration (d ⁻¹) and temperature (°C) for heterotrophic plankton calculated with Equation (5.5).	162

TABLE OF EQUATIONS

CO_2 (atmospheric) \leftrightarrow CO_2 (dissolved)	(1.1)	5
CO_2 (dissolved) + $\text{H}_2\text{O} \leftrightarrow \text{H}_2\text{CO}_3$	(1.2)	5
$\text{H}_2\text{CO}_3 \leftrightarrow \text{H}^+ + \text{HCO}_3^-$ (bicarbonate ion)	(1.3)	5
$\text{HCO}_3^- \leftrightarrow \text{H}^+ + \text{CO}_3^{2-}$ (carbonate ion)	(1.4)	5
CO_2 (dissolved) + $\text{H}_2\text{O} + \text{CO}_3^{2-} \leftrightarrow 2\text{HCO}_3^-$	(1.5)	5
$\log_{10} R = a + b \log_{10} [\text{BM}] + c [\text{T}]$	(2.1)	40
$\log_{10} R = a + b \log_{10} [\text{BM}] + c [\text{T}] + b \log_{10} [\text{BM}] \cdot c[\text{T}]$	(2.2)	40
$\frac{\partial \text{MAC}}{\partial t} = \sum_k g_{F_k}^{\text{mac}} \cdot F_k \cdot \text{MGE} \cdot \text{MAC} - m^{\text{mac}} \cdot T$	(4.1)	105
$g_{F_k}^{\text{mac}} = g_{\text{max}}^{\text{mac}}(T) \frac{p_{F_k}^{\text{mac}} \left(\frac{1 - H^{\text{mac}}}{\sum_k p_{F_k}^{\text{mac}} \cdot F_k} \right)}{K_{1/2}^{\text{mac}} + \sum p_{F_k}^{\text{mac}} \cdot F_k - H^{\text{mac}}}$	(4.2)	106
$g_{\text{max}}^{\text{mac}}(T) = g_{0^\circ \text{C}}^{\text{mac}} \cdot a^{T/10}$	(4.3)	106
$\text{MGE} = \min \left(\text{GGE}, \sum g_{F_{Fe}}^{\text{mac}} \cdot \frac{(1 - \zeta)}{\sum g_{F_C}^{\text{mac}} \cdot Fe : C^{\text{mac}}} \right)$	(4.4)	106
$m^{\text{mac}}(T) = m_{0^\circ \text{C}}^{\text{mac}} \cdot b^{T/10} \cdot \text{MAC}$	(4.5)	107
$\frac{\partial \text{DOC}}{\partial t} = \sum \left[(1 - \sigma)(1 - \zeta - \text{MGE}) \sum_k g_{F_k}^{\text{mac}} \cdot \text{MAC} \cdot F_k \right]$	(4.6)	107
$\frac{\partial \text{POC}_l}{\partial t} = \sum \zeta \sum_k g_{F_k}^{\text{mac}} \cdot \text{MAC} \cdot F_k - \sum g_{\text{poc}_l}^{\text{mac}} \cdot \text{MAC} \cdot \text{POC}_l + m^{\text{mac}} \cdot T$	(4.7)	107
$\frac{\partial \text{POC}_s}{\partial t} = \sum g_{\text{poc}_s}^{\text{mac}} \cdot \text{MAC} \cdot \text{POC}_s$	(4.8)	108
$\frac{\partial \text{DIC}}{\partial t} = \sum \sigma(1 - \zeta - \text{MGE}) \sum_k g_{F_k}^{\text{mac}} \cdot \text{MAC} \cdot F_k$	(4.9)	108
$\mu = \mu_{0^\circ \text{C}} (Q_{10}^{0.1})^T$	(4.10)	108
$\text{normalised RSS} = \sqrt{\frac{\left(\sum \frac{\text{observed}}{\mu - 1} \right)^2}{n}}$	(4.11)	109
Grazing rate = $\mu_{\text{max}} / \text{GGE}$	(4.12)	109
$\frac{pn_1 \cdot cn_1 + pn_2 \cdot cn_2 + \dots pn_{11} \cdot cn_{11}}{\sum cn_1 + cn_2 + \dots cn_{11}} = 1$	(4.13)	110
$pn_1 = p_F \cdot \text{relative preference}$	(4.14)	110

Grazing = GGE + ζ + γ + R	(4.15)	111
$\gamma = (1 - \sigma)(1 - \zeta - \text{GGE})$	(4.16)	111
$R = \sigma(1 - \zeta - \text{GGE})$	(4.17)	111
$f[\text{DOC}] + f[\text{DIC}] = 1$	(4.18)	111
$R = R_{0^\circ\text{C}}(Q_{10}^{0.1})^T$	(4.19)	113
Maximum basal respiration rate = R_{max} · (basal:routine respiration)	(4.20)	113
$H = \frac{K_{1/2} \cdot R_{0^\circ\text{C}} \cdot c^{T/10}}{g_{0^\circ\text{C}} \cdot a^{T/10} - R_{0^\circ\text{C}} \cdot c^{T/10}} - 1$	(4.21)	114
$m = m_{0^\circ\text{C}}(Q_{10}^{0.1})^T$	(4.22)	114
(4.23)		114
GGE = grazing rate / growth rate	(5.1)	154
$\text{GGE} = a + b \cdot T$	(5.2)	154
Grazing rate = growth rate / $a + b \cdot T$	(5.3)	155
Grazing rate = growth rate / GGE	(5.4)	155
$\ln R = c + d \cdot T$	(5.5)	155
$\text{GGE} + f[\text{POM}] + f[\text{DOM}] + f[\text{DIC}] = 1$	(5.6)	156

DECLARATION OF AUTHORSHIP

I declare that the thesis entitled: The Role of Macro-zooplankton in the Global Carbon Cycle and the work presented in the thesis are both my own, and have been generated by me as the result of my own original research. I confirm that: 1) this work was done wholly or mainly while in candidature for a research degree at this University, 2) where any part of this thesis has previously been submitted for a degree or any other qualification at this University or any other institution, this has been clearly stated, 3) where I have consulted the published work of others, this is always clearly attributed, 4) where I have quoted from the work of others, the source is always given. With the exception of such quotations, this thesis is entirely my own work, 5) I have acknowledged all main sources of help, 6) where the thesis is based on work done by myself jointly with others, I have made clear exactly what was done by others and what I have contributed myself.

Many aspects of this work were discussed with my supervisors, members of the Dynamic Green Ocean research group and individuals external to this PhD project. All data synthesis, unless otherwise stated, and analysis undertaken during the course of this PhD has been carried out by the author.

I am very grateful to Dr. Marie-Pierre Gosselin who was responsible for the extraction of the raw abundance data from the COPEPOD data base. This was used to calculate the macro-zooplankton abundance and biomass distributions and concentrations presented in Chapter 3.

Dr. Erik Buitenhuis wrote the code for the macro-zooplankton PFT in PlankTOM10. Any changes in the code were discussed between myself, my supervisors (Prof. Corinne Le Quéré and Dr. Erik Buitenhuis) and the group's scientific programmer Dr. Clare Enright.

Apart from macro-zooplankton data (gelatinous and crustacean macro-zooplankton) all other data in Chapter 5 was gathered by members of the Dynamic Green Ocean. All statistical analysis carried out on the data in this chapter was carried out by the author.

ACKNOWLEDGEMENTS

I would like to thank Prof. Corinne Le Quéré for choosing me to undertake this PhD project and for her help in bring this thesis to fruition. I would like to thank Dr. Erik Buitenhuis for his support and the innumerable discussions we had on all aspects of the analysis of data, model equations and the limitations of our data sets; I have learnt how to think like a modeller. I would like to thank Dr. Andrew Hirst for his guidance through the daunting field that is metabolic scaling. I would also like to thank Prof. Eugene Murphy for his support as a supervisor throughout my PhD; I have learnt to be sceptical of models and their formulations.

As a Dynamic Green Ocean PhD student I would like to thank all those involved in the group and all those who participated in the workshops in Villefranche-sur-Mer for animated discussions, information, encouragement and for the pleasure of witnessing such determination, scientific talent and inter-disciplinary communication. I would also like to thank Clare Enright our scientific programmer and administrator at BAS for her patience, understanding, good humour and kindness throughout my PhD.

There are many, many people at BAS who have made themselves available for advice on various subjects and offered hearty encouragement often very early in the morning or late into the night. Among them Andy Clarke, Angus Atkinson, Pete Rothery, Geraint Tarling, Christine Philips, Mandy Thompson, Phil Trathan, Tony Martin, Paul Seear and Nadine Johnston.

A big thank you to all the friends I have made since my arrival in England, there are too many to name (BAS and Cambridge, UEA, ANDREX, and Manchester), for their encouragement and understanding. They have enriched my experience through the appreciation of the realisms that surround us all, while striving to enjoy the world in spite of them.

I would like to thank both my extended real and adoptive families on both sides of the Irish Sea for their unrelenting support, encouragement and love. And finally, Vernon I hope you don't feel that I have take you for granted through all of this. My world would not be the same without you. I love you, my handsome man in the world.

For Ann and Margaret

I must down to the sea again, to the lonely sea and the sky,
And all I ask is a tall ship and a star to steer her by,
And the wheel's kick and the wind's song and the white sail's shaking,
And a grey mist on the sea's face, and a grey dawn breaking.

Sea-Fever, John Masefield

1 INTRODUCTION

1.1 CARBON AND THE FUTURE - AN OPENING STATEMENT

As a species we produce $\sim 20\text{Tg C}$ (tera = 1×10^{12}) a day (Le Quéré et al. 2001). Every facet of our day-to-day lives involves the release of energy from carbon. Through our endless thirst for energy, energy for the most part derived from fossil fuels, we have altered (Hegerl et al. 2007) and will continue to alter the global carbon cycle. We must endeavour to investigate changes in the natural carbon cycle and the implications these changes have for its various components. Little is known of the feedbacks that may be associated with different components of the global carbon cycle, in particular biological feedbacks (Denman et al. 2007). We must open our minds to the possibility that the human contribution to climate change may change the face of the planet with serious consequences for all that inhabit it. The impact will be greatest for those of limited means in some of the poorest regions of the world.

1.2 THE GLOBAL CARBON CYCLE

The carbon cycle links four carbon pools; the atmosphere, the terrestrial biosphere, the oceans and geological reservoirs. Carbon moves between these four pools on varying timescales-from one to many thousands of years. The carbon exchange, 120 Pg C y^{-1} , between the two smaller pools, the atmosphere and the terrestrial biosphere, is the largest (Ciais et al. 1997). Atmospheric CO_2 is incorporated into plant biomass through photosynthesis. Around half of the carbon fixed in photosynthesis is returned to the atmosphere, as CO_2 , through autotrophic respiration. The remaining biomass returns to the atmosphere on a time scale of tens to hundreds of years; through the heterotrophic respiration of herbivores, bacteria and fungi and through natural and anthropogenic land fires (Prentice et al. 2001). The second largest flux occurs between the atmosphere and the ocean, 90 Pg C y^{-1} , through physical air-sea exchange. This will be described in more detail in Section 1.2.1. The largest of the carbon pools is the geological reservoir, composed of fossil organic carbon and carbonate rock formed through the lithification of inorganic biogenic CaCO_3 and the diagenesis of organic sediments (Chester 2003). The natural cycling of carbon to and from this reservoir occurs over a time scale of millions of years and plays a minor role in the natural carbon cycling occurring between terrestrial, atmospheric and oceanic carbon pools. Anthropogenic interference in the carbon cycle, particularly the

acceleration of CO₂ release from the geological reservoir will be described in more detail in Section 1.2.2.

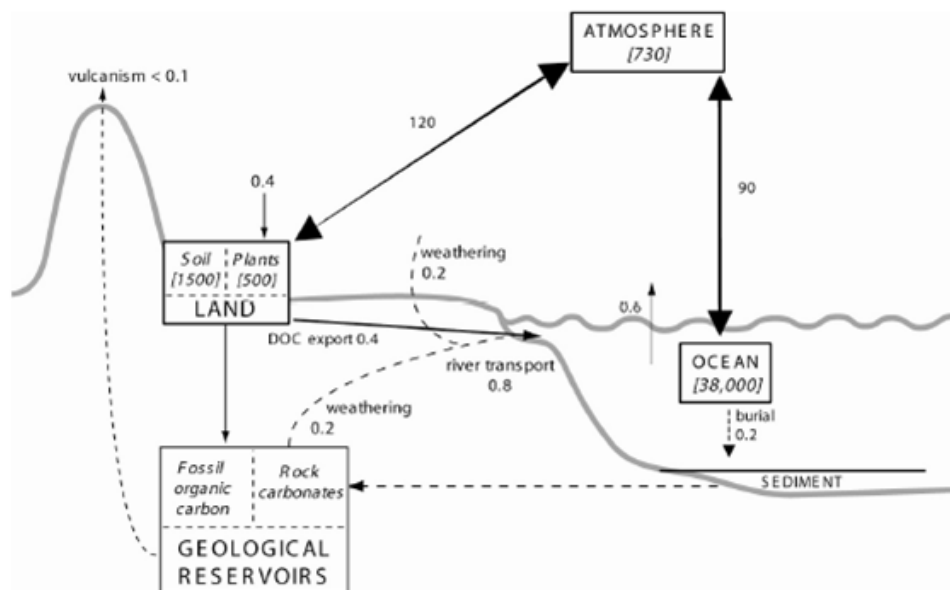


Figure 1.1: The global carbon cycle: reservoirs (Pg C) and fluxes (Pg C y⁻¹) of preindustrial estimate.
Figure reproduced from Prentice et al. (2001).

1.2.1 THE MARINE CARBON CYCLE

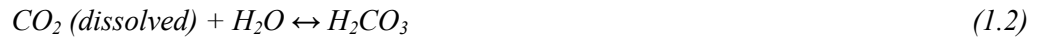
There are two pathways that lead to the storage of carbon in the deep ocean reservoir: the carbon solubility pump and the biological carbon pump. Both pumps operate as a vehicle for the transfer of carbon from the surface pool to the deep ocean reservoir. The physical pump enriches the deep ocean because CO₂ is more soluble in the cold waters of high latitude, where deep water formation occurs, than in low latitude areas. Thus CO₂ is removed from surface layers of the world ocean through deep water formation. It will eventually return to the surface as part of the meridional overturning circulation over a time scale of hundreds to a thousand years. A recent modelling study has, however, suggested that the Southern Ocean has already become saturated with CO₂ (Le Quéré et al. 2007). So even though the absorption of CO₂, including anthropogenically produced CO₂, is usually higher in high latitude cold water regions like the Southern Ocean (caused by lower temperatures and more intense mixing regimes) the saturation of these waters in relation to CO₂ means that more anthropogenically produced CO₂ will remain in the atmosphere.

After dissolution CO_2 can be found in three dissolved forms CO_2 , HCO_3^- and CO_3^{2-} which constitute dissolved inorganic carbon (DIC) in the ocean. Increases in atmospheric CO_2 mean an increase in dissolved CO_2 in surface seawater. Most of the added CO_2 will be transformed to HCO_3^- . The addition of this in turn causes a decrease in CO_3^{2-} . Less CO_3^{2-} means any further addition of CO_2 will remain in dissolved form (Equation 1.5).

Solution:



Conversion to carbonic acid:



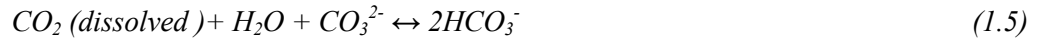
First ionisation:



Second ionisation:



Overall:



In the biological carbon pump, carbon dioxide in the surface of the ocean is used by autotrophic organisms in photosynthesis causing a decrease in the partial pressure of CO_2 which results in the drawdown of CO_2 .

Transport of carbon fixed in the sunlit layers across the surface ocean-deep ocean boundary means that the fixed carbon is out of contact with the atmosphere. Material of biological origin lost from the surface ocean will only come back in contact with the atmosphere when it is up-welled via the ocean currents. Similar to what happens in the terrestrial biosphere around half (Prentice et al. 2001) of the carbon fixed by autotrophs in the ocean is respired and returned to the DIC pool in surface waters. The remainder, 45 Pg C y^{-1} (Behrenfeld & Falkowski 1997), is either phyto-detritus or available for heterotrophic consumption. Heterotrophs consume and respire 34 Pg C y^{-1} (Calbet 2001, Prentice et al. 2001, Ducklow 2002, Calbet & Landry 2004), the greater part of net primary production. The part of primary

production that escapes the surface layer of the ocean is known as export production. Export production in the form of dissolved organic carbon (DOC) and particulate organic carbon (POC) has been estimated at $\sim 11 \text{ Pg C y}^{-1}$ (Schlitzer 2000). Only a fraction of export production, 0.01 Pg C y^{-1} , ever reaches the sea floor (Prentice et al. 2001). Most of the export is respired by heterotrophs and returned to the DIC pool where it is eventually returned to the surface ocean by ocean currents. Both autotrophic and heterotrophic organisms contribute to the particulate phase of inorganic cycling in the ocean by producing shells of CaCO_3 . Although the export of CaCO_3 to the deep sea is only a fraction of the organic carbon exported, 0.4 Pg C y^{-1} , it makes a much larger contribution to sedimentation, 0.2 Pg C y^{-1} , the remainder is dissolved, returning to DIC. The production of CaCO_3 in the ocean surface partly offsets the effect of biological production on pCO_2 because it shifts the carbonate balance of Equation 1.5 to the left. This is sometimes referred to as the carbonate pump.

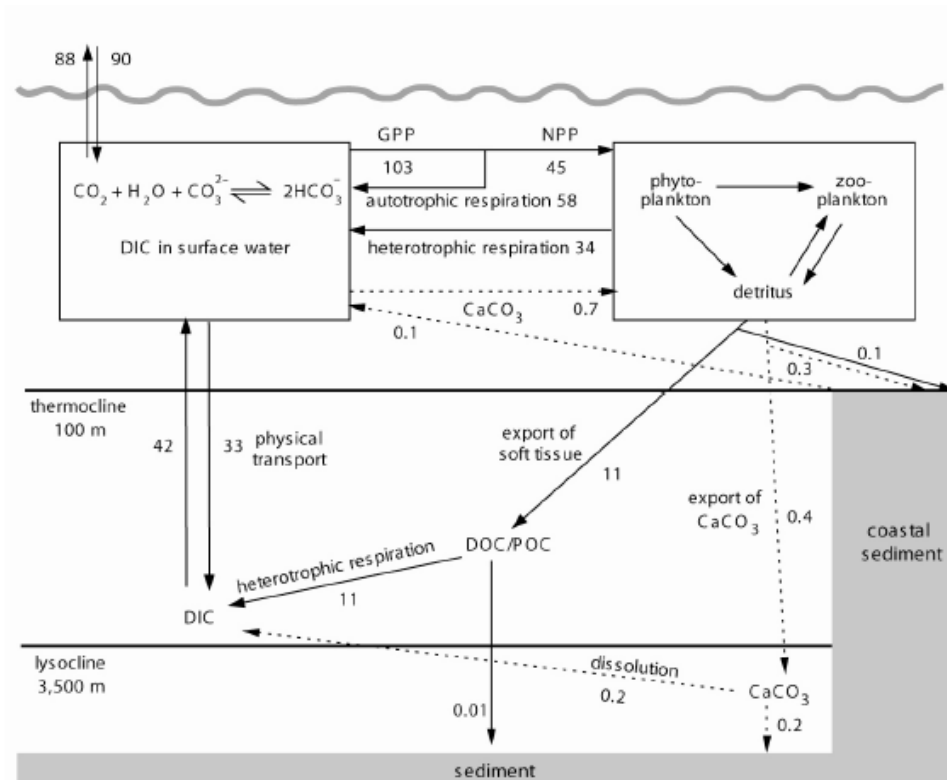


Figure 1.2: Carbon cycling in the ocean: fluxes (Pg C y^{-1}) estimated for the 1980s. Figure reproduced from Prentice et al. (2001).

1.2.2 ANTHROPOGENIC CLIMATE CHANGE

Prior to the industrial revolution the concentration of atmospheric CO₂ was constant at 280 parts per million (ppm) varying by about 10 ppm over a few thousand years (Indermuhle et al. 1999). In 2008 the concentration of atmospheric CO₂ was 386 ppm. There is no doubt that the observed increase in atmospheric CO₂ is the result of anthropogenic interference in the global carbon cycle (Hegerl et al. 2007). The majority of this increase is caused by the anthropogenic release of CO₂ from fossil fuels ($9.1 \pm 0.9 \text{ Pg C y}^{-1}$ from 2000 to 2006 (Canadell et al. 2007), this includes the small fraction of CO₂ released from cement production) and changes in land use. There is however an imbalance between anthropogenic CO₂ emissions and the increase in CO₂ in the atmosphere. This imbalance is caused by the uptake of anthropogenic CO₂ by the terrestrial biosphere and the oceans. As a result, the increase of CO₂ in the atmosphere is on average about 45% of the emissions, or $4.1 \pm 0.1 \text{ Pg C}$ for 2000 to 2006 (Figure 1.3).

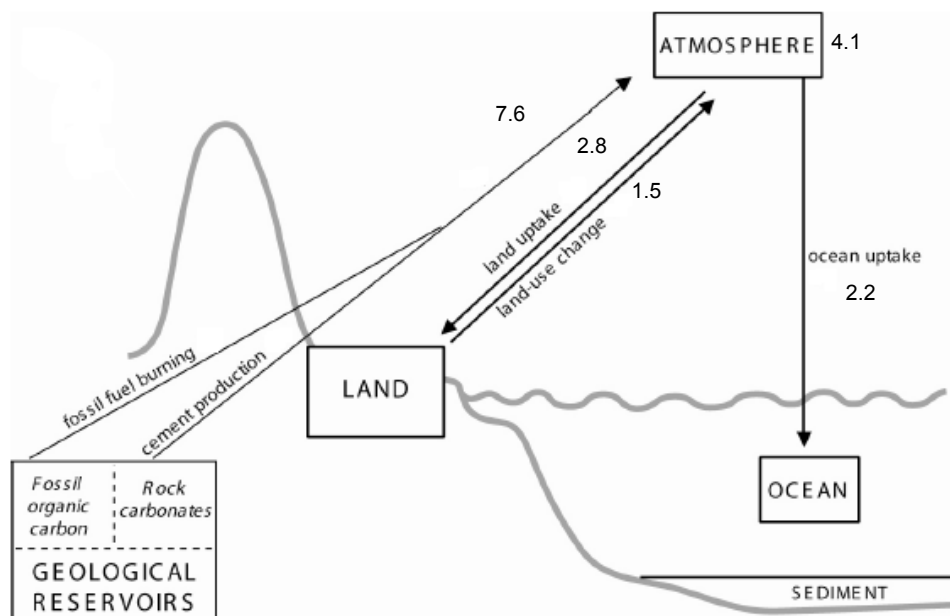


Figure 1.3: Anthropogenic disturbance of the global carbon cycle: fluxes (Pg C y⁻¹) estimated for 2000-2006. Figure reproduced from Prentice et al. (2001) with updated flux values from Canadell et al. (2007).

The continued increase of atmospheric CO₂ and its impact on climate will affect the ocean's capacity as a sink for anthropogenic CO₂. The chemical and physical processes that will influence the uptake of anthropogenic CO₂ include:

1. a decrease in the amount of dissolved CO_2 in the ocean caused by changes in buffering (Equation 1.5),
2. surface warming results in a reduction of the dissolution of CO_2 in the oceans,
3. warming and other changes in atmospheric forcing may change surface stratification and ocean circulation, which will affect the ventilation time of carbon stored in the deep ocean, and the uptake of anthropogenic CO_2 .

While physical processes seem more likely to reduce the capacity of the oceans as a sink for CO_2 (Prentice et al. 2001), biological processes may increase or decrease its capacity as a sink for anthropogenic CO_2 . Some of the processes that may play a role in changes in the ocean CO_2 sink include:

1. effect of surface warming on primary and secondary production and bacterial respiration,
2. changes in the supply of major nutrients or currently limiting nutrients such as iron in high nutrient low chlorophyll (HNLC) areas like the Southern Ocean, which may affect primary production and export,
3. shifts in ecosystem components as a result of regional and global environmental changes. For example, ocean acidification may decrease calcification rates in organisms with hard body parts composed of calcium carbonate, which could lead to an increase in the capacity of the oceans as a carbon sink by increasing carbonate ion concentration in the surface ocean.

Physical and biological processes in the oceans are responsible for important changes in atmospheric CO_2 on glacial/interglacial time scales, but the exact mechanism driving the CO_2 variations is difficult to determine (Watson & Liss 1998, Prentice et al. 2001, Denman et al. 2007). The ocean's importance is known because deep-sea $\delta^{13}\text{C}$ records, used to reconstruct the terrestrial storage of carbon during glacial and interglacial periods, suggest that the terrestrial biosphere stored less carbon during glacial periods, and cannot explain the low atmospheric CO_2 . The oceanic mechanisms responsible for the changes in atmospheric CO_2 remain elusive mirroring the uncertainties about the mechanisms and/or the complexities involved in the uptake

of anthropogenic CO_2 by the oceans under conditions where its concentration in the atmosphere is increasing.

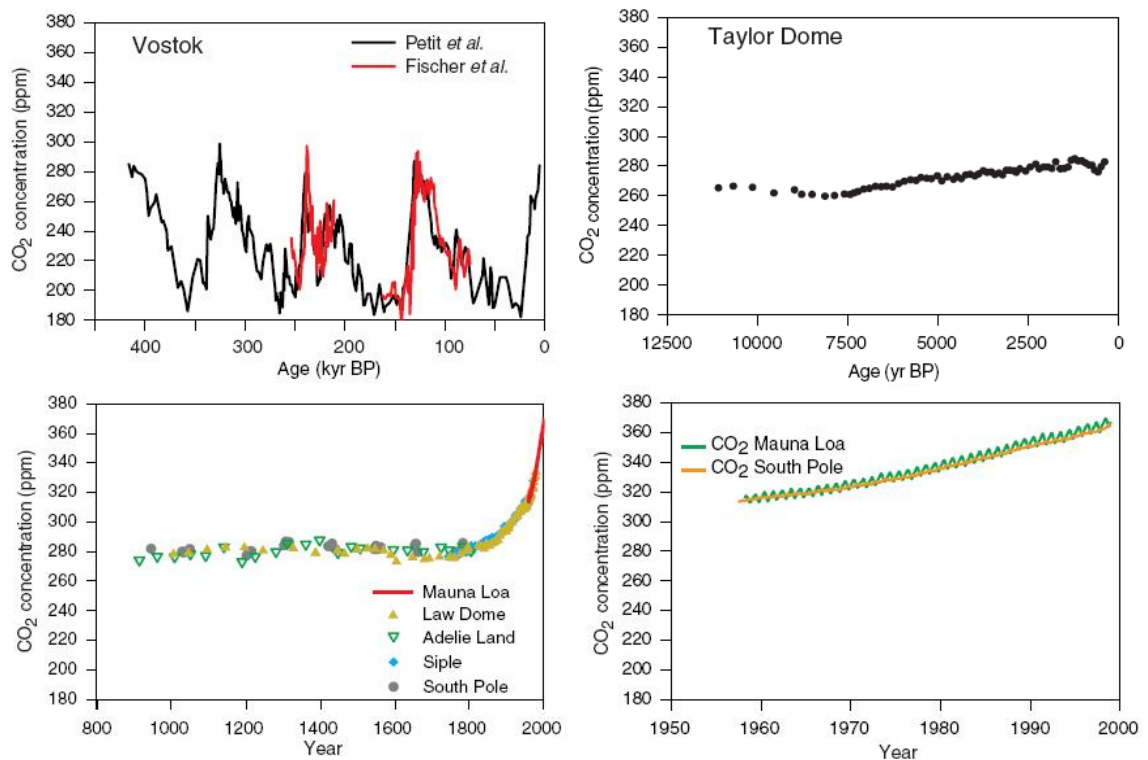


Figure 1.4: Concentrations of CO_2 on different time scales. Top-left: concentrations of CO_2 reconstructed from the Vostok Antarctic ice core over the last 420,000 years (Fischer et al. 1999, Petit et al. 1999). Top-right: CO_2 concentrations in the Taylor Dome Antarctic ice core (Indermuhle et al. 1999). Bottom-left: Concentration of CO_2 in Antarctic ice cores over the last thousand years (Siegenthaler et al. 1988, Barnola et al. 1993, Neftel et al. 1994, Etheridge et al. 1996, Keeling & Whorf 2000). Bottom-right: measurements of contemporary changes in atmospheric CO_2 (Keeling & Whorf 2000). Figures reproduced from Prentice et al. (2001).

1.3 PLANKTON FUNCTIONAL TYPE MODELLING AND MACRO-ZOOPLANKTON

1.3.1 THE EVOLUTION OF PLANKTON FUNCTIONAL TYPE MODELLING

Plankton Functional Type (PFT) modelling has evolved through the necessity to understand interactions between marine ecosystems and climate and the possible feedback mechanisms that link the m. It was not possible to address these interactions with either Nutrient-Phytoplankton-Zooplankton-Detritus (NPZD) type models or primitive ocean biogeochemical models as described below. A new type of model was necessary in order to study the impact of anthropogenic climate change on the biology of the oceans and provide insight into the resulting changes that occur in both ocean and atmosphere. PFT models allow a suite of questions,

relating to controls on atmospheric gases and the interaction between components of the marine ecosystem and climate, to be addressed as outlined in Le Quéré et al. (2005). They can help elucidate patterns in the variation of CO₂ concentrations during the Quaternary ice age cycles, and increase understanding of the controls on preindustrial CO₂ levels. They can help to track both the evolution of CO₂ concentrations since the mid 18th century and any future changes in the uptake of anthropogenic CO₂ by the oceans. They can also help address other questions regarding the role of the oceans in the regulation of trace gases, aerosols, DMS and halogenated organic species in the atmosphere and their role in controlling the abundance of isotopic tracers in the oceans and in the atmosphere. Finally, PFT models can help address questions regarding the role that marine ecosystems or particular groups within the ecosystem play in processes such as the regulation of surface temperature and mixing regimes, regional and global ecosystem-climate feedback, the combined effects of climate change and management of commercially viable groups, e.g. fish, and the possibility to evaluate the effectiveness of CO₂ sequestration in the ocean and understanding the effects it would have on marine ecosystems. These questions are all centred around components of the marine ecosystem that are explicitly represented in PFT type models.

The forerunners of PFT models shall be examined briefly in order to demonstrate the need for the development of models that are capable of addressing the concerns related to marine ecosystem-climate feedbacks mentioned above. NPZD models are simple representations of marine ecosystems (Anderson 2005) where nutrients, phytoplankton, zooplankton and detritus form the backbone of the model (e.g., Steele 1974)(Figure 1.5). NPZD models were usually developed for a particular region to address a particular concern, e.g. Station P in the open subarctic Pacific Ocean where possible mechanisms of high production rate were examined (Frost 1993). NPZD models usually operate with one or two elements as model currency, usually nitrogen and/or carbon (e.g., Frost 1987, Fasham et al. 1993, Anderson et al. 2007). The simple food web components of these models are usually based on predator-prey type equations based on Lotka-Volterra equations, e.g. Moloney & Field (1991). The regional and simplistic nature of these models means that they may not be employed to address

questions regarding global marine ecosystem-climate feedbacks. The simple approach to ecosystem modelling adopted in NPZD type models was partly caused by the limits of the computational facilities available at the time (1970s).

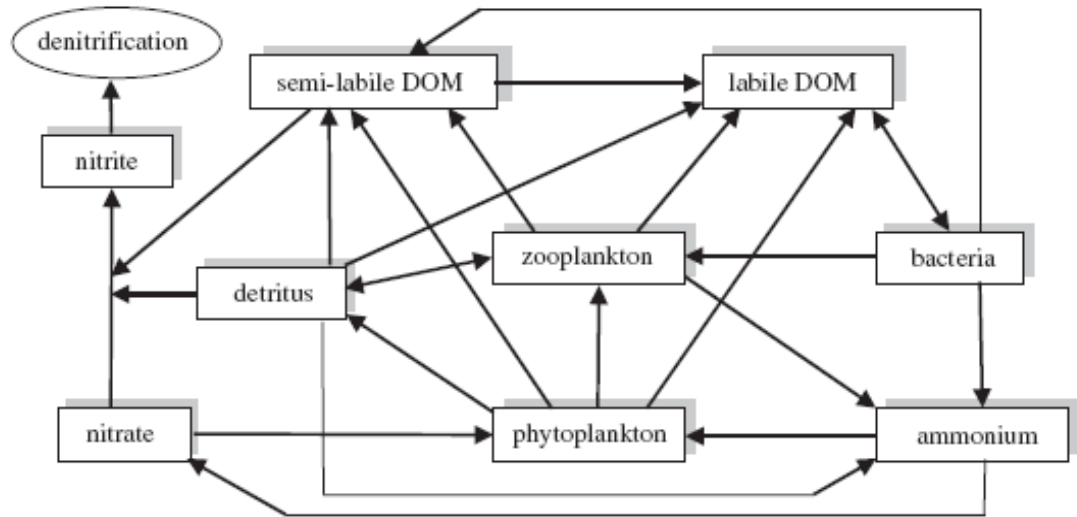


Figure 1.5: A simple NPZD model with carbon and nitrogen cycles. Figure reproduced from Anderson et al. (2007).

Global ocean biogeochemical models are a relatively more recent development (Najjar et al. 1992, Maier-Reimer 1993). Ocean biogeochemical models parameterise biological processes important in carbon, nitrogen and sulphur cycles using geochemical observations. The biological processes and their sensitivities to changes in climate are ignored as they are implicitly represented. Ocean biogeochemical models also render geochemical data sets useless as validation tools as they have been used to constrain biological activity, while ignoring the wealth of physiological and ecological data available to characterise ecosystem processes (Le Quéré et al. 2005). Implicit biological processes are not expressed or parameterised in their own right and, as such, are inbuilt in geochemical processes such as the carbon, nitrogen and sulphur cycles of ocean biogeochemical models. In the case of ocean biogeochemical models these cycles are parameterised from geochemical observations. The implicit representation of biological processes means that biogeochemical models may be able to project how the ocean will respond to increases in CO_2 but they will not elucidate the nature of biological processes involved as they depend entirely on physical processes (Le Quéré 2006).

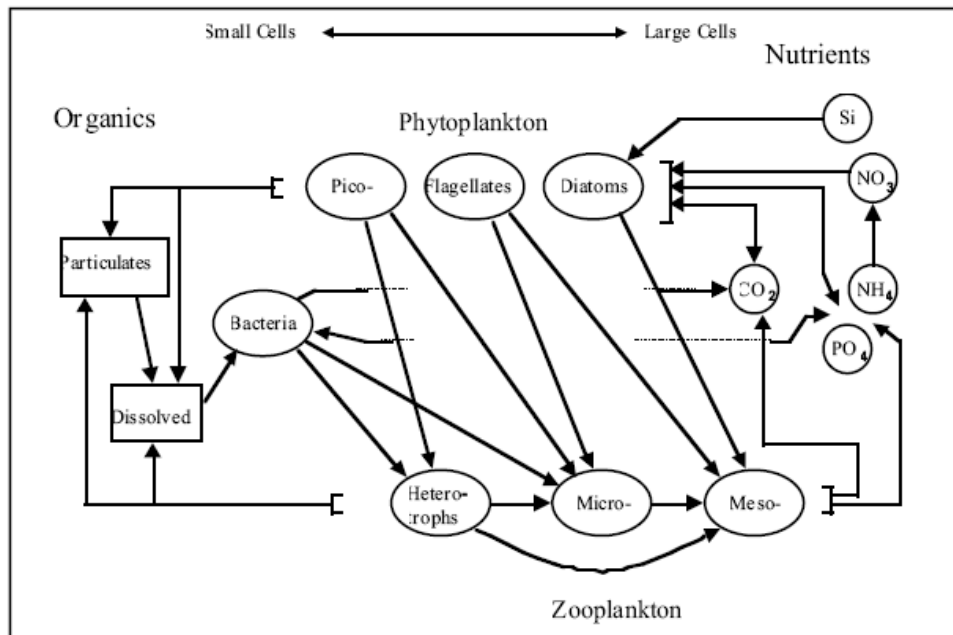


Figure 1.6: Ocean biogeochemical model with ecosystem composed of PFTs with a more sophisticated pelagic food web than that presented in Figure 1.4 and representations of nitrogen, phosphorus and silicate cycles. Figure reproduced from Allen et al. (2001).

PFT models include the explicit representation of biological processes which enables the response of the biological components to increases in CO_2 to be examined. The inclusion of ecology or the ecosystem in PFT models enables the focus to fall on the ecological system, the groups within it, or biological processes occurring within those groups, making it easier to identify the effect of increasing CO_2 on the biological system and the implications that these effects have for the rest of the climate system. PFT models take advantage of the data related to the ecological and physiological processes within ocean ecosystems enabling them to parameterise biological processes explicitly (Figure 1.6). Currently PFT models are limited by the lack of precise understanding of the mechanisms that control marine ecosystems (Le Quéré et al. 2005), and by the insufficient availability of data to parameterise all physiological and ecological rates. This thesis uses the PlankTOM10 PFT model, which will be discussed in more detail later in this section.

Developments in ocean biogeochemical models have followed the successful approaches used in their terrestrial counterparts. Global Vegetation Models (GVMs) were developed to model the impact of climate on terrestrial ecosystems. A number of GVMs were successful in predicting the geographic distribution of vegetation types, e.g. BIOME (Prentice et

al. 1992), BIOME-3 (Haxeltine & Prentice 1996), MAPSS (Neilson 1995) and DOLY (Woodward et al. 1995). Subsequently versions of GVMs were developed to allow changes in climate to influence the geographical distribution of plant types through biological, physiological and ecological processes (Levis et al. 1999). These models were named Dynamic Global Vegetation Models (DGVMs). When DGVMs such as IBIS (Levis et al. 1999) were coupled to atmospheric general circulation models (AGCMs), e.g. GENESIS in Levis et al. (1999), a number of feedbacks between terrestrial ecosystems and climate were identified, e.g. the resultant increase in land surface temperature from a decrease in high latitude albedo as a consequence of tundra-to-forest transition (Moorcroft 2003). DGVMs have also been used in Earth System models where they are coupled to an ocean–atmosphere model (HadCM3) (Gordon et al. 2000) and an ocean carbon-cycle model (HadOCC) and used to examine the feedbacks between ecosystem and climate caused by increasing anthropogenic CO₂ (Cox et al. 2000).

Employing a similar strategy, Dynamic Green Ocean Models (DGOMs) are now being used to investigate the feedbacks between marine ecosystems and climate (e.g., Le Quéré et al. 2005). It has been suggested by Le Quéré et al. (2005) that the inability of ocean biogeochemical models to reproduce the observed interannual variability in chlorophyll *a* may in part be attributed to the lack of sufficient complexity, at course resolution, in ecosystem processes. Biogeochemical processes in marine systems are intimately linked to PFTs (Falkowski et al. 2003, Anderson 2005) therefore grouping organisms that have a similar biogeochemical function enables a fuller representation of the ecosystem without the inherent complexity associated with species-specific ecosystem models. As the number of PFTs explicitly represented in the ecosystem increases the complexity of the interactions in the system also increases. Plankton groups may be considered a PFT, as defined by Le Quéré et al. (2005), if the following four criteria are met:

1. the group must play an explicit role in ocean biogeochemical cycling,
2. the physiological and/or ecological rates or environmental conditions of the group must be distinct from those of other PFTs,

3. the group must directly impact one or more of the other PFTs and
4. the group must be of quantitative importance in at least one region of the world ocean.

PlankTOM10 is a model based on PFTs that has evolved directly from one lineage of ocean biogeochemistry models. PISCES, a model developed by Aumont et al. (2003), was based on an ocean biogeochemical model originally developed by Maier-Reimer (1993) to describe the effect of the biological pump on carbon distribution. The PISCES model included two phytoplankton and two zooplankton groups. Further developments to PISCES by Buitenhuis et al. (2006) resulted in a PFT model called PISCES-T. All subsequent models in this lineage belong to the PlankTOM series of DGOM models. These models contain the full biogeochemical cycles of phosphate, silicate, carbon, oxygen and a simplified iron cycle. PlankTOM10 is the most complex model in this series so far. It represents ten PFTs: pico-heterotrophs, pico-autotrophs, N₂-fixers, calcifiers, DMS-producers, silicifiers, mixed phytoplankton, proto-, meso- and macro-zooplankton. These ten PFTs capture some of the major biological processes thought to be important in ocean biogeochemical cycling.

There are a number of other global and regional PFT type DGOM models used to examine a variety of biogeochemical processes. Global models are used to examine the response of the global ocean to variations in dust input (Moore et al. 2005), global fluxes in carbon or, more specifically, changes associated with these fluxes (Bopp et al. 2001) and the impacts associated with them (Friedlingstein et al. 2001). PFT type DGOM models with a focus on specific regions of the world ocean include ERSEM (Blackford et al. 2004) which monitors plankton dynamics in the North Sea and NEMURO (Kishi et al. 2004, Kishi et al. 2007) with a focus on the North Pacific.

1.3.2 MACRO-ZOOPLANKTON

Plankton consists of autotrophic and heterotrophic organisms that drift, passively transported by ocean currents. The heterotrophic component of the plankton is divided into three broad groups: the prokaryotes (bacteria) and eukaryotic protozoan and metazoan zooplankton. Zooplankton range in size from a few μm in flagellates to 2 m in large jellyfish or pyrosomes (Harris et al.

2000) covering six orders of magnitude in length and eighteen orders of magnitude in mass. They are commonly classified by size, an artificial division, of which there are a number of classification schemes (see Schütt 1892, Omori & Ikeda 1984, Sieburth et al. 1987). Perhaps the most widely accepted classification was published by Sieburth et al. (1987) where zooplankton are split into five different size classes; nano- (2-20 μm), micro- (20-200 μm), meso- (0.2-20 mm), macro- (2-20 cm) and mega-zooplankton (20-200cm). Each size class spans one order of magnitude except for meso-zooplankton which spans two. Nano- and micro-zooplankton are often combined and referred to as proto-zooplankton, and macro-zooplankton are often accepted as the largest size class (Le Quéré et al. 2005). For the purpose of this thesis macro-zooplankton were defined, by scientific consensus, as zooplankton greater than 2 mm in size by Le Quéré et al. (2005). They are separated from nekton, metazoans that reside within the pelagic realm, by the locomotive capacity of the nekton which enables them to overcome ocean currents (Omori & Ikeda 1984).

Table 1.1: The number of species in holoplanktic and meroplanktic macro-zooplankton. Numbers in bold are rough estimates. Reproduced from Table 1.1 in Harris et al. (2000).

Taxonomic groups	No. of species
<i>Holoplankton</i>	
Thaliacea	45
Ctenophores	80
Siphonophores	150
Polychaetes	100
Heteropods	30
Pteropods	100
Chaetognaths	50
Mysids	600
Amphipods (Hyperidea)	300
Euphausiids	90
Decapods	200
Appendicularians	60
<i>Meroplankton</i>	
Scyphomedusae	250
Hydromedusae	500
Polychete larvae	3000
Veliger larvae	10000
Decapods larvae	6000

Table 1.2: Taxonomic classification of groups within the macro-zooplankton (classification is restricted to groups based on species data presented in Chapters 2, 3 and 4).

Phylum	Subphylum	Class	Subclass	Superorder	Order	Superfamily
Ctenophora	Medusozoa	Scyphozoa	Trachylina Hydroidolina		Limnomedusae	Heteropoda
Cnidaria		Hydrozoa			Trachymedusae	
					Anthoathecatae	
					Leptothecatae	
					Siphonophorae	
Mollusca		Gastropoda	Opisthobranchia		Thecosomata	
					Neotaenioglossa	
					Gymnosomata	
Annelida	Crustacea	Polychaeta	Eumalacostraca	Peracarida	Amphipoda	
Chaetognatha					Mysida	
Arthropoda		Malacostraca			Decapoda	
					Euphausiacea	
					Stomatopoda	
	Tunicata			Hoplocarida		
Chordata		Thaliacea Appendicularia				

Macro-zooplankton is a diverse collection of organisms that come from a number of different phyla. They include the holoplanktic and meroplanktic members of the thalicia, ctenophores, cnidaria, gastropods, heteropods, pteropods, chaetognaths, polychaetes, amphipods, stomatopods, mysids, decapods, euphausiids each containing many species (Table 1.1). The size of organisms in this open ended definition of macro-zooplankton varies. Ctenophores, chaetognaths, appendicularians, doliolids and hydromedusae all have smaller member species ranging a few millimetres in length. The crustaceans (mysids, amphipods, euphausiids), scyphomedusae, ctenophores, salps, pteropods, heteropods and pelagic polychaetes have species of a medium size ranging from tens of millimetres to a few centimetres. Some groups, in particular the hydromedusae, siphonophores, scyphomedusae, pyrosomes and salps have species that can reach 2 m in length.

Table 1.3: Dry mass content (as % of wet mass) and carbon mass (as % of dry mass). Dry mass and polychaete data reproduced from Larson (1986 and references therein) and carbon data reproduced from Schneider (1989).

Group	Dry mass % wet mass	Carbon mass % dry mass	Carbon mass % dry mass			
			Mean	Stdev.	Min.	Max.
<i>Gelatinous</i>						
Ctenophores	3.5	5.0	03.8	3.0	0.9	32.4
Salps	3.5	5.0	08.1	2.7	4.2	11.6
Scyphomedusae	4.0	5.0	10.7	5.9	4.3	25.4
Hydromedusae	3.5	5.0	11.7	8.3	2.8	32.4
Siphonophores	3.5	5.0	13.1	6.2	3.0	26.8
<i>Semi-gelatinous</i>						
Molluscs	3.5	30	28.7	8.1	17.0	52.0
Chaetognaths	5.0	15	33.6	9.3	19.3	52.0
Polychaetes	--	--	35.0	--	--	--
<i>Crustacean</i>						
Decapods	10	30	38.1	7.4	23.4	59.6
Euphausiids & mysids	10	30	41.8	3.9	31.1	55.4
Other crustaceans	10	30	35.0	6.9	22.5	48.4
<i>Appendicularian</i>						
Appendicularians	--	--	57.1	6.1	50.4	62.3

Macro-zooplankton may be distinguished according to their chemical composition. Gelatinous organisms have the lowest carbon and nitrogen values as a proportion of dry mass. Gelatinous forms belong to a number of systematic groups including the cnidaria, ctenophora, and thaliacea. The soft-bodied or semi-gelatinous group contains the pelagic molluscs and chaetognaths, which have about two to ten times the carbon content as a proportion of dry mass of the gelatinous organisms. Hard-bodied forms belonging to the crustacea have four to fifteen times more carbon as a proportion of dry mass than gelatinous forms. Appendicularians may be included in the gelatinous group, although strictly speaking a non-gelatinous group, they effectively occupy, with their jelly house, a total body volume that is similar to that of gelatinous organisms (Hirst et al. 2003). However if only the animal and not the gelatinous house is considered they have much higher carbon content than the crustaceans.

Although macro-zooplankton are largely at the mercy of the surrounding water mass they do have powers of locomotion sufficient to change their vertical position in the water column and to locate food. Macro-zooplankton use a variety of mechanisms to facilitate locomotion. Members of the ctenophores, salps and cnidaria use rhythmic pulsations, propelling

themselves through the water by driving water through their body cavities, e.g. salps, or out from beneath body structures, e.g. some ctenophores and cnidarians. Some members of the ctenophores move using cilia. In these species the cilia have fused to create comb rows which beat, moving the animal through the water. Lobate ctenophores may also employ lateral undulation. Siphonophores employ gas filled chambers to change position in the water column by adding or releasing gas to the chamber. A number of siphonophore and chondrophore species keep their pneumatic float above the water where it functions as a sail, the most notable species among these are *Physalia physalis* and *Velella velella*. Pelagic molluscs have modified the molluscan foot into a swimming appendage. In heteropods the foot appears as a ventral fin and the animal swims belly up. The modified foot in pteropods is different to that of the heteropods. Pteropods have developed two parapodia lateral to the foot. These flap open and closed in broad strokes. Pelagic polychaetes have modified the parapodia from those of their benthic relations into swimming appendages and move through a combination of backward moving paddle like parapodia and lateral body undulation. Crustaceans have developed large fringed pereopods as their principal swimming mechanisms allowing them to hover. Backwards darting movements are also possible through the ventral flexion of the uropods. Chateognaths combine the contraction of longitudinal muscles, dorsoventral undulations, and fin movements to propel themselves forward. Appendicularia beat their tails while enclosed within their feeding houses, creating a current that passes through the house. Many species within the macro-zooplankton have large volume to surface area ratios which means that they will sink fast. In an effort to reduce sinking some groups, e.g. salps and ctenophores have increased their buoyancy by reducing their density.

Many species of macro-zooplankton migrate vertically, a behaviour that is usually linked to feeding and predator avoidance (Hays 2002). Migrations can occur on a daily basis. Crustaceans are perhaps the most well studied group with diel vertical migrations. Diel vertical migration is the migration from depth to surface or epipelagic waters, where zooplankton spend the hours of darkness, and the return to depth during sunlight hours. The most well known examples come from within the crustacean macro-zooplankton particularly euphausiids, e.g.

Euphausia superba (Russell 1927), *Euphausia pacifica* (Endo & Yamano 2006) and *Meganyctiphanes norvegica* (Mauchline & Fisher 1969, Mauchline 1980) but species belonging to other groups including salps e.g. *Salpa aspera* (Madin et al. 2006) and chaetognaths, e.g. *Sagitta hispida* (Sweatt & Forward 1985) are also known to carry out diel vertical migrations. Much work has been carried out to identify triggers and controls for diel vertical migration. Light is thought to be the most important environmental cue (Ringelberg 1995). Diel vertical migration in some species of macro-zooplankton means there are both diurnal and seasonal variations, related to food supply in the latter case.

In all macro-zooplankton species, locomotion, the movement of body parts, may also be associated with the collection or capture of food. In some cases, e.g. the crustaceans, body parts that originated as feeding apparatus were adapted for use in locomotion. Within the macro-zooplankton there are herbivores, carnivores, omnivores and detritivores. The thaliacea are the true filter feeders, filtering water that is pumped through mucus sieves capturing small particles (Madin & Deibel 1998). The carnivorous ctenophores employ two different feeding techniques. Some ctenophores use long tentacles to fish for other planktic animals or take direct bites from other gelatinous organisms including other ctenophores. Cnidarians also employ fishing techniques to catch prey items casting tentacles like nets. However there are some species of scyphomedusae that are suspension feeders, e.g. *Aurelia*, trapping plankton on mucus covered tentacles. Pelagic polychaetes are active predators capturing prey using a rapidly eversible pharynx. The pelagic molluscs belonging to the heteropods are also active predators, some species only preying on specific pteropod species. Pteropods can be divided into active predators and suspension feeders. Some pteropods such as *Gleba* and *Corolla* secrete enormous mucus feeding nets to capture particles, ingesting particles from the mucus web using cilia on their proboscis. Carnivorous pteropods, gymnosomes, prey exclusively on the mucus net producing thecosomes. Chaetognaths use their locomotive powers to ascend the water column and then float downwards detecting movement of prey. Once a prey item has been detected they dart towards it and capture it with grasping spines which sometimes contain poison with which they paralyse their prey (Ruppert & Barnes 1994). Many crustaceans are also suspension

feeders, removing particles from the water using a current created by beating both feeding and locomotor appendages. The appendicularians produce feeding houses to which they are either attached, e.g. *Fritillaria*, or enclosed in, e.g. *Oikopleura*. Tail beating creates a current strong enough to draw water through the house, and fine particles $< 10 \mu\text{m}$ are collected and ingested. Once these feeding structures have become clogged they are discarded and a new feeding house is secreted by the animal.

The life history of many macro-zooplankton species may play a role in both the patchiness of their biomass distribution and in their capacity to achieve very high biomass concentrations. Life history is another trait that varies greatly within the macro-zooplankton. Alternation of generations dominates much of the life of salps (Ruppert & Barnes 1994) and has significant implications; blooms of some species occur only at certain times of the year. Blooms are made possible by the rapidity of blastozoid production by budding and to a lesser extent by the remarkably rapid growth of the individual. The life cycle of *Thalia* may be completed in 48 hours (Heron 1972). High densities can last for several months. In the cnidarians there is a sessile benthic polyp and adult planktic medusa, the latter is the part of the life cycle that exists in the pelagic realm. Reproduction is usually seasonal and many forms are paedomorphic, where an adult of the species retains some of the features of the juvenile. Many species of scyphomedusae and hydromedusae can be found in large swarms at certain times of the year as mentioned above. Of the cnidarians, one group, the siphonophores, have lost their benthic stage and are now entirely planktic (Bouillon 1999). Very little is known about the life span of different members of this group. It is thought that smaller species live for a few months, while larger species may survive for ten or more years (Bouillon 1999). Ctenophores may reach high biomass concentrations as one aspect of the reproductive biology in lobate and cydippid ctenophores is that they can precociously attain sexual maturity and successfully reproduce (Ruppert et al. 2004).

The pelagic polychaetes like the pelagic molluscs and the crustaceans all have larval stages that develop through a number of stages before the juvenile and adult forms are reached. For many species within these groups swarming occurs during sexual reproduction.

Chaetognaths on the other hand have direct and rapid development once they emerge as hatchlings. Development is sometimes known to occur in less than one day (Ruppert & Barnes 1994). Decapod larvae which contribute to the meroplankton come in two distinct types; the zoëa and the megalopa larvae. Zoëa emerge from eggs and usually hatch at night. After the final zoëa stage a metamorphosis occurs and it then molts to a megalopa. Adult decapods produce 200 to 80,000 eggs (Pohle et al. 1999). Other crustacean groups also produce high numbers of eggs, e.g. amphipod brood sizes range between two and 750 eggs, and more than one brood a year is common. Mysids have a marsupium between pleopods in which to keep embryos. Larval development time varies, e.g. between 7 to 15 days in *Neomysis intermedia* (Murano 1999). Macro-zooplankton species often show a highly seasonal life cycle, for example groups bloom or swarm and reproduce and the adults die off over winter while their offspring are developing. Many of the strategies mentioned above exploit favourable conditions, e.g. high food concentrations.

Species belonging to the macro-zooplankton are found throughout the world ocean. Crustaceans, e.g. euphausiids, are particularly important at high latitudes, because of their importance in the food chain, but all groups are ubiquitous throughout the world ocean. Thaliacea and appendicularians are important in some areas of the world ocean but are not as wide spread as the crustaceans, although they can reach extremely high biomass concentrations when environmental conditions are favourable. Cnidarians and ctenophores are often associated with coastal and inshore areas but they are present to a lesser extent in oligotrophic ocean basins. Macro-zooplankton are of both ecological and commercial importance in the world ocean. They channel carbon from the microbial loop, primary and secondary producers, to higher trophic level predators such as fish, birds, seals, whales and turtles. They are commercially important as they serve as food sources for exploited species. A number of macro-zooplankton species are also directly exploited commercially for both human consumption and as agricultural feed. In 1978 twenty species of zooplankton, including crustacean macro-zooplankton and scyphomedusae, were being commercially exploited (Omori

1978). At the height of commercial operation in the 1980s half a million tonnes of *Euphausia superba* were removed from the Southern Ocean each year (Kawaguchi & Nicol 2007).

1.3.3 MACRO-ZOOPLANKTON AS A PFT

It is difficult to summarise the attributes of a diverse group of organisms such as the macro-zooplankton as demonstrated above. Members of the macro-zooplankton come from a myriad of species from a number of different phyla. Despite the inherent differences between species and indeed across phyla, the group shares a number of traits and satisfy the criteria set down in Section 1.3.2 that allow it to be considered a PFT. Macro-zooplankton meets these criteria as follows:

1. Macro-zooplankton produce large and fast sinking faecal pellets contributing to the export of material to the deep ocean and thus play an explicit role in biogeochemical cycling of carbon and nutrients.
2. The physiological rates of macro-zooplankton are distinct from those of other zooplankton; some of the highest growth rates in the animal kingdom occurring among member species.
3. The diversity of the taxa belonging to the macro-zooplankton means that there are many variations in feeding behaviour and a variety of prey are consumed by the group as a whole. Macro-zooplankton have a direct influence on not only meso-zooplankton, which are placed one trophic level below them in a traditional food pyramid, but feed on all lower trophic levels and are involved in an intricate trophic web. They also have the capacity to short-circuit the microbial loop.
4. It is not difficult to assess the quantitative importance in a particular region of the world ocean for the more familiar members of the macro-zooplankton, e.g. *Euphausia superba* in the Southern Ocean. Member species of the cnidaria are often in the news as they occur in such high numbers that they disrupt aquaculture and tourism. Macro-zooplankton abundance is exploited not only by their marine predators but by humans who also consume them in vast quantities. Macro-zooplankton may not be

quantitatively important in all regions of the world ocean, e.g. Arctic where it is benthic fauna that provide food for grey whales and walrus (Smetacek & Nicol 2005). However there are regions where they are the crucial link between higher and lower trophic levels, e.g. *Euphausia superba* in the Southern Ocean.

1.3.4 CARBON EXPORT BY MACRO-ZOOPLANKTON

There is no global estimation of the contribution of macro-zooplankton to the sedimentary flux of carbon from the sunlit layers of the world ocean to the deep sea. Faecal pellets are the main vehicle through which carbon is repackaged by macro-zooplankton, and transported to the deep sea. There is limited data on the production, composition and sinking rates of faecal pellets produced by macro-zooplankton which make the qualitative and quantitative assessment of this flux difficult. Macro-zooplankton are capable of feeding across a multitude of species from varying trophic levels both higher and lower than themselves. They repackage autotrophic, heterotrophic and detrital material in the epipelagic layer of the world ocean. Part of this repackaged carbon moves to higher trophic levels through predation on macro-zooplankton (Deibel 1998). The portion of the carbon that is not assimilated by macro-zooplankton is packaged into faecal pellets. The faecal pellets of some macro-zooplankton sink up to one order of magnitude faster than marine snow and phyto-detritus (Turner 2002). The higher sinking speeds of macro-zooplankton faecal pellets mean that faecal pellets spend less time in the surface layers of the ocean and there is less opportunity for microbial decomposition and coprophagy. In contrast, the faecal pellets of smaller zooplankton do not sink fast enough to escape microbial degradation and coprophagy and are recycled and repackaged in the euphotic zone (Turner 2002). This means that macro-zooplankton faecal pellets play a smaller role in the recycling and repackaging of carbon and nutrients that occurs in the surface layers of the ocean, and, correspondingly, a larger role in the export of carbon to depth.

Table 1.4: Sinking rates of zooplankton faecal pellets, marine snow and phytoplankton detritus. Sinking rate is in meters per day. Reproduced from Turner (2002). Note: Macro-zooplankton groups are italicised.

Particles	Sinking rate (m d ⁻¹)	Reference
Faecal pellets		
Copepods	5-220	Smayda 1971, Turner 1977, Honjo & Roman 1978, Paffenhofer & Knowles 1979, Small et al. 1979, Bienfang 1980, Yoon, 2001
<i>Euphausiids</i>	16-862	Fowler & Small 1972, Youngbluth et
<i>Doliolids</i>	41-504	Bruland & Silver 1981, Deibel 1990
<i>Appendicularians</i>	25-166	Gorsky et al. 1984
<i>Chaetognaths</i>	27-1313	Dilling & Alldredge 1993
<i>Pteropods</i>	120-1800	Bruland & Silver 1981, Yoon et al.
<i>Heteropods</i>	120-646	Yoon et al. 2001
<i>Salps</i>	43-2700	Madin 1982, Yoon et al. 2001
Marine snow	16-368	Taguchi 1982
Phyto-detritus	100-150	Billett et al. 1983, Lampitt 1985

Macro-zooplankton also contribute to the downward flux of carbon through their contribution of dead tissues to marine snow. Abandoned feeding structures such as the abandoned houses of appendicularians (Alldredge & Gotschalk 1988, Robison et al. 2005), discarded mucus feeding nets of some species of pteropods (Hamner et al. 1975), crustacean molts (Alldredge & Gotschalk 1988), episodic mass sedimentation of gelatinous macro-zooplankton carcasses, e.g. thaliacea (Lebrato & Jones 2009) and cnidarians (Billett et al. 2006), in part make up the contribution of macro-zooplankton to marine snow. Marine snow and phyto-detritus are also important in the sedimentation of carbon to the deep sea. The degree to which faecal pellets, marine snow and phyto-detritus contribute to carbon export is highly variable. The slower sinking speeds of marine snow and phyto-detritus mean that they spend more time in the surface ocean and are more likely to meet a similar fate as the faecal pellets of smaller zooplankton. The tendency of macro-zooplankton to ‘bloom’ during favourable environmental conditions (Purcell 2005) means they contribute to carbon export during mass export events, for salps and pteropods in particular, where faecal pellets (Bruland & Silver 1981, Madin 1982, Bathmann 1988, Perissinotto & Pakhomov 1998) and discarded feeding structures (Turner 2002) sink from the euphotic zone to the deep sea.

1.4 THESIS OUTLINE

1.4.1 THESIS OBJECTIVE

Much is still lacking with regards to information on the influence of macro-zooplankton on the global carbon cycle. There is a need for better understanding of biogeochemical pathways that exert control on the export of carbon from the surface to the deep ocean. The goal of this PhD thesis was to investigate the role of macro-zooplankton for global biogeochemical cycles, and in particular to provide constraints on the contribution of macro-zooplankton to global export production. An important step of this work was to synthesize and analyse data on macro-zooplankton physiological and ecological process rates and derive functional relationships with temperature to allow the parameterisation of macro-zooplankton for their inclusion in the biogeochemical model PlankTOM10.

1.4.2 THESIS STRUCTURE

Chapter 2 presents a data synthesis and analysis of macro-zooplankton respiration data, complemented with mass-specific respiration rates in carbon units and metadata that includes geographical location, temperature and experimental protocol. This data synthesis is used to investigate the relationship between respiration and both body mass and temperature in the macro-zooplankton. In Chapter 3 macro-zooplankton abundance and biomass data sets are constructed which are used to produce a first quantification of macro-zooplankton biomass and to validate the macro-zooplankton distribution and biomass concentration in PlankTOM10. In Chapter 4 the macro-zooplankton PFT is parameterised and incorporated this group into the global ocean biogeochemical model PlankTOM10. Model simulations, optimisations and sensitivity analysis were undertaken. The model results have been used to investigate and quantify the contribution of macro-zooplankton to global export production. In Chapter 5 heterotrophic physiological process rate data, collected on behalf of the Dynamic Green Ocean Group, is compiled and summarised. The relationship between physiological rates such as uptake, grazing and respiration and temperature is investigated. The temperature-dependence of

physiological rates is examined in order to determining the possible implications of global warming on heterotrophic groups and its implications for climate.

REFERENCES

- Allredge A L, Gotschalk C (1988) Insitu settling behavior of marine snow. *Limnology and Oceanography* 33:339-351
- Allen J I, Blackford J, Holt J, Proctor R, Ashworth M, Siddorn J (2001) A highly spatially resolved ecosystem model for the North West European Continental Shelf. *Sarsia* 86:423-440
- Anderson T R (2005) Plankton functional type modelling: running before we can walk? *Journal of Plankton Research* 27:1073-1081
- Anderson T R, Ryabchenko V A, Fasharna M J R, Gorchakov V A (2007) Denitrification in the Arabian Sea: a 3D ecosystem modelling study. *Deep-Sea Research Part I-Oceanographic Research Papers* 54:2082-2119
- Aumont O, Maier-Reimer E, Blain S, Monfray P (2003) An ecosystem model of the global ocean including Fe, Si, P colimitations. *Global Biogeochemical Cycles* 17
- Barnola J M, Anklin M, Porcheron J, Raynaud D, Schwander J, Stauffer B (1993) CO₂ evolution during the last millennium as recorded by antarctic and greenland ice. 4th Atmospheric CO₂ International Conference, Carqueiranne, France
- Bathmann U V (1988) Mass occurrence of *Salpa fusiformis* in the Spring of 1984 off Ireland - Implications for sedimentation processes. *Marine Biology* 97:127-135
- Behrenfeld M J, Falkowski P G (1997) Photosynthetic rates derived from satellite-based chlorophyll concentration. *Limnology and Oceanography* 42:1-20
- Bienfang P K (1980) Herbivore Diet Affects Fecal Pellet Settling. *Canadian Journal of Fisheries and Aquatic Sciences* 37:1352-1357
- Billett D S M, Bett B J, Jacobs C L, Rouse I P, Wigham B D (2006) Mass deposition of jellyfish in the deep Arabian Sea. *Limnology and Oceanography* 51:2077-2083
- Billett D S M, Lampitt R S, Rice A L, Mantoura R F C (1983) Seasonal sedimentation of phytoplankton to the deep-sea benthos. *Nature* 302:520-522
- Blackford J C, Allen J I, Gilbert F J (2004) Ecosystem dynamics at six contrasting sites: a generic modelling study. *Journal of Marine Systems* 52:191-215
- Bopp L, Monfray P, Aumont O, Dufresne J L, Le Treut H, Madec G, Terray L, Orr J C (2001) Potential impact of climate change on marine export production. *Global Biogeochemical Cycles* 15:81-99
- Bouillon J (1999) Hydromedusae. In: D Boltovskoy (ed) *South Atlantic zooplankton*, Vol 1. Backhuys, Leiden, p 385-466
- Bruland K W, Silver M W (1981) Sinking rates of fecal pellets from gelatinous zooplankton (salps, pteropods, doliolids). *Marine Biology* 63:295-300
- Buitenhuis E T, Le Quéré C, Aumont O, Beaugrand G, Bunker A, Hirst A, Ikeda T, O'Brien T, Piontkovski S, Straile D (2006) Biogeochemical fluxes through mesozooplankton. *Global Biogeochemical Cycles* 20

- Calbet A (2001) Mesozooplankton grazing effect on primary production: A global comparative analysis in marine ecosystems. *Limnology and Oceanography* 46:1824-1830
- Calbet A, Landry M R (2004) Phytoplankton growth, microzooplankton grazing, and carbon cycling in marine systems. *Limnology and Oceanography* 49:51-57
- Canadell J G, Le Quere C, Raupach M R, Field C B, Buitenhuis E T, Ciais P, Conway T J, Gillett N P, Houghton R A, Marland G (2007) Contributions to accelerating atmospheric CO₂ growth from economic activity, carbon intensity, and efficiency of natural sinks. *Proceedings of the National Academy of Sciences of the United States of America* 104:18866-18870
- Chester R (2003) *Marine Geochemistry* Blackwell Science Ltd., Oxford
- Ciais P, Denning A S, Tans P P, Berry J A, Randall D A, Collatz G J, Sellers P J, White J W C, Troler M, Meijer H A J, Francey R J, Monfray P, Heimann M (1997) A three-dimensional synthesis study of delta O-18 in atmospheric CO₂ .1. Surface fluxes. *Journal of Geophysical Research-Atmospheres* 102:5857-5872
- Cox P M, Betts R A, Jones C D, Spall S A, Totterdell I J (2000) Acceleration of global warming due to carbon-cycle feedbacks in a coupled climate model. *Nature* 408:750-750
- Deibel D (1990) Still water sinking velocity of fecal material from the pelagic Tunicate *Doliolotta gegenbauri*. *Marine Ecology-Progress Series* 62:55-60
- Deibel D (1998) Feeding and metabolism in Appendicularia. In: Q Bone (ed) *The Biology of Pelagic Tunicates*. Oxford University Press, New York, p 340
- Denman K L, Brasseur G, Chidthaisong A, Ciais P, Cox P M, Dickinson R E, Hauglustaine D, Heinze C, Holland E, Jacob D, Lohmann U, Ramachandran S, da Silva Dias P L, Wofsy S C, Zhang X (2007) Couplings between changes in the climate system and biogeochemistry. In: S Solomon, Qin D, Manning M, Chen Z, Marquia M, Averyt K B, Tignor M, Miller H L (eds) *Climate Change: The Physical Basis Contribution of Working Group I to the Fourth Assessment Report of the Intergovernmental Panel on Climate Change*. Cambridge University Press, Cambridge, United Kingdom and New York, NY, USA
- Dilling L, Alldredge A L (1993) Can chaetognath fecal pellets contribute significantly to carbon flux. *Marine Ecology-Progress Series* 92:51-58
- Ducklow H (2002) Bacterial production and biomass in the ocean. In: D L Kirchman (ed) *Microbial Ecology of the Oceans*. Wiley-Liss, Inc.
- Endo Y, Yamano F (2006) Diel vertical migration of *Euphausia pacifica* (Crustacea, Euphausiacea) in relation to molt and reproductive processes, and feeding activity. *Journal of Oceanography* 62:693-703
- Etheridge D M, Steele L P, Langenfelds R L, Francey R J, Barnola J M, Morgan V I (1996) Natural and anthropogenic changes in atmospheric CO₂ over the last 1000 years from air in Antarctic ice and firn. *Journal of Geophysical Research-Atmospheres* 101:4115-4128
- Falkowski P G, Laws E A, Barber R T, Murry J (2003) Phytoplankton and their role in primary, new, and export production. In: M J R Fasham (ed) *Ocean Biogeochemistry: The Role of the Ocean Carbon Cycle in Global Change*. Springer, Berlin, p 99-121

- Fasham M J R, Sarmiento J L, Slater R D, Ducklow H W, Williams R (1993) Ecosystem behavior at Bermuda Station-S and Ocean Weather Station India - a general-circulation model and observational analysis. *Global Biogeochemical Cycles* 7:379-415
- Fischer H, Wahlen M, Smith J, Mastroianni D, Deck B (1999) Ice core records of atmospheric CO₂ around the last three glacial terminations. *Science* 283:1712-1714
- Fowler S W, Small L F (1972) Sinking rates of euphausiid fecal pellets. *Limnology and Oceanography* 17:293-296
- Friedlingstein P, Bopp L, Ciais P, Dufresne J L, Fairhead L, LeTreut H, Monfray P, Orr J (2001) Positive feedback between future climate change and the carbon cycle. *Geophysical Research Letters* 28:1543-1546
- Frost B (1987) Grazing control of phytoplankton stock in the open subarctic Pacific Ocean: a model assessing the role of mesozooplankton, particularly the large calanoid copepods *Neocalanus* species. *Marine Ecology Progress Series*:49-68
- Frost B W (1993) A modeling study of processes regulating plankton standing stock and production in the open sub-Arctic Pacific Ocean. *Progress in Oceanography* 32:17-56
- Gordon C, Cooper C, Senior C A, Banks H, Gregory J M, Johns T C, Mitchell J F B, Wood R A (2000) The simulation of SST, sea ice extents and ocean heat transports in a version of the Hadley Centre coupled model without flux adjustments. *Climate Dynamics*:147-168
- Gorsky G, Fisher N S, Fowler S W (1984) Biogenic debris from the pelagic tunicate, *Oikopleura dioica*, and its role in the vertical transport of a trans-uranium element. *Estuarine Coastal and Shelf Science* 18:13-23
- Hamner W M, Madin L P, Alldredge A L, Gilmer R W, Hamner P P (1975) Underwater observations of gelatinous zooplankton - sampling problems, feeding biology, and behavior. *Limnology and Oceanography* 20:907-917
- Harris R, Weibe P, Lenz J, Skjoldal H-R, Huntley M (2000) *ICES Zooplankton Methodology Manual*. Academic Press, London
- Haxeltine A, Prentice I C (1996) BIOME3: An equilibrium terrestrial biosphere model based on ecophysiological constraints, resource availability, and competition among plant functional types. *Global Biogeochemical Cycles* 10:693-709
- Hays G C (2002) A review of the adaptive significance and ecosystem consequences of zooplankton diel vertical migrations. 37th European Marine Biology Symposium, Reykjavik, Iceland
- Hegerl G C, Zwiers F W, Braconnont P, Gillett N P, Luo Y, Marengo Orsini J A, Nicholls N, Penner J E, Stott P A (2007) Understanding and attributing climate change. In: S Solomon, Qin D, Manning M, Chen Z, Marquia M, Averyt K B, Tignor M, Miller H L (eds) *Climate Change 2007: The Physical Science Basis Contribution of Working Group I to the Fourth Assessment Report of the Intergovernmental Panel on Climate Change*. Cambridge University Press, Cambridge, UK and New York, NY, USA
- Heron A C (1972) Population ecology of a colonizing species - pelagic tunicate *Thalia democratica*. 1. Individual growth rate and generation time. *Oecologia* 10:269-293

- Hirst A G, Roff J C, Lampitt R S (2003) A synthesis of growth rates in marine epipelagic invertebrate zooplankton. *Advances in Marine Biology* 44:1-142
- Honjo S, Roman M R (1978) Marine copepod fecal pellets - production, preservation and sedimentation. *Journal of Marine Research* 36:45-57
- Indermuhle A, Stocker T F, Joos F, Fischer H, Smith H J, Wahlen M, Deck B, Mastroianni D, Tschumi J, Blunier T, Meyer R, Stauffer B (1999) Holocene carbon cycle dynamics based on CO₂ trapped in ice at Taylor Dome, Antarctica. *Nature* 398:121-126
- Kawaguchi S, Nicol S (2007) Learning about Antarctic krill from the fishery. 19:219-230
- Keeling C D, Whorf T P (2000) Atmospheric CO₂ records from sites in the SIO air sampling network. In: *Trends: A Compendium of Data on Global Change*. Carbon Dioxide Information Analysis Centre, Oak Ridge, Tennessee, USA
- Kishi M J, Kashiwai M, Ware D M, Megrey B A, Eslinger D L, Werner F E, Noguchi-Aita M, Azumaya T, Fujii M, Hashimoto S, Huang D J, Iizumi H, Ishida Y, Kang S, Kantakov G A, Kim H C, Komatsu K, Navrotsky V V, Smith S L, Tadokoro K, Tsuda A, Yamamura O, Yamanaka Y, Yokouchi K, Yoshie N, Zhang J, Zuenko Y I, Zvalinsky V I (2007) NEMURO - a lower trophic level model for the North Pacific marine ecosystem. 11th PICES Annual Meeting, Qingdao, PEOPLES R CHINA
- Kishi M J, Okunishi T, Yamanaka Y (2004) A comparison of simulated particle fluxes using NEMURO and other ecosystem models in the western North Pacific. *Journal of Oceanography* 60:63-73
- Lampitt R S (1985) Evidence for the Seasonal deposition of detritus to the deep-sea floor and its subsequent resuspension. *Deep-Sea Research Part I-Oceanographic Research Papers* 32:885-897
- Larson R J (1986) Water-content, organic content, and carbon and nitrogen composition of medusae from the Northeast Pacific. *Journal of Experimental Marine Biology and Ecology* 99:107-120
- Le Quéré C (2006) Reply to Horizons Article 'Plankton functional type modelling: running before we can walk' Anderson (2005): I. Abrupt changes in marine ecosystems? *Journal of Plankton Research* 28:871-872
- Le Quéré C, Aumont O, Bopp L, Bousquet P, Ciais P, Francey R, Heimann M, Keeling C D, Keeling R F, Khesghi H, Peylin P, Piper S C, Prentice I C, Rayner P J (2001) Two decades of ocean CO₂ sink and variability. 6th International Carbon Dioxide Conference, Sendai, Japan
- Le Quéré C, Harrison S P, Prentice I C, Buitenhuis E T, Aumont O, Bopp L, Claustre H, Da Cunha L C, Geider R, Giraud X, Klaas C, Kohfeld K E, Legendre L, Manizza M, Platt T, Rivkin R B, Sathyendranath S, Uitz J, Watson A J, Wolf-Gladrow D (2005) Ecosystem dynamics based on plankton functional types for global ocean biogeochemistry models. *Global Change Biology* 11:2016-2040
- Le Quéré C, Rödenbeck C, Buitenhuis E T, Conway T J, Langenfelds R, Gomez Q, Labuschagne C, Ramonet M, Nakazawa T, Metzl N, Gillett N, Heimann M (2007) Saturation of the Southern ocean CO₂ sink due to recent climate change. *Science* 316:1735-1738
- Lebrato M, Jones D O B (2009) Mass deposition event of *Pyrosoma atlanticum* carcasses off Ivory Coast (West Africa). *Limnology and Oceanography* 54:1197-1209

- Levis S, Foley J A, Brovkin V, Pollard D (1999) On the stability of the high-latitude climate-vegetation system in a coupled atmosphere-biosphere model. *Global Ecology and Biogeography* 8:489-500
- Madin L P (1982) Production, composition and sedimentation of salp fecal pellets in oceanic waters. *Marine Biology* 67:39-45
- Madin L P, Deibel D (1998) Feeding and energetics of Thaliacea. In: Q Bone (ed) *The Biology of Pelagic Tunicates* Oxford University Press, New York, p 81-104
- Madin L P, Kremer P, Wiebe P H, Purcell J E, Horgan E H, Nemazie D A (2006) Periodic swarms of the salp *Salpa aspera* in the Slope Water off the NE United States: Biovolume, vertical migration, grazing, and vertical flux. *Deep-Sea Research Part I-Oceanographic Research Papers* 53:804-819
- Maier-Reimer E (1993) Geochemical cycles in an ocean general circulation model: preindustrial tracer distributions. *Global Biogeochemical Cycles* 7
- Mauchline J (1980) The biology of mysids and euphausiids. *Advances in Marine Biology* 33:1-637
- Mauchline J, Fisher L R (1969) The biology of euphausiids. *Advances in Marine Biology* 7
- Moloney C L, Field J G (1991) The size based dynamics of plankton food webs.1. A simulation model of carbon and nitrogen flows. *Journal of Plankton Research* 13:1003-1038
- Moorcroft P R (2003) Recent advances in ecosystem-atmosphere interactions: an ecological perspective. *Proceedings of the Royal Society B-Biological Sciences* 270:1215-1227
- Moore J K, Doney S C, Lindsay K, Mahowald N, Michaels A F (2005) Nitrogen fixation amplifies the ocean biogeochemical response to decadal timescale variations in mineral dust deposition. 7th International Carbon Dioxide Conference (CO₂), Boulder, CO
- Murano M (1999) Mysidacea. In: D Boltovskoy (ed) *South Atlantic Zooplankton*, Vol 2. Backhuys, Leiden, p 1099-1140
- Najjar R G, Sarmiento J L, Toggweiler J R (1992) Downward transport and fate of organic matter in the ocean: simulations with a general circulation model. *Global Biogeochemical Cycles*:45-76
- Neftel A, Friedli H, Moor E, Lötscher H, Oeschger H, Siegenthaler U, Stauffer B (1994) Historical CO₂ record from the Siple station ice core. In: T A Boden, Kaiser D P, Sepanski R J, Stoss F W (eds) *Trends '93: A Compendium of Data on Global Change*. Carbon Dioxide Information Analysis Centre, Oak Ridge, Tennessee, USA, p 11-14
- Neilson R P (1995) A model for predicting continental-scale vegetation distribution and water-balance. *Ecological Applications* 5:362-385
- Omori M (1978) Zooplankton fisheries of world - review. *Marine Biology* 48:199-205
- Omori M, Ikeda T (1984) *Methods in marine zooplankton ecology*. Wiley-Interscience Publications, John Wiley & Sons, Japan
- Paffenhofer G A, Knowles S C (1979) Ecological implications of fecal pellet size, production and consumption by Copepods. *Journal of Marine Research* 37:35-49
- Perissinotto R, Pakhomov E A (1998) Contribution of salps to carbon flux of marginal ice zone of the Lazarev Sea, Southern Ocean. *Marine Biology* 131:25-32
- Petit J R, Jouzel J, Raynaud D, Barkov N I, Barnola J M, Basile I, Bender M, Chappellaz J, Davis M, Delaygue G, Delmotte M, Kotlyakov V M, Legrand M, Lipenkov V Y, Lorius C, Pepin L, Ritz C,

- Saltzman E, Stievenard M (1999) Climate and atmospheric history of the past 420,000 years from the Vostok ice core, Antarctica. *Nature* 399:429-436
- Pohle G, Fransozo A, Negreiros-Fransozo M L, Medina Mantelatto F L (1999) Larval Decapoda (Brachyura). In: D Boltovskoy (ed) South Atlantic zooplankton, Vol 2. Backhuys, Leiden, p 1281-1352
- Prentice I C, Cramer W, Harrison S P, Leemans R, Monserud R A, Solomon A M (1992) A Global Biome Model Based on Plant Physiology and Dominance, Soil Properties and Climate. *Journal of Biogeography* 19:117-134
- Prentice I C, Farquhar G D, Fasham M J R, Goulden M L, Heimann M, Jaramillo V J, Kheshgi H S, Le Quéré C, Scholes R J, Wallace D W R (2001) The carbon cycle and atmospheric carbon dioxide. In: J T Houghton, Ding Y, Griggs D J, Noguer M, van der Linden P J, Dai X, Maskell K, Johnson C A (eds) *Climate Change 2001: The Scientific Basis Contributions of Working Group I to the Third Assessment Report of the International Panel on Climate Change*. Cambridge University Press, Cambridge
- Purcell J E (2005) Climate effects on formation of jellyfish and ctenophore blooms: a review. *Journal of the Marine Biological Association of the United Kingdom* 85:461-476
- Ringelberg J (1995) Changes in light intensity and diel vertical migration: a comparison of marine and freshwater environments. *Cambridge Journals Online*, p 15-25
- Robison B H, Reisenbichler K R, Sherlock R E (2005) Giant larvacean houses: rapid carbon transport to the deep sea floor. *Science* 308:1609-1611
- Ruppert E E, Barnes R D (1994) *Invertebrate Zoology*, Sixth Edition. Saunders College Publishing., California
- Ruppert E E, Fox R S, Barnes R D (2004) *Invertebrate Zoology: A Functional Evolutionary Approach*. Brooks/Cole-Thomson Learning
- Russell F S (1927) The vertical distribution of plankton in the sea. *Biological Reviews of the Cambridge Philosophical Society* 2: 213–262
- Schlitzer R (2000) Carbon export fluxes in the Southern Ocean: results from inverse modeling and comparison with satellite-based estimates. 3rd International Symposium on Climatic Changes and the Cycle of Carbon, Brest, France
- Schneider G (1989) Carbon and nitrogen content of marine zooplankton dry material, a short review. *Plankton Newsletter* 11:4-7
- Schütt F (1892) *Analytische Planktonstudien*. Lipsius and Tischer, Kiel
- Sieburth J M, Smetacek V, Lenz J (1987) Pelagic ecosystem structure: heterotrophic compartments of the plankton and their relationship to plankton size fraction. *Limnology and Oceanography* 23:1256-1263
- Siegenthaler U, Friedli H, Loetscher H, Moor E, Neftel A, Oeschger H, Stauffer B (1988) Stable-isotope ratios and concentration of CO₂ in air from polar ice cores. *Annals of Glaciology* 10:1-6
- Small L F, Fowler S W, Unlu M Y (1979) Sinking rates of natural copepod fecal pellets. *Marine Biology* 51:233-241
- Smayda T J (1971) Normal and accelerated sinking of phytoplankton in sea. *Marine Geology* 11:105-122

- Smetacek V, Nicol S (2005) Polar ocean ecosystems in a changing world. *Nature* 437:362-368
- Steele J H (1974) *The Structure of Marine Ecosystems*. Harvard University Press, Cambridge, Massachusetts
- Sweatt A J, Forward R B (1985) Diel vertical migration and photoresponses of the chaetognath *Sagitta hispida* Conant. *Biological Bulletin* 168:18-31
- Taguchi S (1982) Seasonal study of fecal pellets and discarded houses of appendicularia in a sub-tropical inlet, Kaneohe Bay, Hawaii. *Estuarine Coastal and Shelf Science* 14:545-555
- Turner J T (1977) Sinking rates of fecal pellets from marine copepod *Pontella meadii*. *Marine Biology* 40:249-259
- Turner J T (2002) Zooplankton fecal pellets, marine snow and sinking phytoplankton blooms. *Aquatic Microbial Ecology* 27:57-102
- Watson A J, Liss P S (1998) Marine biological controls on climate via the carbon and sulphur geochemical cycles. *Philosophical Transactions of the Royal Society of London Series B-Biological Sciences* 353:41-51
- Woodward F I, Smith T M, Emanuel W R (1995) A global land primary productivity and phytogeography model. *Global Biogeochemical Cycles* 9:471-490
- Yoon W D, Kim S K, Han K N (2001) Morphology and sinking velocities of fecal pellets of copepod, molluscan, euphausiid, and salp taxa in the northeastern tropical Atlantic. *Marine Biology* 139:923-928
- Youngbluth M J, Bailey T G, Davoll P J, Jacoby C A, Bladeseckelbarger P I, Griswold C A (1989) Fecal pellet production and diel migratory behavior by the euphausiid *Meganyctiphanes norvegica* effect benthic-pelagic coupling. *Deep-Sea Research Part I-Oceanographic Research Papers* 36:1491-1501

2 RESPIRATION RATES IN THE EPIPELAGIC MACRO-ZOOPLANKTON: RELATIONSHIP WITH BODY MASS & TEMPERATURE

Published in parts as a data set:

R. Moriarty (2009). Respiration in epipelagic macro-zooplankton: a data set. PANGAEA
<http://doi.pangaea.de/10.1594/PANGAEA.718139>

2.1 ABSTRACT

A synthesis of respiration rate data points and the accompanying body mass, in wet, dry and carbon terms, and temperature measurements is presented for 139 species of macro-zooplankton across 42 studies. For all the data taken together, epipelagic macro-zooplankton respiration rate increases with increasing carbon mass and temperature ($\log_{10} R = -1.75 + 0.82 \log_{10} [BM] + 0.0329 [T]$, $r^2 = 0.92$, $n = 1988$). Patterns in inter- and intraspecific levels are investigated. Regardless of the type of macro-zooplankton, i.e. gelatinous, semi-gelatinous, crustacean or appendicularian, the carbon-specific respiration is similar at similar body mass. The relationship between metabolic (respiration) rate (R) and body mass (M), which is usually described as a power function, $R = aM^b$, where b is the metabolic scaling exponent is examined. The interspecific metabolic scaling exponent was $b = 0.70 \pm 0.03$ and there was a variety of b -values (0.5 to 1.3) for intraspecific metabolic scaling exponent the mean of which is $b = 0.90 \pm 0.20$. This shows that interspecific and intraspecific relationships between metabolic rate and body mass scale differently. This is in contrast to the model of West et al. (1997) which suggests that both interspecific and intraspecific have a b -value of 0.75. The interspecific temperature dependence (Q_{10}) of metabolic rate was 1.94 and the mean intraspecific Q_{10} had a value of 3.06. These findings support the theory that optimisations occurring at species level are constrained by a variety of both internal (physical and chemical) and external (ecological) factors rather than one single factor.

2.2 INTRODUCTION

Macro-zooplankton are zooplankton that can attain a size $> 2000 \mu\text{m}$ as adults (e.g., Le Quéré et al. 2005). They include the meroplanktic and holoplanktic members of many taxa including: thalassia, ctenophores, cnidaria, gastropods, heteropods, pteropods, chaetognaths, polychaetes, amphipods, stomatopods, mysids, decapods, and euphausiids. They are important in the sunlit waters of the world's ocean as they consume both autotrophic and heterotrophic organisms, repackaging primary and secondary production. Some groups within the macro-zooplankton consume microbial sized prey and even bacteria, in effect short circuiting the microbial loop and making small particulate organic matter available to higher trophic levels such as fish (Gorsky

& Fenaux 1998). Macro-zooplankton contribute to the export of carbon, in the form of faecal pellets (Turner 2002) and dead bodies (Lebrato & Jones 2009), from the epipelagic zone (~top 200 m) to the deep sea. To understand and quantify the role they play in carbon export to the deep sea it is necessary to characterise both their metabolic gains and losses, i.e. ingestion, growth and respiration. Respiration is an important loss rate as carbon is lost during metabolism, e.g. energy is required for the catabolism of macromolecules which in turn release energy that is used in the synthesis of macromolecules necessary for the maintenance, growth and a variety of other functions within the organism. Carbon gained through grazing is utilised in part by the animal to respire and to grow.

The consumption of oxygen is often referred to as respiration. Respiration is composed of two discrete processes. The first is the transport of oxygen from the surrounding environment to the cells within the organism while carbon dioxide is transported in the opposite direction. The second component is referred to as cellular respiration where oxygen is used in the production of adenosine triphosphate (ATP). ATP is generated aerobically using oxygen as the final electron acceptor. If ATP is generated anaerobically the oxygen debt incurred is usually repaid once oxygen becomes available once again (Ikeda et al. 2000). Respiration or oxygen consumption can be used as a measure of metabolic rate, in other words the measure of power utilisation of an organism (Clarke & Fraser 2004). Respiration rate of marine organisms is not usually determined by the amount of carbon dioxide produced by the organism as the buffering capacity of sea water hampers such a determination. It is much simpler to determine the amount of oxygen consumed using the traditional Winkler titration (Winkler 1888) or using oxygen-electrodes (Halcrow 1963).

Studies of metabolic rate usually measure the basal or maintenance respiration of an animal. Basal metabolism is defined as the metabolic rate of an organism where there is no net change in body mass, i.e. where food intake balances the ATP production necessary for essential maintenance within the organism (Clarke & Fraser 2004). The functional definition of basal respiration originates from the study of mammals and birds (Brody 1945) and is not particularly suitable when studying the metabolism of pelagic zooplankton. Pelagic zooplankton

require a certain level of activity to maintain themselves in the water column. For this reason routine respiration, where the animal is not feeding and their activity is not controlled (Ikeda 1985), is usually measured when investigating metabolic rates in pelagic zooplankton.

Much work has been carried out on the respiration rates of pelagic zooplankton, particularly the relationship with body mass and to a lesser extent temperature. Epipelagic macro-zooplankton respiration rates have been the subject of several major studies (Ikeda 1970, Biggs 1977, Ivleva 1980, Ikeda 1985, Larson 1987). The search for patterns and rules in metabolic scaling with body mass and temperature within epipelagic zooplankton respiration rates are well documented in the literature (Krüger 1968, Ikeda 1985, Schneider 1992, Glazier 2005, Glazier 2006). There are two reasons why it is necessary to express respiration rate in epipelagic macro-zooplankton in carbon terms. The first is that ecosystem modellers require physiological and ecological process rates to be parameterised in carbon units as ecosystem models usually operate with a currency of carbon. The second reason is more fundamental; previous studies indicate similar oxygen requirements per gram of carbon mass across a range of macro-zooplankton taxa (Schneider 1992). Using carbon as the unit of mass allows a more direct comparison between individuals that have different wet mass/carbon mass ratios and dry mass/carbon mass ratios (Schneider 1992). Unfortunately respiration data and body mass in pelagic zooplankton are not always recorded in carbon units; wet mass and dry mass being easier to determine. Previous syntheses have been updated with as many respiration measurements as possible allowing the diversity among the macro-zooplankton to be captured. The construction of this data set has allowed the further investigation of general patterns in interspecific, intra-group and intraspecific relationships between respiration rate, body mass, in carbon units, and temperature.

The relationship between metabolic rate and body mass is usually described in the form of a power function: $R = aM^b$, where R is metabolic (respiration) rate, M is body mass and b is the metabolic scaling exponent. Since Rubner first proposed an allometric ($b = 0.66$) metabolic scaling exponent in 1883 there have been a variety of proposed values for b and a variety of models to explain why metabolic rate scales with body mass. As yet none of these models have

been generally accepted by the scientific community. Many authors have suggested that there is one single constraint that causes metabolic rate to scale with body mass with a unified exponent. This constraint could be ecological (external) and/or physical or chemical (both internal) in nature. A scaling exponent of $b = 0.66$ (Rubner 1883) has traditionally been associated with heat loss in endothermic birds and mammals: as heat loss through the organisms' external surface area, which generally scales at $b = 0.66$ with body mass, the production of heat through metabolism would have the same scaling. A scaling exponent of $b = 0.75$ is another commonly assumed value. It was first suggested by Kleiber (1932) who observed that scaling in mammals was closer to $b = 0.75$ than $b = 0.66$. It is best known today through the work of West et al. (1997) who have provided a theoretical basis for this particular scaling exponent. The model of West et al. (1997) purports to explain both interspecific* and intraspecific metabolic scaling. It is based on space filling fractal distribution networks, i.e. circulatory and respiratory systems. More recently a temperature dependence of biochemical reactions, in the form of the Boltzmann factor (Gillooly et al. 2001), has been added to this model.

Epipelagic macro-zooplankton are an extremely diverse group of organisms with members across seven phyla. The results of this search for interspecific and intraspecific patterns within the epipelagic macro-zooplankton will allow metabolic scaling within and between species to be tested and determine if it scales at $b = 0.75$. It is worth noting that some of the phyla with members among the epipelagic macro-zooplankton do not have internal respiratory or circulatory systems but rely on diffusion, e.g. cnidarians, ctenophores, and chaetognaths, or open circulatory systems, e.g. molluscs and crustacea. The deviation from $b = 0.75$ in interspecific and/or intraspecific metabolic scaling exponents is examined along with and some of the existing theories that might explain metabolic scaling. The scaling of metabolic

*The term interspecific literally means between species. Later in the chapter results are presented for intra-group metabolic scaling exponents. Intra-group relationships are drawn across species within the same taxonomic group, e.g. euphausiids, chaetognaths or salps. By definition interspecific also covers intra-group as they are also concerned with between species relationships.

rate with temperature is examined and the temperature dependence theory proposed by Gillooly et al. (2001) is tested.

2.3 METHODS

An extensive literature search was carried out for data relating to the respiration rate of marine epipelagic macro-zooplankton. Approximately seventy papers relating to respiration in macro-zooplankton were found. There are a number of studies that contributed many data points for particular species, e.g. Thill (1937), Paranjape (1967), Small & Hebard (1967), Rakusa-Suszczewski & Klekowski (1973), Svetlichny et al. (2004), and others that contributed many data points for a variety of species, e.g. Ikeda (1974), Larson (1987) and Biggs (1982). The information extracted was used to create a comprehensive data set that included: species name, body mass, body mass conversion factors to allow for conversion to wet, dry, and carbon equivalents, respiration rate, and temperature. Previous syntheses often included data on meso-zooplankton which was removed to create a strictly macro-zooplankton data set. Experimental method and geographic location, where provided, were also included. If data did not exist in a tabular form it was digitised from suitable graphs in the original papers.

Only data for macro-zooplankton species identified as epipelagic found within the top 200 metres of the ocean were considered. Data were excluded when: 1) temperature deviated during an experiment by 2°C or more, 2) there was major uncertainty over experimental procedures, e.g. the activity level of the animal was unknown or there may have been a systematic error in the data for a variety of species in a single study, i.e. Biggs (1977) where although the slope of the relationship between respiration rate and body mass was similar to those reported in other studies the intercept was two orders of magnitude higher, and 3) if active or feeding respiration was measured rather than routine respiration. If several methods had been used to determine respiration for a single species, the data which was most representative of the in situ environment, e.g. experiments that were carried out soon after capture were preferred to experiments where animals were held for a prolonged period before experimentation, was used. All data were converted to a wet, dry, and carbon equivalents. For conversions there was a

preference for species-specific data when it could be found. There was a limited use of genus-specific and group-specific conversions for mass. They were used in the absence of reported species-specific data. There was a preference for proportional mass-type conversion data e.g., in *Aurelia aurita* carbon mass is 0.16% of wet mass (Larson 1986), with a limited use of mass-types calculated from regressions relating different mass types or mass and length. The complete respiration data set, and a supplementary data set of mass conversions compiled during data synthesis and used in this chapter (Moriarty 2009) can be found online at <http://doi.pangaea.de/10.1594/PANGAEA.718139> the Publishing Network for Geoscientific & Environmental Data (PANGAEA).

A general linear model (GLM) was used to examine the effect of body mass and temperature on respiration of the form:

$$\log_{10} R = a + b \log_{10} [BM] + c [T] \quad (2.1)$$

where R is respiration rate (mg C individual⁻¹ day⁻¹), BM is body mass (mg ind⁻¹), and T is temperature (°C). A GLM was also used to examine the effect of the interaction between body mass and temperature on respiration of the form:

$$\log_{10} R = a + b \log_{10} [BM] + c [T] + b \log_{10} [BM] \cdot c [T] \quad (2.2)$$

The entire data set (n=1988) was used to determine the coefficients a , b , and c for the three different body mass types (wet mass, dry mass and carbon mass). To analyse metabolic scaling for different types of body mass, temperature was adjusted to 15°C using a Q_{10} of 2.14 as calculated from Equation 2.1 above. A similar GLM to Equation 2.1 was used to investigate the effect of carbon mass and temperature on specific respiration rate in carbon (mg C mg C⁻¹ d⁻¹ or d⁻¹) and the relationship between specific respiration (carbon, d⁻¹) and body mass in carbon.

To investigate the relationship between respiration rate and carbon mass on an interspecific level, respiration rate and carbon mass were both log transformed (\log_{10}) before analysis. Within species regression was carried out for individual species where the number of data points (n) was greater than three and there was a range of body mass (Table 2.6). To

investigate the relationship between respiration rate and temperature, respiration rate was log transformed (\log_{10}) before analysis. For interspecific analysis of respiration and carbon mass (or temperature) each species was reduced to a single data point. Representing each species by a single data point allows each species the same effect on the fit regardless of how many measurements of respiration rate have been taken for that species. Species regressions for respiration rate and carbon mass (or temperature) were used to predict respiration rate at a carbon mass (or temperature) representative of that species. Where the number of data points for a species was low ($n \leq 3$), carbon mass or temperature were constant, no regression was performed and mean values of respiration rate, carbon mass and temperature were calculated. All interspecific, intra-group and intraspecific respiration rates and body masses are expressed in terms of carbon.

To analyse the effect of temperature on respiration rate, body mass was corrected to a value of 500 mg. This means extrapolation outside the body mass range of some of the species. In an effort to minimise the error associated with extrapolation a correction calculated from the relationship between respiration rate, body mass and temperature for the entire data set ($n=1988$) was applied. In the preliminary analysis of the intraspecific data each species was corrected for body mass using species-specific relationships and tested if the slopes of the entire data set and species-specific corrections were different. In the majority of cases the slopes were not significantly different at $P \leq 0.05$.

Multiple comparisons are made on group and species data. The more statistical tests that are performed on a set of data it is more likely that the null hypothesis may be rejected when it is in fact true. This is known as a 'Type I' error. To avoid making this type of error the Bonferonni correction has been applied where more than one test has been carried out. Applying this correction results in a more stringent test of significance. This means that a significance test is only considered significant if the associated probability is smaller than:

$$\alpha [PT] = \alpha [PF] / C \quad (2.3)$$

where α [PT] is the probability of making a ‘Type I’ error when dealing with a specific test, it is also known as test-wise significance level, α [PF] is the probability of making a ‘Type I’ error when dealing with a suite of tests, it is also known as experiment-wise significance level, and C is the number of statistical tests carried out on a set of data. Although the risk of making a ‘Type I’ error is reduced the risk of making a ‘Type II’ error, where it is more likely that the null hypothesis may be accepted when it is in fact false, is increased. In this instance it is more important to avoid making a ‘Type I’ error which in which we reject the null hypothesis when it is in fact true than avoiding a ‘Type II’ error. It is better to remove the chance of significant results based on rare events that are more likely to be detected when multiple comparisons are carried out than the inclusion of these events which are not a true representation of the population at large.

2.4 RESULTS

2.4.1 GENERAL PATTERNS

The data synthesis produced 1988 data points for respiration rate in marine epipelagic macro-zooplankton. The data included 19 groups and 139 species. The data set consisted of respiration rate data for euphausiids ($n = 527$, where n equals the number of data points), scyphomedusae ($n = 407$), hydromedusae ($n = 240$), ctenophores ($n = 238$), amphipods ($n = 203$), chaetognaths ($n = 101$), appendicularia ($n = 64$), thaliacea ($n = 44$), trachymedusae ($n = 29$), decapods ($n = 28$), limnomedusae ($n = 23$), naked pteropods ($n = 36$), shelled pteropods ($n = 16$), siphonophores ($n = 7$), pelagic polychaetes ($n = 7$), mysids ($n = 7$), heteropods ($n = 6$), stomatopods ($n = 4$) and pelagic gastropods ($n = 1$). Body mass covers nine orders of magnitude from 20 ng C ind^{-1} to $4.44 \text{ g C ind}^{-1}$ (larval and juvenile individuals $< 2000 \mu\text{m}$ were included as macro-zooplankton if adult members of the species were large enough to be defined as macro-zooplankton). Temperature of incubations ranged from -1.7 to 30°C . Respiration rates uncorrected for mass and temperature ranged from $11 \text{ ng C ind}^{-1} \text{ d}^{-1}$ in the ctenophore *Beroë ovata* to $522 \text{ mg C ind}^{-1} \text{ d}^{-1}$ in the scyphomedusae *Stomolophus meleagris*. Specific respiration (carbon) uncorrected for mass and temperature ranged from $940 \text{ ng C mg C}^{-1} \text{ d}^{-1}$ in the

scyphozoan *Aequorea victoria* to $5.77 \text{ mg C mg C}^{-1} \text{ d}^{-1}$ in the amphipod *Synopia ultramarine*. From the coefficients calculated using the GLM in Equation 1 (Table 2.1) a Q_{10} of 2.14 was calculated. Including an interaction term (Equation 2) in the equation did not increase the predictability of respiration rate from body mass and temperature.

Table 2.1: The relationship between respiration rate, body mass (BM, mg ind^{-1}) and temperature (T, $^{\circ}\text{C}$) presented for this study and Ikeda's (1985) study of epipelagic zooplankton. Note: the GLM used in this study was used on \log_{10} transformed data whereas the regression analysis carried out in Ikeda (1985) used \ln transformed data.

$\log[R] = a + b \log[BM] + c [T]$			Q_{10}	r^2	n	
a	b	c				
-1.75	0.82	0.033	2.14	0.92	1988	this study
0.53	0.83	0.064	1.89	0.93	721	Ikeda (1985)

Respiration rates were corrected to 15°C to remove the effects of temperature and examine the effect of body mass on respiration rates. The three panels in Figure 2.1 show a decrease in the scatter in the data from wet (top) to dry (middle) to carbon mass (bottom). Within the scatter, particularly in the top panel (see circles in Figure 2.1) it is possible to see three distinct branches within the data. Branch A is made up of data points from the two appendicularian species in the data set. Branch B is predominantly made up of crustacean data but also contains data on chaetognaths, pelagic molluscs, pelagic polychaetes and a small portion of data from ctenophores ($n = 3$ data points) and salps ($n = 2$ data points). Branch C is predominantly made up of ctenophore, salp and cnidarians data with some overlap with branches A and B. As body mass type changes these branches become less apparent, as seen in dry mass (middle), and are not apparent when body mass is expressed in units of carbon (bottom).

Table 2.2: Regression analysis of respiration rate (R, $\text{mg C ind}^{-1} \text{ d}^{-1}$) and body mass (BM, mg ind^{-1}), the correlation coefficient (r^2) and minimum and maximum body mass for each mass type. Temperature is corrected to 15°C using a Q_{10} of 2.14

	log ₁₀ [R] vs. log ₁₀ [BM]				Mass range (mg)		n
	Intercept	Slope	r ²	P	Min. x10 ⁻³	Max. x10 ³	
Wet mass	-2.30	0.60	0.70	0.0001	22.00	954	1988
Dry mass	-1.78	0.71	0.85	0.0001	0.53	41.5	1988
Carbon	-1.26	0.82	0.92	0.0001	0.02	4440	1988

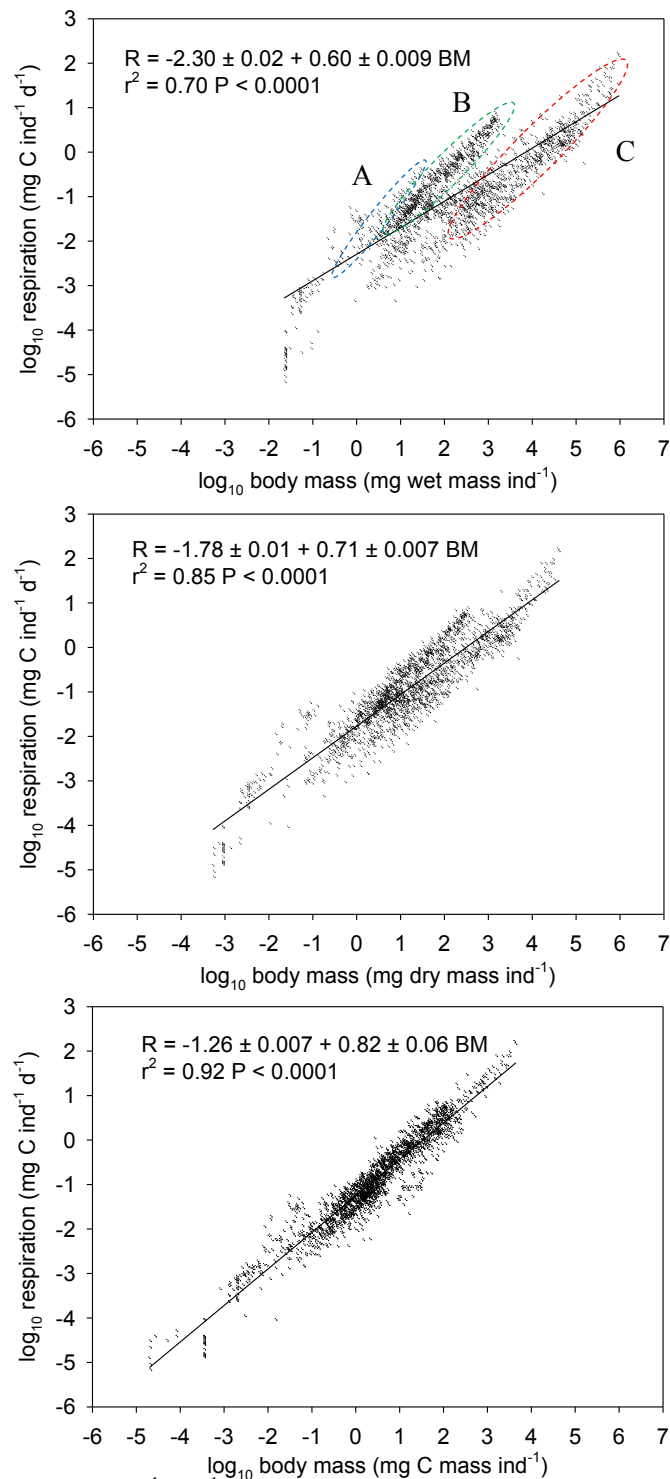


Figure 2.1: Respiration rate (mg C ind⁻¹ day⁻¹) of marine epipelagic macro-zooplankton against body mass (mg ind⁻¹): wet mass [top], dry mass [middle] and carbon mass [bottom]. Symbols: A is appendicularian spur (barely visible), B is the crustacean spur and C is the gelatinous spur. Temperature is corrected to 15°C using a Q_{10} of 2.14 see Table 2.1 for regression analysis.

Regression analysis of respiration rate (mg C ind⁻¹ d⁻¹) and body mass, over the entire data set (n=1988), for three different body mass types, wet, dry, and carbon mass (Table 2.2)

revealed an increase in metabolic scaling exponent from 0.60 to 0.82 across mass types from wet mass to carbon mass. The correlation coefficient (r^2) also increased across mass types. In each instance the relationship was highly significant ($P \leq 0.0001$). Analysis of carbon-specific respiration rate (d^{-1}) and body mass ($mg\ C\ ind^{-1}$) revealed similar rates of carbon-specific respiration in macro-zooplankton of similar carbon mass (Table 1.3 and Figure 2.2).

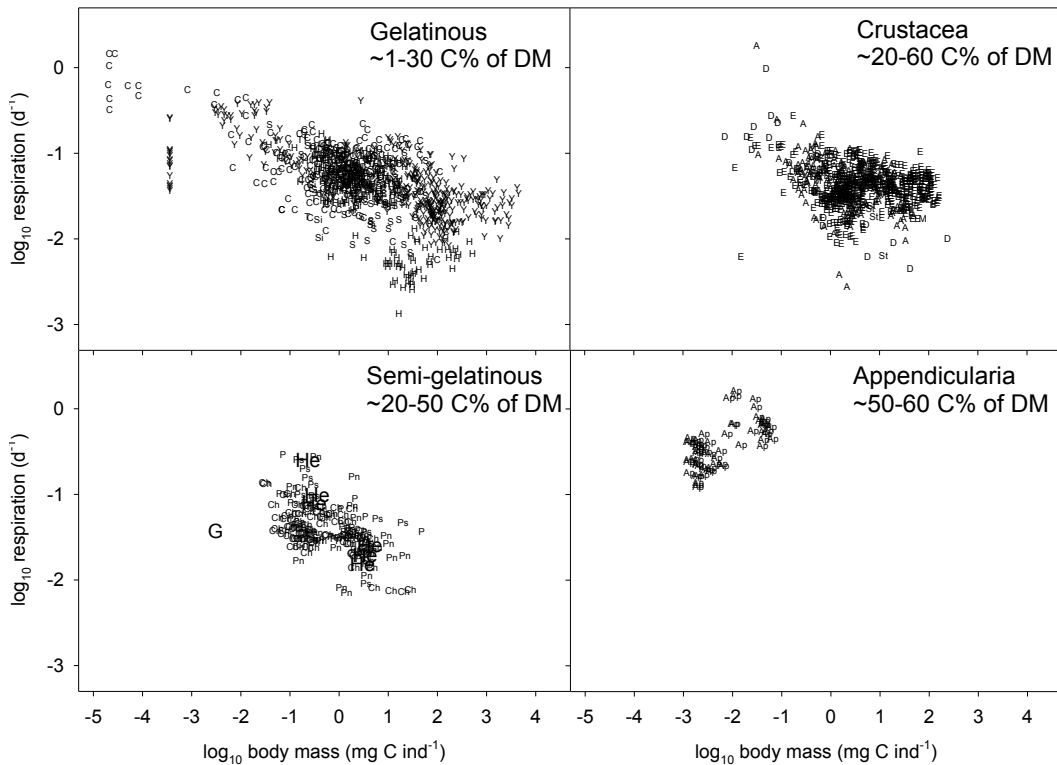


Figure 2.2: Carbon-specific respiration (d^{-1}) rates of different marine epipelagic macro-zooplankton against body mass ($mg\ C\ ind^{-1}$). The data set was separated into four according to the mean carbon as a percentage dry mass in each group, see Table 1.3. Rates were corrected to $15^{\circ}C$ using a Q_{10} of 2.14.

Symbols: ctenophores (C), salps (S), scyphomedusae (Y), limnomedusae (L), trachymedusae (T), hydromedusae (H), siphonophores (Si), gastropod molluscs (G), heteropod molluscs (He), shelled pteropods (Ps), naked pteropods (Pn), polychaetes (P), chaetognaths (Ch), amphipods (A), stomatopoda (St), decapods (D), mysids (M), euphausiids (E), appendicularians (Ap).

2.4.2 INTERSPECIFIC RESPIRATION

Analysis of interspecific metabolic scaling exponents reveal an allometric relationship where $b = 0.70 \pm 0.03$, $r^2 = 0.77$) between respiration rate and body mass across species (Figure 2.3).

Similar analysis of the relationship between respiration rate and temperature revealed a Q_{10} of 1.94 across species (Figure 2.4). Both relationships are significant ($P = 0.0001$). When the metabolic scaling exponent from this analysis to previously published values, $b = 0.66$, 0.75 , 0.90 and 1.0 , are compared it is not significantly different, to $b = 0.66$, at $P \leq 0.05$, but it is

significantly different from both $b = 0.75$, 0.90 and 1.0 at $P \leq 0.05$. Significant differences were determined using a t -test.

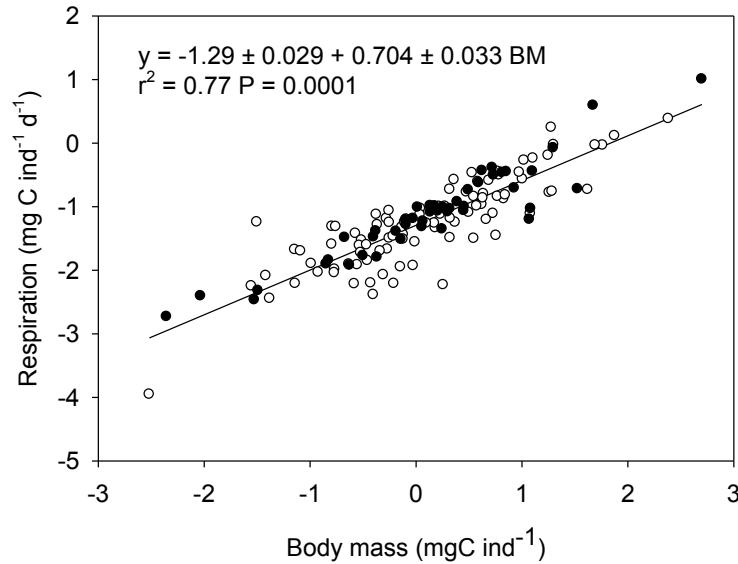


Figure 2.3: Regression of interspecific respiration rate (mg C ind⁻¹ d⁻¹) against temperature (°C). A regression was fit to all data points, each originally calculated to represent an individual species. Symbols: data points calculated using regression and mid-point body mass to predict respiration (●) and data points calculated using within species mean body mass and mean within species respiration rate (○).

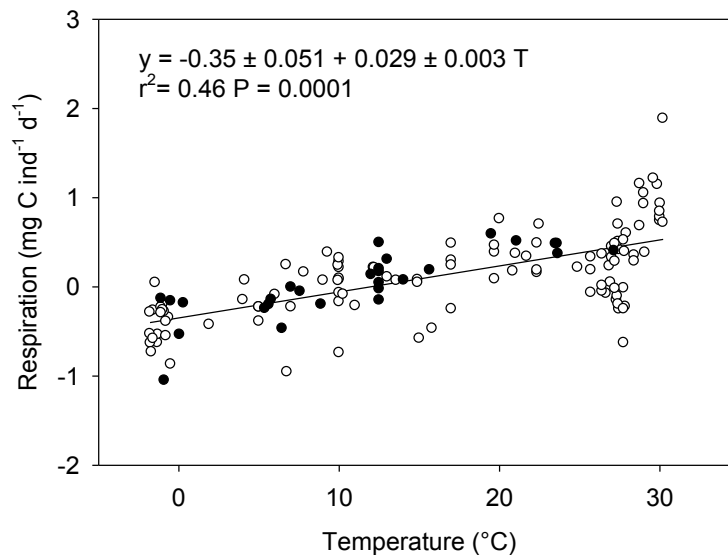


Figure 2.4: Regression of interspecific respiration rate (mg C ind⁻¹ d⁻¹) against temperature (°C). A regression was fit to all data points, each originally calculated to represent an individual species. Symbols: data points calculated using regression and mid-point temperature to predict respiration (●) and data points calculated using intraspecific mean temperature and mean intraspecific respiration rate (○).

2.4.3 INTRA-GROUP RESPIRATION

Table 2.3: Results of intra-group (interspecific) regressions using the species midpoint. n = number of species per group, P = significance, bold = significant at $P \leq 0.025$ (after application of Bonferroni correction), r^2 = the correlation coefficient, -- = no data, mass is measured in mg C ind^{-1} .

Group	n	log ₁₀ R vs. log ₁₀ [BM]			Mass range (mg C ind ⁻¹)			Temp. range (°C)						
		Intercept	Slope	r ²	P	Min.	Max.	Mean	Q ₁₀	r ²	P	Min.	Max.	Mean
Ctenophores	9	-1.14	0.77	0.95	1E-04	0.03	58	2.3	2.23	0.77	0.002	-1.6	23.5	10.42
Thaliacea	9	-1.24	0.67	0.81	0.001	0.038	19	1.6	1.66	0.47	0.042	-1.47	29	18.55
Scyphomedusae	3	-1.13	0.86	0.96	0.125	0.65	500	25	1.65	0.53	0.482	12.5	30	19.38
Limnomedusae	2	--	--	--	--	5.3	7.1	6.1	--	--	--	10	10	10.00
Trachymedusae	2	--	--	--	--	0.26	0.94	0.5	--	--	--	5.6	26.9	16.30
Hydromedusae	9	-1.3	0.41	0.68	0.007	0.15	34	1.9	2.25	0.07	0.506	10	17	12.17
Siphonophores	5	-1.67	1.05	0.88	0.018	0.28	5.9	0.89	1.73	0.63	0.109	-1.77	27.45	21.24
Gastropod molluscs	1	--	--	--	--	0.003	0.003	0.003	--	--	--	15.8	15.8	15.80
Heteropod molluscs	3	-1.27	0.35	0.78	0.31	0.27	4.2	1.2	6.66	0.68	0.384	22.35	30.03	26.93
Pteropods (shelled)	8	-1.27	0.68	0.75	0.005	0.14	20	1.6	1.57	0.47	0.06	-1.1	30	16.27
Pteropods (naked)	6	-1.39	0.8	0.51	0.111	0.42	10	1.8	1.25	0.09	0.559	-1.3	27.85	8.65
Polychaetes	6	-1.13	0.68	0.82	0.013	0.072	13	0.92	2.06	0.71	0.036	-0.9	30.2	19.18
Chaetognaths	7	-1.55	0.55	0.92	0.001	0.042	12	0.41	2.79	0.90	0.001	-0.9	29.07	18.74
Amphipods	25	-1.23	0.6	0.51	1E-04	0.031	49	1.3	2.12	0.45	0.0001	-1.8	30.2	12.31
Stomatopods	2	--	--	--	--	7	12	9.2	--	--	--	27.2	27.4	27.30
Decapods	18	-1.4	0.57	0.8	1E-04	0.028	240	1.1	2.4	0.43	0.003	-1.7	30	20.19
Mysids	5	-1.21	0.69	0.96	0.003	0.43	75	1.8	2.22	0.82	0.034	-1.6	27.75	12.19
Euphausiids	17	-1.22	0.75	0.82	1E-04	0.1	18	1.6	2.29	0.71	0.0001	-1.1	28.75	12.62
Appendicularians	2	--	--	--	--	0.0044	0.0093	0.0064	--	--	--	19.5	20	19.75

Using the mid-point and mean values of within species respiration rate and body mass and temperature regressions are fit to describe the metabolic scaling exponent and temperature dependence of each group, e.g. ctenophores, gastropod molluscs, chaetognaths and appendicularians. The relationship between respiration rate and body mass and the temperature dependence of intra-group respiration in macro-zooplankton are presented in Table 2.3. Body mass ranges within each group range from less than one to three orders of magnitude. The temperature range for most groups is $\geq 20^{\circ}\text{C}$, data on respiration rate in the scyphomedusae, heteropod molluscs and hydromedusae were lower with a range of 17°C , 8°C and 7°C respectively. In four groups, the limnomedusae, gastropod molluscs, stomatopods and appendicularians, data were limited and respiration rate was only recorded at one temperature. Where the number of data points was less than or equal to three the data was not fit with the model for either the relationship between respiration rate and body mass or temperature.

Table 2.4: Results of analysis of differences between the scaling exponent of respiration rate with mass and 0.66, 0.75, 0.90 and 1.0 for each of the groups where a linear regression through species mid-points was preformed. Notes: bold = b is significant at $P \leq 0.0125$ (after application of the Bonferonni correction) and NS = difference from b is not significant.

Group	n	b	Stdev.	0.66	0.75	0.90	1.00
				P	P	P	P
Ctenophores	9	0.77	0.06	NS	NS	NS	0.01
Thaliacea	9	0.67	0.12	NS	NS	NS	0.01
Hydromedusae	9	0.41	0.11	0.002	0.002	0.001	0.002
Siphonophores	5	1.05	0.22	NS	NS	NS	NS
Pteropods (shelled)	8	0.68	0.16	NS	NS	NS	NS
Polychaetes	6	0.69	0.16	NS	NS	NS	NS
Chaetognaths	7	0.55	0.07	NS	0.01	NS	0.002
Amphipods	25	0.60	0.12	NS	NS	0.001	0.002
Decapods	18	0.57	0.07	NS	0.002	0.001	0.002
Mysids	5	0.69	0.08	NS	NS	0.001	0.01
Euphausiids	17	0.75	0.09	NS	NS	NS	0.01

Regression analysis was carried out for the relationship between respiration rate and body mass for 19 groups and respiration rate and temperature for 14 groups. For the relationship with body mass, 11 of these relationships were significant ($P \leq 0.025$, after application of Bonferonni correction), whilst for the relationship with temperature, 5 were significant ($P \leq 0.025$, after application of Bonferonni correction). Metabolic scaling exponents in these groups

ranged from 0.41 in the hydromedusae to 1.05 in the siphonophores. Q_{10} values range from 1.27 in the naked pteropods to 2.8 in chaetognaths in those species where the regression relationship proved statistically significant. Further analysis of intra-group metabolic scaling reveals that fewer scaling exponents are significantly different from $b=0.66$ (9%) than $b=0.75$ (27%), $b=0.90$ (36%) and $b=1.0$ (72%) at $P \leq 0.0125$, after application of Bonferonni correction.

2.4.4 INTRASPECIFIC RESPIRATION

The relationship between intraspecific respiration rate, body mass and temperature is presented in Table 2.5. Body mass ranged between less than one and seven orders of magnitude, the majority of species only ranging across one to two orders of magnitude. Overall within species respiration rate temperature ranges were much lower than between species temperature ranges. Typical within species temperature ranges are $\geq 5^{\circ}\text{C}$ but many species had very narrow temperature ranges of less than 3°C . Only one species *Clione sp.* had a temperature range of $\sim 30^{\circ}\text{C}$ unfortunately the number of respiration data points for this species was only three. Where $n \leq 3$ the data was not fit with the model for either the relationship between respiration rate and body mass or respiration rate and temperature. Similarly, if body mass or temperature was the same for all respiration data within a species then no relationship could be fit because of insufficient data relating to either body mass or temperature. A relationship between respiration rate and body mass was determined for 49 species of which 38 were significant ($P \leq 0.025$, after application of Bonferonni correction). It was possible to determine a Q_{10} for 28 species of which 16 were significant ($P \leq 0.025$, after application of Bonferonni correction), only 14 where temperature range was $\geq 5^{\circ}\text{C}$.

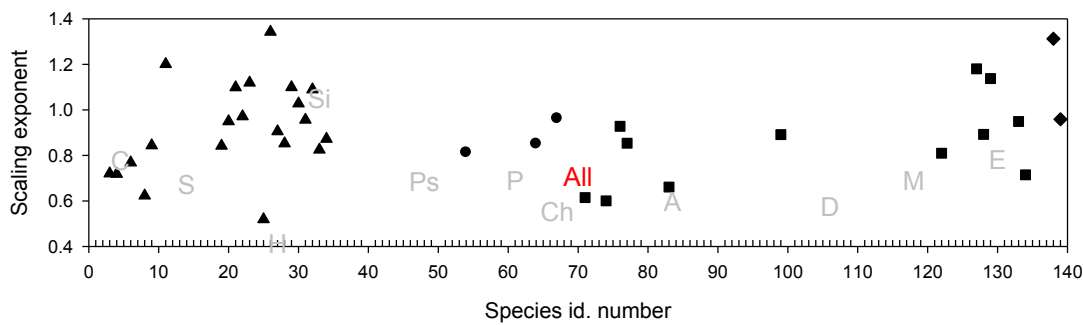
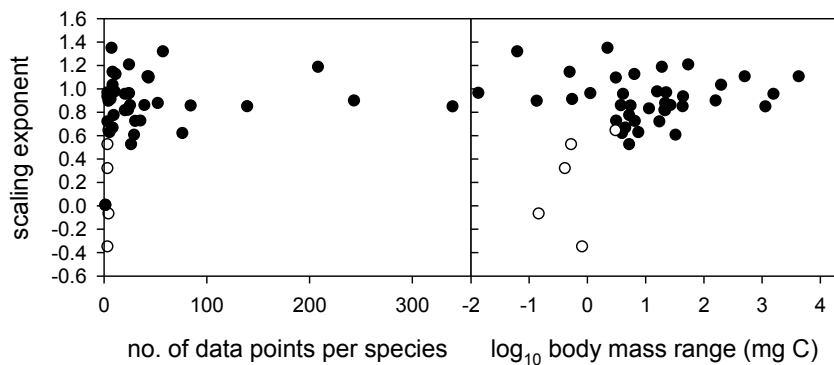


Figure 2.5: Intraspecific and intra-group and interspecific respiration to body mass scaling exponents for marine epipelagic macro-zooplankton. Symbols: gelatinous (▲), semi-gelatinous (●), crustacean (■) and appendicularians (◆). For species id number see Table 2.5. Symbols in grey: ctenophores (C), salps (S), hydromedusae (H), siphonophores (Si), heteropod molluscs (He), shelled pteropods (Ps), polychaetes (P), chaetognaths (Ch), amphipods (A), decapods (D), mysids (M) and euphausiids (E) see Table 2.4. Interspecific metabolic scaling exponent is represented by All in red see Figure 2.3. Note: only scaling exponents significant at ($P \leq 0.025$, after application of Bonferonni correction) are shown.



Figure

2.6: Intraspecific metabolic scaling exponents expressed against sample size and \log_{10} body mass range (mg C) for marine epipelagic macro-zooplankton. Symbols: scaling exponents significant at $P \leq 0.025$ (after application of Bonferonni correction) (●) and non-significant scaling exponents (○).

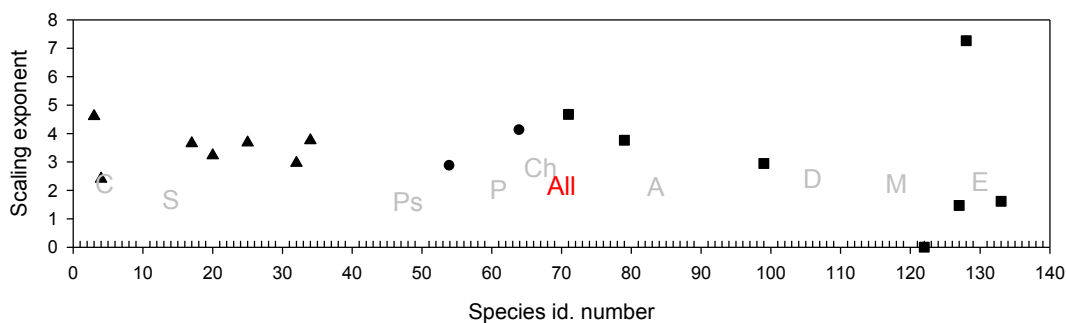


Figure 2.7: Intraspecific and intra-group and interspecific respiration Q_{10} s for marine epipelagic macro-zooplankton. Symbols and notes: as in Figure 2.3.

Metabolic scaling exponents ($P \leq 0.025$, after application of Bonferonni correction) ranged from 0.52 in *Aglantha digitale* ($n = 27$, $r^2 = 0.82$, $P = 0.0001$) and 1.34 in *Sarsia princeps* ($n = 8$, $r^2 = 0.93$, $P = 0.0001$). There is a general trend within the intraspecific respiration data for

the metabolic scaling exponents with the highest number of data points (> 80) to converge between ~ 0.8 and ~ 1.2 (Figure 2.5). There is a trend in the body mass data but only for the data sets with the largest number of data points (Figure 2.5). Q_{10} ranged from 1.62 ($n = 21$, $r^2 = 0.58$, $P = 0.0001$) in *Thysanoessa spp.* to 4.61 ($n = 36$, $r^2 = 0.70$, $P = 0.0001$) in *Pleurobrachia brachei*. Metabolic scaling exponents and Q_{10} s are summarised by species in Figures 2.3 and 2.4. I investigate if epipelagic macro-zooplankton have a higher metabolic scaling exponent than would be predicted by the $b = 0.66$ or $b = 0.75$ metabolic scaling exponents. I tested them against four different values for $b = 0.66$, 0.75 , 0.90 and 1.0 . Further analysis of intraspecific metabolic scaling reveals that fewer scaling exponents are significantly different from $b = 0.90$ (33%), than $b = 0.75$ (38%), $b = 1.0$ (43%) and $b = 0.66$ (48%) at $P \leq 0.0125$ (after application of Bonferonni correction) (Table 2.6).

Table 2.5. Results of regression analysis of relationship between respiration rate ($\text{mg C ind}^{-1} \text{ d}^{-1}$) and body mass (mg C ind^{-1}) in 139 marine epipelagic macro-zooplankton species, where $n < 4$, n = number of species per group, **bold** = significant at $P \leq 0.05$, r^2 = the correlation coefficient, P = significance, NS = difference is not significant, -- = no data, mass is measured in mg C ind^{-1}

Group	Id.	Species	n	log ₁₀ R vs. log ₁₀ [BM]			Mass (mg C ind ⁻¹)			Temp (°C)			Original Reference				
				Intercept	Slope	r ²	P	Min.	Max.	Mean	Q ₁₀	r ²		P	Min.	Max.	Mean
Ctenophores	1	<i>Mertensiidae</i> sp.	1	--	--	--	--	--	--	10	--	--	--	--	-1.6	16	
	2	<i>Hormiphora palmate</i>	1	--	--	--	--	--	--	2.3	--	--	--	--	6.7	11	
	3	<i>Pleurobrachia bachei</i>	36	-1.14	0.72	0.69	0.0001	0.19	3.4	1	4.61	0.70	0.0001	10	15	12.5	25
	4	<i>Pleurobrachia pileus</i>	31	-1.02	0.72	0.94	0.0001	0.16	6.9	1.1	2.41	0.90	0.0001	2	24	12.27	9, 12
	5	<i>Bolinopsis infundibulum</i>	10	-0.78	0.54	0.43	0.04	3	130	29	--	--	--	--	--	6	1
	6	<i>Mnemiopsis mcecradyi</i>	10	-1.21	0.77	0.97	0.0001	0.55	5.9	1.8	--	--	--	--	--	21	23
	7	<i>Beroë</i> sp.	3	--	--	--	--	36	150	58	--	--	--	-1.7	-0.8	-1.33	15, 16
Thaliacea	8	<i>Beroë cucumis</i>	6	-1.2	0.62	0.98	0.0001	0.32	8	1.9	6.01	0.31	0.248	12.7	15.35	14.81	12
	9	<i>Beroë ovata</i>	140	-1.18	0.84	0.93	0.0001	0.00002	44	0.39	1.8	0.04	0.025	21	26	23.21	5, 37
	10	<i>Pyrosoma verticillatum</i>	2	--	--	--	--	4.5	10	6.8	--	--	--	--	--	25.7	12
	11	<i>Cyclosalpa bakeri</i>	25	-1.82	1.2	0.9	0.0001	1.3	57	8.3	--	--	--	--	--	11	27
	12	<i>Iasia zonaria</i>	1	--	--	--	--	--	--	0.76	--	--	--	--	--	27	12
	13	<i>Ihleia recovitzai</i>	1	--	--	--	--	--	--	1.1	--	--	--	--	--	-1	15
	14	<i>Pegea confederata</i>	3	--	--	--	--	10	28	18	--	--	--	--	--	25.7	12
Scyphomedusae	15	<i>Salpa fusiformis</i>	4	-1.19	0.52	0.39	0.379	0.23	0.77	0.53	--	--	--	--	--	27.4	12
	16	<i>Salpa thompsoni</i>	3	--	--	--	--	5.4	58	19	--	--	--	-1.7	-1.1	-1.47	15, 16
	17	<i>Thalia democratica</i> (sol.)	4	-1.62	0.31	0.34	0.415	0.17	0.59	0.35	3.66	0.97	0.013	17.3	30	20.48	11, 12
	18	<i>Thalia democratica</i> (col.)	1	--	--	--	--	--	--	0.038	--	--	--	--	--	29	11
	19	<i>Aurelia aurita</i>	340	-1.23	0.84	0.97	0.0001	0.00036	1200	5.5	1.15	0.00	0.214	10	21.3	15.25	6, 21, 25, 28, 34, 38, 39
	20	<i>Cyanea capillata</i>	24	-1	0.95	0.96	0.0001	1.4	1600	18	3.23	0.33	0.003	10	15	11.46	25
	21	<i>Stomolophus meleagris</i>	43	-1.96	1.1	0.93	0.0001	56	4400	850	--	--	--	--	--	30	25
Limnomedusae	22	<i>Eperemus typus</i>	11	-1.28	0.97	0.75	0.0001	2.7	19	7.2	--	--	--	--	--	10	25
	23	<i>Gonionemus vertens</i>	12	-1.19	1.12	0.85	0.0001	2.9	9.5	4	--	--	--	--	--	10	25
Trachymedusae	24	<i>Liriope tetryphylla</i>	2	--	--	--	--	0.22	0.31	0.26	--	--	--	26.85	27	26.93	25
	25	<i>Aglantha digitale</i>	27	-1.18	0.52	0.82	0.0001	0.16	5.5	1.2	3.68	0.33	0.002	1.1	10.15	9.39	11, 12, 14, 25

6, 21, 25, 28, 34, 38, 39

25

Table 2.5: [continued]

Group	Id.	Species	n	log ₁₀ R vs. log ₁₀ [BM]				Mass (mg C ind ⁻¹)			Temp (°C)			Original Reference			
				Intercept	Slope	r ²	P	Min.	Max.	Mean	Q ₁₀	r ²	P		Min.	Max.	Mean
Hydromedusae	26	<i>Sarsia princeps</i>	8	-1.39	1.34	0.93	0.0001	0.47	2.8	0.98	--	--	--	--	10	24	
	27	<i>Sarsia tubulosa</i>	7	-1.1	0.91	0.97	0.0001	0.037	0.6	0.16	--	--	--	--	17	28	
	28	<i>Stomatoca atra</i>	26	-1.34	0.85	0.57	0.0001	0.85	4.7	1.8	1.58	0.12	0.085	10	15	12.12	25
Siphonophores	29	<i>Aequorea victoria</i>	44	-2.4	1.1	0.87	0.0001	2.2	520	35	--	--	--	--	--	10	25
	30	<i>Aequorea vitrina</i>	9	-2.3	1.03	0.96	0.0001	0.68	200	39	--	--	--	--	--	15	28
	31	<i>Clytia lomae</i> *	25	-1.1	0.96	0.68	0.0001	0.12	1.3	0.5	--	--	--	--	--	10	25
	32	<i>Clytia gregaria</i> *	44	-1.3	1.09	0.77	0.0001	0.38	3.6	1.3	2.97	0.36	0.0001	10	15	12.16	25
	33	<i>Eutonia indicans</i>	24	-1.3	0.83	0.87	0.0001	0.36	12	2.7	--	--	--	--	--	10	25
	34	<i>Mitrocoma cellularia</i>	53	-1.17	0.87	0.8	0.0001	0.43	23	6	3.76	0.39	0.0001	10	15	11.89	25
	35	<i>Ceratocymba leuckartii</i> *	1	--	--	--	--	--	--	0.4	--	--	--	--	--	27.45	12
	36	<i>Crystallonia</i> sp.	1	--	--	--	--	--	--	2.3	--	--	--	--	--	26.85	12
	37	<i>Diphyes</i> sp.	1	--	--	--	--	--	--	0.28	--	--	--	--	--	27	12
	38	<i>Diphyes antaretica</i>	3	--	--	--	--	4.5	9.4	5.9	--	--	--	-1.8	-1.7	-1.77	16
Gastropods	39	<i>Diphyes dispar</i>	1	--	--	--	--	--	--	0.37	--	--	--	--	--	26.65	12
	40	Veliger larva	1	--	--	--	--	--	--	0.003	--	--	--	--	--	15.8	12
Heteropoda	41	<i>Cardiapoda sublaevis</i>	3	--	--	--	--	0.36	3.4	1.5	--	--	--	--	--	28.4	12
	42	<i>Firoloida desmaresti</i>	2	--	--	--	--	0.23	0.31	0.27	--	--	--	29.85	30.2	30.03	11
Pteropods (shelled)	43	<i>Oxygyrus keraudreni</i>	1	--	--	--	--	4.2	4.2	4.2	--	--	--	--	--	22.35	12
	44	<i>Cavolinia gobulosa</i>	2	--	--	--	--	2.8	3.6	3.2	--	--	--	22.35	27.4	24.88	12
	45	<i>Cavolinia uncinata</i>	1	--	--	--	--	--	--	3.8	--	--	--	--	--	19.7	12
	46	<i>Cleodora sulcata</i>	1	--	--	--	--	--	--	20	--	--	--	--	--	-1.1	15
	47	<i>Creseis acicula clava</i>	1	--	--	--	--	--	--	0.31	--	--	--	--	--	30	11
	48	<i>Diareea trispinosa</i>	1	--	--	--	--	--	--	3.5	--	--	--	--	--	27.3	12
	49	<i>Euclio cuspidate</i>	1	--	--	--	--	--	--	6.1	--	--	--	--	--	22.35	12
	50	<i>Limacina helicina</i>	5	-1.54	-0.07	0.003	0.934	0.15	0.3	0.21	0.001	0.70	0.076	-1	0	-0.8	2, 16

Table 2.6: [continued]

Group	Id.	Species	n	log ₁₀ R vs. log ₁₀ [BM]				Mass (mg C ind ⁻¹)				Temp (°C)				Original Reference	
				Intercept	Slope	r ²	P	Min.	Max.	Mean	Q ₁₀	r ²	P	Min.	Max.		Mean
Pteropods (naked)	51	<i>Limacina helicina helicina</i>	4	-1.21	0.82	0.95	0.026	0.069	0.29	0.14	2.91	0.88	0.062	5	10.15	7.18	11, 12
	52	<i>Clione</i> sp.	3	--	--	--	--	0.11	2	0.42	--	--	--	-1	29.9	9.3	2
	53	<i>Clione antarctica</i>	1	--	--	--	--	--	--	10	--	--	--	--	--	-1.3	15
	54	<i>Clione limacina</i>	24	-1.55	0.81	0.95	0.0001	0.14	22	1.2	2.85	0.82	0.0001	-0.1	13	8.48	4
	55	<i>Clione limacina antarctica</i> *	3	--	--	--	--	1.6	2.2	1.9	--	--	--	-0.9	-0.5	-0.63	15
	56	<i>Clione limacina limacina</i>	2	--	--	--	--	2.1	9.1	4.3	--	--	--	--	7.8	12.7	10.25
	57	<i>Hydromyles gobulosa</i>	3	--	--	--	--	0.15	1.4	0.62	--	--	--	--	27.4	28.75	27.85
Pelagic polychaetes	58	<i>Trochophora larva</i>	1	--	--	--	--	--	--	0.072	--	--	--	--	--	29.85	11
	59	<i>Lepidasthenia grimaldi</i>	1	--	--	--	--	--	--	0.29	--	--	--	--	--	30.2	11
	60	<i>Naiades cantrainii</i>	1	--	--	--	--	--	--	1.1	--	--	--	--	--	19.7	12
	61	<i>Tomopteris</i> sp.	1	--	--	--	--	--	--	0.98	--	--	--	--	--	28.4	11
	62	<i>Tomopteris carpenter</i>	2	--	--	--	--	3.4	48	13	--	--	--	-1	-0.8	-0.9	12
	63	<i>Tomopteris septentrionalis</i>	1	--	--	--	--	--	--	2.1	--	--	--	--	--	7.8	15
	64	<i>Parasagitta elegans</i>	85	-1.49	0.85	0.92	0.0001	0.032	5.7	0.48	4.11	0.60	0.0001	-1.5	12.25	-0.78	11, 12, 17, 41
Chaetognaths	65	<i>Sagitta bipunctata</i>	2	--	--	--	--	0.21	0.26	0.23	--	--	--	27.45	27.45	27.45	12
	66	<i>Flaccisagitta enflata</i> *	3	--	--	--	--	0.22	0.45	0.35	--	--	--	27.35	30	29.07	11, 12
	67	<i>Pseudosagitta gazellae</i> *	4	-2.07	0.96	1	0.0001	5.2	28	14	0	0.88	0.061	-1.1	-0.7	-0.93	18
	68	<i>Mesosagitta minima</i> *	2	--	--	--	--	0.031	0.056	0.042	--	--	--	--	--	14.9	12
	69	<i>Ferosagitta robusta</i> *	3	--	--	--	--	0.17	0.52	0.34	--	--	--	27.35	29	27.92	11, 12
	70	<i>Serratosagitta serratodentata</i> *	2	--	--	--	--	0.24	0.38	0.3	--	--	--	--	--	27.4	12
	71	<i>Paramoera walkeri</i>	77	-1.43	0.62	0.82	0.0001	0.13	4.2	0.94	4.67	0.27	0.0001	-1.9	2	0.41	22
Amphipods	72	<i>Pleustes panopla</i>	1	--	--	--	--	--	--	0.81	--	--	--	--	--	9	12
	73	<i>Synopia ultramarina</i>	1	--	--	--	--	--	--	0.031	--	--	--	--	--	30.2	11
	74	<i>Waldeckia obesa</i>	30	-1.1	0.6	0.66	0.0001	4.2	38	16	--	--	--	--	--	-1.8	31
	75	<i>Cyphocaris challangeri</i>	1	--	--	--	--	--	--	2.1	--	--	--	--	--	5	42

Table 2.5: [continued]

Group	Id.	Species	n	log ₁₀ R vs. log ₁₀ [BM]			Mass (mg C ind ⁻¹)			Temp (°C)			Original Reference				
				Intercept	Slope	r ²	P	Min.	Max.	Mean	Q ₁₀	r ²		P	Min.	Max.	Mean
	76	<i>Orchomenella</i> sp.	4	-1.19	0.93	0.98	0.008	0.64	46	3.6	--	--	--	--	-1	2	
	77	<i>Orchomene plebs</i>	40	-1.16	0.85	0.8	0.0001	1.5	29	10	--	--	--	--	-1.8	31	
	78	<i>Hyperia</i> sp.	3	--	--	--	--	0.034	0.56	0.12	--	--	--	6.7	17	13.57	11
	79	<i>Hyperia galba</i>	5	-1.35	0.64	0.67	0.09	1.7	4.8	2.9	3.76	0.91	0.012	5.6	12.15	6.91	3, 11
	80	<i>Hyperia gaudichaudii</i>	1	--	--	--	--	--	--	49	--	--	--	--	--	-0.8	15
	81	<i>Parathemisto japonica</i> *	7	-1.07	0.6	0.48	0.085	0.79	2.4	1.5	5.1	0.64	0.032	5	9	7.79	12, 42
	82	<i>Themisto libellula</i> *	3	--	--	--	--	0.28	0.98	0.53	--	--	--	-0.1	6.7	4.12	11, 17
	83	<i>Themisto gaudichaudii</i> *	9	-0.85	0.66	0.76	0.002	2.5	7.1	4.4	--	--	--	--	10	2	
	84	<i>Themisto pacifica</i>	1	--	--	--	--	--	--	0.56	--	--	--	--	--	5	42
	85	<i>Themisto compressa</i> *	3	--	--	--	--	1.5	1.7	1.7	--	--	--	--	--	4	3
	86	<i>Phronima</i> sp.	1	--	--	--	--	--	--	3	--	--	--	--	--	28.75	11
	87	<i>Phronima sedentaria</i>	4	-1.32	-0.35	0.31	0.446	0.49	1.3	0.78	0.51	0.73	0.145	19.7	27.5	23.56	12
	88	<i>Prinno abyssalis</i>	1	--	--	--	--	--	--	3.5	--	--	--	--	--	5	42
	89	<i>Brachyseelus latipes</i>	1	--	--	--	--	--	--	0.081	--	--	--	--	--	29	11
	90	<i>Thamneus platyrhynchus</i>	2	--	--	--	--	0.75	1.2	0.94	--	--	--	--	--	27.35	12
	91	<i>Streetsia porcella</i>	1	--	--	--	--	--	--	0.56	--	--	--	--	--	27.35	12
	92	<i>Hemityphis tenuimanus</i>	2	--	--	--	--	0.47	0.51	0.49	--	--	--	--	--	26.4	12
	93	<i>Viblia</i> sp.	2	--	--	--	--	1.5	2.2	1.8	--	--	--	--	--	27.75	12
	94	<i>Viblia antarctica</i>	1	--	--	--	--	--	--	4.9	--	--	--	--	--	-1.1	15
	95	<i>Scina crassicornis</i> *	2	--	--	--	--	0.5	0.58	0.54	--	--	--	--	--	22.35	12
Stomatopods	96	<i>Alima larva</i>	1	--	--	--	--	--	--	12	--	--	--	--	27.4	12	
Decapods	97	<i>Coroniderichus larva</i>	3	--	--	--	--	6.5	7.7	7	--	--	--	--	27.2	12	
	98	<i>Brachyuran megalopa larva</i>	2	--	--	--	--	0.063	0.41	0.16	--	--	--	17	27.95	22.48	11
	99	<i>Brachyuran zoea larva</i>	5	-0.99	0.89	0.89	0.015	0.0071	0.15	0.04	2.95	0.90	0.014	12.15	30	20.51	11, 12
	100	<i>Chorismus antarcticus</i>	1	--	--	--	--	--	--	240	--	--	--	--	--	-1.7	16

Table 2.6: [continued]

Group	Id.	Species	n	log ₁₀ R vs. log ₁₀ [BM]			Mass (mg C ind ⁻¹)			Temp (°C)			Original Reference				
				Intercept	Slope	r ²	P	Min.	Max.	Mean	Q ₁₀	r ²		P	Min.	Max.	Mean
Mysids	101	<i>Crangon affinis</i> juv.	1	--	--	--	--	--	--	5.4	--	--	--	--	17	11	
	102	<i>Eualus gracilirostris</i>	1	--	--	--	--	--	--	5.7	--	--	--	--	6.75	12	
	103	<i>Leptochela gracilis</i> juv.	1	--	--	--	--	--	--	0.74	--	--	--	--	17	11	
	104	<i>Lucifer typus</i>	1	--	--	--	--	--	--	0.028	--	--	--	--	17	11	
	105	<i>Lysmata</i> sp.	1	--	--	--	--	--	--	0.56	--	--	--	--	30	11	
	106	Macruran decapodid larva	1	--	--	--	--	--	--	0.17	--	--	--	--	7	12	
	107	Macruran mysis larva	2	--	--	--	--	0.025	0.21	0.073	--	--	15.4	28	21.7	11	
	108	Macruran post mysis larva	2	--	--	--	--	--	--	0.16	--	--	29	30.2	29.6	12	
	109	Megolopa A larva	2	--	--	--	--	0.71	0.72	0.72	--	--	--	--	27.75	12	
	110	Megolopa B larva	1	--	--	--	--	--	--	1.5	--	--	--	--	26.4	12	
	111	Megolopa C larva	2	--	--	--	--	2	2.2	2.1	--	--	--	--	26.4	12	
	112	<i>Penaeus</i> sp.	1	--	--	--	--	--	--	5.9	--	--	--	--	12.15	11	
	113	Phyllosoma larva	1	--	--	--	--	--	--	42	--	--	--	--	27.75	12	
	114	<i>Portunidae</i> sp.	2	--	--	--	--	0.45	0.47	0.46	--	--	--	--	27.8	12	
	115	Puerulus larva	1	--	--	--	--	--	--	19	--	--	--	--	27.2	12	
Mysids	116	<i>Antarctomysis maxima</i>	1	--	--	--	--	--	--	75	--	--	--	--	-1.6	16	
	117	<i>Siriella</i> spp.	1	--	--	--	--	--	--	0.43	--	--	--	--	9.95	12	
	118	<i>Siriella thompsoni</i>	2	--	--	--	--	0.55	0.68	0.61	--	--	--	--	27.75	12	
	119	<i>Xenacanthomysis</i> sp.*	1	--	--	--	--	--	--	0.78	--	--	--	--	9.95	12	
	120	<i>Xenacanthomysis pseudomacropsis</i> *	2	--	--	--	--	--	--	1.3	--	--	--	--	14.9	12	
Euphausiids	121	Cyrtopia larva	3	--	--	--	--	0.11	0.23	0.17	--	--	6.9	27.8	20.83	12	
	122	<i>Euphausia crystallorophias</i>	21	-1.11	0.81	0.77	0.0001	0.67	23	2.5	0	0.58	0.0001	-1.7	-0.5	-0.94	2,16,13
	123	<i>Euphausia diomedea</i>	2	--	--	--	--	1.3	2.3	1.7	--	--	--	--	27.2	12	

Table 2.5: [continued]

Group	Id.	Species	n	log ₁₀ R vs. log ₁₀ [BM]				Mass (mg C ind ⁻¹)				Temp (°C)				Original Reference	
				Intercept	Slope	r ²	P	Min.	Max.	Mean	Q ₁₀	r ²	P	Min.	Max.		Mean
Appendicularians	124	<i>Euphausia distinguenda</i>	2	--	--	--	--	--	0.6	0.96	0.76	--	--	--	--	25.7	12
	125	<i>Euphausia krohnii</i> juv.	2	--	--	--	--	--	0.098	0.11	0.1	--	--	--	--	19.7	12
	126	<i>Euphausia mutica</i>	1	--	--	--	--	--	--	--	0.18	--	--	--	--	28.75	11
	127	<i>Euphausia pacifica</i>	209	-1.54	1.18	0.8	0.0001	0.41	20	1.9	1.47	0.18	0.0001	5	20	11.12	11, 12, 29
	128	<i>Euphausia superba</i>	244	-1.21	0.89	0.94	0.0001	0.011	160	21	7.27	0.20	0.0001	-1.8	2.4	-0.11	10, 13, 14, 15, 16, 19, 20, 30, 32, 35, 36,
	129	<i>Euphausia tenera</i>	9	-1.21	1.14	0.95	0.0001	0.093	0.6	0.25	0.04	0.09	0.432	26.85	27.45	27.19	12
	130	<i>Euphausia triacantha</i>	1	--	--	--	--	--	--	9.5	--	--	--	--	--	-0.8	15
	131	<i>Meganyctiphanes norvegica</i>	1	--	--	--	--	--	--	18	--	--	--	--	--	13	33
	132	<i>Thysanoessa</i> sp.	2	--	--	--	--	3	3.9	3.4	--	--	--	--	--	10	2
	133	<i>Thysanoessa</i> spp.	21	-1.16	0.95	0.6	0.0001	0.48	4.7	1.8	1.62	0.49	0.0001	4	20	9.33	40
	134	<i>Thysanoessa inermis</i>	4	-1.2	0.72	0.98	0.009	0.33	18	1.7	2.74	0.89	0.055	0.1	11.45	6.15	11, 17
	135	<i>Thysanoessa longipes</i>	1	--	--	--	--	--	--	3.8	--	--	--	--	--	12.2	12
	136	<i>Thysanoessa macrura</i>	3	--	--	--	--	3.7	4.6	4.3	--	--	--	-0.5	6.7	1.9	13
	137	<i>Thysanoessa raschii</i>	1	--	--	--	--	--	--	4.6	--	--	--	--	--	-0.5	11
	138	<i>Oikopleura dioica</i>	58	0.26	1.31	0.94	0.0001	0.0013	0.066	0.0062	0.91	0.00	0.823	15	24	15.97	8, 26
	139	<i>Oikopleura (Coecaria) longicauda</i>	6	-0.47	0.96	0.96	0.001	0.0013	0.015	0.0045	--	0.91	--	--	--	--	7

References:¹Bailey et al. 1994, ²Biggs 1982, ³Conover 1960, ⁴Conover & Lalli 1974, ⁵Finenko et al. 2001, ⁶Frandsen & R isgaard 1997, ⁷Gorsky et al. 1984, ⁸Gorsky et al. 1987, ⁹Gyllenberg & Greve 1979, ¹⁰Ikeda 1974, ¹¹Ikeda 1974, ¹²Ikeda & Hing Fay 1981, ¹³Ikeda 1981, ¹⁴Ikeda & Mitchell 1982, ¹⁵Ikeda & Mitchell 1982, ¹⁶Ikeda & Bruce 1986, ¹⁷Ikeda & Skjoldal 1989, ¹⁸Ikeda & Kirkwood 1989b, ¹⁹Ikeda & Kirkwood 1989a, ²⁰Ishii et al. 1987, ²¹Kinoshita et al. 1997, ²²Klekowski et al. 1973, ²³Kremer 1982, ²⁴Larson 1987, ²⁵Larson 1985, ²⁶Lombard et al. 2005, ²⁷Madin & Purcell 1992, ²⁸M  ller & R isgaard 2007, ²⁹Paranjape 1967, ³⁰Rakusa-Suszczewski & Opalinski 1978, ³¹Rakusa-Suszczewski 1990a, ³²Rakusa-Suszczewski 1990b, ³³Salomon et al. 2000, ³⁴Schneider 1988, ³⁵Segawa et al. 1982, ³⁶Small & Hebard 1967, ³⁷Svetlichny et al. 2004, ³⁸Thill 1937, ³⁹Uye & Shimauchi 2005, ⁴⁰Vidal & Whitley 1982, ⁴¹Welch et al. 1996 and ⁴²Yamada & Ikeda 2003.

Table 2.6: Results of analysis of differences between the scaling exponent of respiration rate with mass 0.66, 0.75 and 1 for each of the species where a linear regression was performed. Notes: bold = b is significant at $P \leq 0.0125$ (after application of Bonferonni correction), Stdev. = standard deviation and NS = difference from b is not significant.

Group	Species	n	b	Stdev.	0.66	0.75	0.9	1
					P	P	P	P
Ctenophores	<i>Pleurobrachia bachei</i>	36	0.72	0.08	NS	NS	0.01	0.002
	<i>Pleurobrachia pileus</i>	31	0.72	0.03	NS	NS	0.001	0.002
	<i>Bolinopsis infundibulum</i>	10	0.54	0.22	NS	NS	NS	0.01
	<i>Mnemiopsis mccradyi</i>	10	0.77	0.05	NS	NS	0.01	0.002
	<i>Beroë cucumis</i>	6	0.62	0.05	NS	NS	0.001	0.002
	<i>Beroë ovate</i>	140	0.84	0.02	0.002	0.002	0.001	0.002
Thaliacea	<i>Cyclosalpa bakeri</i>	25	1.20	0.08	0.002	0.002	0.01	NS
Scyphomedusae	<i>Aurelia aurita</i>	340	0.84	0.008	0.002	0.002	0.001	0.002
	<i>Cyanea capillata</i>	24	0.95	0.04	0.002	0.002	NS	NS
	<i>Stomolophus meleagris</i>	43	1.10	0.05	0.002	0.002	0.001	NS
Limnomedusae	<i>Eperetmus typus</i>	11	0.97	0.19	NS	NS	NS	NS
	<i>Gonionemus vertens</i>	12	1.12	0.15	NS	NS	NS	NS
Trachymedusae	<i>Aglantha digitale</i>	27	0.52	0.05	0.002	0.002	0.001	0.002
Hydromedusae	<i>Sarsia princeps</i>	8	1.34	0.15	NS	NS	NS	NS
	<i>Sarsia tubulosa</i>	7	0.91	0.07	0.01	NS	NS	NS
	<i>Stomotoca atra</i>	26	0.85	0.15	NS	NS	NS	NS
Siphonophores	<i>Aequorea Victoria</i>	44	1.10	0.07	0.002	0.002	NS	NS
	<i>Aequorea vitrina</i>	9	1.03	0.08	0.01	0.01	NS	NS
	<i>Clytia loma*</i>	25	0.97	0.14	NS	NS	NS	NS
	<i>Clytia gregaria*</i>	44	1.09	0.09	0.002	0.002	NS	NS
	<i>Eutonina indicans</i>	24	0.83	0.07	0.01	NS	NS	0.01
	<i>Mitrocoma cellularia</i>	53	0.87	0.06	0.002	NS	NS	NS
Pteropods (shelled)	<i>Limacina helicina</i>	4	0.82	0.13	NS	NS	NS	NS
Pteropods (naked)	<i>Clione limacine</i>	24	0.81	0.04	0.002	NS	0.01	0.002
Chaetognaths	<i>Parasagitta elegans</i>	85	0.85	0.03	0.002	0.002	NS	0.002
	<i>Pseudosagitta gazellae*</i>	4	0.96	0.04	0.02	NS	NS	NS
Amphipods	<i>Paramoera walkeri</i>	77	0.62	0.03	0.05	0.002	0.001	0.01
	<i>Waldeckia obesa</i>	30	0.60	0.08	NS	0.01	0.001	0.002
	<i>Orchomenella sp.</i>	4	0.93	0.09	NS	NS	NS	NS
	<i>Orchomene plebs</i>	40	0.85	0.07	0.01	NS	NS	0.01
	<i>Themisto gaudichaudii*</i>	9	0.66	0.14	NS	NS	NS	NS
	<i>Brachyuran zoea larva</i>	5	0.89	0.18	NS	NS	NS	NS
Decapods	<i>Euphausia</i>	21	0.81	0.1	NS	NS	NS	NS
Euphausiids	<i>Euphausia pacifica</i>	209	1.18	0.04	0.002	0.002	NS	0.002
	<i>Euphausia superba</i>	244	0.89	0.02	0.002	0.002	NS	0.002
	<i>Euphausia tenera</i>	9	1.14	0.1	0.01	NS	NS	NS
	<i>Thysanoessa spp.</i>	21	0.95	0.18	NS	NS	0.001	NS
	<i>Thysanoessa inermis</i>	4	0.71	0.07	NS	NS	NS	NS
Appendicularians	<i>Oikopleura dioica</i>	58	1.31	0.05	0.002	0.002	NS	0.002
	<i>Oikopleura longicauda</i>	6	0.96	0.1	NS	NS	NS	NS

2.4.5 COMPARISON OF INTERSPECIFIC, INTRA-GROUP AND INTRASPECIFIC RESPIRATION

A comparison of the interspecific, including intra-group and intraspecific metabolic scaling exponents analysed during this study shows a lower metabolic scaling exponent in the interspecific analysis. The highest occurrence of metabolic scaling exponents for the intra-group occur between 0.5 and 0.7 while for intraspecific they occurred between 0.7 and 0.9 (Figure

2.8). The value for interspecific and the mean values for intra-group and intraspecific metabolic scaling exponents were 0.70 ± 0.006 (95% CL), 0.68 ± 0.095 (95% CL) and 0.90 ± 0.062 (95% CL) respectively, which shows that relationship between metabolic rate and body mass across species scales differently to that within species. Although the mean of the intra-group metabolic scaling exponents is lower than the interspecific metabolic scaling exponent they are not significantly different at $P \leq 0.05$.

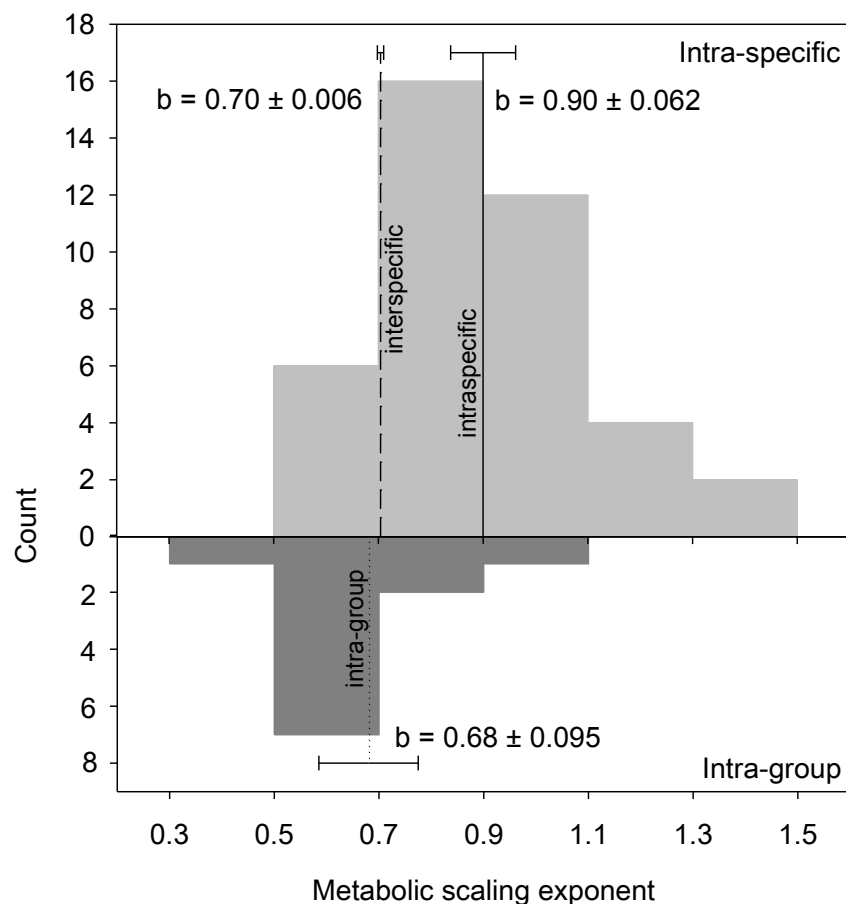


Figure 2.8: Frequency of intraspecific and intra-group metabolic scaling exponents of marine epipelagic macro-zooplankton. Dashed line = interspecific metabolic scaling exponent, solid line = mean intraspecific metabolic scaling exponent, dotted line = mean intra-group metabolic scaling exponent. Whiskers are 95% confidence limits.

2.4.6 INTRASPECIFIC RESPIRATION: COMPARISON WITH GLAZIER (2005)

Intraspecific metabolic scaling exponents from this study and Glazier (2005) are compared in Figure 2.9. While the metabolic scaling exponents from this study are lower than those presented by Glazier (2005) they are not significantly different at $P \leq 0.05$ using a t-test. Examination of the intraspecific metabolic scaling exponents for both studies reaffirms this

observation. The mean intraspecific metabolic scaling exponent from this study has slightly greater 95% confidence intervals (0.062) than the Glazier (2005) data (0.056). While this indicates that the range of possible values for the mean intraspecific metabolic scaling exponent is greater, it also indicates that the mean intraspecific scaling exponent from this study is not greater than that of Glazier's (2005) study.

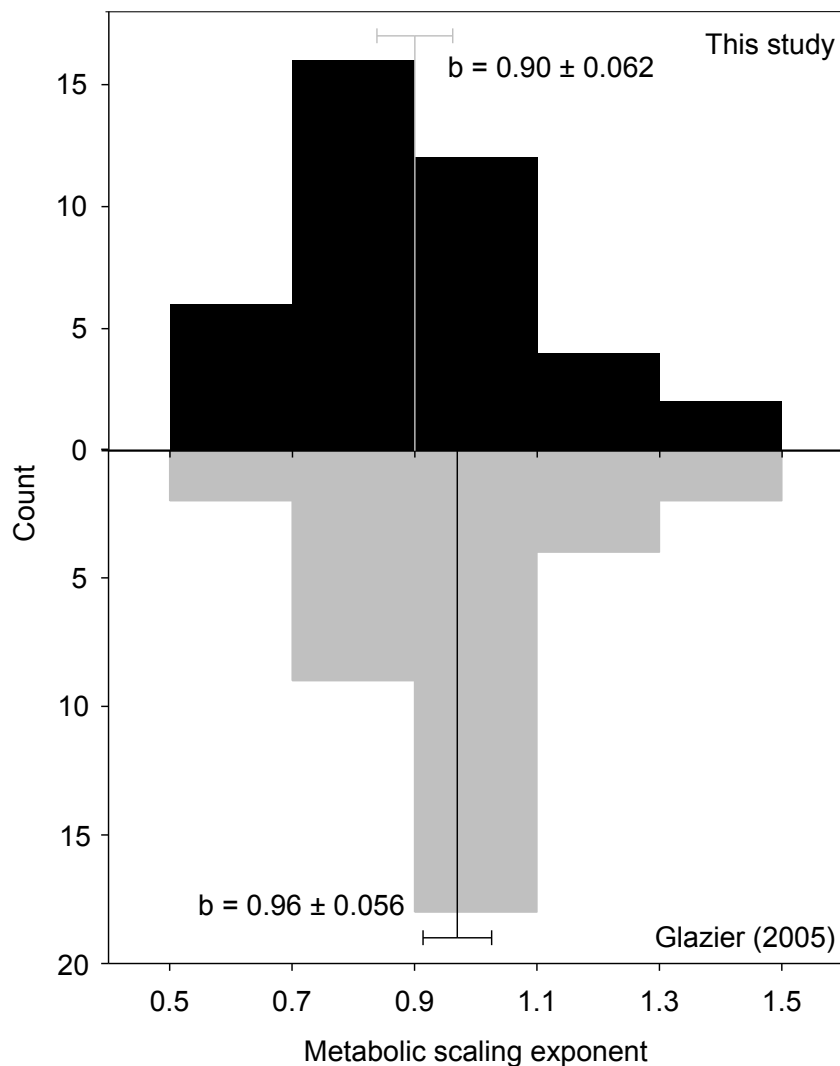


Figure 2.9: Comparison of metabolic scaling exponents from this study (top) and those presented in Glazier (2005). Whiskers are 95% confidence limits.

2.5 DISCUSSION

2.5.1 GENERAL PATTERNS

The data presented in Figure 2.1 represents the most comprehensive collection of respiration rates, body mass and temperature data for epipelagic macro-zooplankton to date. This data set is not only a syntheses of respiration rates, body mass and temperature but also of the conversion

data necessary to provide a complete data set for each mass type. A synthesis of this nature is well suited to address general patterns in the respiration of epipelagic macro-zooplankton. It also enables investigation of both interspecific and intra-group relationships between respiration rate, body mass and temperature. I have endeavoured to search for intra-group and intraspecific patterns within the synthesis and this is where the limitations of this data set become apparent. The limitations of the data set will be discussed in more detail in the section of the discussion that deals with intra-group and intraspecific metabolic scaling and temperature dependence.

In my search for general patterns within this synthesis I was able to reproduce the general patterns observed in epipelagic zooplankton. In my search for a statistical characterisation of relationship between respiration rate, body mass and temperature in epipelagic macro-zooplankton I use a similar model (Equation 1.1) to Ikeda (1985). However instead of assuming that body mass and temperature are independent I first tested the interaction between these two variables (Equation 1.2). The results of this analysis show that the inclusion of the interaction term between body mass and temperature lead to only a negligible increase in predictability. The coefficients for body mass and temperature are similar to those presented in Ikeda (1985) (Table 2.1). There is some overlap between Ikeda's (1985) data set and the synthesis presented here. Ikeda only presents data from publications where he was involved in the respiration experiments. He also presents data for copepods, ostracods, cumacea and fish as he was interested in all members of the epipelagic zooplankton. I have been selective in different ways; experimental method was controlled for by excluding those studies where I was unsure of the experimental method used or where the experimental method was outside the preferred criteria. I focused only on macro-zooplankton. Despite these difference in the data set there was a similar relationship between respiration rate, body mass and temperature.

Respiration rate was corrected to 15°C using a Q_{10} of 2.14 to remove the effect of temperature which allowed me to investigate the relationship between respiration and body mass for three different mass types. The findings support earlier work carried out by Ikeda (1970) on epipelagic marine zooplankton where the wet, dry and carbon mass was known. Using a much larger data set of $n = 1988$, compared to $n = 98$ in Ikeda (1970), I show highly

significant relationships between respiration rate and each mass type and a much clearer increase in correlation coefficient (r^2), from wet to dry mass and dry mass to carbon mass. I find that of the three mass types used to determine the relationship between respiration rate and body mass, carbon mass gives the highest correlation. Branching that is visible in wet mass and dry mass disappears when carbon is used as body mass type.

This result is not surprising. It shows that respiration rate measurements based on carbon body mass is a valuable measure of metabolism as it ties carbon turnover within an organism to the carbon mass of that organism. It is a much more meaningful measure than a metabolic rate given as a function of wet mass or dry mass because body mass varies enormously with changes in water and ash content across taxa. In contrast, respiration rates correlate highly with carbon mass in epipelagic macro-zooplankton, as would be expected, as energy rich organic molecules are catabolised to drive the synthesis of macromolecules, and macromolecules are created from many precursor organic molecules. Both of these processes involve most of what happens to carbon inside not only the cells of macro-zooplankton but in all other organisms. The predominance of gelatinous organisms to the right of the top panel in Figure 2.1 results from gelatinous organisms having a low wet mass to carbon ratio. This enables them to increase in size without increasing the materials (carbon) required for metabolic processes.

Body mass in carbon terms is more meaningful when considering the metabolism of an organism as the functioning of that organism is primarily carbon based. To clarify this further I examined carbon-specific respiration rate and carbon mass by type of epipelagic macro-zooplankton. I found that regardless of the type of macro-zooplankton, i.e. gelatinous, semi-gelatinous, crustacean or appendicularian, the carbon-specific respiration is similar at similar body mass. Other studies have examined this previously using smaller data sets most recent Schneider (1992) ($n = 470$). Schneider went as far as recommending that all mass-specific metabolic rates should be expressed in carbon terms ($\text{mg C mg C}^{-1} \text{ d}^{-1}$) to enable accurate comparisons between individuals that have different wet mass/carbon and/or dry mass/carbon ratios.

2.5.2 INTERSPECIFIC RESPIRATION

There are many different models that attempt to explain the scaling of metabolism with body mass. As yet there is still much controversy over which explanatory model is best, or indeed if any model explains the various patterns seen. An allometric metabolic scaling of $b = 0.70 \pm 0.03$ across 139 species of epipelagic macro-zooplankton is revealed. The value of b for epipelagic macro-zooplankton is statistically indistinguishable from $b = 0.66$. Many of the models used to try and explain metabolic scaling with body mass predict metabolic scaling exponents of $b = 0.66$ and $b = 0.75$ for interspecific metabolic scaling (Rubner 1883, McMahon 1973, Witting 1995, Kozlowski & Weiner 1997, West et al. 1997, Banavar et al. 1999, Darveau et al. 2002, Rau 2002, Demetrius 2003, Fujiwara 2003), yet other studies have shown metabolic scaling exponents of $b = 0.83$ or $b = 0.33$ (Witting 1995, Dodds et al. 2001, Santillan 2003) or a range of b -values (Davison 1955, Bejan 2001).

As I have approached this study from an empirical perspective it is difficult to ascertain which model explains interspecific metabolic scaling of $b = 0.70$ in epipelagic macro-zooplankton. A number of studies have pointed to the ‘lumping’ together of data from heterogeneous taxa, with physiological and ecological differences, resulting in the b -values of ~ 0.75 (Prothero 1986, Kozlowski et al. 2003b). Metabolic scaling exponent has been shown to be sensitive to the taxonomic groups included in the analysis (Prothero 1986). Model predictions such as $b=0.66$ or $b = 0.75$ in interspecific studies may be useful estimates to the scaling of mass with metabolic rate (Glazier 2005) but they are not the only values for metabolic scaling exponent b as I have demonstrated. The variety of values presented throughout the literature suggests that they result from multiple internal constraints (Kooijman 2000) or whole-organism optimisation and constraints, be they physical or ecological (Kozlowski et al. 2003a, Glazier 2005).

2.5.3 INTRA-GROUP RESPIRATION

Again I examine interspecific metabolic scaling exponents and temperature dependence, this time, however, within taxonomic groups (intra-group). I used the species mid-point and mean data as used in the inter-specific analysis. Although sample values are low, out of fourteen

groups that had a range of body mass (as opposed to a constant body mass value) to be analysed, eleven relationships were significant. Within the cnidaria there is both the highest and the lowest metabolic scaling exponents $b = 1.05$ in the siphonophores and 0.41 in the hydromedusae. All other significant b -values fall between 0.55 and 0.77. There are also a range of values for intra-group Q_{10} ranging between 1.66 in thaliaceans and 2.79 in chaetognaths. I identified a range of values for both the metabolic scaling exponent and the temperature dependence in intra-group metabolic rate. This finding supports Glazier's (2005) findings that there is a range of interspecific metabolic scaling exponents rather than one single value of $b \sim 0.75$ as proposed by West et al.(1997).

2.5.4 INTRASPECIFIC RESPIRATION

I will address the limitations associated with creating this synthesis and identify areas where improvement would make a difference to the results. Of 139 species I could only determine the relationship between respiration and body mass for 48 of which 38 relationships were significant. For temperature dependence only 16 species could be tested and of these 14 were significant. Problems associated with collecting body mass data range from the original publication only reporting average values rather than the full suite of measurements taken during the experiment. Experiments are often only carried out on one stage in the animals' life cycle. Thus, if there are changes in metabolic scaling exponent associated with different types of growth (von Bertalanffy 1951) they are not always captured. Body mass conversions are not always from the same study and there is variation in wet, dry and carbon mass within a species and within individuals for a multitude of reasons, such as different stages of development within an individual, differing environmental conditions (food concentration) and seasonal differences. Not all the conversions used were species-specific, genus- and group-specific conversions were used to convert mass types. Another limitation in the body mass data for a number of species was a limited range in body mass. A minimum range of one order of magnitude for body mass is recommended (LaBarbera 1989) to study relationships with body mass. If this minimum is not satisfied, it is more likely that the metabolic scaling exponent will be distorted by sampling

error caused by noise within biological data. A number of species within this study do not meet this minimum requirement, yet highly correlated and highly significant relationships between respiration rate and body mass were found in some species. This might be explained by higher sample numbers for these species. There were similar problems within the temperature data. Many species exist in a narrow range of temperatures, such as *Euphausia superba* where temperatures, reported in this synthesis, range from -1.8 to 2.4°C only. Larger sample values, mass ranges and temperature ranges for many of the species examined in this study would have made a quantitative difference to the results, both in terms of increasing the number of interspecific relationships it was possible to examine and the significance of those relationships.

2.5.5 COMPARISON OF INTERSPECIFIC, INTRA-GROUP AND INTRASPECIFIC RESPIRATION

I have assessed interspecific scaling in epipelagic macro-zooplankton in two different ways: across all species of macro-zooplankton, and across the various taxonomic groups. Both sets of analysis lead to an overall or mean metabolic scaling exponents that are not statistically different to $b = 0.66$ yet are statistically different to $b = 0.75$ at $P \leq 0.05$ (Figure 2.6). This analysis of intraspecific scaling in macro-zooplankton shows that the mean b -value is 0.90 and which is significantly different to both $b = 0.66$ and $b = 0.75$ at $P \leq 0.05$. I have shown that there is a range of metabolic scaling exponents to be found in intraspecific relationships and that more of these scaling exponents are significantly different to $b = 0.75$ than to $b = 0.90$. These results show that allometric scaling where $b = 0.75$ is not the case for either interspecific or intraspecific metabolic scaling in epipelagic macro-zooplankton. Interspecific and mean intra-group metabolic scaling have a value that is not significantly different to $b = 0.66$ with a range of values for different groups. While these results do not fit with the model of West et al. (1997) they do perhaps reflect a situation where multiple constraints (Kozłowski et al. 2003a, b) or metabolic boundaries are at work (Kooijman 2000) and these values are the result of the ‘lumping’ together of data from physiologically and ecologically different taxa (Glazier 2005).

There is an ongoing debate in the literature as to why and how metabolic rate scales with temperature. The effect of temperature on metabolic rate must either be direct (e.g.,

Gillooly et al. 2001) or indirect (e.g., Clarke & Fraser 2004). If the effect of temperature is direct this means that temperature controls metabolic rate in a mechanistic way. Gillooly et al. (2001) assume that temperature controls the kinetic energy of cellular constraints. If the effect of temperature is indirect it influences metabolic rate through a combination of energetic trade offs (Clarke & Fraser 2004). Advocates of the indirect effect of temperature on metabolism argue that if the effects of temperature are indirect, then intraspecific temperature dependence will be greater than intra-group (interspecific) temperature dependence (Clarke & Fraser 2004). While this analysis reveals a wider range of Q_{10} in intraspecific data than in intra-group data, this argument cannot be supported definitively. The values of Q_{10} for intra-group and intraspecific relationship with temperature are quite different for each set of data, $2.15 (\pm 0.24, 95\% \text{ CL})$ and $3.06 (\pm 1.45, 95\% \text{ CL})$ respectively, yet they cannot be clearly separated as the mean intraspecific Q_{10} does not fall outside the 95% confidence interval of the intra-group Q_{10} .

2.5.6 INTRASPECIFIC RESPIRATION: COMPARISON WITH GLAZIER (2005)

The results of the analysis of intraspecific metabolic scaling exponents are in general agreement with the data presented by Glazier (2005, 2006). Our results show a scaling of $b = 0.9$ in epipelagic macro-zooplankton rather than allometric scaling where b would be equal to 0.75 (West et al. 1997). At first glance it is obvious that Glazier (2005) presents more metabolic scaling exponents for epipelagic macro-zooplankton than in this study. The higher metabolic scaling exponents of Glazier (2005) can be explained by a different data set and approach. Glazier (2005) uses the metabolic scaling exponent as reported in the literature and presents multiple metabolic scaling exponents at different temperatures for a single species. In contrast, I present only one relationship for any individual species corrected to one temperature of 15°C. Furthermore this synthesis of respiration rates was subject to strict selection criteria and this meant the exclusion of many studies. One of the studies that was excluded was that of Biggs (1977), a data-rich study of gelatinous species. Of the metabolic scaling exponents that are reported in Glazier (2005) around 20% came from the Biggs (1977) data set. The high respiration rates presented in Biggs (1977) have not been reproduced by other experimentalists

as demonstrated in Kremer et al. (1986). There is no explanation for the consistently higher respiration rates presented in Biggs (1977). There was no difference in the range of intraspecific metabolic scaling exponent found across the data set, but there was a twofold difference in intercept. This data set was excluded from the synthesis because of these higher rates of respiration and the effect that they would have on the regression analysis that was planned, as the interest lay in intercepts and not simply slopes of relationships. The Biggs (1977) data set is also used by Schneider (1992) and this explains why he finds comparatively higher rates in salps than in other gelatinous groups.

2.5.7 METABOLIC SCALING IN EPIPELAGIC MACRO-ZOOPLANKTON

Epipelagic macro-zooplankton contain a group of diverse organisms. Ecologically, these organisms have filled a multitude of niches in the epipelagic realm through modification at a species level. There are many obvious differences between the various phyla and species that compose the epipelagic macro-zooplankton, e.g. body forms, feeding mechanisms and life histories. General relationships are necessary to describe both across and within species physiological processes, and so that broad predictions can be made when modelling biogeochemistry and estimating rate processes in the upper ocean.

The focus has been on explaining these descriptive relationships with one explanatory variable. A species is the results of modifications that in some way increase its suitability to its surrounding environment. As I was examining the scaling of metabolic rate with body mass and temperature it is necessary to look at the optimisation of biochemical and physical processes involved in metabolism within the organism and the ecological constraints within which an organism resides. The machinery of metabolism is a collection of complex interactions and for each there must be an optimal. Each species is a package of different optimisations and variation in metabolic scaling exponent and Q_{10} , as seen in the macro-zooplankton, reflect this.

Their diversity is partly caused by broad differences in their evolutionary history, i.e. at the level of phyla, and differences between species from similar lineages. Temperature is linked indirectly to metabolic processes by the optimisation occurring between the structure, function

and stability of enzymes involved in metabolic processes (Clarke 2003). There are overall limits, rather than bottle-necks (Glazier 2005), e.g. the physical constraints of resource supply (West et al. 1997), within which optimisation occurs, i.e. physical constraints; surface area limits on substrate/waste and limits on power production associated with body mass (Kooijman 2000), or ‘general optimisation’ (Kozłowski et al. 2003b, Glazier 2005) where body size and metabolic rate have been optimised against the size-specific mortality of a species (Kozłowski et al. 2003b). The assumptions associated with ‘general optimisation’ allow for differences between interspecific and intraspecific metabolic scaling. Optimisation of processes mediated by temperature are finally beginning to be elucidated. The stability of an enzyme and its activity, at the temperature at which the species exists, are key when considering differences in metabolic temperature dependence in different species (Clarke & Fraser 2004).

Species within the epipelagic macro-zooplankton have evolved to exploit the realm in which they exist. They are bound by similar ecological pressures such as high predation pressure and problems associated with remaining afloat (Glazier 2005). There is plasticity in metabolism and increased basal metabolism brings benefits along with its higher costs (Clarke & Fraser 2004). Those species with the metabolic capabilities (plasticity) that predispose them to 1) higher growth and/or reproductive outputs and 2) satisfy the higher energy requirements demanded for living in the pelagic environment were able to adapt and prosper in the pelagic environment. Metabolic rate may have increased, relative to body mass, as a result of necessary optimisations associated with survival in the pelagic environment.

2.6 CONCLUSIONS

There are strong patterns in epipelagic macro-zooplankton in the relationship between respiration rate, body mass and temperature. The similarities between the results of Ikeda (1985) and this study suggest that these patterns can be found in the epipelagic meso- and macro-zooplankton. Examining respiration rate in terms of carbon-specific body mass is important, as authors of previous syntheses, particularly Ikeda (1985), Larson (1985, 1986) and Schneider (1992), have documented as it places all groups within the macro-zooplankton in equivalent

terms. Even though this is generally understood by researchers, wet and dry mass units are still used when reporting experimental results. The need for rates in carbon units is particularly important today to satisfy the needs of ecosystem modellers. Without adequate information assumptions are made to convert wet/dry mass into carbon or energy terms. The error associated with such assumptions of this kind will always be greater than if data on the carbon composition of these organisms had been determined experimentally.

Only statistical relationships can be used to describe the relationship between respiration rate and body mass, in carbon, and temperature as interspecific and intraspecific metabolic scaling is inherently complicated by optimisations that have occurred throughout the evolution of any particular species (Clarke & Fraser 2004). I presented these statistical relationships to characterise the metabolic rates of epipelagic macro-zooplankton as a group and to investigate the contribution of each different species. As Glazier (2006) pointed out, there are robust patterns within pelagic zooplankton and it seems plausible that the pelagic environment has forced this convergence. Further investigation along multiple lines of enquiry would be necessary to achieve a mechanistic understanding of epipelagic macro-zooplankton metabolic scaling with body mass and temperature. These include the employment of rigorous statistical testing, exploring metabolic scaling at different scales, undertaking quantitative genetic studies, undertaking comparative studies of little studied taxa, employing experimental manipulations, testing the assumptions and the predictions of theoretical models and creating a unification between physiological and ecological interpretations (Glazier 2005). While I agree with the recommendations that Glazier makes for future investigations I am not quite sure whether there is an impetus within the community to carry out such a comprehensive investigation of metabolic scaling. The last two of Glazier's recommendations show the most promise. The theoretical models that are currently being employed and the impact of the assumptions on predictions needs to be thought of in the light of the exceptions to the 'general tendency' and these models need to be parameterised from experimental results. It is important to try and understand more clearly the effect of physiological and ecological constraints and the different ways both influence metabolic scaling. It is necessary to understand the interplay between the

two in order to discover how metabolic scaling really works. If a descriptive relationship between metabolic rate, body mass and temperature is all that is necessary then more information on intraspecific metabolic scaling is sufficient. The analysis presented here provides important information required to parameterise and evaluate models that represent macro-zooplankton processes.

REFERENCES

- Bailey T G, Youngbluth M J, Owen G P (1994) Chemical composition and oxygen consumption rates of the ctenophore *Bolinopsis infundibulum* from the Gulf of Maine. *Journal of Plankton Research* 16:673-689
- Banavar J R, Maritan A, Rinaldo A (1999) Size and form in efficient transportation networks. *Nature* 399:130-132
- Bejan A (2001) The tree of convective heat streams: its thermal insulation function and the predicted 3/4-power relation between body heat loss and body size. *International Journal of Heat and Mass Transfer* 44:699-704
- Biggs D C (1977) Respiration and ammonium excretion by open ocean gelatinous zooplankton. *Limnology and Oceanography* 22:108-117
- Biggs D C (1982) Zooplankton excretion and NH_4^+ cycling in near-surface waters of the Southern Ocean.1. Ross Sea, Austral summer 1977-1978. *Polar Biology* 1:55-67
- Brody S (1945) *Bioenergetics and Growth*. Reinhold Publishing Corporation, New York
- Clarke A (2003) Costs and consequences of evolutionary temperature adaptation. *Trends in Ecology & Evolution* 18:573-581
- Clarke A, Fraser K P P (2004) Why does metabolism scale with temperature? *Functional Ecology* 18:243-251
- Conover R J (1960) The feeding behavior and respiration of some marine planktonic Crustacea. *Biological Bulletin*:399-415
- Conover R J, Lalli C M (1974) Feeding and growth in *Clione limacina* (Phipps), a pteropod mollusk.2. Assimilation, metabolism, and growth efficiency. *Journal of Experimental Marine Biology and Ecology* 16:131-154
- Darveau C A, Suarez R K, Andrews R D, Hochachka P W (2002) Allometric cascade as a unifying principle of body mass effects on metabolism. *Nature* 417:166-170
- Davison J (1955) Body weight, cell surface, and metabolic rate in anuran amphibia. *Biological Bulletin* 109:407-419
- Demetrius L (2003) Quantum statistics and allometric scaling of organisms. *Physica a-Statistical Mechanics and Its Applications* 322:477-490
- Dodds P S, Rothman D H, Weitz J S (2001) Re-examination of the "3/4-law" of metabolism. *Journal of Theoretical Biology* 209:9-27

- Finenko G A, Anninsky B E, Romanova Z A, Abolmasova G I, Kideys A E (2001) Chemical composition, respiration and feeding rates of the new alien ctenophore, *Beroë ovata*, in the Black Sea. *Hydrobiologia* 451:177-186
- Frandsen K T, Riisgard H U (1997) Size dependent respiration and growth of jellyfish, *Aurelia aurita*. *Sarsia* 82:307-312
- Fujiwara N (2003) Origin of the scaling rule for fundamental living organisms based on thermodynamics. *Biosystems* 70:1-7
- Gillooly J F, Brown J H, West G B, Savage V M, Charnov E L (2001) Effects of size and temperature on metabolic rate. *Science* 293:2248-2251
- Glazier D S (2005) Beyond the '3/4-power law': variation in the intra- and interspecific scaling of the metabolic rate in animals. *Biological Reviews of the Cambridge Philosophical Society*:611-662
- Glazier D S (2006) The 3/4-power law is not universal: evolution of isometric, ontogenetic metabolic scaling in pelagic animals. *Bioscience* 56:325-332
- Gorsky G, Fenaux R (1998) The role of Appendicularia in marine food webs. In: Q Bone (ed) *The biology of Pelagic Tunicates*. Oxford University Press, New York, p 161-170
- Gorsky G, Palazzoli I, Fenaux R (1984) Some preliminary observations on the respiration of appendicularians (Pelagic Tunicates). *Comptes Rendus De La Academie Des Sciences Serie III-Sciences De La Vie-Life Sciences* 298:531-534
- Gorsky G, Palazzoli I, Fenaux R (1987) Influence of temperature changes on oxygen uptake and ammonia and phosphate excretion in relation to body size and weight in *Oikopleura dioica* (Appendicularia). *Marine Biology*:191-201
- Gyllenberg G Y, Greve W (1979) Studies on oxygen uptake in ctenophores. *Annales Zoologici Fennici*:44-49
- Halcrow K (1963) Acclimation to temperature in the marine copepod, *Calanus finmarchicus* (Gunner). *Limnology and Oceanography* 8:1-8
- Hirche H J (1983) Excretion and respiration of the Antarctic krill *Euphausia superba*. *Polar Biology* 1:205-209
- Ikeda T (1970) Relationship between respiration rate and body size in marine plankton animals as a function of temperature of habitat. *Bulletin of the Faculty of Fisheries, Hokkaido University* 21:91-112
- Ikeda T (1974) Nutritional ecology of marine zooplankton. Member of the Faculty Fisheries, Hokkaido University:1-97
- Ikeda T (1981) Metabolic activity of larval stages of Antarctic krill. *Antarctic Journal of the United States* 16:161-162
- Ikeda T (1985) Metabolic rates of epipelagic marine zooplankton as a function of body mass and temperature. *Marine Biology* 85:1-11
- Ikeda T, Bruce B (1986) Metabolic activity and elemental composition of krill and other zooplankton from Prydz Bay, Antarctica, during early summer (November-December). *Marine Biology*:545-555

- Ikeda T, Hing Fay E (1981) Metabolic activity of zooplankton from the Antarctic Ocean. *Australian Journal of Marine and Freshwater Research* 32:921-930
- Ikeda T, Kirkwood R (1989a) Metabolism and body composition of two euphausiids (*Euphausia superba* and *E. crystallorophias*) collected from under the pack-ice off Enderby Land, Antarctica. *Marine Biology* 100:301-308
- Ikeda T, Kirkwood R (1989b) Metabolism and elemental composition of a giant chaetognath *Sagitta gazellae* from the Southern Ocean. *Marine Biology* 100:261-267
- Ikeda T, Mitchell A W (1982) Oxygen uptake, ammonia excretion and phosphate excretion by krill and other Antarctic zooplankton in relation to their body size and chemical composition. *Marine Biology* 71:283-298
- Ikeda T, Skjoldal H R (1989) Metabolism and elemental composition of zooplankton from the Barents Sea during early Arctic Summer. *Marine Biology* 100:173-183
- Ikeda T, Torres J J, Hernández-León S, Geiger S P (2000) Metabolism. In: R Harris, Weibe P, Lenz J, Skjoldal H-R, Huntley M (eds) ICES Zooplankton Methodology Manual. Academic Press
- Ishii H, Omori M, Maeda M, Watanabe Y (1987) Metabolic rates and elemental composition of the Antarctic krill, *Euphausia superba* Dana. *Polar Biology* 7:379-382
- Ivleva I V (1980) The dependence of crustacean respiration rate on body mass and habitat temperature. *Internationale Revue Der Gesamten Hydrobiologie* 65:1-47
- Kinoshita J, Hiromi J, Kadota S (1997) Do respiratory metabolic rates of the scyphomedusa *Aurelia aurita* scale isometrically throughout ontogeny in a sexual generation? *Hydrobiologia* 347:51-55
- Kleiber M (1932) Body size and metabolism. *Hilgardia*:315-353
- Klekowski R Z, Opalinski K W, Rakusa-Suszczewski S (1973) Respiration of the Antarctic Amphipoda *Paramorea walkeri* Stebbing during the winter season. *Polskie archiwum hydrobiologii* 20:301-308
- Kooijman S A L M (2000) Dynamic Energy and Mass Budgets in Biological Systems. Cambridge University Press, Cambridge
- Kozłowski J, Konarzewski M, Gawelczyk A T (2003a) Cell size as a link between noncoding DNA and metabolic rate scaling. *Proceedings of the National Academy of Sciences of the United States of America* 100:14080-14085
- Kozłowski J, Konarzewski M, Gawelczyk A T (2003b) Intraspecific body size optimization produces interspecific allometries. In: T M Blackburn, Gaston K J (eds) *Macroecology: Concepts and Consequences*. Blackwell, Malden, Massachusetts, p 299-320
- Kozłowski J, Weiner J (1997) Interspecific allometries are by-products of body size optimization. *The American Naturalist* 149:352-380
- Kremer P (1982) Effect of food availability on the metabolism of the ctenophore *Mnemiopsis mccradyi*. *Marine Biology* 71:149-156
- Kremer P, Canino M F, Gilmer R W (1986) Metabolism of epipelagic tropical ctenophores. *Marine Biology* 90:403-412
- Krüger F (1968) Metabolism and growth in Scyphomedusae. *Helgoländer Wissenschaftliche Meeresuntersuchungen* 18:367-383

- LaBarbera M (1989) Analyzing Body Size as a Factor in Ecology and Evolution. *Annual Review of Ecology and Systematics* 20:97-117
- Larson R J (1985) Trophic ecology of gelatinous predators (Cnidaria and Ctenophora) in Saanich Inlet, Vancouver Is., B.C., Canada. University of Victoria
- Larson R J (1986) Water-content, organic content, and carbon and nitrogen composition of medusae from the Northeast Pacific. *Journal of Experimental Marine Biology and Ecology* 99:107-120
- Larson R J (1987) Respiration and carbon turnover rates of medusae from the NE Pacific. *Comparative Biochemistry and Physiology a-Physiology* 87:93-100
- Le Quéré C, Harrison S P, Prentice I C, Buitenhuis E T, Aumont O, Bopp L, Claustre H, Da Cunha L C, Geider R, Giraud X, Klaas C, Kohfeld K E, Legendre L, Manizza M, Platt T, Rivkin R B, Sathyendranath S, Uitz J, Watson A J, Wolf-Gladrow D (2005) Ecosystem dynamics based on plankton functional types for global ocean biogeochemistry models. *Global Change Biology* 11:2016-2040
- Lebrato M, Jones D O B (2009) Mass deposition event of *Pyrosoma atlanticum* carcasses off Ivory Coast (West Africa). *Limnology and Oceanography* 54:1197-1209
- Lombard F, Sciandra A, Gorsky G (2005) Influence of body mass, food concentration, temperature and filtering activity on the oxygen uptake of the appendicularian *Oikopleura dioica*. *Marine Ecology-Progress Series* 301:149-158
- McMahon T (1973) Size and shape in biology. *Science* 179:1201-1204
- Moriarty R (2009) Respiration rates in epipelagic macro-zooplankton: a data set. PANGAEA
- Paranjape M A (1967) Molting and respiration of Euphausiids. *Journal of the Fisheries Research Board of Canada* 24:1229-&
- Prothero J (1986) Scaling of energy metabolism in unicellular organisms - a reanalysis. *Comparative Biochemistry and Physiology a-Physiology* 83:243-248
- Rakusa-Suszczewski S, Klekowski R Z (1973) Biology and respiration of the Antarctic amphipod (*Paramoera walkeri* Stebbing) in the summer. *Polskie Archiwum Hydrobiologii* 20:475-488
- Rau A R P (2002) Biological scaling and physics. *Journal of Biosciences* 27:475-478
- Rubner M (1883) Über den Einfls der Körpergrösse auf Stoffund Kraftwechsel. *Zeitschrift für Biologie (Munich)*:535-562
- Salomon M, Mayzaud P, Buchholz F (2000) Studies on metabolic properties in the Northern krill, *Meganyctiphanes norvegica* (Crustacea, Euphausiacea): influence of nutrition and season on pyruvate kinase. *Comparative Biochemistry and Physiology a-Molecular and Integrative Physiology* 127:505-514
- Santillan M (2003) Allometric scaling law in a simple oxygen exchanging network: possible implications on the biological allometric scaling laws. *Journal of Theoretical Biology* 223:249-257
- Schneider G (1988) Chemical-composition and biomass parameters of the common jellyfish *Aurelia aurita*. *Helgolander Meeresuntersuchungen* 42:319-327
- Schneider G (1992) A comparison of carbon-specific respiration rates in gelatinous and nongelatinous zooplankton - a search for general rules in zooplankton metabolism. *Helgoländer Wissenschaftliche Meeresuntersuchungen* 46:377-388

- Segawa S, Kato M, Murano M (1982) Respiration and ammonia excretion rates of the Antarctic krill, *Euphausia superba* Dana. Transactions of the Tokyo University of Fisheries 5:177-187
- Small L F, Hebard J F (1967) Respiration of a vertically migrating marine crustacean *Eupausia pacifica* Hansen. Limnology and Oceanography:272-280
- Svetlichny L S, Abolmasova G, Hubareva E S, Finenko G A, Bat L, Kideys A E (2004) Respiration rates of *Beroë ovata* in the Black Sea. Marine Biology 145:585-593
- Thill H (1937) Beiträge zur kenntnis der *Aurelia aurita* (L.). Zeitschrift fuer wissenschaftliche Zoologie:51-96
- Turner J T (2002) Zooplankton fecal pellets, marine snow and sinking phytoplankton blooms. Aquatic Microbial Ecology 27:57-102
- Uye S, Shimauchi H (2005) Population biomass, feeding, respiration and growth rates, and carbon budget of the scyphomedusa *Aurelia aurita* in the Inland Sea of Japan. Journal of Plankton Research 27:237-248
- Vidal J, Whitley T E (1982) Rates of metabolism of planktonic crustaceans as related to body-weight and temperature of habitat. Journal of Plankton Research 4:77-84
- von Bertalanffy L (1951) Metabolic types and growth types. The American Naturalist:111-117
- Welch H E, Siferd T D, Bruecker P (1996) Population densities, growth, and respiration of the chaetognath *Parasagitta elegans* in the Canadian high Arctic. Canadian Journal of Fisheries and Aquatic Sciences 53:520-527
- West G B, Brown J H, Enquist B J (1997) A general model for the origin of allometric scaling laws in biology. Science 276:122-126
- Winkler L W (1888) Die Bestimmung des Wasser gelösten Sauerstoffes und die Löslichkeit des Sauerstoffes in Wasser. Beriche ser Deutschen Chemischen Gesellschaft zu Berlin 21:2843-2855
- Witting L (1995) The body mass allometries as evolutionarily determined by the foraging of mobile organisms. Journal of Theoretical Biology 177:129-137
- Yamada Y, Ikeda T (2003) Metabolism and chemical composition of four pelagic amphipods in the Oyashio region, western subarctic Pacific Ocean. Marine Ecology-Progress Series 253:233-241

3 MACRO-ZOOPLANKTON BIOMASS: A VALIDATION DATA SET

3.1 ABSTRACT

A global data set is presented for the validation of macro-zooplankton abundance and biomass in ocean biogeochemical models. Data has been compiled from two sources: KRILLBASE (Atkinson et al. 2004) and the Coastal & Oceanic Plankton Ecology, Production & Observation Database (COPEPOD) (O'Brien 2005). Macro-zooplankton abundance data were standardised to individuals per litre (ind. L⁻¹). Maps produced from abundance data give an indication of the global distribution of macro-zooplankton. At low latitudes abundance ranges between 0 and 0.05 ind. L⁻¹ and at high latitudes abundance ranges from 0 to ≤ 30 ind. L⁻¹. In general terms macro-zooplankton abundance is more homogenous in the tropics with constant low levels of abundance. At high latitudes the background abundance is lower yet there are patches of very high abundance. Abundance data is converted to biomass where species, as opposed to a higher taxonomic classification, data accompanied abundance measurements and species-specific conversions from abundance to carbon biomass were available. Species-specific data on one euphausiid species (*Euphausia superba*) and two salp species (*Salpa thompsoni* and *Ihleia racovitzai*) were converted to carbon biomass as was the species-specific data from the COPEPOD data base (~5% of data). The result of this reduction in data from abundance to biomass is apparent as biomass data are restricted to the higher latitudes whereas there are abundance data for both the high latitudes and the tropics. Biomass distribution is patchy with concentrations ranging between 0 and ~1000 $\mu\text{M C}$. The median biomass of macro-zooplankton, 0.006 $\mu\text{M C}$, is low compared to those of meso- and proto-zooplankton, at 0.61 and 0.43 $\mu\text{M C}$, respectively, yet they have the capability to reach very high biomass concentrations, e.g. 973 $\mu\text{M C}$ compared to the lower biomass concentrations of meso- and proto-zooplankton, 9 and 25 $\mu\text{M C}$, respectively.

3.2 INTRODUCTION

Every model needs an independent data set against which its performance may be evaluated. There are a number of different criteria a biogeochemical PFT model must satisfy. The model's ability to reproduce mean state and variability in CO₂ and O₂ fluxes and the reproduction of the seasonal cycle in chlorophyll *a* in today's oceans is a strong indicator of good overall

performance (Le Quéré et al. 2005). In order to determine the performance of individual PFT parameterisations it is necessary to evaluate the model against observations of abundance and biomass for that group. Macro-zooplankton are governed by physical, chemical and biological processes that occur on a vast temporal and spatial scale. This makes it difficult to piece together a global distribution for the group. Measurements of zooplankton abundance and biomass have been collected since the end of the 19th century (Mills 1989). What is known about macro-zooplankton abundance, biomass and distribution has been pieced together from discrete sampling events that have taken place at different times and different locations over the years. Currently all zooplankton abundance and biomass data are collected from direct *in situ* observations. Zooplankton biomass cannot be detected from space using the same technology that is used in the remote detection of phytoplankton as they do not contain photosynthetic pigments. Detection of chlorophyll *a*, in phytoplankton, by ocean colour sensors, such as the SeaWiFS satellite, provides information on sea surface chlorophyll *a*. Remote sensing of chlorophyll *a* allows a global estimation of phytoplankton biomass and provides information on the seasonal cycle (Yoder & Kennelly 2003) and interannual variability (Behrenfeld et al. 2001, Yoder & Kennelly 2003, Behrenfeld et al. 2006). There is no such equivalent global estimation for zooplankton.

To build a global validation data set for macro-zooplankton, discrete estimates of macro-zooplankton abundance and biomass are necessary. Many government institutions and funding bodies require that data collected with public funding be deposited in the corresponding national data centres. Abundance and biomass data measured by scientists at sea are now commonly being collected and catalogued. These data sets also contain the metadata associated with collection. This includes exact location and date of sampling along with varying degrees of taxonomic and sampling information. Data sets submitted to data centres must undergo fidelity checks and standardisation. Over the next few years, abundance and biomass data for macro-zooplankton will become available to the modelling community through such data centres, e.g. COPEPOD-SAR, the historical plankton data search and rescue project from the National Marine Fisheries Service (NMFS) and the Ocean Biogeographical Information System (OBIS) from the Institute for Marine and Coastal Sciences, Rutgers University. For now, a data set for the validation of macro-

zooplankton biomass in PlankTOM10 has been produced from currently available data sets; the raw KRILLBASE database (Atkinson et al. 2004) and the Coastal & Oceanic Plankton Ecology, Production & Observation Database (COPEPOD): The Global Plankton Database at <http://www.st.nmfs.noaa.gov/plankton> (O'Brien 2005).

3.3 METHODS

Data on macro-zooplankton abundance were gathered from two sources: the KRILLBASE database (Atkinson et al. 2004) and COPEPOD (O'Brien 2005). KRILLBASE is a Southern Ocean data set for the euphausiid, *Euphausia superba*, and two salps, *Salpa thompsoni* and *Ihlea racovitzai*. It is the result of the sampling effort of nine countries (UK, Germany, USA, Ukraine, South Africa, Japan, Australia, Poland and Spain) and subsequent collaboration. The original authors (Atkinson et al. 2004) gathered the data through their institutions, collaborators, and from the published literature. All data are from oblique or vertical net hauls with a pre-defined geographic position. Data within KRILLBASE was standardised to ind. m⁻². KRILLBASE data was converted from ind. m⁻² to ind. L⁻¹ using the depth over which the samples were gathered. Mean body mass of *Euphausia superba*, 140 mg dry mass ind.⁻¹ (Atkinson pers. comm.), was estimated from a length frequency distribution data set containing 535,581 length measurements of *Euphausia superba* recovered from scientific nets between October and April from 1926-1939 and 1976-2006 (Atkinson et al. 2009). A dry mass to carbon conversion of 45% (Pakhomov et al. 2002) was used to convert dry mass to carbon individual. Body mass, for both species of salp was estimated at 120 mg dry mass ind.⁻¹ (Dubischar et al. 2006). A dry mass to carbon conversion of 20% (Dubischar et al. 2006) was used to convert dry mass to carbon per individual.

The COPEPOD data set contains data on fifteen higher groupings of macro-zooplankton: salps, doliids and pyrosomes, ctenophores, cnidaria, scyphozoa, hydrozoa, anthozoa, pelagic molluscs, pelagic polychaetes, chaetognaths, amphipods, mysids, stomatopods, decapods, euphausiids, and appendicularians. The data from COPEPOD were extracted by M.-P. Gosselin, as part of the EUROCEANS global PFT biomass database for model evaluation (Le Quéré 2008). Within COPEPOD, NMFS data comes from NMFS ecosystem survey and sampling programs,

historical plankton data search and rescue work and institutional and project data. There are also individual submissions from researchers. All taxonomic data within COPEPOD were standardised to the Integrated Taxonomic Information System (ITIS, <http://www.itis.gov>). Abundance measurements within COPEPOD were standardized to individuals per m^3 . The taxonomic data in the COPEPOD data set is organized at a number of different levels. For ease of extraction the major group level was used. At this level data within these groups may provide additional information under the COPEPOD headings of minor group, focus group, special group and species name. Data was not resolved to species level in the majority of measurements. This means that abundance measurements are usually under a higher heading such as minor group, giving only general taxonomic details of a related group of species where size range may be large. There were only 19,649 entries of a total 206,514 where the organism was identified to species level. A total of 274 different species were recorded. COPEPOD data were converted from individual per m^3 to ind. L^{-1} . For the COPEPOD data set only species-specific abundance data was converted to biomass. Abundance measurements that were not accompanied by a species level classification were not converted to biomass. Body mass data was compiled for 32 of the 274 species found in the COPEPOD data set (for individual species conversions see Table 3.1). Adult mean body mass of the species was used for the conversion to carbon. This allowed 11,186 or ~57% of species data points to be converted directly from abundance to carbon.

Abundance and biomass were plotted on a 4D grid of the world ocean. Month, latitude and longitude data directly from COPEPOD and KRILLBASE were used as co-ordinates. In both data sets a top depth and bottom depth of sampling was recorded. The mean depth of each abundance and biomass measurement is calculated from these values. This calculated mean depth was then used as the depth of the sample. Only data gridded in the top 200 m of the ocean were used to calculate the annual average abundance and biomass. Distribution maps of macro-zooplankton annual average abundance (ind. L^{-1}) and biomass ($\mu\text{M C}$) in the top 200 meters of the world ocean were created for each macro-zooplankton group and total macro-zooplankton. Both the raw and the gridded macro-zooplankton data extracted from COPEPOD are available from http://lgmacweb.env.uea.ac.uk/green_ocean/macro.html.

3.4 RESULTS

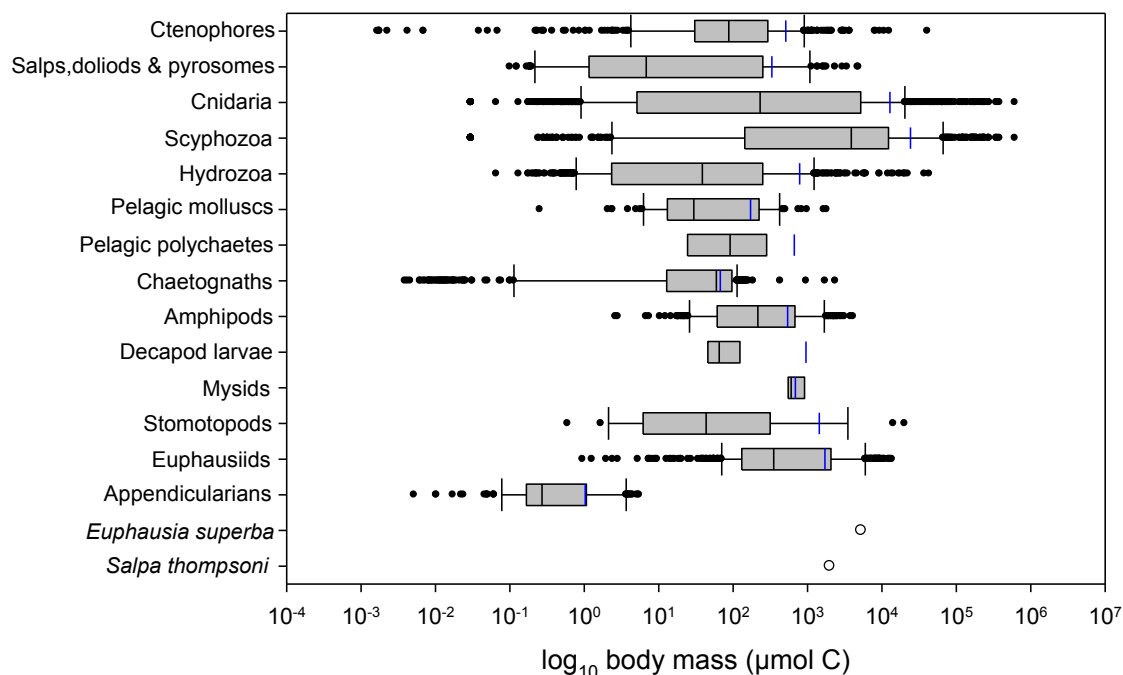


Figure 3.1: Body mass of COPEPOD groups and KRILLBASE species-specific conversions. Box plot shows median (black), mean (blue), upper and lower quartile (whiskers), upper and lower range of data (●) and species-specific conversion data (○). Data from Hirst & Bunker 2003 and Moriarty 2009. Euphausiid data excludes body mass data of *Euphausia superba*.

Body mass data compiled from two macro-zooplankton data sets (Hirst & Bunker 2003, Moriarty 2009) were used to calculate the mean and median body mass for the major groups extracted from the COPEPOD (Figure 3.1). At a major group level the body mass gathered from these two data sets gives a good indication of the range of body mass within the group. As there is a range of body mass of ~8 orders of magnitude within some groups, e.g. the scyphozoa and the ctenophores, the mean body mass could lead to under-estimation or over-estimation of the carbon body mass of any individual within these groups. Figure 3.1 shows the range of body mass ($\mu\text{mol C}$) for each of the groups involved in this study.

Table 3.1: Mean body mass values used to convert COPEPOD species abundance data to biomass. N = number of data points, Stdev. = standard deviation, all units are $\mu\text{M C}$.

Species	Group	n	Mean	Stdev.	% Stdev.	Min.	Max.
<i>Bolionopsis infundibulum</i>	Ctenophore	12	3896	4062	104	131	10764
<i>Pleurobrachia pileus</i>		31	166	181	109	13	571
<i>Cyaena capillata</i>	Scyphozoa	25	10283	28330	276	114	13515
<i>Aglantha digitale</i>	Hydrozoa	27	139	110	80	13	461
<i>Eutonina indicans</i>		24	311	230	74	30	1013
<i>Gonionemus vertens</i>		12	359	171	48	242	793
<i>Philalidium gregarium</i>		44	125	62	50	31	297
<i>Sarsia princeps</i>		8	101	73	73	39	230
<i>Sarsia tubulosa</i>		22	19	16	82	1.1	54
<i>Stomotoca atra</i>		26	164	75	46	75	392
<i>Agalma elegans</i>		7	1.6	1.4	89	0.5	4.6
<i>Clione limacine</i>	Pelagic mollusc	31	198	357	180	12	1819
<i>Diacrea trispinosa</i>		1	293	--	--	293	293
<i>Limacina helicina</i>		5	17	4.9	28	13	25
<i>Sagitta elegans</i>	Chaetognath	530	54	44	82	0.0	187
<i>Sagitta enflata</i>		3	31	11	36	18	38
<i>Cyphocaris challengerii</i>	Amphipod	1	176	--	--	176	176
<i>Hyperia galba</i>		5	258	106	41	139	401
<i>Parathemisto japonica</i>		55	96	128	135	0.5	492
<i>Themisto libellula</i>		1	80	--	--	80	80
<i>Phronima sedentaria</i>		4	72	35	49	41	111
<i>Themisto pacifica</i>		1	47	--	--	47	47
<i>Acanthomysis pseudomacropsis</i>	Mysid	2	106	25	23	89	124
<i>Euphausia pacifica</i>	Euphausiid	234	195	186	96	0.2	1674
<i>Meganycitiphanes norvegica</i>		2	1476	--	--	1477	1477
<i>Thysanoessa inermis</i>		31	373	377	101	0.8	1495
<i>Thysanoessa longipes</i>		1	321	--	--	321	321
<i>Thysanoessa raschi</i>		5	166	108	65	51	309
<i>Thysanoessa spinifera</i>		6	619	548	89	26	1330
<i>Fritillaria borealis sargassi</i>	Appendicularian	8	0.01	0.01	100	0.0	0.02
<i>Fritillaria haplostomai</i>		8	0.01	0.01	100	0.0	0.02
<i>Oikopleura dioica</i>		151	0.9	1.42	158	0.0	5.5

Abundance information gives no indication of size or species, where specific taxonomic information was not recorded. This is the case in the majority of the COPEPOD data set (~95%). In order to reduce error, only species-specific conversions were carried out. The standard deviation of the mean carbon per individual used in species-specific conversion to biomass ranged from 23 to 276% (Table 3.1) while the standard deviation of the mean carbon per individual calculated for group-specific conversions to biomass ranged from 30 to 518% .

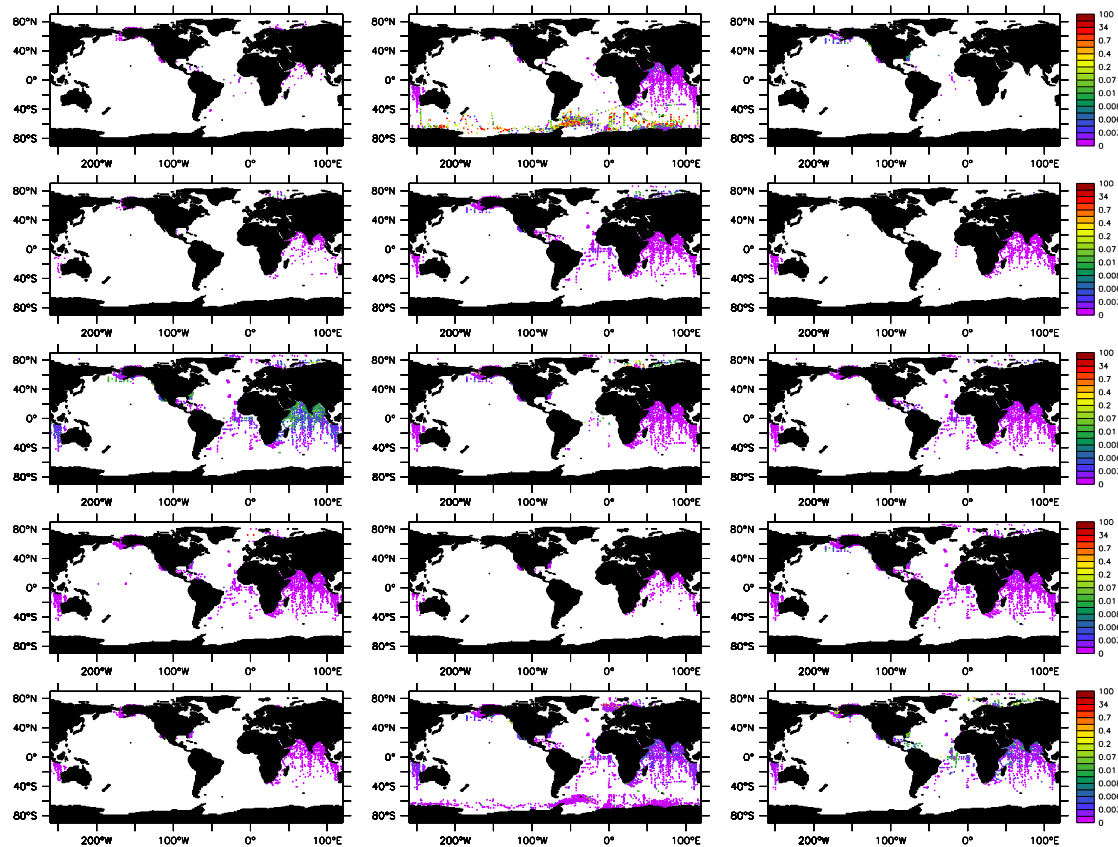


Figure 3.2: The annual average abundance (ind. L^{-1}) in the top 200 meters of the world ocean. Panels show the distribution of ctenophore [top row left], salp*, doliolid, and pyrosome [top row centre], cnidarians [top row right], scyphozoan [2nd row left], hydrazoan [2nd row centre], anthazoan [2nd row right], chaetognath [3rd row left], pelagic mollusc [3rd row centre], pelagic polychaete [3rd row right], decapods [4th row left], stomatopod [4th row centre], amphipod [4th row right], mysid [5th row left], euphausiid* [5th row centre] and appendicularian [5th row right]. All distribution data, unless otherwise stated, are from COPEPOD.

*data from COPEPOD and KRILLBASE. White indicates no data.

Global distribution of abundance is presented for all taxonomic groups of macro-zooplankton represented in the COPEPOD and KRILLBASE data sets (Figure 3.2). It is clear from the gridded distribution maps that the majority of the abundance data can be found in the Indian and Southern Oceans. Further examination of the global distribution of macro-zooplankton abundance reveals constant low levels of abundance, between 0 and 0.05 ind. L^{-1} , in the tropics. In contrast to the low latitudes abundance values for macro-zooplankton at high latitudes are variable showing much greater spatial heterogeneity. Abundance values at high latitude range between 0 and 30 ind. L^{-1} (Figure 3.3).

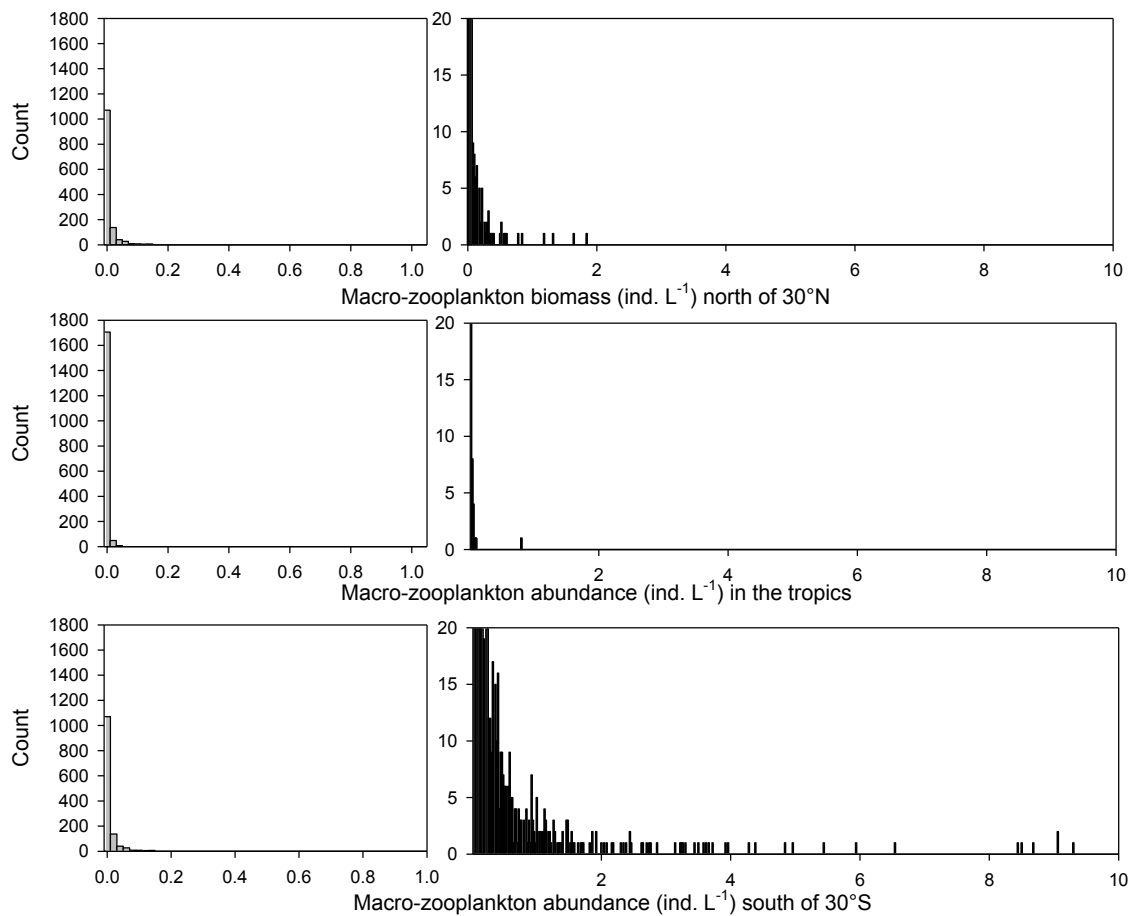


Figure 3.3: The annual average of total abundance in the top 200 meters three areas of the world ocean. Panels show the frequency of macro-zooplankton abundance north of 30°N[top], in the tropics [centre] and south of 30°S [lower] in (ind. L⁻¹). Note: entire range of abundance is not shown at high latitudes.

The loss of data associated with the conversion of abundance to biomass using species specific conversions is apparent when annual average of total macro-zooplankton abundance and annual average of total macro-zooplankton biomass distributions are compared (Figure 3.4). There is no biomass data for the tropics, the wealth of abundance data in the Indian Ocean disappears as the abundance data were not resolved to species level. There is also less biomass data than abundance data available in the higher latitudes, particularly in the Northern hemisphere. Overall the loss of data associated with the conversion of abundance data to carbon specific biomass data using species-specific conversions leads to a fragmented impression of macro-zooplankton biomass.

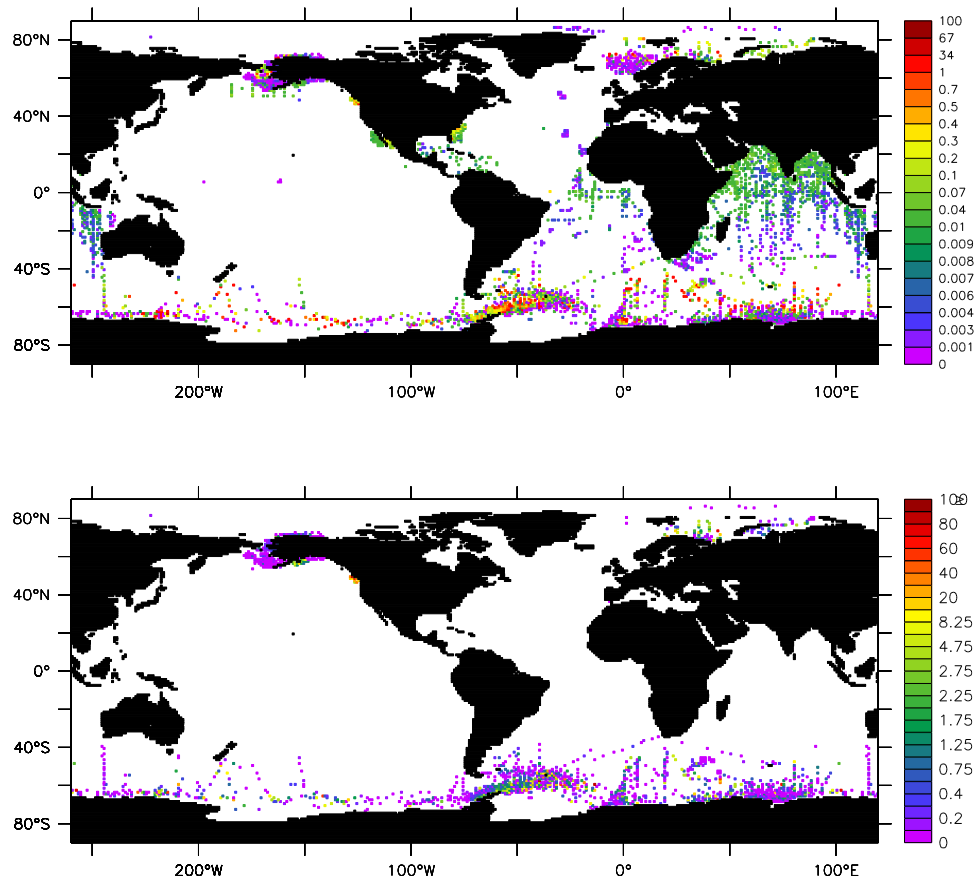


Figure 3.4: The annual average distribution of macro-zooplankton in the top 200 meters of the world ocean. The panels show the total abundance (ind. L⁻¹) [top] and the total biomass (μM C) [bottom] in the top 200 meters of the world ocean. White indicates no data.

Global distribution of biomass is presented for all species of macro-zooplankton represented in the COPEPOD and KRILLBASE data sets (Figure 3.4). For biomass distribution species-specific data were only available for some data in nine of the fifteen taxonomic groups represented in COPEPOD. Species from the same taxonomic group were plotted together. The median observed macro-zooplankton biomass was calculated as 0.006 (± 0.59 absolute deviation) μM C from the global annual average macro-zooplankton biomass in the top 200 meters of the global ocean. The mean observed macro-zooplankton biomass concentration calculated from the global annual average macro-zooplankton biomass in the top 200 meters of the global ocean is 0.75 (± 0.59 absolute deviation) μM C is much higher than the median. Patchiness or heterogeneity of macro-zooplankton biomass distribution is evident at high latitudes where concentrations range between 0 and 100 μM C.

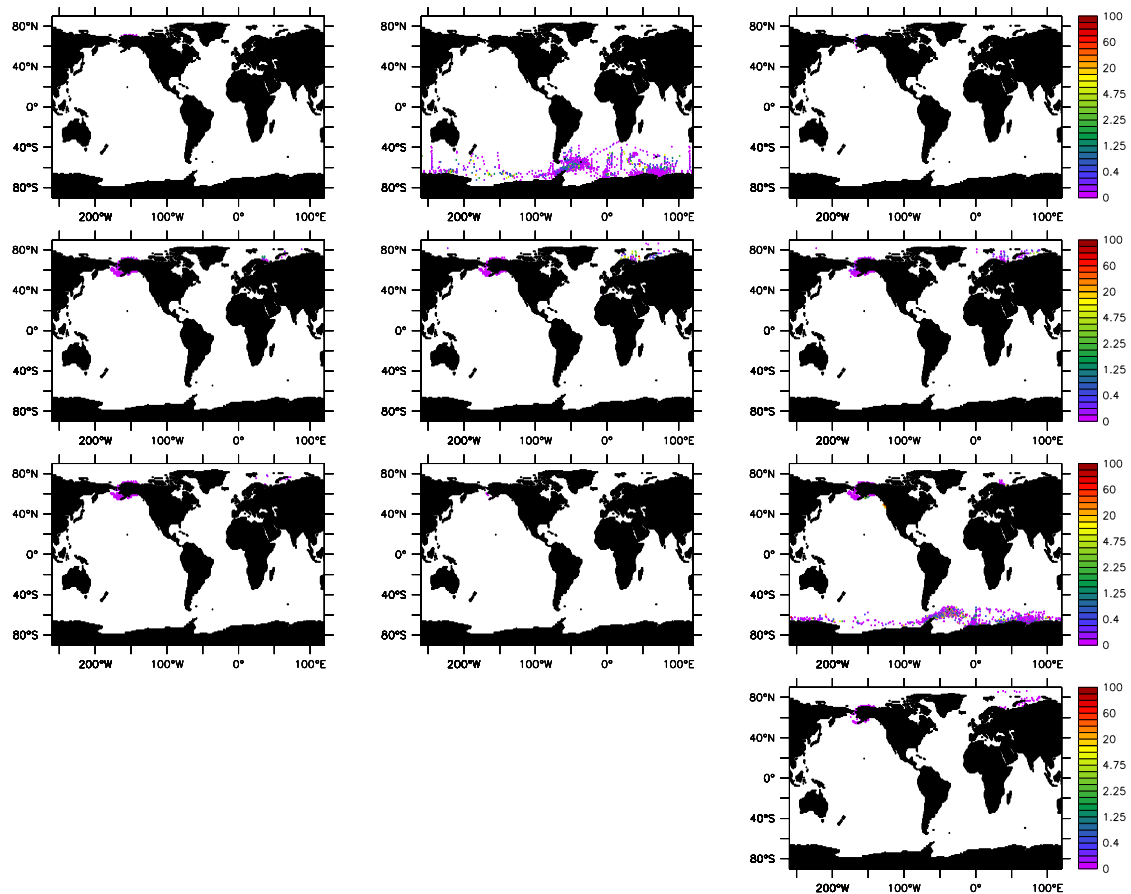


Figure 3.5: The annual average biomass ($\mu\text{M C}$) in the top 200 meters of the world ocean. Panels show the distribution of *Bolionopsis infundibulum* and *Pleurobrachia pileus* (ctenophores) [top row left], *Salpa thompsoni* and *Ihlea racovitzai* (salps) (KRILLBASE) [top row centre], *Cyaena capillata* (scyphozoan) [top row right], *Agalantha digitale*, *Eutonina indicans*, *Gonionemus vertens*, *Philalidium gregarium*, *Sarsia princes*, *Sarsia tubulosa*, *Stomatocystis atra* and *Agalma elegans* (hydrozoan) [2nd row left], *Clione limacina*, *Diacrea trispinosa* and *Limacina helicina* (pelagic molluscs) [2nd row centre], *Sagitta elegans* and *Sagitta enflata* (chaetognaths) [2nd row right], *Cyphocaris challengeri*, *Hyperia galba*, *Parathemisto japonica*, *Themisto libellula*, *Phronima sedentaria* and *Themisto pacifica* (amphipods) [3rd row left], *Acanthomysis pseudomacropsis* (mysid) [3rd row centre], *Euphausia superba*, *Euphausia pacifica*, *Meganyctiphanes norvegica*, *Thysanoessa inermis*, *Thysanoessa longipes*, *Thysanoessa raschi* and *Thysanoessa spinifera* (euphausiids)* [3rd row right] and *Fritillaria borealis sargassi*, *Fritillaria haplostomai* and *Oikopleura dioica* [bottom row right]. All distribution data, unless otherwise stated, are from COPEPOD.* data from COPEPOD and KRILLBASE. White indicates no data.

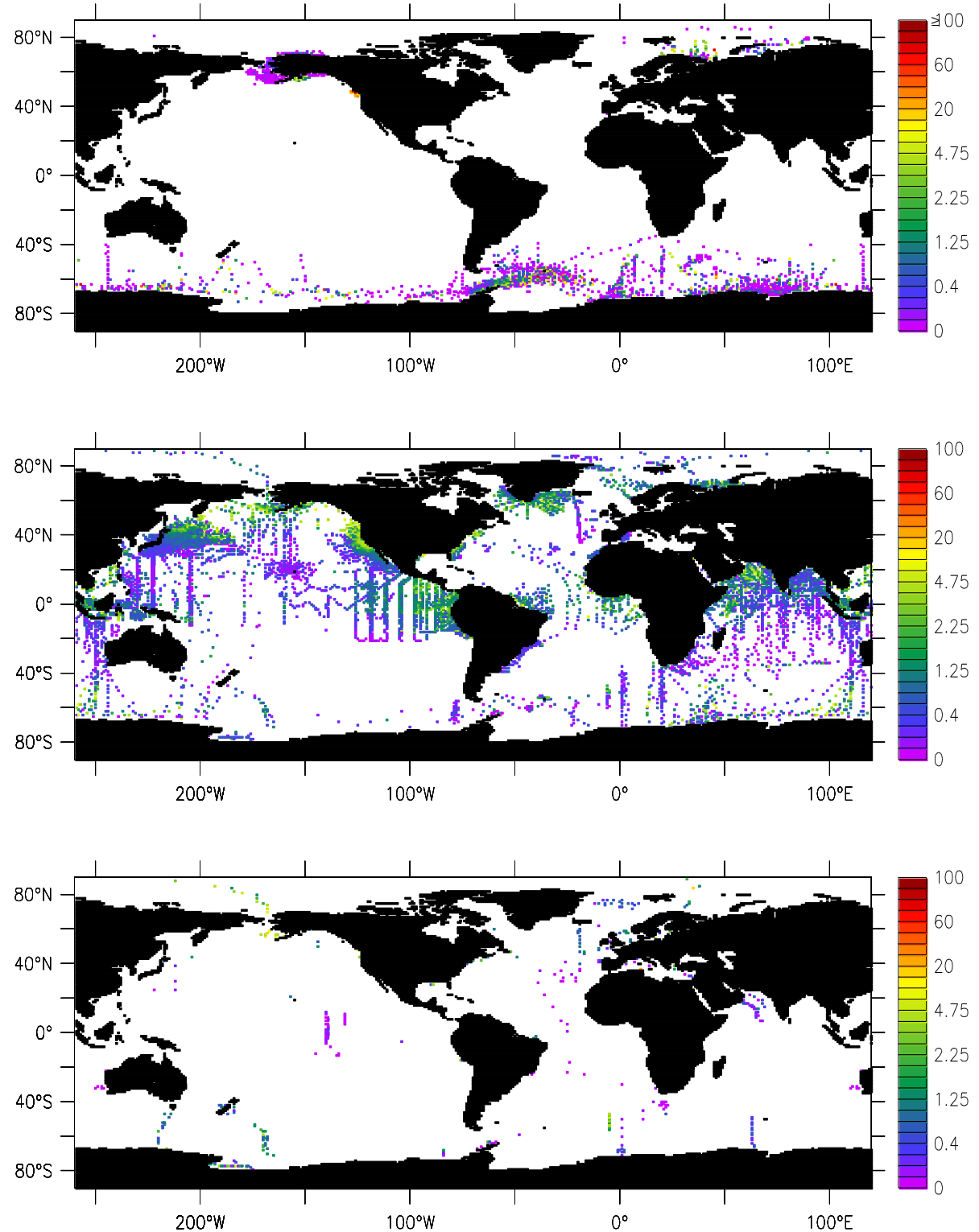


Figure 3.6: The annual average of total biomass of in the top 200 meters of the world ocean. Panels show the frequency of macro-zooplankton [top], meso-zooplankton [centre] (Buitenhuis et al. 2006) and proto-zooplankton [lower] biomass ($\mu\text{M C}$) (Buitenhuis et al. 2009). White indicates no data.

For comparison sake the global annual average biomass distribution of macro-, meso- and proto-zooplankton (Figures 3.6 and 3.7) are compared. Meso-zooplankton have the most comprehensive biomass data set and consequently distribution. The macro-zooplankton data set

follows and then the relatively data poor data set of the proto-zooplankton. The macro- and proto-zooplankton share a similar frequency distribution with low background biomass compared to meso-zooplankton yet they can sustain levels of high biomass comparable if not greater than the meso-zooplankton. This is particularly evident in the macro-zooplankton (Figure 3.6).

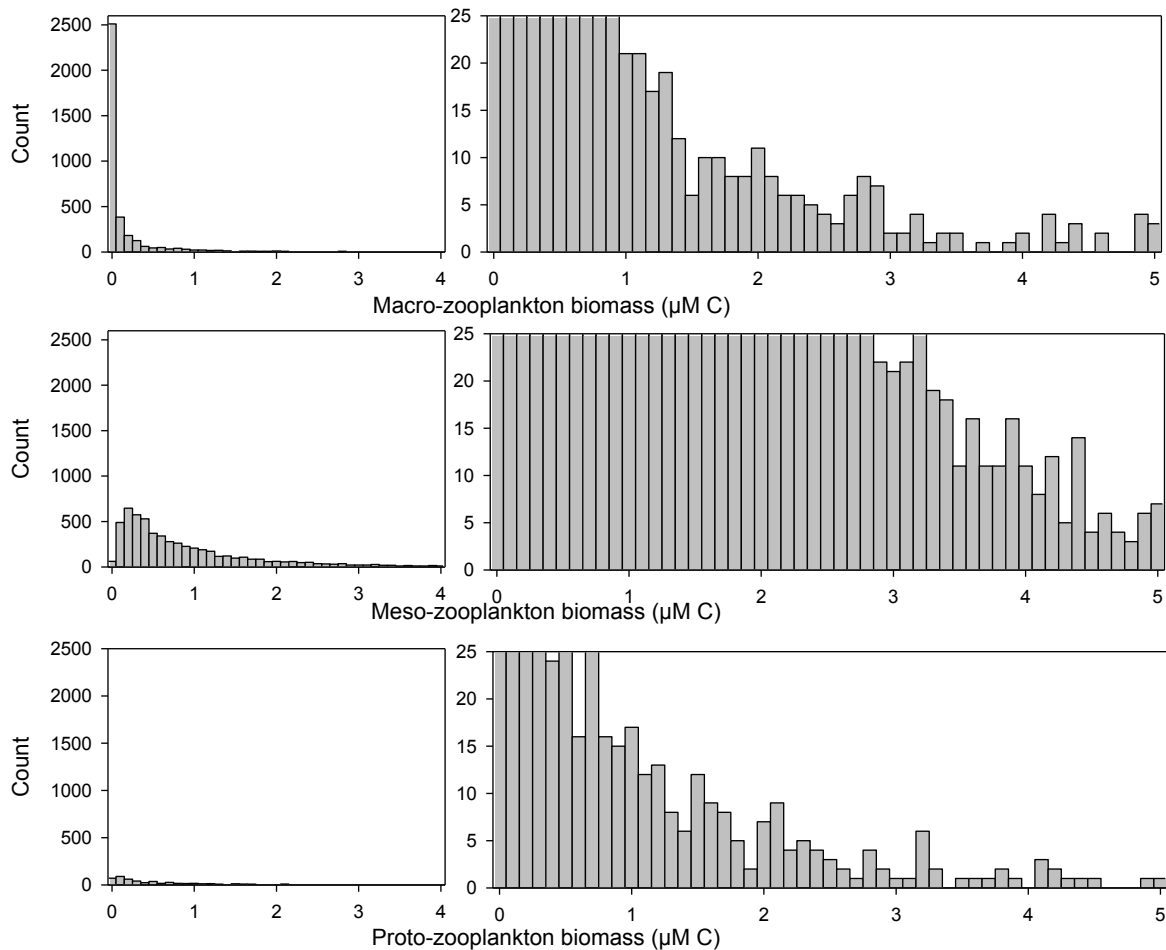


Figure 3.7: The annual average distribution of total biomass of macro-zooplankton [top] ($\mu\text{M C}$), meso-zooplankton [centre] ($\mu\text{M C}$) (Buitenhuis et al. 2006) and proto-zooplankton [lower] ($\mu\text{M C}$) (Buitenhuis et al. 2009) in the top 200 meters of the world ocean. Note: not all abundance data shown.

3.5 DISCUSSION

Abundance data are not readily convertible to biomass data without introducing appreciable error.

To obtain a realistic distribution and biomass measure it was necessary to try to constrain the error as much as possible. Therefore, two sets of distribution maps were produced; abundance and biomass. The abundance map indicates where in the global ocean macro-zooplankton can be found, how many individuals are present, and the coherence of their abundance, i.e. even or

patchy. The biomass map indicates realistic biomass values in the regions where abundance data was amenable to carbon conversion. Error was minimised at every level. To reduce the error, carbon conversions at a group level (Figure 3.1) was not used to convert from abundance to biomass because in some groups body mass ranged over ~8 orders of magnitude. Converting abundance data where animal size spans such a range introduced a major uncertainty. Species-specific conversion were preferred even though only 19,649 out of 206,514 abundance data points from COPEPOD were resolved to species level. Of the 19,649, species-specific conversions could only be applied to the 11,186 abundance data points where taxonomic data extended as far as species. Where taxonomic data did extend as far as species level, species-specific data were not available to convert all 274 taxa. The standard deviation associated with species-specific conversions used to convert COPEPOD abundance data to biomass is shown in Table 3.1. Although the standard deviation of species-specific body mass is high in many cases this error is lower than the error calculated for the groups presented in Figure 3.1. Standard deviation, as percentage of mean value, of species-specific carbon conversion ranged between 23-276% with a mean of 84% while the standard deviation of group-specific carbon conversion ranged between 30-518% with a mean of 276%.

The type and magnitude of error associated with COPEPOD and KRILLBASE data sets are quite different. The KRILLBASE data set refers only to three species; *Euphausia superba*, *Salpa thompsoni* and *Ihlea racovitzia*. There is a huge amount of literature associated with the abundance data contained in KRILLBASE (e.g., Nishikawa et al. 1995, Quetin et al. 1996, Loeb et al. 1997, Pakhomov et al. 2002, Atkinson et al. 2004, Pakhomov 2004). Other studies of these species in the Southern Ocean include length and mass measurements of *Euphausia superba* (Morris et al. 1988) and *Salpa thompsoni* (Heron et al. 1988, Huntley et al. 1989, Dubischar et al. 2006), information on their chemical composition (Raymont et al. 1971) and information on community biomass in different regions of the Southern Ocean (Hopkins 1971, 1985, Hopkins & Torres 1988, Lancraft et al. 1989, Hernandez-Leon et al. 1999, Pakhomov et al. 2006). In this instance converting first from individual to realistic dry mass calculated from length frequency data gives a more accurate estimation of carbon body mass when applying a carbon conversion.

KRILLBASE (Atkinson et al. 2004) is restricted to the Southern Ocean and these three species. COPEPOD is a global data base with varying taxonomic resolution, i.e. animals identified at varying taxonomic levels from phylum to species. In order to locate all the associated literature, a detailed review of macro-zooplankton abundance and biomass literature would be necessary. Even then the taxonomic resolution would remain limiting. This type of review was outside the scope of this investigation.

COPEPOD data were converted directly from abundance to carbon biomass using species-specific carbon conversions. There was no estimation of body size for the individuals. Without detailed information on the size range, length or mass, of individual species it was difficult to assess the variation in carbon composition within a species over the size range of that species. The carbon conversion used is based on limited data for many of the species considered in the COPEPOD data set. Compared to the detailed information available for the KRILLBASE data, the error was much greater. Lack of taxonomic resolution, species size and carbon composition data explain why all KRILLBASE data and only ~5% of the COPEPOD data was used to produce the biomass distribution map. From the abundance distribution it is clear that there are three distinct regions with respect to data coverage: 1) well covered, e.g. the Southern Ocean, Indian Ocean, North Sea, eastern North Pacific, Californian coast and the east coast of the USA, 2) covered, e.g. the South Atlantic, Caribbean and the Arctic, 3) regions where there are no abundance data, e.g. large parts of the Pacific Ocean and the North Atlantic. Gaps in the distribution of biomass are even more apparent as only three areas are covered with data; the Southern Ocean, the eastern North Pacific and the Arctic.

The primary sources of data for this study have come from NMFS and the British Antarctic Survey (BAS). There are a number of sources in the US and the UK that were originally targeted in an effort to gather all the available data. Three of these data sets shall be discussed here in brief. Currently data sets such as the Continuous Plankton Recorder (CPR) north Atlantic macro-zooplankton distribution and abundance data are not available to those working outside the Sir Alistair Harvey Foundation for Ocean Science (SAHFOS). Restriction of access to this data set is the main limitation facing those interested in using this data for model evaluation or

parameterization purposes. If the CPR macro-zooplankton data was published as a data set with its own digital object identifier (doi) it would allow the wider scientific community access to the data while those responsible for sample collection and analysis are recognized and credited through citation. It is currently possible to publish data sets in this manner but it is by no means the 'norm'. There are other limitations associated with macro-zooplankton data collected using the CPR. Some species of macro-zooplankton actively avoid capture in the CPR and others are too large to fit through the device opening. This means that only small macro-zooplankton species are represented in CPR data. This data can only be used as a presence/absence guide for these smaller macro-zooplankton species across the north Atlantic. It is difficult to assess whether the data contained in this data set can be useful in estimating abundance of macro-zooplankton in the north Atlantic. The accurate identification and live size estimate of macro-zooplankton species captured on the CPR may allow a more precise carbon conversion which could possibly be useful in converting abundance estimates to biomass.

The Hawaii Ocean Time-series Study (HOTS) and Bermuda Atlantic Time-series Study (BATS) Joint Global Ocean Flux Study (JGOFS) data sets were not originally investigated as part of the data trawl because of their limited spatial coverage and the time constraints of the project. JGOFS was a interdisciplinary study initiated to bring about understanding of the biological, chemical and physical processes that control the oceanic carbon cycle and to understand the role of the oceans in the large scale processes associated with global change. HOTS and BATS are two long term time series oceanographic sites that were chosen to represent the North Pacific subtropical gyre and the western North Atlantic, respectively. Repeated and comprehensive studies of hydrography, chemistry and biology have been undertaken at both sites, in an effort to describe the processes occurring at these sites, which are representative of the region. HOTS data is currently available on line and it is possible to extract location, depth, abundance, wet, dry and carbon mass for macro-zooplankton. BATS data is currently being incorporated into COPEPOD in much the same way as the California Cooperative Oceanic Fisheries Investigations (CalCOFI) data has been, and as such is included in this analysis, but macro-zooplankton data from BATS is not readily available yet. Here the main limitation was the data availability of the BATS data set.

Maps produced from abundance data give an indication of the global distribution of macro-zooplankton in ind. L⁻¹ in the top 200 m of the world ocean. It is clear from the data presented in Figure 3.2 that there are differences in the distribution of macro-zooplankton abundance between low and high latitudes. At low latitudes abundance ranges between 0 and 0.05 ind. L⁻¹. At high latitudes abundance is patchy and ranges from 0 to 30 ind. L⁻¹. Spatial heterogeneity has long been associated with zooplankton (Haeckel 1891). Patchiness in zooplankton is the result of both physical and biological processes operating on a variety of spatial scales. Physical processes such as micro-scale turbulence, Langmuir circulation, currents and eddies can drive patchiness in macro-zooplankton and occur over a variety of scales (1 mm to 1000s km) (Pinel-Alloul 1993, Folt & Burns 1999). Over smaller scales (1 mm to 10 m) biological processes are often more important (Folt & Burns 1999). Individual behaviour, e.g. mating, predator avoidance and searching for food (Folt & Burns 1999), and variables such as food concentration, swimming behaviour (Pinel-Alloul 1993) and species interactions (Mackas et al. 1985) are important examples of small scale biological processes. From the abundance data presented in Figure 3.4 it appears that spatial heterogeneity in macro-zooplankton abundance is less pronounced in the tropics compared to the high latitudes. The high latitudes are high energy and high productivity regions (Longhurst 1998). A combination of high productivity, decreased stability of the water column, physical and biological processes on a variety of temporal and spatial scales is most likely responsible for the differences in abundance seen between the high latitudes and the relatively stable tropics (in terms of mixed layer depth and energy input).

Some of the difference between abundance at low and high latitudes may be attributed to the ‘bloom’ capabilities of some species associated with high latitudes e.g. *Salpa thompsoni*, location, seasonal and/or species sampling bias. High abundance in the Southern Ocean is in part explained by a bias towards seasons of high productivity as sampling is not usually carried out during the winter months. Sampling, in the case of the KRILLBASE data, targeted specific species and sampling was designed around areas where a particular species might be found. *Euphausia superba* and *Salpa thompsoni*, in particular, can occur at high concentrations (i.e., ~30 ind. L⁻¹) (Perissinotto & Pakhomov 1998, Atkinson et al. 2004) so it is not surprising that there

are patches of high concentration found in the Southern Ocean. Data from the COPEPOD data set is a collection of data on different groups of macro-zooplankton. It is a record of all groups or species that were in the region that was sampled, high concentrations of a particular species were not targeted.

There is less information for biomass distribution. Data are restricted to the higher latitudes. Biomass distribution is patchy with concentrations ranging between 0 and 100 $\mu\text{M C}$. Macro-zooplankton have a low median concentration yet are capable of reaching very high (>100 $\mu\text{M C}$) biomass concentrations (Figure 3.5). As this is the first global validation data set for the macro-zooplankton it is difficult to assess it other than in general terms, i.e. are the macro-zooplankton where they are expected to be found and are they present at reasonable concentrations? As the only data on biomass is found in higher latitudes it is not possible to compare regions of high and low productivity.

To place macro-zooplankton biomass distribution in context, it is necessary to look at the biomass distribution of the meso- and proto-zooplankton (Figure 3.6). Global data sets of meso- and proto-zooplankton biomass distribution have recently been produced for the validation of these PFTs in PlankTOM10. For meso-zooplankton a comprehensive biomass distribution has been put together by Buitenhuis et al. (2006) including 184,278 data points. Buitenhuis et al. (2009) have also produced a proto-zooplankton biomass distribution including 4629 data points. From biomass presented for the three zooplankton groups it is clear that areas associated with high productivity, e.g. continental shelf waters, have higher zooplankton biomass than areas associated with low productivity, e.g. high nutrient low chlorophyll (HNLC) areas. It is difficult to extrapolate outside of this general pattern as there are too many gaps in the biomass data sets belonging to each group, perhaps with the exception of meso-zooplankton. The distribution and median biomass of macro-zooplankton, 0.006 (± 1.33 absolute deviation) $\mu\text{M C}$, is lower than that of meso- and proto-zooplankton, 0.61 (± 0.34 absolute deviation) and 0.43 (± 0.45 absolute deviation) $\mu\text{M C}$ respectively (Figure 3.7). Macro- and proto-zooplankton share similar frequency distributions occurring at low concentrations overall with patches of very high concentration. Macro- and proto-zooplankton have a lower mean biomass, 0.75 (± 0.59 standard deviation) and

0.66 (\pm 0.22 standard deviation) $\mu\text{M C}$, respectively compared to that of meso-zooplankton, 0.98 (\pm 0.03 standard deviation) $\mu\text{M C}$ for the meso-zooplankton, all mean values are significantly different at a 95% confidence level. Macro- and proto-zooplankton occur in patches with a much higher concentration of biomass than meso-zooplankton. Under favourable environmental conditions both macro- and proto-zooplankton can occur at very high biomass ($>100 \mu\text{M C}$). Proto-zooplankton have growth rates similar to those in phytoplankton and respond to phytoplankton blooms by dampening bloom formation through grazing (Le Quéré et al. 2005). Growth rates for a number of groups within the macro-zooplankton, particularly the gelatinous members, salps, ctenophores, cnidarians and appendicularians are higher than those of meso-zooplankton copepods (Hirst et al. 2003). The ability of these groups to ‘bloom’ or to swarm, through a combination of high grazing rates, growth rates and life history, when food concentration or other environmental factors are favourable, means that macro-zooplankton may reach high biomass concentrations in areas where they amass resulting in a spatially heterogeneous distribution. Meso-zooplankton on the other hand have a higher mean concentration and have a more homogenous distribution (Buitenhuis et al. 2006).

In order to place macro-zooplankton biomass in a wider context total heterotrophic biomass is examined in relation to total autotrophic biomass in the open ocean (Figure 3.8). The mean concentration for each group is considered and the heterotrophic component relative to the autotrophic component of the plankton is calculated. Lower biomass in the autotrophic component of the ecosystem reflects the higher turnover and metabolic costs of these small organisms (Odum 1971). With higher turnover and metabolic costs a low standing crop with high productivity can supply higher trophic levels with the energy that is then stored in their biomass because of lower turnover and metabolic costs. As the data for each plankton group presented in Figure 3.8 are mainly representative of the open ocean environment it is not surprising that an inverted pyramid with a high H:A (heterotroph:autotroph) ratio as predicted by Gasol et al., (1997) is found. Judging from the standard deviation associated with the macro-zooplankton (Figure 3.8) much work needs to be carried out before a more precise representation of heterotrophic plankton may be presented. Although data is not presented for trophic levels higher

than macro-zooplankton a recent study by Jennings et al. (2008) maps the spatial distribution of marine fish biomass ($>1 \times 10^{-5}$ g wet mass). The modelled biomass distributions of teleost fish from Jennings et al. (2008) look as if they are in spatial agreement with the biomass distribution of macro-zooplankton presented here.

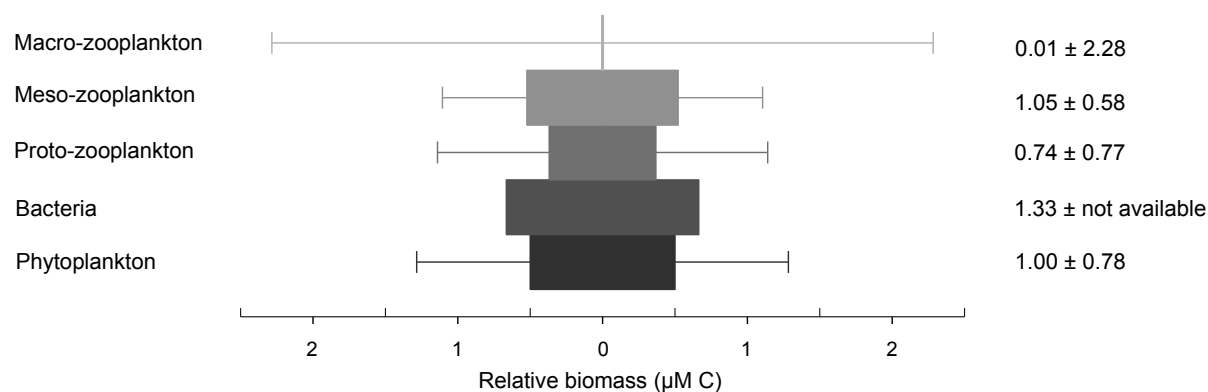


Figure 3.8: Median and absolute deviation of heterotrophic phytoplankton (bacteria (Whitman et al. 1998), proto- (Buitenhuis et al. 2009), meso- (Buitenhuis et al. 2006) and macro-zooplankton) biomass relative to that of autotrophic (Conkright et al. 2002) biomass for the global ocean. Numbers are the relative median concentration ($\mu\text{M C}$) of each group \pm the relative absolute deviation for the group. There is no data on the error associated with heterotrophic bacterial biomass as there was no information on the error of the original estimate. For phytoplankton chlorophyll concentration was converted to biomass using a C:Chl ratio of 50 (Uitz et al. 2006).

3.6 CONCLUSIONS

A partial picture of macro-zooplankton abundance and biomass distribution is presented here.

Despite the obvious gaps in both abundance and biomass distribution some insight on the varying distribution of abundance and biomass of macro-zooplankton from the poles to the tropics has been gained. It has also been possible to estimate the global biomass of macro-zooplankton. This work is presented as a first step towards a quantitative global distribution of macro-zooplankton biomass. A qualitative and to some extent a quantitative, $0.006 (\pm 1.33 \text{ absolute deviation}) \mu\text{M C}$, estimate of macro-zooplankton biomass in the global ocean has been provided through this work. This data set may be improved; additional information may be found in the published literature, national data centres and with the original experimentalists. Systems for the dissemination of data sets, such as data useful in model validation, are currently being implemented. Experimentalists are being encouraged to submit their data to national data centres. Through these data centres data

will become available to the wider scientific community. Undertaking a detailed review of the macro-zooplankton biomass literature was outside the scope of this investigation and apart from COPEPOD no other national data centre was in a position to facilitate requests for data. Communication between biogeochemical modellers, data managers and experimentalists is continually improving (Le Quéré & Pesant 2009) and there is an ever increasing impetus within the modelling community to acquire and share the data necessary to parameterise and validate models.

The validation of macro-zooplankton the PFT in PlankTOM10 will be discussed in the next chapter.

REFERENCES

- Atkinson A, Siegel V, Pakhomov E, Rothery P (2004) Long-term decline in krill stock and increase in salps within the Southern Ocean. *Nature* 432:100-103
- Atkinson A, Siegel V, Pakhomov E A, Jessopp M J, Loeb V (2009) A re-appraisal of the total biomass and annual production of Antarctic krill. *Deep-Sea Research Part I-Oceanographic Research Papers* 56:727-740
- Behrenfeld M J, O'Malley R T, Siegel D A, McClain C R, Sarmiento J L, Feldman G C, Milligan A J, Falkowski P G, Letelier R M, Boss E S (2006) Climate-driven trends in contemporary ocean productivity. *Nature* 444:752-755
- Behrenfeld M J, Randerson J T, McClain C R, Feldman G C, Los S O, Tucker C J, Falkowski P G, Field C B, Frouin R, Esaias W E, Kolber D D, Pollack N H (2001) Biospheric primary production during an ENSO transition. *Science* 291:2594-2597
- Buitenhuis E T, Le Quéré C, Aumont O, Beaugrand G, Bunker A, Hirst A, Ikeda T, O'Brien T, Piontkovski S, Straile D (2006) Biogeochemical fluxes through mesozooplankton. *Global Biogeochemical Cycles* 20
- Buitenhuis E T, Rivkin R, Sailley S, Le Quéré C (2009) Global biogeochemical fluxes through microzooplankton. *Limnology and Oceanography*
- Conkright M E, O'Brien T D, Stephens C, Locarnini R A, Garcia H E, Boyer T P, Antonov J I (2002) World Ocean Atlas 2001, Volume 6: Chlorophyll. In: S Levitus (ed) NOAA Atlas NESDIS 52. U.S. Government Printing Office, Washington, D.C., p CD-ROMs. B. 46
- Dubischar C D, Pakhomov E A, Bathmann U V (2006) The tunicate *Salpa thompsoni* ecology in the Southern Ocean II. Proximate and elemental composition. *Marine Biology* 149:625-632
- Folt C L, Burns C W (1999) Biological drivers of zooplankton patchiness. *Trends in Ecology & Evolution* 14:300-305

- Gasol J M, del Giorgio P A, Duarte C M (1997) Biomass distribution in marine planktonic communities. *Limnology and Oceanography* 42:1353-1363
- Haeckel E (1891) Plankton Studien. *Jenn Zeitschrift für Naturwissenschaft* 25:232-336
- Hernandez-Leon S, Torres S, Gomez M, Montero I, Almeida C (1999) Biomass and metabolism of zooplankton in the Bransfield Strait (Antarctic Peninsula) during austral spring. *Polar Biology* 21:214-219
- Heron A C, McWilliam P S, Dalpont G (1988) Length weight relation in the salp *Thalia democratica* and potential of salps as a source of food. *Marine Ecology-Progress Series* 42:125-132
- Hirst A G, Bunker A J (2003) Growth of marine planktonic copepods: global rates and patterns in relation to chlorophyll *a*, temperature, and body weight. *Limnology and Oceanography* 48:1988-2010
- Hirst A G, Roff J C, Lampitt R S (2003) A synthesis of growth rates in marine epipelagic invertebrate zooplankton. *Advances in Marine Biology* 44:1-142
- Hopkins T L (1971) Zooplankton standing crop in the Pacific sector of the Antarctic. In: G W Llano, Wallen I E (eds) *Biology of the Antarctic Seas IV Antarctic Research Service Vol 17*
- Hopkins T L (1985) The zooplankton community of Croker Passage, Antarctic Peninsula. *Polar Biology* 4:161-170
- Hopkins T L, Torres J J (1988) The zooplankton community in the vicinity of the ice edge, Western Weddell Sea, March 1986. *Polar Biology* 9:79-87
- Huntley M E, Sykes P F, Marin V (1989) Biometry and trophodynamics of *Salpa thompsoni* Foxton (Tunicata, Thaliacea) near the Antarctic Peninsula in Austral Summer, 1983-1984. *Polar Biology* 10:59-70
- Jennings S, Melin F, Blanchard J L, Forster R M, Dulvy N K, Wilson R W (2008) Global-scale predictions of community and ecosystem properties from simple ecological theory. *Proceedings of the Royal Society B-Biological Sciences* 275:1375-1383
- Lancraft T M, Torres J J, Hopkins T L (1989) Micronekton and macrozooplankton in the open waters near Antarctic Ice Edge Zones (Ameriez-1983 and Ameriez-1986). *Polar Biology* 9:225-233
- Le Quéré C (2008) The EUROCEANS global PFT biomass database for model evaluation, British Antarctic Survey, Cambridge, UK
- Le Quéré C, Harrison S P, Prentice I C, Buitenhuis E T, Aumont O, Bopp L, Claustre H, Da Cunha L C, Geider R, Giraud X, Klaas C, Kohfeld K E, Legendre L, Manizza M, Platt T, Rivkin R B, Sathyendranath S, Uitz J, Watson A J, Wolf-Gladrow D (2005) Ecosystem dynamics based on plankton functional types for global ocean biogeochemistry models. *Global Change Biology* 11:2016-2040
- Le Quéré C, Pesant S (2009) Plankton Functional Types in a new generation of biogeochemical models. *EOS : Transactions American Geophysical Union*
- Loeb V, Siegel V, HolmHansen O, Hewitt R, Fraser W, Trivelpiece W, Trivelpiece S (1997) Effects of sea-ice extent and krill or salp dominance on the Antarctic food web. *Nature* 387:897-900
- Longhurst A (1998) *Ecological Geography of the Sea*. Academic Press, London
- Mackas D L, Denman K L, Abbott M R (1985) Plankton patchiness: biology in the physical vernacular. *Bulletin of Marine Science* 37:652-674

- Mills E L (1989) Biological Oceanography. An early history. Cornell University Press, Ithaca
- Moriarty R (2009) Respiration rates in epipelagic macro-zooplankton: a data set. PANGAEA
- Morris D J, Watkins J L, Ricketts C, Buchholz F, Priddle J (1988) An assessment of the merits of length and weight measurements of Antarctic krill *Euphausia superba*. British Antarctic Survey Bulletin:27-50
- Nishikawa J, Naganobu M, Ichii T, Ishii H, Terazaki M, Kawaguchi K (1995) Distribution of salps near the South Shetland Islands During Austral Summer, 1990-1991 with special reference to krill distribution. Polar Biology 15:31-39
- O'Brien T D (2005) COPEPOD: A global plankton database, U.S. Dep. Commerce, NOAA Technical Memorandum. NMFS-F/SPO-73
- Odum E P (1971) Fundamentals of Ecology. W. B. Saunders, Philadelphia
- Pakhomov E A (2004) Salp/krill interactions in the eastern Atlantic sector of the Southern Ocean. Deep-Sea Research Part II-Topical Studies in Oceanography 51:2645-2660
- Pakhomov E A, Dubischar C D, Strass V, Brichta M, Bathmann U V (2006) The tunicate *Salpa thompsoni* ecology in the Southern Ocean. I. Distribution, biomass, demography and feeding ecophysiology. Marine Biology 149:609-623
- Pakhomov E A, Froneman P W, Perissinotto R (2002) Salp/krill interactions in the Southern Ocean: spatial segregation and implications for the carbon flux. Deep-Sea Research Part II-Topical Studies in Oceanography 49:1881-1987
- Perissinotto R, Pakhomov E A (1998) Contribution of salps to carbon flux of marginal ice zone of the Lazarev Sea, Southern Ocean. Marine Biology 131:25-32
- Pinel-Alloul B (1993) Spatial Heterogeneity as a Multiscale Characteristic of Zooplankton Community. 2nd International Joint Conference on Limnology and Oceanography, Evian, France
- Quetin L B, Ross R M, Frazer T K, Haberman K L (1996) Factors affecting distribution and abundance of zooplankton, with an emphasis on Antarctic krill, *Euphausia superba*. Antarctic Research Series:357-371
- Raymont J E G, Srinivas R T, Raymont J K B (1971) Biochemical studies on marine zooplankton.9. Biochemical composition of *Euphausia superba*. Journal of the Marine Biological Association of the United Kingdom 51:581-588
- Uitz J, Claustre H, Morel A, Hooker S B (2006) Vertical distribution of phytoplankton communities in open ocean: an assessment based on surface chlorophyll. Journal of Geophysical Research-Oceans 111:23
- Whitman W B, Coleman D C, Wiebe W J (1998) Prokaryotes: The unseen majority. Proceedings of the National Academy of Sciences of the United States of America 95:6578-6583
- Yoder J A, Kennelly M A (2003) Seasonal and ENSO variability in global ocean phytoplankton chlorophyll derived from 4 years of SeaWiFS measurements. Global Biogeochemical Cycles 17:14

4 MACRO-ZOOPLANKTON IN THE GLOBAL OCEAN BIOGEOCHEMICAL MODEL PLANKTOM10v1.0

4.1 ABSTRACT

Macro-zooplankton play an important part in the removal of carbon from the surface layers of the ocean to the deep ocean. Their role in the export of large particulate organic carbon distinguishes them from other types of zooplankton. The explicit representation of macro-zooplankton in a Plankton Functional Type (PFT) model is essential to capture the effect of macro-zooplankton on the natural carbon cycle. Specially synthesised data sets for process rate measurements allow the representation of macro-zooplankton in the biogeochemical model PlankTOM10. Following a set of model simulations based on parameterisations of macro-zooplankton and its component groups: gelatinous, semi-gelatinous, crustacean and appendicularians, the crustacean parameterisation was chosen for the standard simulation of macro-zooplankton. Macro-zooplankton activity affected other PFTs, with the largest impact on PFTs of the highest trophic level represented. Macro-zooplankton exerted strong control on the biomass of meso- and proto-zooplankton. Without tuning, the standard model simulation using crustacean parameterisation reproduced a biomass for meso- and macro-zooplankton of 0.52 and 0.003 Pg C, close to observations. The contribution of macro-zooplankton to carbon export production ranged from 0.26 Pg C y⁻¹ in the standard model simulation to 0.57 Pg C y⁻¹ in an optimised simulation where grazing threshold, grazing rate and particulate egestion were increased. The model was unable to reproduce the patchy distribution and high biomass concentrations (> 100 µM C) observed for biomass and this had implications for their contribution to export production.

4.2 INTRODUCTION

Macro-zooplankton are a diverse collection of metazoan groups whose adult body size is ≥ 2 mm in length. The macro-zooplankton data synthesised for this study includes information on the following groups: ctenophores, salps, doliolids, pyrosomes, cnidaria, pelagic molluscs, pelagic polychaetes, chaetognaths, amphipods, decapods, mysids, stomatopods, euphausiids and appendicularians. These groups are divided into four categories based on their carbon composition; gelatinous, semi-gelatinous, crustacean and appendicularian (Table 4.1). Macro-zooplankton repackage both autotrophic and heterotrophic production through a variety of

feeding strategies such as predation, ‘true’ filter feeding and suspension feeding, and through their food preferences.

Table 4.1: Carbon composition of groups within the macro-zooplankton (see Table 2.3 for greater detail).

	Group	Carbon (% dry mass)
Gelatinous	Ctenophores, salps, doliolids, pyrosomes & cnidaria	~ 1 to 30
Semi-gelatinous	Pelagic molluscs, pelagic polychaetes & chaetognaths	~ 15 to 50
Crustacean	Amphipods, decapods, stomatopods, mysids & euphausiids	~ 20 to 60
Appendicularian	Appendicularians	~ 50 to 60

Macro-zooplankton are intricately linked to both higher and lower trophic levels. Some macro-zooplankton feed directly on the trophic level below them following the classical food web. They are also capable of feeding on much smaller prey with the ‘true’ filter feeders salps, doliolids and appendicularians effectively ‘short circuiting’ the microbial loop through the consumption of bacteria and small particles, making this material available to higher trophic levels (Deibel 1998) and/or exporting it in part to the deep sea. The unassimilated carbon is removed from the surface of the ocean through the rapid sinking of faecal pellets. The faecal pellets of some macro-zooplankton sink up to one order of magnitude faster than marine snow and phyto-detritus (Turner 2002). There is variation within the sinking rates of macro-zooplankton faecal pellets (Table 1.4). This reflects both the collection of different groups that comprise the macro-zooplankton and the composition of the faecal pellets. Faecal pellets produced by doliolids are not very compact and sink only tens to hundreds of meters per day (Madin 1982, Deibel 1990) whereas the compact faecal pellets of salps and pteropods sink tens to thousands of meters per day (Bruland & Silver 1981). The tendency of macro-zooplankton to ‘bloom’ during favourable environmental conditions (Purcell 2005) means they can contribute to carbon export during mass export events where faecal pellets, of salps in particular (Bathmann 1988, Perissinotto & Pakhomov 1998), discarded feeding structures and unconsumed biomass (Lebrato & Jones 2009) sink from the euphotic zone to the deep sea.

Changes to the pelagic realm, e.g. stratification caused by warming or the removal of fish biomass, have knock on effects for macro-zooplankton. As these and other changes are occurring at the same time it becomes increasingly difficult to establish a baseline for macro-

zooplankton distribution and biomass in the global ocean. To assess how macro-zooplankton and their role in carbon export may be changing, it is important to understand the natural variability of macro-zooplankton. For most researchers or experimentalists that work with macro-zooplankton it is necessary to collect or monitor specimens in their natural environment. This is costly in terms of time and funding. The returns from this type of work give a temporally and spatially limited picture of macro-zooplankton. Field work is fundamental to gain information about macro-zooplankton but it is slow and it does not provide a global baseline. Models are useful tools to gain a global insight into the distribution and variability in macro-zooplankton in a changing environment. Models such as PlankTOM10 may be used to identify macro-zooplankton sensitivities that are associated with changes in temperature, stratification, food concentration or availability, changes in ecosystem structure on physiological or ecological process rates. Changes in these process rates may have implication for both biomass concentration and distribution.

Macro-zooplankton have been included as a PFT in the biogeochemical model PlankTOM10. Macro-zooplankton were parameterised using syntheses of observed physiological and community process rates. The PlankTOM model already included representations of proto- and meso-zooplankton (Buitenhuis et al. 2006, Buitenhuis et al. 2009). The addition of a third zooplankton group, the macro-zooplankton allows a fuller appreciation of lower trophic levels and their interactions. An independent biomass data set (Chapter 3) was constructed to validate the macro-zooplankton in PlankTOM10. Model simulations were carried out to identify if it was possible to reproduce primary production, export, chlorophyll *a* distribution and PFT biomass distributions, using macro-zooplankton parameterisation. The same approach was applied with parameterisations based at group level, i.e. gelatinous, semi-gelatinous, crustacean and appendicularians. The macro-zooplankton parameterisation that gave results closest to observations without tuning was chosen as the standard run. The standard run was then tuned to observational data. Tuning of macro-zooplankton was achieved by varying parameter values within the constraints of the data.

4.3 METHODS

4.3.1 MODEL

PlankTOM10 is coupled to the physical model NEMO v2.3 (Madec 2008). NEMO is a general circulation model. It describes a non-linear equation of state and the motion of fluid using equations based on Navier-Stokes equations. It has a horizontal resolution of 2° longitude and $\sim 1.1^\circ$ latitude. The vertical resolution is 10 m in the top 100 m and decreases to 500 m at depth. NEMO is coupled to a thermodynamic sea-ice model LIM (Timmermann et al. 2005). This sea-ice model is particularly suited to climate model studies where the ice edge is examined from coarse grid resolutions. Vertical mixing is calculated at all depths using a turbulent kinetic energy model (Gaspar et al. 1990) and sub-grid eddy induced mixing (Gent & McWilliams 1990).

There are a total of 39 biogeochemical tracers in PlankTOM10. There are full biogeochemical cycles for phosphate, nitrate, silicate, carbon and oxygen, and a simplified iron cycle. The biogeochemical cycles were originally based on the PISCES model of Aumont et al. (2003) and modified by Buitenhuis et al. (2006). Details of the modifications that lead to the creation of the PlankTOM10 model may be found on <http://www.eur-oceans.eu/integration/wp3.2/> under description and code. Here information is provided that is relevant for understanding simulations presented in this chapter only. Phosphorus and nitrogen in the organic carbon pools are not independent but fixed to the Redfield ratio. There are three dissolved inorganic compartments: dissolved inorganic carbon (DIC), dissolved oxygen and alkalinity. There are seven detrital compartments: dissolved organic carbon (DOC), large and small particulate organic matter (POC_l and POC_s), CaCO_3 , SiO_2 and the iron content of POC (POFe_l and POFe_s). The model includes a representation of the ballasting effect on the sinking of particles based on Stokes' Law (Buitenhuis et al. 2001, Ploug et al. 2008) where differential sinking and turbulence cause both the refractory sinking of CaCO_3 and SiO_2 , and the aggregation of large and small particles.

There are ten Plankton Functional Types (PFTs) in the biogeochemical model PlankTOM10: three zooplankton PFTs (proto-, meso- and macro-zooplankton), six

phytoplankton PFTs (pico-autotrophs, N₂-fixers, calcifiers, mixed phytoplankton, DMS-producers and diatoms) and bacteria. For the phytoplankton PFTs, biomass (carbon), chlorophyll, iron and silicate are modelled. For heterotrophic PFTs only biomass is modelled. The C:N:P:O ratio of all PFTs is constant whereas the Fe:C and Chl:C ratios of the phytoplankton are variable and fully determined by the phytoplankton model. Si:C ratio is determined only for the diatoms.

The model is forced with daily wind stress, cloud cover and precipitation from NCEP/NCAR reanalysed fields (Kalnay et al. 1996). Sensible and latent heat fluxes are calculated using bulk equations based on the difference between surface temperature calculated by NEMO and observed air temperature with local humidity taken into account. The water balance is calculated and a uniform water flux correction is applied to conserve mass. The model is initialised with biological state variables from previous model simulations. The World Ocean Atlas 2005 is used to initialise temperature (Locarnini et al. 2006), salinity (Antonov et al. 2006), PO₃⁻⁴, NO₃⁻, SiO₃ (Garcia et al. 2006b), O₂ (Garcia et al. 2006a), DIC and alkalinity from GLODAP (Key et al. 2004). Dust is deposited at the surface using monthly dust fluxes (Jickells et al. 2005) which have been interpolated to daily values, assuming an Fe constant in dust of 3.5% and an Fe solubility of 2%. The model receives riverine input with annual riverine fluxes of C and N, Si, P and Fe (da Cunha et al. 2007). Model simulations were run from 1990 to 1999, and all results are annual averages for 1999.

4.3.2 MACRO-ZOOPLANKTON EQUATIONS

The equations used for macro-zooplankton in PlankTOM10 are similar to the equations presented for meso-zooplankton in PISCES-T (Buitenhuis et al. 2006). The biomass of macro-zooplankton in PlankTOM10 is determined by the following equation:

$$\frac{\partial MAC}{\partial t} = \sum_k g_{F_k}^{mac} \cdot F_k \cdot MGE \cdot MAC - m^{mac} \cdot T \quad (4.1)$$

where MAC is the biomass concentration of macro-zooplankton. All other terms are defined in the following equations. Grazing or ingestion by macro-zooplankton in the model is calculated using:

$$g_{F_k}^{mac} = g_{max}^{mac}(T) \frac{p_{F_k}^{mac} \left(\frac{1 - H^{mac}}{\sum_k p_{F_k}^{mac} \cdot F_k} \right)}{K_{1/2}^{mac} + \sum p_{F_k}^{mac} \cdot F_k - H^{mac}} \quad (4.2)$$

where $g_{F_k}^{mac}$ is the grazing of macro-zooplankton on food source F_k , $g_{max}^{mac}(T)$ is the maximum grazing rate of macro-zooplankton, $p_{F_k}^{mac}$ is the preference of macro-zooplankton for F_k , $K_{1/2}^{mac}$ is the half-saturation concentration of grazing in macro-zooplankton and H^{mac} is the threshold food concentration below which the macro-zooplankton starve. Grazing rate of macro-zooplankton in the model is calculated using:

$$g_{max}^{mac}(T) = g_{0^\circ C}^{mac} \cdot a^{T/10} \quad (4.3)$$

where $g_{0^\circ C}^{mac}$ is the maximum grazing rate at 0 °C, a is the Q_{10} of grazing and T is temperature.

Model growth efficiency (MGE) of macro-zooplankton in the model is calculated using:

$$MGE = \min \left(GGE, \sum g_{F_{Fe}}^{mac} \cdot \frac{(1 - \zeta)}{\sum g_{F_C}^{mac} \cdot Fe : C^{mac}} \right) \quad (4.4)$$

where \min is the minimum function, ζ is unassimilated grazing, GGE is gross growth efficiency, $g_{F_{Fe}}^{mac}$ and $g_{F_C}^{mac}$ are the grazing of iron and carbon, respectively from food sources, and $Fe : C^{mac}$ is the fixed iron to carbon ratio in macro-zooplankton. Equation 4.4 reduces the growth efficiency if the Fe:C in the food is lower than what is required by the macro-zooplankton.

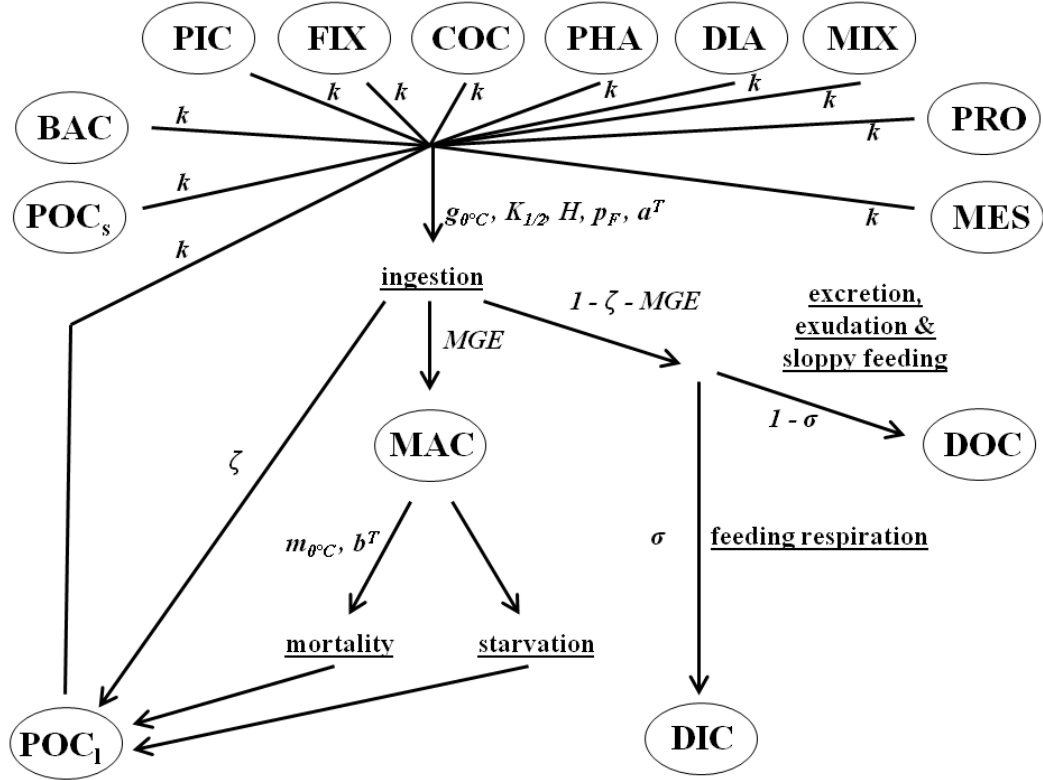


Figure 4.1: Macro-zooplankton mediated fluxes in PlankTOM10. Circles represent state variables; underlined texts represent fluxes and italic texts represent parameters. BAC = pico-heterotrophs, PIC = pico-autotrophs, FIX = N₂-fixers, COC = calcifiers, PHA = DMS-producers, DIA = silicifiers, MIX = mixed phytoplankton, PRO = proto-zooplankton, MES = meso-zooplankton, MAC = macro-zooplankton, DOC = dissolved organic carbon, DIC = dissolved inorganic carbon, POC_s = small particulate organic matter and POC_l = large particulate organic matter. Parameters are described in Table 4.4.

Mortality rate of the macro-zooplankton in the model is calculated using:

$$m^{mac}(T) = m_{0^\circ C}^{mac} \cdot b^{T/10} \cdot MAC \quad (4.5)$$

where $m_{0^\circ C}^{mac}$ is the mortality rate at 0 °C, b is the Q₁₀ of mortality and MAC is macro-zooplankton biomass.

Fluxes of dissolved and particulate carbon from macro-zooplankton excretion, exudation and sloppy feeding and unassimilated digestion of macro-zooplankton in the model are calculated using:

$$\frac{\partial DOC}{\partial t} = \sum \left[(1 - \sigma)(1 - \zeta - MGE) \sum_k g_{F_k}^{mac} \cdot MAC \cdot F_k \right] \quad (4.6)$$

$$\frac{\partial POC_l}{\partial t} = \sum \zeta \sum_k g_{F_k}^{mac} \cdot MAC \cdot F_k - \sum g_{poc_l}^{mac} \cdot MAC \cdot POC_l + m^{mac} \cdot T \quad (4.7)$$

$$\frac{\partial POC_s}{\partial t} = \sum g_{poc_s}^{mac} \cdot MAC \cdot POC_s \quad (4.8)$$

$$\frac{\partial DIC}{\partial t} = \sum \sigma(1 - \zeta - MGE) \sum_k g_{F_k}^{mac} \cdot MAC \cdot F_k \quad (4.9)$$

where $1 - \sigma$ is the fraction of grazing by macro-zooplankton that is converted to DOC and ζ is the fraction of unassimilated grazing.

4.3.3 PARAMETERISATION

Data were gathered from the literature to parameterise macro-zooplankton. If it was not possible to obtain the original data set from the author, data was extracted from tables. If data did not exist in a tabular form it was digitised from suitable graphs. When necessary, data was standardised to carbon units.

Much work has been carried out on the grazing and/or clearance rates for different species of macro-zooplankton. In the majority of cases where grazing and/or clearance rates were reported, essential data on animal body mass, food type, size and concentration, and/or carbon composition, that allow the calculation or conversion of grazing half-saturation concentration and grazing threshold, were not usually reported (Harbison & Gilmer 1976, Harbison & McAlister 1979, Fulton 1982, Madin & Cetta 1984, Harbison et al. 1986, McClatchie 1988, McClatchie et al. 1991, Bochdansky & Deibel 1999, Acuna & Kiefer 2000, Titelman & Hansson 2006). Grazing rates were calculated from growth rate and gross growth efficiency (GGE). Growth rate data was compiled by Hirst et al. (2003). Eppley's (1972) approach was extended to macro-zooplankton by describing maximum growth rates as an exponential function:

$$\mu = \mu_{0^\circ C} (Q_{10}^{0.1})^T \quad (4.10)$$

where $\mu_{0^\circ\text{C}}$ is the growth rate at 0 °C , Q_{10} is the increase in μ for a 10°C increase in temperature, and T is temperature. The values of $\mu_{0^\circ\text{C}}$ and Q_{10} were estimated using growth rate observations and the minimum of the following cost function of the fit is calculated using:

$$\text{normalised } RSS = \sqrt{\frac{\left(\sum \frac{\text{observed}}{\mu - 1}\right)^2}{n}} \quad (4.11)$$

The standard procedure when minimizing the residual sum-of-squares (RSS) is biased towards high temperature data. The normalised RSS is used to remove the bias in the fit to the high temperature data allowing data points at low and high temperatures to be fit equally well. Maximum growth rate (μ_{max}) is calculated as the 99% upper limit of the data after Eppley (1972). This approach ensures that growth rate is characterised at the maximum possible rate that could be expected for macro-zooplankton and that grazing is high enough to allow maximum growth under suitable conditions in the model. In the absence of growth rate data for every species within the macro-zooplankton it is assumed that there will be species to fill the gaps on the maximum exponential fit. From this maximum growth rate grazing rate is calculated using:

$$\text{Grazing rate} = \mu_{\text{max}} / \text{GGE} \quad (4.12)$$

The portion of grazing that is converted to biomass is called gross growth efficiency (GGE). GGE has been studied for two groups of macro-zooplankton. Both of these were gelatinous forms; scyphomedusae and ctenophores (Reeve et al. 1989, Straile 1997, Bamstedt et al. 2001, Purcell & Arai 2001). In an effort to make the GGE parameterisation more robust, crustacean data from unpaired experiments on grazing and growth were used (Dagg 1976). The GGE of macro-zooplankton was calculated as the mean of the GGE data. Mean GGE was also calculated for gelatinous and crustacean macro-zooplankton.

The temperature dependence of growth rate is taken as the temperature dependence of grazing rate. There were no food concentration measurements accompanying the growth rate

data set used to calculate grazing rate. Thus the half-saturation of macro-zooplankton grazing could not be parameterised based on observation. Data from a review of zooplankton growth and grazing (Hansen et al. 1997) was used.

Knowledge of natural foods of various macro-zooplankton species is limited (Ikeda 1985). A number of studies have been undertaken in an attempt to identify the preferred foods of a few individual species of macro-zooplankton (Fulton 1982, Stoecker et al. 1987a, Stoecker et al. 1987b, Haywood & Burns 2003). The preferred foods of the few species that have been studied are not well known because of the myriad difficulties in collecting such information including but not limited to difficulties inherent in measuring prey preference, e.g. exposing the predator to prey types and concentrations that it would encounter in the ocean. There were not enough data from groups within the macro-zooplankton to parameterise food preferences from data found in the literature. In order to parameterise food preference for macro-zooplankton each food type was assigned a logical preference based on the carbon content of the food type. Meso-zooplankton were twice the preference of micro-zooplankton, silicifiers, mixed-phytoplankton, calcifiers and DMS-producers while the preference for pico-phytoplankton, N₂-fixers, POC_s and POC_l is one twentieth that of meso-zooplankton. In the standard run the preference for bacteria is zero. A total food biomass weighted mean of one was used to calculate food preference as (Buitenhuis et al. 2006):

$$\frac{pn_1 \cdot cn_1 + pn_2 \cdot cn_2 + \dots pn_{11} \cdot cn_{11}}{\sum cn_1 + cn_2 + \dots cn_{11}} = 1 \quad (4.13)$$

$$pn_1 = p_F \cdot \text{relative preference} \quad (4.14)$$

where pn_1 to pn_{11} are the preference of macro-zooplankton for pico-heterotrophs, pico-autotrophs, N₂-fixers, calcifiers, DMS-producers, silicifiers, mixed phytoplankton, proto-zooplankton, meso-zooplankton, POC_s and POC_l and cn_1 to cn_{11} are the biomass

concentrations of the foods listed above and p_F is the preference of macro-zooplankton for food source F (Table 4.4).

Macro-zooplankton grazing is broken up into four reservoirs: macro-zooplankton biomass, large POC (POC_l), DOC, and DIC:

$$Grazing = GGE + \zeta + \gamma + R \quad (4.15)$$

$$\gamma = (1 - \sigma) (1 - \zeta - GGE) \quad (4.16)$$

$$R = \sigma (1 - \zeta - GGE) \quad (4.17)$$

where GGE is gross growth efficiency, ζ is unassimilated grazing, σ is excretion, exudation and sloppy feeding and R is total respiration.

The proportion of grazing that is converted to POC_l comes from unassimilated grazing. To calculate the unassimilated grazing as a proportion of grazing, data on grazing, assimilation efficiency, and egestion, all in carbon terms, were required. Sufficient information, in carbon terms, was found in a number of studies (Conover & Lalli 1972, Cosper & Reeve 1975, Nagasawa 1985, Madin & Kremer 1995, Madin et al. 1997, Dilling et al. 1998, Madin unpublished). Where ash measurements are used to calculate unassimilated grazing (Cosper & Reeve 1975) it is assumed that a similar assimilation efficiency for carbon and ash. Studies employing Conover's (Conover 1966) ratio method were not considered as this method has been shown to underestimate assimilation efficiency (Cosper & Reeve 1975).

The proportion of grazing that is converted to DOC comes from excretion, exudation and sloppy feeding. There were two studies of DOC production in macro-zooplankton (i.e., Kremer 1977, Steinberg et al. 2000). In both studies DOC is measured in relation to respiration not grazing. These measurements were used as a fraction of respiration. The proportion of grazing that is respired is converted to DIC. DOC measurements were used to calculate DIC as follows:

$$f[DOC] + f[DIC] = 1 \quad (4.18)$$

where $f[\]$ is the fraction of DOC or DIC.

The parameterisation of macro-zooplankton partitioning of grazing to body mass, POC, DOC and DIC (Table 4.3) yields similar results to those of proto- and meso-zooplankton (Chapter 5). There is more variation between macro-zooplankton for the proportion of grazing that is partitioned to POC. A number of studies suggest that carnivorous and omnivorous groups feeding on heterotrophic prey have a lower proportion of grazing that is partitioned to POC (Conover 1978). When the predator preys only on specific prey species assimilation efficiency may be even higher. This is the case with the pteropod *Clione limacina* which preys exclusively on *Spiratella (Limacina) retroversa* and *Spiratella helicina* where the mean proportion of grazing that is partitioned to POC is only 5% (Conover & Lalli 1974). Chaetognaths are a carnivorous group whereas euphausiids and salps will consume both heterotrophic and autotrophic prey and the differences in POC production between macro-zooplankton groups may be explained in part by the type of prey they consume. Other explanations for differences in POC production may include differences in experimental technique, e.g. Nagasawa (1985) stored faecal pellets in 5% buffered sea-water formalin for a month before they were examined. The preservative may have decreased the dry mass of the faecal pellet leading to an underestimation of POC production. There were only two studies where the production of DOC by macro-zooplankton was measured as a proportion of respiration. There were no studies where DOC was measured as a proportion of grazing. Each of these studies used different groups, crustaceans and polychaetes (Steinberg et al. 2000) and ctenophores (Kremer 1977). In Kremer (1977) the metabolic rate of the ctenophore *Mnemiopsis leidyi* was found to be independent of size. Metabolic rate was higher than what would be expected from metabolic theory and this may explain the 10% difference between the means of the studies. In the absence of data on the production of DIC it is calculated from DOC production. This estimation of DIC is only as accurate as the determination of DOC production as discussed above.

An extensive literature search was carried out on data relating to the respiration rate of macro-zooplankton (Chapter 2). Information extracted from the literature was used to create a comprehensive data set that included species name, body mass, respiration rate, and weight-

specific respiration. Selection criteria were applied to the data. This meant the exclusion of any animals that are usually found at depths greater than 200 metres. Data was also excluded where temperature deviated during an individual experiment by 2°C. Uncertainty over experimental procedure also led to the exclusion of particular studies, i.e. Biggs (1977), from the data set. If data did not exist in the required units, e.g. $\mu\text{mol C } \mu\text{mol C}^{-1} \text{ day}^{-1}$, and $\mu\text{mol C ind}^{-1}$ a suitable conversion was found in the literature and applied to the data. There was a preference for species-specific conversion data when they could be found. Genus-specific and sub-group-specific conversion data were used in the absence of reported species-specific conversion data. There was a preference for amount per measured-weight type conversion data with a limited use of relationship regression calculations. Ultimately it was basal respiration rate in macro-zooplankton that was of interest. However it is difficult to measure the metabolism of any macro-zooplankton species at rest (Chapter 2). It is however possible to measure routine respiration and calculate basal respiration using a ratio, as calculated by Buitenhuis (2006) from average swimming speeds in euphausiids (Torres & Childress 1983). The relationship between routine respiration and temperature is described using an exponential function similar to that in Equation 4.10:

$$R = R_{0^\circ\text{C}} (Q_{10}^{0.1})^T \quad (4.19)$$

where $R_{0^\circ\text{C}}$ is the mass-specific respiration rate at 0°C. The cost function of the fit is calculated using Equation 4.11. As the grazing rate has been calculated as the 99% upper limit of the growth data the same strategy is applied here for consistency with the grazing rate calculation. Maximal routine respiration rate was calculated from the 99% upper limit of the data and temperature dependence was calculated from the exponential function. Maximal basal respiration is calculated as:

$$\text{Maximum basal respiration rate} = R_{\text{max}} \cdot (\text{basal:routine respiration}) \quad (4.20)$$

Grazing threshold could not be parameterised from observations and was calculated using:

$$H = \frac{K_{1/2} \cdot R_{0^\circ C} \cdot c^{T/10}}{g_{0^\circ C} \cdot a^{T/10} - R_{0^\circ C} \cdot c^{T/10}} - 1 \quad (4.21)$$

where $K_{1/2}$ is the half-saturation constant of grazing, R is the maximal basal respiration rate at 0°C , g is the maximum grazing rate at 0°C , a and c are the Q_{10} of grazing and respiration, respectively, and T is temperature. The threshold at 15°C was used to parameterise the model (Table 4.4). Buitenhuis et al. (2009) point out that the equation is sensitive to high temperature dependences of respiration, as both numerator and denominator are temperature dependent, underestimating grazing threshold. This sensitivity is apparent in both macro-zooplankton and gelatinous model outputs where loss is underestimated when a calculated grazing threshold is used (Figure 4.7). It is difficult to assess the accuracy of the grazing threshold equation without measurements of grazing threshold for the macro-zooplankton.

Mortality is the characteristic of a population rather than the individual (Hirst & Kiørboe 2002). Because of this, abundance-specific rather than mass-specific mortality rate is usually measured. It was assumed that abundance-specific mortality is the equivalent of mass-specific mortality for the purpose of this analysis. If abundance-specific mortality was reported but temperature data was absent in the original publication temperature data from the World Ocean Atlas 2005 was used to assign a temperature to mortality rate where location of sampling was provided. The relationship between predation mortality and temperature is described using an exponential function similar to that in Equation 4.10 and 4.18:

$$m = m_{0^\circ C} (Q_{10}^{0.1})^T \quad (4.22)$$

with a standard deviation of the fit calculated using:

$$stdev. = \sqrt{\frac{(\sum X - \bar{X})^2}{n}} \quad (4.23)$$

Mortality rate is characterised slightly differently than growth and respiration rates, e.g. Equations 4.10 and 4.18. It was not possible to fit an exponential with a normalised residual

sum-of-squares (RSS) to this data with a reasonable Q_{10} because of the data distribution (Chapter 5). The fitted predation mortality rate and its temperature dependence are used to describe macro-zooplankton mortality in the model. Mortality data for crustaceans is fit to Equation 4.22. Using the standard deviation calculated in Equation 4.23 it was possible to fit an exponential function to the mortality data. However the highest two data points had to be removed from the data set.

In order to use mortality data collected from the literature a number of assumptions had to be made. It was assumed that 1) the population in which mortality is being measured is in steady state, i.e. mortality is balanced by recruitment, 2) production of offspring is constant and 3) mortality is independent of age, i.e. mortality is constant at all times during the life cycle of an organism. Of course these assumptions do not allow for the dynamic situation in which species exist. In any population where mortality is being measured, steady state is achieved over longer time periods as the species remains viable. On shorter time scales recruitment may not always balance with mortality. Mortality will not be constant with age as some stages of the life cycle, particularly eggs and juveniles, are particularly vulnerable to predation and, in the case of the latter, starvation is also a consideration. These assumptions are employed in all models used to describe mortality rates in zooplankton. When there is limited data on mortality rates, as is the case with macro-zooplankton, the greater uncertainty in the parameterisation of the rate originates with the observations rather than the assumptions.

4.4 RESULTS

4.4.1 PARAMETERISATION

A maximum growth rate of 1.14 d^{-1} at 15°C with a Q_{10} of 3.8 results from a fit of the entire macro-zooplankton data set (Equation 4.10). Maximum growth is converted to grazing using Equation 4.12. This results in a grazing rate of 4.85 d^{-1} at 15°C . Q_{10} is assumed to be the same as the Q_{10} for growth rate. The values of grazing calculated from growth for groups within the macro-zooplankton are presented in Table 4.1. For the half-saturation of grazing rate a mean value of $20 \mu\text{M C}$ (Hansen et al. 1997) was used. Although macro-zooplankton are not included

in the Hansen et al. (1997) study the half-saturation rate of grazing was found to be independent of body size within the zooplankton groups tested.

Table 4.2: A summary of macro-zooplankton grazing, respiration and mortality rates at 15°C, their temperature dependence and the breakdown of these rates between the umbrella groups that make up the macro-zooplankton. Notes: error was calculated for grazing rate and respiration in Equation 4.11 and for mortality in Equation 4.23, n = number of data points. For references see Table 4.4.

Group	Macro-zooplankton			Gelatinous			Semi-gelatinous			Crustacean			Appendicularian			Units
	error	n		error	n		error	n		error	n		error	n		
Grazing	4.85	0.77	643	3.14	0.75	193	3.80	0.76	107	0.94	0.48	253	4.55	0.53	90	d ⁻¹
Q ₁₀	3.80			3.86			1.79			3.16			1.99			--
Basal respiration	0.54	0.76	2001	0.39	0.75	988	0.19	0.70	167	0.26	0.58	769	1.42	0.54	64	d ⁻¹
Q ₁₀	5.46		2001	5.06		988	2.3		167	4.07		769	0.81		64	--
Threshold	2.53		--	2.80		--	1.04		--	7.80		--	5.25		--	μM C
Mortality	--		--	0.26		1	--		--	0.02	0.01	39	--		--	d ⁻¹
Q ₁₀	--		--	--		--	--		--	3.00		39	--		--	--

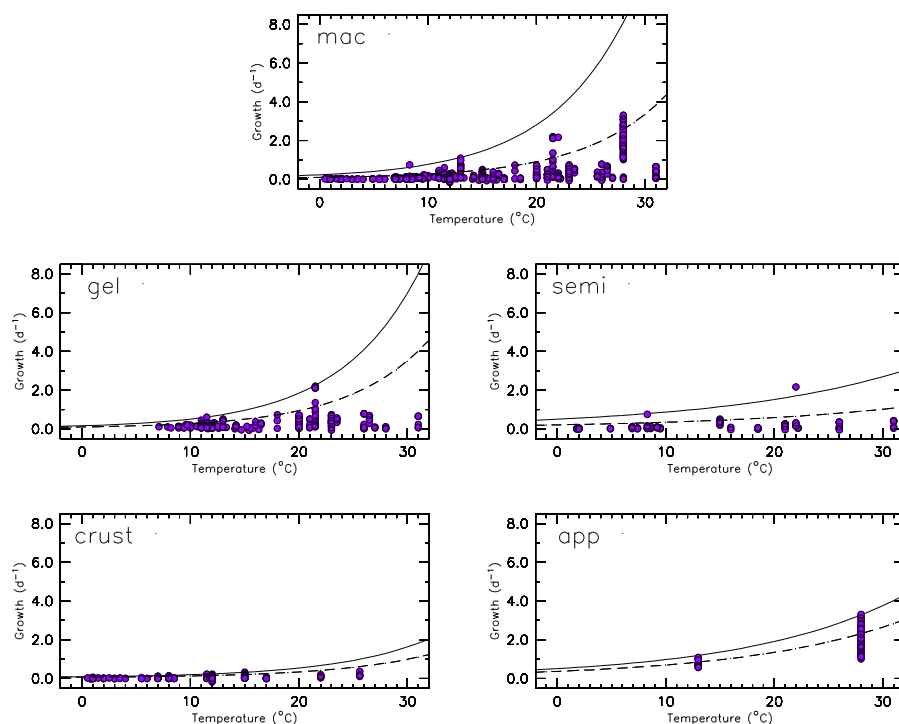


Figure 4.1: The relationship between mass-specific growth rate (d⁻¹) and temperature for macro-zooplankton [top] and four macro-zooplankton groups. Dashed line represents the normalised fit, the solid line represents the maximum growth rate with the temperature dependence of the original fit. Notes: gel = gelatinous, semi = semi-gelatinous, crust = crustacean and app = appendicularian.

Table 4.3: The partitioning of grazing in macro-zooplankton and the different groups within the macro-zooplankton. Note: there was no data for appendicularians. There is no standard deviation for DOC and DIC as DOC has been recalculated as a fraction of grazing and DIC was calculated from GGE, POC and DOC. n = number of data points, -- = no data. For references see Table 4.4.

Group	Macro-zooplankton			Gelatinous			Semi-gelatinous			Crustacean		
	%	Stdev.	n	%	Stdev.	n	%	Stdev.	n	%	Stdev.	n
<i>Partitioning of grazing</i>												
to biomass	0.29	0.24	251	0.29	0.23	195	--	--	--	0.30	0.16	56
to POC	0.18	0.12	30	0.28	0.10	4	0.13	0.11	22	0.26	0.08	4
to DOC	0.16	--	46	0.16	--	37	--	--	--	--	--	--
to DIC	0.37	--	--	0.27	--	--	--	--	--	--	--	--

The proportion of grazing that was converted to body mass (GGE) was similar for all three groups; ctenophores 0.28 ± 0.16 , $n = 69$, scyphomedusae 0.29 ± 0.27 , $n = 126$ and amphipods 0.30 ± 0.14 , $n=56$. The mean GGE calculated for the complete data set was 0.29 ± 0.22 , $n = 251$. There were a number of publications where POC_1 production in various groups of macro-zooplankton was reported. POC_1 production ranged from 0.39 of grazing in gelatinous macro-zooplankton (Madin et al. 1997) to 0.05 in semi-gelatinous macro-zooplankton. The mean POM_1 calculated for the complete data set, using a mean weighted by the number of data points per study, was 0.18. DOC production was reported to be 0.24 (Steinberg et al. 2000) and 0.34 (Kremer 1977) of feeding respiration. A weighted mean of 0.30 was calculated using data from both papers. From this result for DOC a value of 0.70 was calculated for the proportion of feeding respiration that was converted to DIC.

A maximum routine respiration rate of 0.064 d^{-1} at 15°C with a Q_{10} of 5.46 results from a fit to the entire macro-zooplankton respiration data set (Equation 4.18). Maximum routine respiration was converted to maximum basal respiration rate using Equation 4.19. This results in a maximum basal respiration rate of 0.043 d^{-1} at 15°C . Maximal basal respiration is used to calculate grazing threshold in macro-zooplankton (Equation 4.20).

Observations of grazing threshold in proto-zooplankton indicate a threshold of $7 \mu\text{M C}$ (Buitenhuis et al. 2009), around one-third of the half-saturation of grazing in this group. Preliminary calculations of grazing threshold in meso-zooplankton indicate a grazing threshold equal to one-tenth of half-saturation of grazing. Grazing threshold values calculated using maximum basal respiration rates and temperature dependencies fall in line with the grazing

threshold for other zooplankton groups with values between roughly one-tenth to one-third of the zooplankton half-saturation constant (Table 4.4).

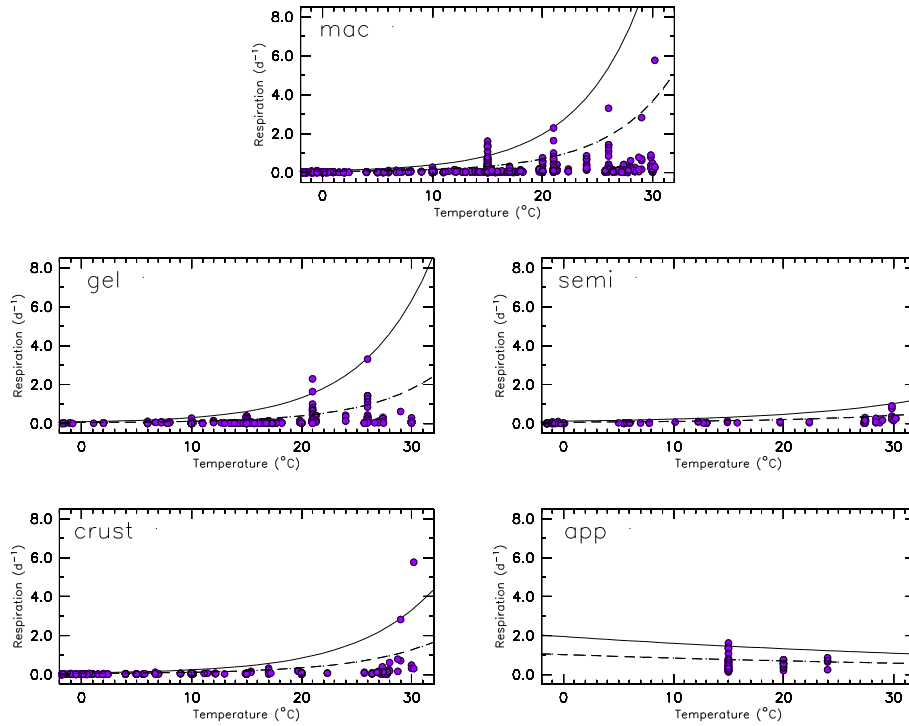


Figure 4.2: The relationship between mass-specific routine respiration rate (d^{-1}) and temperature for macro-zooplankton [top] and four macro-zooplankton groups. Dashed line represents the normalised fit, the solid line represents the maximum growth rate with the temperature dependence of the original fit.

Notes: gel = gelatinous, semi = semi-gelatinous, crust = crustacean and app = appendicularian.

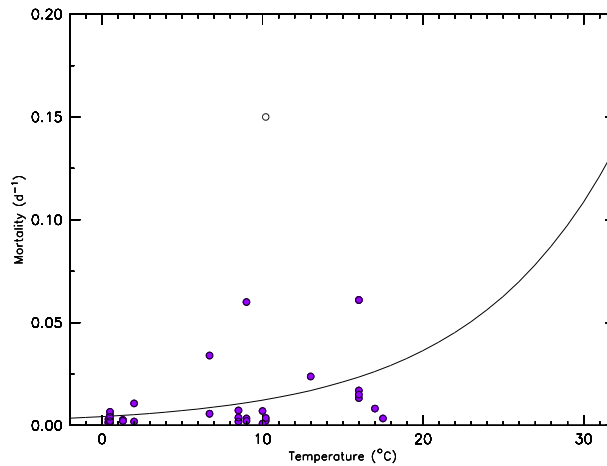


Figure 4.3: The relationship between mass-specific mortality rate (d^{-1}) and temperature for macro-zooplankton. The solid line represents the normalised mortality rate. White circles represent data excluded from the fit.

A mortality rate of 0.021 d^{-1} at 15°C with a Q_{10} of 3.0 results from a fit to the entire macro-zooplankton mortality data set (Equation 4.21). From the data that was collected on

macro-zooplankton mortality rate it is clear that it is highly variable, e.g. 0.0009 to 0.15 d⁻¹ (McGurk 1986). Predation mortality as a two-thirds to three-quarters of total loss was estimated for copepods (Hirst & Kiørboe 2002). If predation mortality in macro-zooplankton is similar to that of copepod predation mortality, a much higher mortality rate than that presented for crustacea in Table 4.1 was expected. Maximum basal respiration rates were used to calculate grazing threshold which effectively allowed loss rates to be adjusted without having to adjust mortality rates. It is clear that there is a need for data on both grazing threshold and mortality rates in macro-zooplankton. Without these data it is difficult to balance the loss between starvation/respiration and predation mortality.

Table 4.4: Parameter values used in the standard model simulation. Note: * = only used to calculate grazing threshold

Flux	Parameter	Units	Macro-zooplankton	Gelatinous	Rates Semi-gelatinous	Crustacean	Append- icularian	References
Grazing	\mathcal{G}_{max}^{mac}	d ⁻¹	0.66	0.41	1.59	0.17	1.62	Hirst et al. 2003
Q ₁₀	a	--	3.80	3.86	1.79	3.16	1.99	--
Half-saturation	$K_{1/2}^{mac}$	μMC	20.0	20.0	20.0	20.0	20.0	Hansen et al. 1997
Threshold at 15°C	H^{mac}	μMC	2.53	2.80	1.04	7.80	5.25	--
Feeding preference	$P_{F_k}^{mac}$	--			--			--
Meso-zooplankton	F_{mes}	--			4.15			--
Proto-zooplankton	F_{pro}	--			2.08			--
Mixed-phytoplankton	F_{mix}	--			2.08			--
Silicifiers	F_{dia}	--			2.08			--
DMS-producers	F_{pha}	--			2.08			--
Calcifiers	F_{coc}	--			2.08			--
N ₂ -fixers	F_{fix}	--			0.21			--
Pico-phytoplankton	F_{pic}	--			0.21			--
Bacteria	F_{bac}	--			0.00			--
POC _s	F_{poc_s}	--			0.21			--
POC _l	F_{poc_l}	--			0.21			--
GGE	GGE	--	0.29	0.29	0.29	0.30	0.29	Dagg 1976, Reeve et al. 1989, Straile 1997, Bamstedt et al. 2001, Purcell & Arai 2001
Particulate egestion	ζ	--	0.18	0.28	0.13	0.26	0.18	Conover & Lalli 1972, Cosper & Reeve 1975, Nagasawa 1985, Madin & Kremer 1995, Madin et al. 1997, Dilling et al. 1998, Madin unpublished in Madin & Kremer 1995
Inorganic fraction of excretion	σ	--	0.70	0.62	0.70	0.70	0.70	Kremer 1977, Steinberg et al. 2000
Mortality (predation)	$m_{0^\circ C}^{mac}$	d ⁻¹	0.004	0.004	0.004	0.004	0.004	Matthews 1973, McGurk 1986, Labat & CuzinRoudy 1996, Siegel 1999
Q ₁₀	b	--	3.00	3.00	3.00	3.00	3.00	--
Respiration (basal*)	$R_{0^\circ C}^{mac}$	d ⁻¹	0.043	0.036	0.054	0.032	1.273	Moriarty 2009
Q ₁₀ *	c	--	5.46	4.86	2.3	4.07	0.82	--

4.4.2 MODEL

The selection of the standard simulation for macro-zooplankton in PlankTOM10 was determined on the basis of model simulations for five sets of parameterisation. The five parameterisations were based on total macro-zooplankton and four groups within the macro-zooplankton. Group data were split into gelatinous, semi-gelatinous, crustacean and appendicularian groups (Table 4.4). No tuning of parameter values took place at this point. The results of these model simulations are based on fit to observations. Where observations for a group were missing, the parameter value used in the total macro-zooplankton parameterisation was used as a substitute.

PlankTOM10 is a new ocean biogeochemical model, that has not yet been published. Previous (simpler) model versions have reproduced the spatial distribution of phytoplankton PFTs (Vogt et al. submitted) of surface chlorophyll *a* and proto- and meso-zooplankton biomass within the constraints of the observations, the global primary production and carbon export at 100 m (Buitenhuis et al. 2006, Buitenhuis et al. 2009). In this version of PlankTOM both primary (33.4 Pg C y^{-1}) and export production (8.2 Pg C y^{-1}) are lower than the observed values for each, $\sim 45 \text{ Pg C y}^{-1}$ (Behrenfeld & Falkowski 1997) and $\sim 11 \text{ Pg C y}^{-1}$ (Schlitzer 2004) respectively and change only slightly as a result of various macro-zooplankton parameterisations implemented in the model simulations (Figure 4.4 and Figure 4.6). These underestimates are most likely caused by poorly constrained growth rates in proto-zooplankton. They should not affect the results presented here as the focus is on the impact of different parameterisations rather than an absolute rate. Phytoplankton biomass is generally overestimated in all model simulations (Figure 4.6) when compared to observations. Low primary production in the model simulations can in part be attributed to low turnover rates in the phytoplankton. All model simulations capture the general distribution of export production at 100 m but fail to reproduce higher rates of export in continental shelf areas of the eastern Pacific and off the west coast of Africa (Figure 4.6). Export production is overestimated in the North Atlantic and along the Antarctic continent in the Southern Ocean.

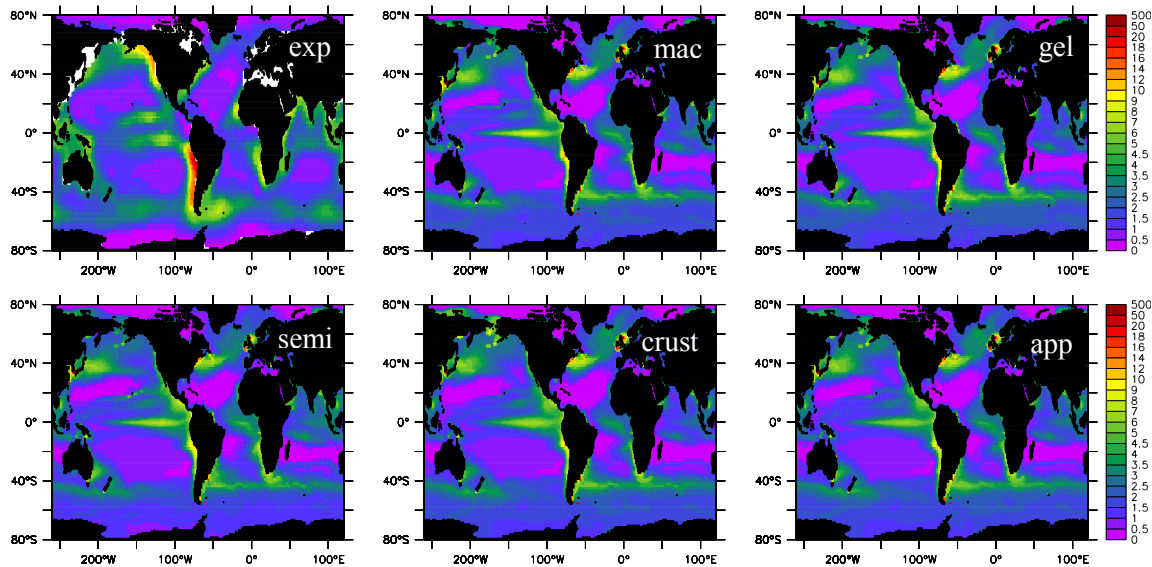


Figure 4.4: Export at 100m ($\text{mol C m}^{-2} \text{ y}^{-1}$) for model simulations. Notes: exp = observations of export production at 100m (Schlitzer 2004), mac = macro-zooplankton, gel = gelatinous, semi = semi-gelatinous, crust = crustacean, app = appendicularian parameterisations.

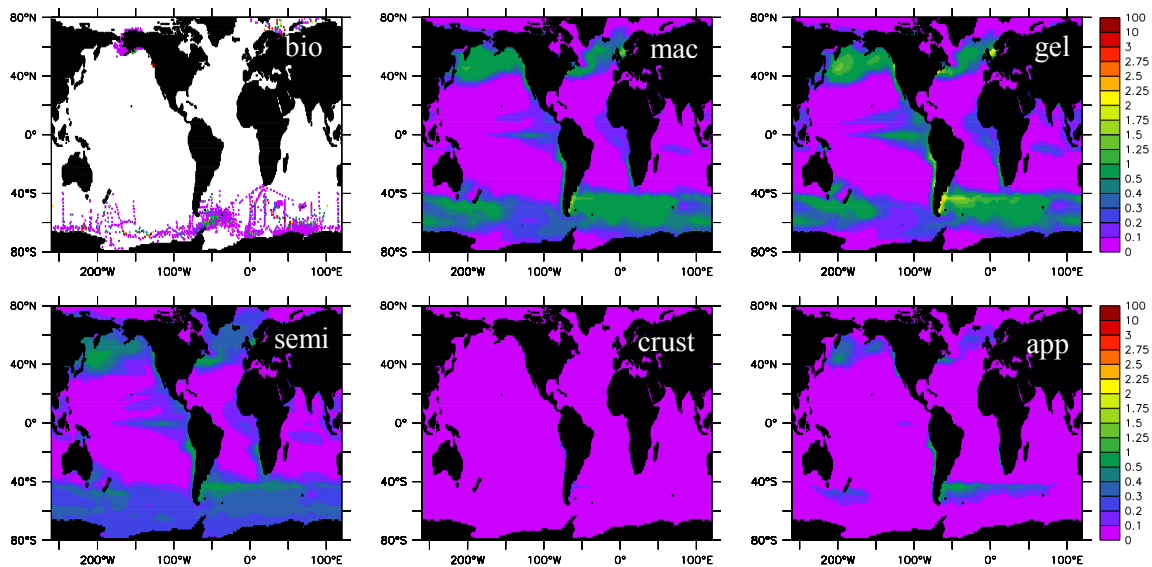


Figure 4.5: Macro-zooplankton biomass ($\mu\text{M C}$) for model simulations. Notes: bio = observations of macro-zooplankton biomass (Chapter 3), others same as Figure 4.4.

The biomass of macro-zooplankton is very different between simulations (Figure 4.5).

Biomass of macro-zooplankton is between 6 and 34 times greater than observed values except for the crustacean simulation where the biomass is, 0.003 PgC y^{-1} , lower than the observed value for macro-zooplankton biomass (0.005 PgC y^{-1}) (Chapter 3). The high macro-zooplankton biomass and patchiness observed in nature is not reproduced in any of the model simulations.

Table 4.5: Results of model simulations using macro-zooplankton and macro-zooplankton group parameterisations.

	Primary production (Pg C y ⁻¹)	Export production (Pg C y ⁻¹)	Zooplankton biomass (Pg C)		
			Proto	Meso	Macro
Data	45 ¹	11 ²	0.37 ³	0.52 ⁴	0.005 ⁵
<i>Parameterisation</i>					
Macro-zooplankton	33.4	8.2	0.14	0.04	0.15
Gelatinous	31.1	8.3	0.13	0.07	0.17
Semi-gelatinous	35.6	8.3	0.08	0.00	0.13
Crustacean	29.7	8.0	0.12	0.50	0.003
Appendicularian	31.8	8.2	0.13	0.24	0.03

Notes: Primary production is particulate primary production. References: ¹Behrenfeld & Falkowski 1997, ²Schlitzer 2004, ³Buitenhuis et al. 2009, ⁴Buitenhuis et al. 2006 and ⁵Chapter 3.

Table 4.6: Phytoplankton concentration results of model simulations using macro-zooplankton and macro-zooplankton group parameterisations.

	Phytoplankton biomass (Pg C)					
	Pico-autotrophs	N ₂ -fixers	Calcifiers	DMS-producers	Silicifiers	Mixed
Data	0.25	0.03	0.13	0.13	0.11	0.13
<i>Parameterisation</i>						
Macro-zooplankton	0.21	0.32	0.28	0.20	0.21	0.28
Gelatinous	0.19	0.31	0.28	0.21	0.21	0.29
Semi-gelatinous	0.23	0.40	0.40	0.15	0.18	0.21
Crustacean	0.20	0.30	0.27	0.19	0.20	0.26
Appendicularian	0.18	0.32	0.29	0.20	0.21	0.27

Notes: References: Uitz et al. 2006 and Alvain et al. 2006.

Biomass values for proto- and meso-zooplankton are lower than observed biomass concentrations for these groups as expected from the biomass of the primary producers. The difference in parameterisations can be clearly distinguished when the biomass concentration of the proto-, meso- and macro-zooplankton PFTs are considered (Table 4.5). In the semi-gelatinous parameterisation, meso-zooplankton have been completely consumed. While the crustacean parameterisation results in lower primary and export production, reasonable values for macro-, 0.003 Pg C y⁻¹, and meso-zooplankton, 0.50 Pg C y⁻¹, biomass are achieved. Proto-zooplankton on the other hand is not particularly affected by this parameterisation and returns a similar value to the other macro-zooplankton parameterisations. Both proto- and meso-zooplankton model spatial distributions are reasonable when compared to observations. The model fails to reproduce the observed patchiness and localised high concentrations of meso-

zooplankton biomass. This is also true of macro-zooplankton biomass, in the crustacean parameterisation.

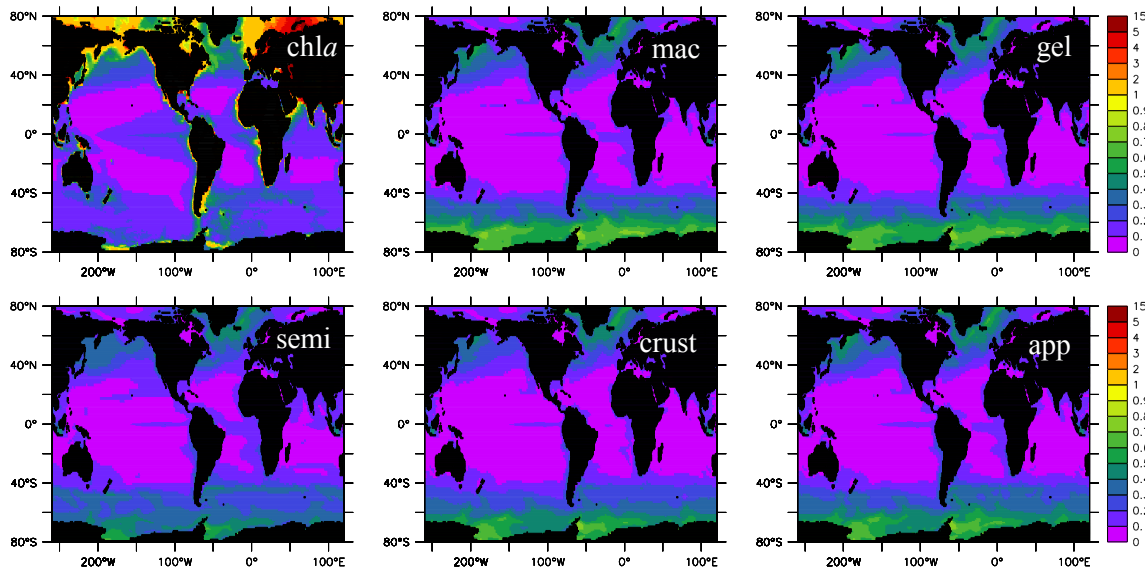


Figure 4.6: Surface chlorophyll a ($\mu\text{g L}^{-1}$) for model simulations. Notes: chl a = surface chlorophyll a observations (SeaWiFS), others same as Figure 4.4.

Phytoplankton biomass is overestimated in all the models ($1.5 - 1.7 \text{ Pg C y}^{-1}$), presented in Table 4.5, when they are compared to phytoplankton biomass observations (0.8 Pg C y^{-1}). When considering surface chlorophyll a as opposed to phytoplankton biomass it is clear that chlorophyll a is underestimated in all model simulations (Table 4.8). It is clear from the model simulations that chlorophyll a is lower, by roughly one order of magnitude, than observations in the equatorial Pacific and Atlantic, Indian Ocean, Arctic Ocean and along the Antarctic continent. Distribution of surface chlorophyll a in the Southern Ocean appears homogenous in model simulations whereas observations suggest it is heterogeneous in both distribution and concentration. The mismatch between phytoplankton biomass, measured in carbon, and chlorophyll a indicates an underestimation of chlorophyll a . This is caused by an overestimation of the C:Chl ratio at low latitudes in the photosynthesis model that is being used in PlankTOM10. Results of model simulations suggest that the various macro-zooplankton parameterisations have a minimal effect on phytoplankton biomass.

Model losses from the calculated grazing threshold in semi-gelatinous macro-zooplankton match respiration observations. In the crustacean macro-zooplankton loss rates in

the model simulations is slightly higher than observations even though the temperature dependence of respiration is high ($Q_{10} = 4.07$). Starvation resulting from the change in grazing threshold in all model simulations brings model macro-zooplankton biomass in line with observations (Table 4.8). Crustacean macro-zooplankton are the only group where model loss rates are closer to observations. In all other groups model loss rate exceed observations.

The response of each parameterisation to a paired half saturation of grazing and grazing threshold based on proto-zooplankton observation where grazing threshold has a value of $7 \mu\text{M C}$ was tested. As the grazing threshold parameter was a derived number this test allows the effect of a threshold value, roughly one-third the concentration of the half-saturation of grazing constant in the model, to be gauged. In all cases the grazing threshold concentration was increased. This increased the food concentration below which the macro-zooplankton starve, resulting in increased losses through starvation (Table 4.8). In all model simulations where the threshold was increased to $7 \mu\text{M C}$, model biomass of both meso- and macro-zooplankton were brought closer to observations. Meso-zooplankton biomass increased and macro-zooplankton biomass decreased (Table 4.8). Biomass concentrations of proto-zooplankton decreased slightly except in the case of the semi-gelatinous parameterisation where there was a slight increase which brought the results of this simulation close to the other simulations.

This analysis shows that all parameterisations are capable of reproducing similar phytoplankton and zooplankton biomass once the grazing threshold is adjusted to $\sim 7 \mu\text{M C}$. Although increasing the grazing threshold allows the observed biomass values of zooplankton to emerge. If the resultant increase in loss rates is examined it is clear that in some cases loss rates are now overestimated (Figure 4.7). In the model simulations of macro-zooplankton and gelatinous macro-zooplankton losses are underestimated. Loss is overestimated in the semi-gelatinous macro-zooplankton when the threshold is increased. The loss rates in the crustacean macro-zooplankton are slightly overestimated. The crustacean parameterisation is the only parameterisation where grazing threshold was decreased to achieve a grazing threshold of $7 \mu\text{M C}$. This decrease results in a closer match to observations. For appendicularians loss is overestimated in both model simulations.

Table 4.7: The contribution of various processes to the POC_1 flux and to total particulate export production. All measurements in Pg C y^{-1} . Bold text identifies the parameterisation used in the standard run.

	Contribution to POC _i				Total Flux to POC _i	Export Production		
	Macro	Meso	Silicifiers & N ₂ -fixers	DOC & POC _s aggregation		POC _s & POC _i	POC _i	Macro
<i>Parameterisation</i>								
<i>Model simulations</i>								
Macro-zooplankton	15.18	4.12	0.53	0.47	20.30	8.20	5.80	6.13
Gelatinous	17.62	6.31	0.57	0.45	24.95	8.25	5.92	5.83
Semi-gelatinous	16.34	0.00	0.30	0.43	17.07	8.30	5.86	7.95
Crustacean	0.91	26.04	0.54	0.36	27.86	8.04	6.09	0.26
Appendicularians	4.47	20.66	0.61	0.42	26.15	8.23	5.97	1.41
<i>Optimisation</i>								
Threshold	1.34	25.79	0.55	0.37	28.04	8.07	6.08	0.38
Grazing	1.03	25.97	0.54	0.36	27.90	8.05	6.09	0.30
Particulate egestion	1.18	25.31	0.53	0.36	27.38	7.93	5.99	0.34
Combined	2.01	25.45	0.55	0.37	28.39	8.10	6.10	0.57

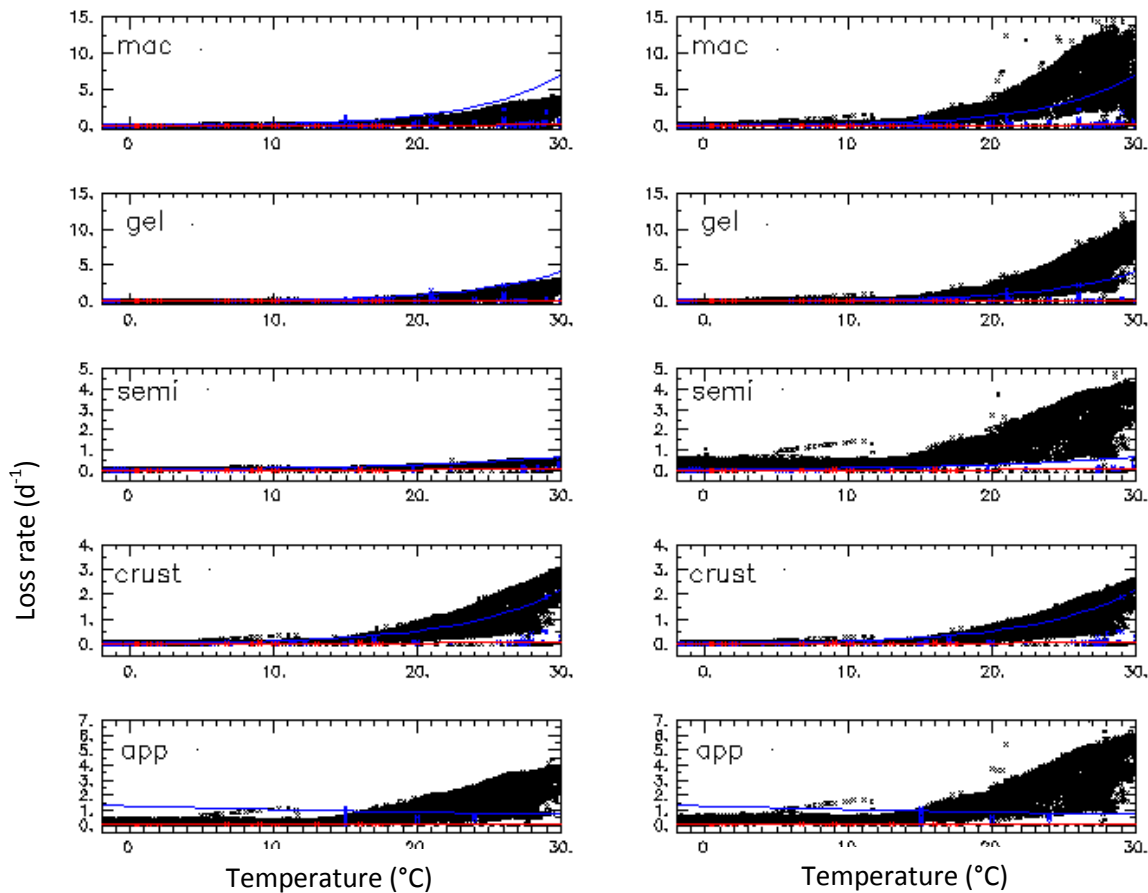


Figure 4.7: Loss rates in model simulations with a calculated grazing threshold [left] and in model simulations with a grazing threshold of $7 \mu\text{M C}$ [right]. Notes: from top to bottom: macro-zooplankton, gelatinous, semi-gelatinous, crustaceans and appendicularians. Black crosses = model loss rates, blue crosses = basal respiration (calculated from routine respiration observations), red crosses = mortality observations, blue line = maximum basal respiration, red line = fit to mortality data, blue crosses = maximum basal respiration, red crosses = mortality, both calculated from observations, black crosses = model loss rates.

The parameterisation that had the most reasonable effect on the model ecosystem and the closest resemblance to observed biomass in the three zooplankton groups, even without tuning the threshold, was chosen as the standard simulation. It was clear from the model simulations that the parameterization of one group, the crustaceans, gave the most reasonable result when zooplankton biomasses were considered. The crustacean parameterisation was selected as the standard simulation upon which the optimisation of macro-zooplankton in PlankTOM10 was based because it resulted in the most realistic reproduction of biomass of all the zooplankton. Selection of the crustacean macro-zooplankton parameterisation as the standard model simulation allows estimates of the fraction of export produced by macro-zooplankton, in an ecosystem close to observed biomass values. In PlankTOM10 there are six model tracers which contribute to the production of POC_i ; these include meso- and macro-zooplankton, silicifiers and N_2 -fixers and the aggregation of DOC and POC_s to POC_i (Table 4.8). In the standard simulation it is clear that meso-zooplankton make the largest contribution to the POC_i flux. The contribution of meso-zooplankton is two orders of magnitude higher than the contribution of other groups. In the standard simulation macro-zooplankton are responsible for only 3.3% or 0.26 Pg C y^{-1} of the total POC (model POC_s and POC_i) export particulate production. Meso-zooplankton on the other hand are responsible for 93.5% or 7.5 Pg C y^{-1} of export production.

Model optimisation was carried out through manipulation of the macro-zooplankton grazing parameters, including the threshold, through the adjustment of maximum basal respiration rate which resulted in a change of grazing threshold as calculated using Equation 4.20. The implementation of the grazing threshold parameter allows the simultaneous tuning of grazing and respiration in PlankTOM10. Attempts were made to augment the amount of POC_i produced by macro-zooplankton. This was done in two ways: 1) by increasing the grazing rate by 30% and 2) by increasing the proportion of grazing to POC_i (faecal pellet production) to the highest observed value (Table 4.8).

Table 4.8: Sensitivity analysis and evaluation of macro-zooplankton in the global biogeochemical model PlankTOM10. Bold text identifies the parameterisation used in the standard run.

	Parameter	Value	Units	Chlorophyll ($\mu\text{g L}^{-1}$)	Primary production (Pg C y^{-1})	Export production (Pg C y^{-1})		Zooplankton biomass (Pg C)		
						Total	Macro	Proto	Meso	Macro
Data				0.35 ¹	46.5 ²	9.6 – 11.1 ³	--	0.37 ⁴	0.52 ⁵	0.005 ⁶
<i>Models</i>										
PISCES ⁷	--	--	--	0.21	66.2	9.9	--	0.23	0.08	--
PISCES-T ⁵	--	--	--	0.15	64.0	8.2	--	0.11	0.09	--
PlankTOM5 ⁴	--	--	--	0.11	48.3	9.0	--	0.12	0.12	--
<i>PlankTOM10</i>										
<i>Parameterisations</i>										
Macro-zooplankton	--		--	0.24	33.44	8.20	6.13	0.14	0.04	0.15
Gelatinous	--	see	--	0.23	31.07	8.25	5.83	0.13	0.07	0.17
Semi-gelatinous	--	Table 4.4	--	0.21	35.55	8.30	7.95	0.08	0.00	0.13
Crustacean	--		--	0.21	29.71	8.04	0.26	0.12	0.50	0.003
Appendicularian	--		--	0.22	31.75	8.23	1.41	0.13	0.24	0.03
<i>Sensitivity analysis</i>										
Macro-zooplankton	H^{mac}			0.21	30.47	8.06	0.52	0.12	0.39	0.007
Gelatinous	H^{mac}			0.21	30.21	8.10	0.58	0.12	0.41	0.004
Semi-gelatinous	H^{mac}	7.0	$\mu\text{M C}$	0.21	30.50	8.06	0.38	0.12	0.39	0.006
Crustacean	H^{mac}			0.21	29.90	8.06	0.33	0.11	0.48	0.004
Appendicularian	H^{mac}			0.21	30.45	8.05	0.51	0.12	0.39	0.006
<i>Augmentation of export production</i>										
Crustacean	H^{mac}	6.8	$\mu\text{M C}$	0.21	30.06	8.07	0.38	0.11	0.46	0.005
Crustacean	$g_{max}^{mac}(T)$	0.22	d^{-1}	0.21	29.79	8.05	0.30	0.11	0.49	0.003
Crustacean	ζ	0.36	--	0.19	29.21	7.93	0.34	0.11	0.50	0.003
Combined	H^{mac} $g_{max}^{mac}(T)$, ζ	last three tests combined		0.21	30.01	8.10	0.57	0.11	0.44	0.005

Notes: Grazing threshold ($\mu\text{M C}$) is macro-zooplankton (crustacean) grazing threshold calculated using maximum basal respiration (d^{-1}). Primary production is particulate primary production. References: ¹Conkright et al. 2002, ²Antoine et al. 1996, Behrenfeld & Falkowski 1997 and Behrenfeld et al. 2005, ³Laws et al. 2000 and Schlitzer 2004, ⁴Buitenhuis et al. 2009, ⁵Buitenhuis et al. 2006, ⁶Chapter 3, and ⁷Aumont et al. 2003.

Changes to macro-zooplankton parameterisations had little effect on the lower trophic ecosystem; phytoplankton PFTs were sensitive to nutrient supply and the effects of micro-zooplankton grazing even though proto-zooplankton biomass in the model is low compared to observations. Changes to the crustacean parameterisation affect macro-zooplankton and meso-zooplankton biomass concentrations and contribution to both POC_1 and total export production. Changes to the grazing threshold, grazing rate and particulate egestion result in an increase to POC_1 flux, except in the case of increased particulate digestion. Proto-zooplankton biomass has decreased by 0.01 Pg C y^{-1} in all cases and meso-zooplankton biomass concentration decreases

in the decreased grazing threshold and increased grazing simulations. Macro-zooplankton biomass concentration matches observations in the decreased grazing threshold model only and is lower than observed in both other simulations. The overall contribution to export production is increased in all model simulations (Table 4.8).

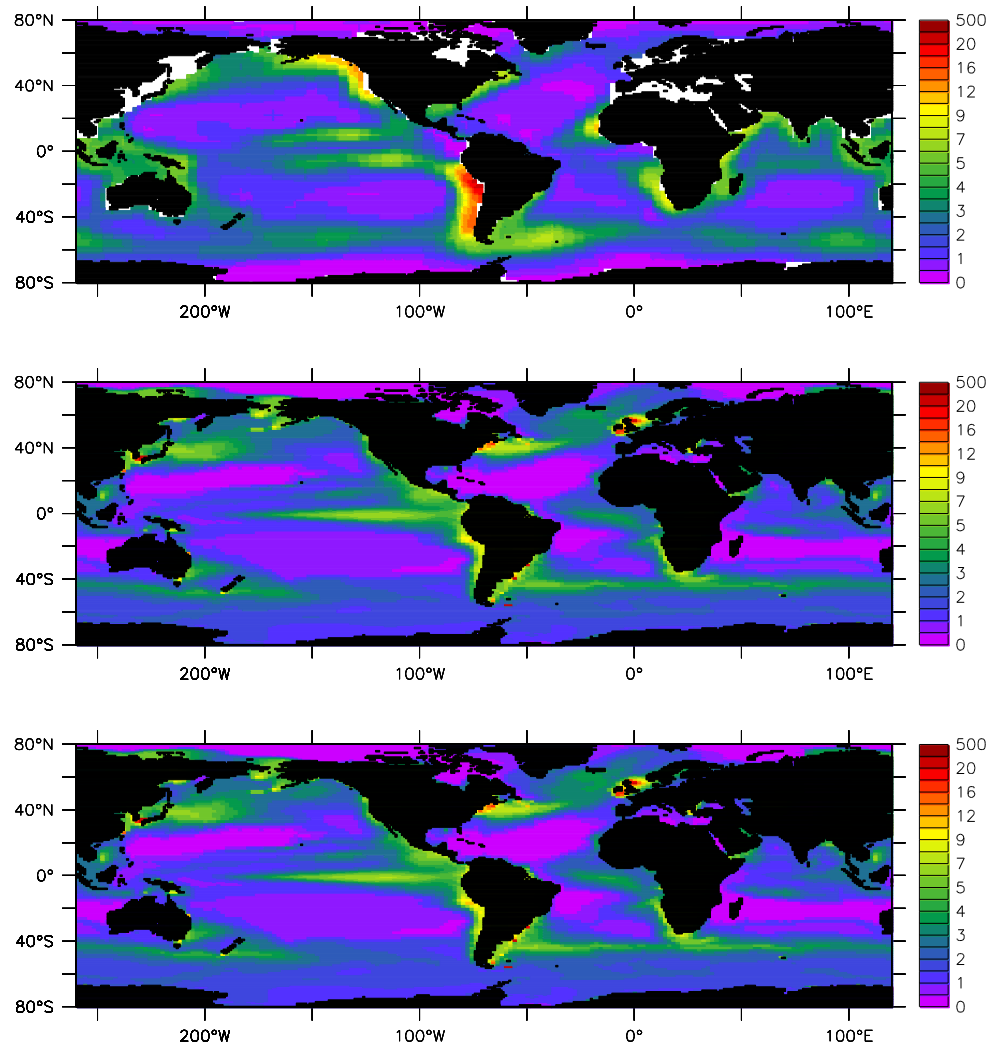


Figure 4.8: Export at 100m ($\text{mol C m}^{-2} \text{y}^{-1}$) for standard and combined simulations. Observations (Schlitzer 2004) [top], standard run [centre] and combined run [bottom].

The decreased grazing threshold was combined with increased grazing and increased particulate egestion in an effort to increase the contribution of macro-zooplankton to the POC_1 flux and to total export particulate production. The combined effects of increasing grazing and particulate egestion results in most of what is gained through grazing is partitioned to particulate egestion. However as there is an increase in macro-zooplankton biomass which may be attributed to the decreased grazing threshold and increased grazing rate, there is a slight increase

in loss rate and this exceeds maximal basal respiration observations slightly. The effect of combining these three changes to the crustacean parameterisation results in an increase in the contribution of macro-zooplankton to both the POC_1 flux, 0.9 to 2.0 Pg C y^{-1} , and in total export production, 0.26 to 0.57 Pg C y^{-1} , in the combined version of the model (Table 4.9 and Table 4.8). The amount of exported POC_1 is increased slightly in the combined model as is primary production. There is no change to proto-zooplankton biomass concentration, a decrease in meso-zooplankton biomass concentration and macro-zooplankton biomass concentration is increased to match observations.

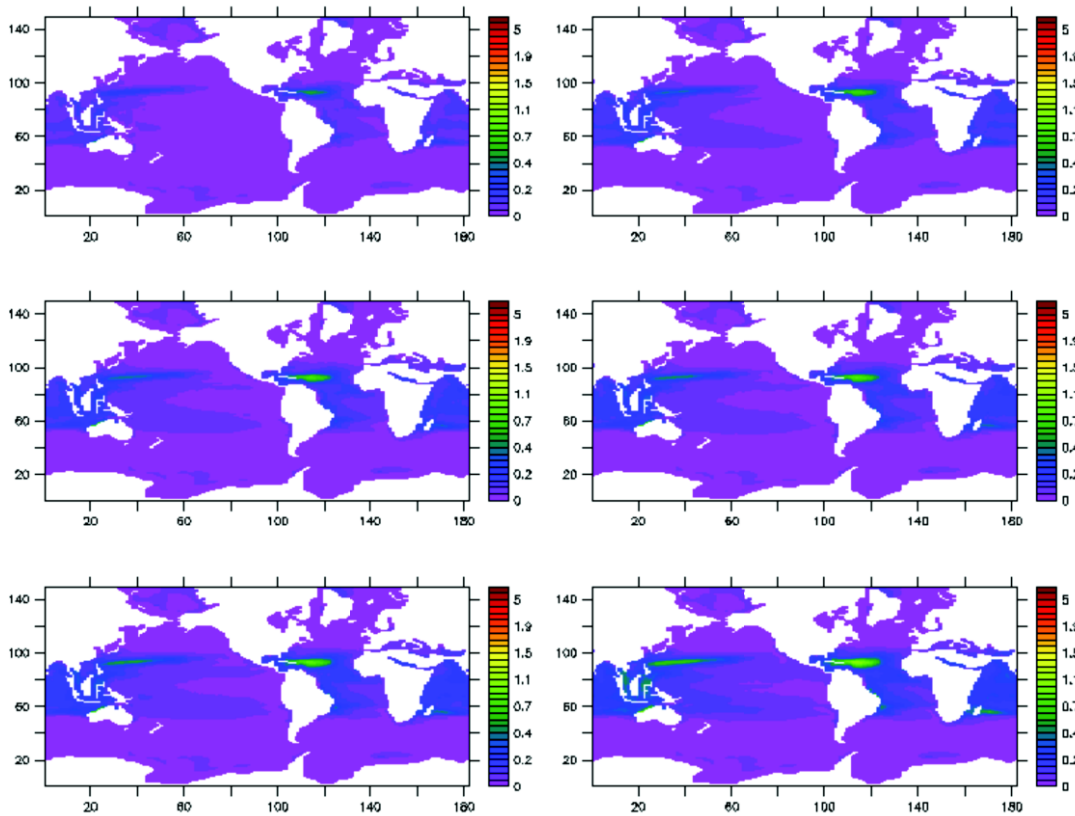


Figure 4.9: Annual average macro-zooplankton grazing in the top 200m (Pg C y^{-1}) for six different temperature dependence (Q_{10}) simulations. $Q_{10} = 2.60$ [top left], $Q_{10} = 3.00$ [top right], standard crustacean run, $Q_{10} = 3.16$ [centre left], $Q_{10} = 3.20$ [centre right], $Q_{10} = 3.30$ [bottom left] and $Q_{10} = 3.60$ [bottom right].

A simple sensitivity analysis of the temperature dependence (Q_{10}) of grazing was carried out to determine the effect that differences in temperature dependence have on processes that involve macro-zooplankton. A range of temperature dependencies were tested (see Table 4.9). Grazing intensity increases spatially and in intensity with increasing temperature dependence

(Q_{10}) as demonstrated in Figure 4.8. Similarly increases in temperature dependence effect macro-zooplankton grazing throughout the year, higher temperature dependences mean greater grazing throughout but particularly during warmer periods. There were only nominal increases in primary production, export, proto-zooplankton and the contribution that macro-zooplankton make to GOC production, nominal decreases in meso-zooplankton and the export of GOC and no change in macro-zooplankton biomass (see Table 4.9).

Table 4.9: Sensitivity analysis of temperature dependence of macro-zooplankton grazing rate using the standard crustacean parameterisation in the global biogeochemical model PlankTOM10. All values are Pg C y^{-1} .

	Primary production (Pg C y^{-1})	Export production (Pg C y^{-1})	Macro- zooplankton contribution to GOC (Pg C y^{-1})	Zooplankton biomass (Pg C)		
				Proto	Meso	Macro
Q_{10}						
2.60	31.12	8.02	0.157	0.112	0.516	0.003
2.85	31.20	8.03	0.178	0.112	0.509	0.003
3.00	31.24	8.03	0.188	0.112	0.505	0.003
3.05	31.25	8.03	0.192	0.112	0.503	0.003
3.10	31.26	8.04	0.195	0.112	0.502	0.003
3.16	31.27	8.04	0.199	0.112	0.501	0.003
3.20	31.28	8.04	0.201	0.112	0.500	0.003
3.25	31.29	8.04	0.204	0.112	0.499	0.003
3.30	31.30	8.04	0.206	0.112	0.498	0.003
3.45	31.33	8.04	0.214	0.113	0.494	0.003
3.60	31.36	8.05	0.223	0.113	0.491	0.003

As with all models this version of PlankTOM10 has both strengths and weaknesses. High phytoplankton biomass, as a result of poorly constrained physiological process rates, and low carbon turnover within these PFTs results in lower than observed primary and export production. Low proto-zooplankton biomass, caused by poorly constrained growth rates, also has implications for the phytoplankton turnover, primary and export production. Apart from low turnover rates associated with the lower trophic levels and the mismatch between phytoplankton biomass and chlorophyll *a* concentration, lower trophic level PFTs are robust in their parameterisations and support meso- and macro-zooplankton PFTs, the highest trophic levels. Meso-zooplankton biomass concentration is closer to observed values than any of the previously published models where they are included as a PFT. Macro-zooplankton are also close to

observed values, although the model does not reproduce the localised high biomass concentrations shown in the observations. PlankTOM10 has a functional ecosystem with reasonable biomass concentrations for the higher trophic level PFTs where macro-zooplankton act as an effective control of meso-zooplankton biomass and their low biomass contribution to carbon export has been realised.

4.5 DISCUSSION

4.5.1 MACRO-ZOOPLANKTON MODEL EQUATIONS

The addition of macro-zooplankton to PlankTOM10 has a similar effect on the representation of meso-zooplankton mortality as the inclusion of meso-zooplankton in PISCES-T (Buitenhuis et al. 2006) had on the representation of proto-zooplankton mortality. For lower trophic levels with high biomass it is important that mortality is represented in a dynamic way, i.e. that their mortality depends on food availability and predation by higher predators. For macro-zooplankton a dynamic representation of mortality is not possible in PlankTOM10 as the group represents the highest trophic level. However it is now possible to represent meso-zooplankton mortality in a dynamic way. Representing meso-zooplankton mortality in a dynamic way means that meso-zooplankton will be more responsive to the availability of their food sources and predation by macro-zooplankton. If the performance of meso-zooplankton in PlankTOM10 are compared to previously published models where their mortality was not represented dynamically there is an improvement in the representation of meso-zooplankton biomass, which is much closer to observations.

4.5.2 MODEL ASSUMPTIONS

There are two main assumptions regarding macro-zooplankton in PlankTOM10. The first is that all macro-zooplankton throughout the water column have the physiological and ecological process rates of those macro-zooplankton that reside in the surface layers of the world ocean. The second is that there is no diel vertical migration among the macro-zooplankton. Both of these assumptions will be addressed in more detail in this section. It is important to remember that a model representation that sufficiently captures the processes that are under investigation is

all that is required. There is uncertainty as to whether adding complexity will benefit the representation of macro-zooplankton processes. Also the addition of processes makes it more difficult to dissect and understand model results.

The physiological and ecological process rates of epi-pelagic macro-zooplankton have been used to parameterize macro-zooplankton the PFT in PlankTOM10. However, macro-zooplankton are found throughout the water column in the ocean and this is carried through to the model. The assumption here is that macro-zooplankton at all depths have the same physiological and ecological process rates. Mid-water species of macro-zooplankton have been shown to have lower rates of oxygen consumption or respiration rates than epi-pelagic species of macro-zooplankton (Childress 1971). The vast majority of physiological and ecological process rate data exists for species of epi-pelagic macro-zooplankton as a result of their accessibility. There is some data available for deeper dwelling macro-zooplankton species but parameterising the macro-zooplankton PFT with epi-pelagic macro-zooplankton species data is a necessary simplicity.

All references to macro-zooplankton distribution are calculated over and examined over only the top 200 m of the world ocean. In both the macro-zooplankton validation data set and the macro-zooplankton model output only those macro-zooplankton found in the top 200 m of the ocean are considered. These macro-zooplankton correspond to epi-pelagic species of macro-zooplankton which are found in the sunlit waters of the ocean. So although there are macro-zooplankton parameterised using epi-pelagic data throughout the ocean only epi-pelagic macro-zooplankton are referred to in this analysis. The primary concern of which is to investigate the role of macro-zooplankton in the export of carbon from the surface sunlit layers of the ocean to the deep ocean. There are ten PFTs in the model and to add deeper dwelling macro-zooplankton species would mean adding another layer of complexity to the model. There is uncertainty as to whether adding more PFTs or varieties to existing PFTs will mean a better representation of the processes that we are interested in capturing. For the moment macro-zooplankton are represented at all depths in the model and the distribution and concentration of macro-

zooplankton throughout the model is dependent on local environmental conditions which are a result of both bottom-up and top-down processes.

It has been shown that diel vertically migrating macro-zooplankton make a significant contribute to DIC, DOC and POC export through respiring, excreting and egesting material ingested in surface waters upon their return to deeper waters (Steinberg et al. 2000). It is not clear whether the contribution of macro-zooplankton to active transport of carbon is significant with some experimentalists suggesting that only fish are large enough and fast enough to contribute in this manner (Angel 1985). The focus of investigations is usually gut passage time (GPT). If an organism is larger than GPT is slower because of the larger size of the gut. Larger organisms may also be able to carry out their diel migration faster. This combination allows these organisms to return to deeper water before what they have ingested at the surface has finished passing through the gut. In smaller and slower migrating organisms much of what is ingested at the surface can be returned while the organism is still feeding in surface waters or lost to intermediate depths on the return migration with little or no surface ingested material remaining upon return to depth (Longhurst & Harrison 1989). However, studies of GPT in species of macro-zooplankton with strong diel vertical migrations have shown that these species have longer GPT and this allows the active export of POC in particular from the surface layers to the deep (Longhurst & Harrison 1989).

Diel vertical migration has not been include in PlankTOM10 although the seasonal vertical migration of meso-zooplankton (mainly copepods) has been included. There are a number of reasons that diel vertical migration of macro-zooplankton has not been included. The primary reason is to try and keep the model as simple as possible and to add to it only when the processes involved are necessary to gain a clearer picture of what is being investigated. The second reason is that it is difficult to model diel vertical migration and there is uncertainty related to the impact vertically migrating macro-zooplankton species have on removing material from the surface layers of the ocean and releasing it at depth as discussed above. Different species of macro-zooplankton carry out diel vertical migrations to and from different depths and some carry out reverse diel migrations. It would be possible to include a crude type of diel

vertical migration in PlankTOM10 but I am uncertain as to whether this would increase the contribution of macro-zooplankton to export from the surface water to the deep ocean in the model.

4.5.3 MODEL

Using PlankTOM10 I have been able to investigate the contribution that macro-zooplankton make to the POC_l flux ($\sim 2 \text{ Pg C y}^{-1}$) and their contribution to both POC_l export (0.43 Pg C y^{-1}) and total export production (0.57 Pg C y^{-1}). If the contribution of macro-zooplankton and meso-zooplankton to total export production is compared meso-zooplankton are responsible for thirteen times more export production. However, macro-zooplankton have a much higher carbon turnover rate, 115 y^{-1} , when compared to meso-zooplankton, 17 y^{-1} . Model simulations show that when macro-zooplankton biomass is high they are responsible for more export production than the meso-zooplankton. It is possible for macro-zooplankton to reach very high biomass concentrations exceeding $100 \mu\text{M C}$ ($0.005 \text{ Pg C y}^{-1} = 0.006 \mu\text{M C}$) in localised patches when environmental conditions are suitable (Chapter 3). In such high biomass patches, macro-zooplankton could become responsible for a large part of the grazing, which is currently attributed to meso-zooplankton in the model. Within high biomass patches the export production from macro-zooplankton fluxes resembles that of simulations using the macro-zooplankton or gelatinous macro-zooplankton parameterisations except in localised patches only. So far PlankTOM10 has been unable to replicate such localised high biomass patches in the macro-zooplankton. However, outside of these events the model has been able to match macro-zooplankton biomass to within observations and it was possible to increase the amount of carbon produced by macro-zooplankton and increase the proportion of carbon export that macro-zooplankton were responsible for through macro-zooplankton tuning.

The results of the temperature dependence sensitivity analysis show that changing the temperature dependence of the process rate makes only small differences to processes that macro-zooplankton are involved in if the process rate, e.g. grazing rate, is low. At higher grazing rates temperature dependence will be more sensitive as differences in temperature dependencies will have a much greater effect at higher process rates. It is clear from the

optimisation and sensitivity analysis carried out during the course of this investigation that parameters associated with grazing processes, particularly grazing rate, half-saturation of grazing and grazing threshold have the greatest effect on processes involving macro-zooplankton and in the optimisation of the model to observations. Unless process rates are high the sensitivity of temperature dependence is small in comparison to the effects that parameters associated with grazing have on macro-zooplankton processes, e.g. the contribution of macro-zooplankton to GOC. Changes in temperature dependence, even slight variations, do however change grazing intensity and spatial coverage of macro-zooplankton grazing.

It is obvious when model results for macro-zooplankton are compared to observations that the model fails to capture the patchy distribution that are characteristic of macro-zooplankton in the global ocean. It is also obvious that localised high macro-zooplankton biomass concentrations are also lacking. There are several reasons for this: 1) the description of macro-zooplankton in the equations presented above is necessarily simplified, 2) knowledge concerning triggers for swarming and ‘bloom/bust’ events is limited and 3) grazing on macro-zooplankton is homogenous rather than heterogeneous in nature. The simplified representation of macro-zooplankton behaviour in PlankTOM10 is caused by the necessity to keep the model as simple as possible while still representing the processes which are deemed important in carbon export by macro-zooplankton. These representations are limited, in turn, by the data that is available to describe and validate the model. There are many records of swarms and ‘blooms’ spread through the literature where the water is literally thick with a particular species of, for example, swarms of *Euphausia superba* in the Southern Ocean, *Pelagia noctiluca* in the Mediterranean, *Velella velella* on the south coast of Ireland (personal observation), *Salpa fusiformis* on the west coast of Ireland (Bathmann 1988), *Thalia democratica* off the coast of California (Berner 1967) and *Salpa thompsoni* in the Southern Ocean. The impact high macro-zooplankton biomass patches on the local ecosystem is also important and can cause early termination of the spring bloom (Bathmann 1988) with repercussions for succession. Future investigations of the role of macro-zooplankton in carbon export will need to focus on the mechanisms that control the patchiness of macro-zooplankton. If these mechanisms can be

described and incorporated into models such as PlankTOM10 the true contribution of macro-zooplankton to the global flux of export production can be appreciated.

There are a variety of mechanisms that are responsible for creating patchiness in the distribution of macro-zooplankton. First, some of the proposed mechanisms responsible for patchiness in plankton will be introduced. Second, in light of the variety of different mechanisms involved, patchiness in macro-zooplankton will be addressed through the separate consideration of a number of groups within the macro-zooplankton and the specific mechanisms that apply to those groups. The main focus here will be on Euphausiids, *Euphausia superba* in particular, salps and jellyfish. Euphausiids are a crustacean group while both salps and jellyfish (Hydromedusae, Scyphomedusae and Siphonophores) are members of the gelatinous macro-zooplankton as defined above. Some of the different types of mechanisms responsible for patchiness in these groups will be discussed in turn.

A wide variety of mechanisms have been proposed to explain the patchiness of plankton in the oceans. Some of these mechanisms are summarised in Brentnall et al. (2003) as follows a) relationships between physical features on which biology depends (Mann & Lazier 1996), b) Turing instability (Levin & Segel 1976), c) randomly varying predation on herbivorous zooplankton by higher trophic levels (Steele & Henderson 1981, 1992), d) turbulent stirring in harness with the slower growth rate of zooplankton as compared to phytoplankton (Abraham 1998) e) differential flow induced instability resulting from the more pronounced diel vertical migration of zooplankton in the presence of vertical shear (Rovinsky et al. 1997). There is some overlap between the mechanisms proposed by Brentnall et al. (2003) and those proposed by (Stavn 1971) who suggests that patchiness in zooplankton is caused by a) vectoral-physical gradients in a vertical plane, b) stochastic-vectoral-advection by currents, c) social-active schooling or swarming for social reasons, d) reproductive-aggregation of young caused by the spawning activities of adults and e) coactive-aggregation or trophic interactions. In both summaries it is clear that patchiness may be explained by either physical or biological mechanisms and often by a combination of the two. Each of these mechanisms is situation specific. So far there is no unified or global theory of patchiness in zooplankton. Although

these mechanisms have been modelled to and in many cases compare favourably to observation, i.e. Abraham (1998), so far mechanisms for zooplankton patchiness have not been included in global biogeochemical models.

Little is known about the causes of swarming or patchiness in krill (*Euphausia superba*) even though it is an important component of their life history (Tarling et al. 2009) and perhaps the fundamental organisational unit in Antarctic krill ecology (Watkins et al. 1986, Murphy et al. 1988). Very few studies have been able to identify clear and consistent relationships between swarm structure and environmental variables (Tarling et al. 2009). A variety of variables have been proposed to explain the causes of swarm structure in krill these include surface fluorescence, photosynthetically active radiation (PAR), krill maturity and length (Tarling et al. 2009) and predator presence (Trathan et al. 2003, Atkinson et al. 2008, Cox et al. 2009). Different krill behaviours are thought to drive patchiness on different scales (Folt & Burns 1999) and it is becoming increasingly more important to consider responses on the appropriate temporal and spatial scales (Murphy et al. 1988) (Brierley & Watkins 2000). At meso-scale level changes in swarms structure , i.e. large tightly packed swarms changing into more diffuse swarms as krill grow and mature. This pattern can be altered according to feeding and light conditions (Tarling et al. 2009). At macro-scale level, low numbers of very large swarms indicate an adaption to pressures associated with the detection of krill by randomly searching predators (Tarling et al. 2009).

The mechanism responsible for swarming in the salp *Salpa thompsoni* has been determined. Through a combination of favourable environmental conditions and life history *Salpa thompsoni* can produce swarms (Daponte et al. 2001). It is known that salps are negatively correlated with years where there was extensive winter sea-ice. In such years krill spawning and recruitment is high. In years where winter sea-ice coverage is poor it seems that salps are capable of outcompeting krill for food (Loeb et al. 1997, Perissinotto & Pakhomov 1998). By comparing salps collected over two winters, one with extensive winter sea-ice coverage and poor winter sea-ice coverage Daponte et al. (2001) determined the mechanism by which *Salpa thompsoni* produce swarms. Under favourable winter-sea ice conditions, i.e. those

that have a negative effect on krill spawning and recruitment, *Salpa thompsoni* produces larger individuals and they produce more aggregate individuals through asexual budding. These aggregate individuals then sexually reproduce to produce more solitary individuals, thus producing swarms (Daponte et al. 2001).

Physical processes may be responsible for the aggregation and patchy distribution in a variety of gelatinous zooplankton, especially medusae. It has been suggested that because of their large size, slow swimming speeds and their ‘simple’ neuro-sensory and locomotive systems (Larson 1992) that they are unable to swarm in a manner similar to that of crustaceans (Wittmann 1976). Although physical processes may be more important than behaviour in terms of patchiness, behaviour might be important on smaller scales (Price, 1988). There are many examples of physical processes effecting gelatinous zooplankton patchiness, (see Larson 1992) however for the purposes of this discussion the focus will be on both physical processes (Langmuir circulation) and the swimming behaviour of the scyphomedusae *Linuche unguiculata*. Patchiness in the scyphomedusae *Linuche unguiculata* results from two processes. The first is the action of the wind on the surface ocean where windrows are produced through horizontal advection caused by Langmuir circulation. At high wind speeds long windrows form whereas at low wind speeds the patches are circular or elliptical (Larson 1992). Wind speeds capable of maintaining Langmuir circulation, over the life time of drifting patches, are not always sustained. It is thought that the simple swimming behaviours observed in *Linuche unguiculata* are sufficient in reducing patch breakup (Larson 1992). This behaviour is also important in terms of reproductive success as more concentrated patches result in less sperm dilution (Larson 1992).

When discussing patchiness in macro-zooplankton it is important to consider the different scales involved as discussed above and whether the scale or resolution in PlankTOM10 is appropriate. Some of the main causes of patchiness, from large to small scale, are fronts, eddies, turbulence, coordinated migration and swarming. Only one of these, fronts, is captured in PlankTOM10. Except for fronts the model resolution is not good enough to represent meso- and micro-scale patchiness. The transport of macro-zooplankton by ocean currents also appears to

be important, and this is controlled by turbulence and eddy activity particularly in the Southern Ocean. Ice dynamics can play an important role in recruitment and mortality avoidance, but only for very specific ice conditions, e.g. Wiedenmann et al. (2009). These are two factors which could potentially be greatly improved in a higher resolution model. The appropriateness of the model resolution to patchiness in macro-zooplankton may not be the right question to ask. There is a direct relationship between unexplained variability in the observations and the spatial resolution at which processes are represented in the model. There is some appropriateness of scale in not combining a lot of biological detail in a coarse resolution model; unfortunately there is uncertainty around how much biological detail is too much at this resolution. It is also important to consider the implications of using mean field values from high resolution observations in coarse resolution models as it is not an accurate picture of plankton dynamics at this scale (Brierley & Watkins 2000).

There is limited data on the many different aspects of macro-zooplankton physiological process rates and behaviour that may be important when modelling their contribution to the export flux. More data on assimilation efficiencies and mass specific rates of egestion in carbon terms would allow the production of faecal pellets to be better constrained (Phillips et al. 2009). Data on food preference and its effect on the sinking speed of faecal pellets is limited in part because of the difficulties associated with carrying out such experiments (Schmidt pers. com.). The behaviour of species within the macro-zooplankton may also be important for their contribution to the export flux. As mentioned above, vertical migration may be important in removing carbon from the surface layers of the ocean, and may hasten the escape of faecal pellets to deep waters where they are less likely to be broken apart.

More information is needed on a global scale to relate the causes and triggers of spawning and blooms to the changes in export production. Environmental variables associated with these processes such as food concentration, temperature and presence of predators, are also important if these events are to be understood and modelled. Without further understanding of the role of macro-zooplankton in the carbon cycle and of their importance as a food source to

higher trophic levels, it will be difficult to quantify better their contribution to carbon export and assess the likely impact of global climate change.

There is sufficient variation in the physiological rates of each macro-zooplankton group to warrant splitting macro-zooplankton into the explicit representations of the four groups. However is this necessary? If the interest is in the function of large zooplankton in the export of carbon from the surface of the world ocean to the deep sea then the use of the combined crustacean parameterisation is recommended. Despite the lack of data on the food preference of macro-zooplankton, this parameterisation is the best representation of the data collected. If however the interest lies with the interaction of a particular group (appendicularians) then the parameterisations for this group could be used. Feeding preferences should reflect the feeding preference of the group rather than macro-zooplankton as a whole, and their model biomass concentration should be a proportion of the observations of total macro-zooplankton biomass concentration. Even if macro-zooplankton are split into one or more PFTs it is difficult to judge if any of the properties mentioned in the previous paragraphs will emerge. Splitting the groups means less data available for parameterisation and observation. There are of course sub-groups within the macro-zooplankton groups used in the parameterisations presented in this chapter, such as pteropods and ctenophores. Such groups have not been parameterised as the purpose of this study was to elucidate the role of macro-zooplankton in carbon export and to assess if macro-zooplankton, with its inherent differences but common functions, may really be considered as a simple group.

Adding compartments to PlankTOM10 has increased the heterogeneous nature of both phytoplankton and zooplankton. Grazing by higher predators is thought to increase patchiness in biomass concentrations in the model. Adding PFTs to higher trophic levels along with improvements to phytoplankton and proto-zooplankton may help increase zooplankton patchiness. Increasing the number of PFTs in the model will ultimately be limited by computing power and storage capacity. Low global “background” biomass concentrations and the associated export production of macro-zooplankton have been reproduced in the model. A better understanding of the processes involved in the creation of high biomass macro-zooplankton

patches, the triggers that lead to macro-zooplankton ‘blooms’ and the subsequent extinction of these ‘blooms’ is necessary to fully capture their role in carbon export. This in turn will lead to the amendment and/or addition of model equations to allow the representation of such processes in the model and therefore an improved representation of the macro-zooplankton PFT.

4.6 CONCLUSIONS

A representation of macro-zooplankton has been included in the PlankTOM10 model and its impact on lower trophic levels and carbon fluxes has been analysed. The crustacean macro-zooplankton parameterisation proved the closest fit to observations without tuning and was chosen to represent macro-zooplankton in the standard model simulations. Through the augmentation of three parameters, grazing threshold/maximal basal respiration rate, grazing rate and particulate egestion, it was possible to obtain biomass of macro-zooplankton and meso-zooplankton that were close to observed levels and increase the contribution of macro-zooplankton to export production. On average macro-zooplankton have very low biomass concentration globally. The contribution of macro-zooplankton to export production in PlankTOM10 captures the low level contribution of $\sim 0.6 \text{ Pg C y}^{-1}$ per macro-zooplankton biomass of 0.005 Pg C (or 120 y^{-1}) compared to $\sim 7 \text{ Pg C y}^{-1}$ for meso-zooplankton of 0.4 Pg C (or 18 y^{-1}). However it is known from observations of macro-zooplankton that they are capable of reaching very high biomass concentrations ($\sim 1000 \mu\text{M C}$) in patches. These high biomass and therefore high contribution to export production patches have not been replicated in the model. Not only do these patches have implication for changes in export production triggered by higher trophic levels (macro- and meso-zooplankton) but also for PFTs of lower levels through the early termination of the spring bloom and the knock on effects for succession and export production associated with primary producers. The lack of quantitative knowledge on the mechanisms controlling patchiness means that the contribution of macro-zooplankton to export production cannot be fully appreciated in models such as PlankTOM10. Until such mechanisms can be included it will be difficult to understand whether or not macro-zooplankton play a role in ecosystem-climate feedbacks.

REFERENCES

- Abraham E R (1998) The generation of plankton patchiness by turbulent stirring. *Nature* 391:577-580
- Acuna J L, Kiefer M (2000) Functional response of the appendicularian *Oikopleura dioica*. *Limnology and Oceanography* 45:608-618
- Alvain S, Moulin C, Dandonneau Y, Loisel H, Breon F M (2006) A species-dependent bio-optical model of case I waters for global ocean color processing. *Deep-Sea Research Part I-Oceanographic Research Papers* 53:917-925
- Angel M V (1985) Vertical migrations in the oceanic realm: possible causes and probable effects. *Contributions in Marine Science* 27
- Antonov J I, Locarnini R A, Boyer T P, Mishonov A V, Garcia H E (2006) World Ocean Atlas 2005, Volume 2: Salinity. NOAA Atlas NESDIS 62, U.S. Government Printing Office, Washington, D.C.
- Atkinson A, Siegel V, Pakhomov E A, Rothery P, Loeb V, Ross R M, Quetin L B, Schmidt K, Fretwell P, Murphy E J, Tarling G A, Fleming A H (2008) Oceanic circumpolar habitats of Antarctic krill. *Marine Ecology-Progress Series* 362:1-23
- Aumont O, Maier-Reimer E, Blain S, Monfray P (2003) An ecosystem model of the global ocean including Fe, Si, P colimitations. *Global Biogeochemical Cycles* 17
- Bamstedt U, Wild B, Martinussen M B (2001) Significance of food type for growth of ephyrae *Aurelia aurita* (Scyphozoa). *Marine Biology* 139:641-650
- Bathmann U V (1988) Mass occurrence of *Salpa fusiformis* in the Spring of 1984 off Ireland - Implications for sedimentation processes. *Marine Biology* 97:127-135
- Behrenfeld M J, Falkowski P G (1997) Photosynthetic rates derived from satellite-based chlorophyll concentration. *Limnology and Oceanography* 42:1-20
- Berner L D (1967) Distribution atlas of the Thaliacea in the Californian Current region. *Californian Cooperative Oceanic Fisheries Investigations Atlas* 8:1-322
- Biggs D C (1977) Respiration and ammonium excretion by open ocean gelatinous zooplankton. *Limnology and Oceanography* 22:108-117
- Bochdansky A B, Deibel D (1999) Functional feeding response and behavioral ecology of *Oikopleura vanhoeffeni* (Appendicularia, Tunicata). *Journal of Experimental Marine Biology and Ecology* 233:181-211
- Brentnall S J, Richards K J, Brindley J, Murphy E (2003) Plankton patchiness and its effect on larger-scale productivity. *Journal of Plankton Research* 25:121-140
- Brierley A S, Watkins J L (2000) Effects of sea ice cover on the swarming behaviour of Antarctic krill, *Euphausia superba*. *Canadian Journal of Fisheries and Aquatic Science* 57:24-30
- Bruland K W, Silver M W (1981) Sinking rates of fecal pellets from gelatinous zooplankton (salps, pteropods, doliolids). *Marine Biology* 63:295-300
- Buitenhuis E T, Le Quéré C, Aumont O, Beaugrand G, Bunker A, Hirst A, Ikeda T, O'Brien T, Piontkovski S, Straile D (2006) Biogeochemical fluxes through mesozooplankton. *Global Biogeochemical Cycles* 20

- Buitenhuis E T, Rivkin R, Sailley S, Le Quéré C (2009) Global biogeochemical fluxes through microzooplankton. *Limnology and Oceanography*
- Buitenhuis E T, Rivkin R, Sailley S, Le Quéré C (2009) Global biogeochemical fluxes through microzooplankton. *Limnology and Oceanography*
- Buitenhuis E T, van der Wal P, de Baar H J W (2001) Blooms of *Emiliania huxleyi* are sinks of atmospheric carbon dioxide: A field and mesocosm study derived simulation. *Global Biogeochemical Cycles* 15:577-587
- Childress J J (1971) Respiratory Rate and Depth of Occurrence of Midwater Animals. *Limnology and Oceanography* 16:104-&
- Conkright M E, O'Brien T D, Stephens C, Locarnini R A, Garcia H E, Boyer T P, Antonov J I (2002) World Ocean Atlas 2001, Volume 6: Chlorophyll. In: S Levitus (ed) NOAA Atlas NESDIS 52. U.S. Government Printing Office, Washington, D.C., p CD-ROMs. B. 46
- Conover R J (1966) Assimilation of organic matter by zooplankton. *Limnology and Oceanography* 11:338-345
- Conover R J (1978) Transformation of organic matter. In: O Kinne (ed) *Marine Ecology*, Vol 4. Wiley & Sons, New York, p 221-449
- Conover R J, Lalli C M (1972) Feeding and growth in *Clione limacina* (Phipps), a pteropod mollusc. *Journal of Experimental Marine Biology and Ecology* 9:279-302
- Conover R J, Lalli C M (1974) Feeding and growth in *Clione limacina* (Phipps), a pteropod mollusk. 2. Assimilation, metabolism, and growth efficiency. *Journal of Experimental Marine Biology and Ecology* 16:131-154
- Cosper T C, Reeve M R (1975) Digestive efficiency of chaetognath *Sagitta hispida* Conant. *Journal of Experimental Marine Biology and Ecology* 17:33-38
- Cox M J, Demer D A, Warren J D, Cutter G R, Brierley A S (2009) Multibeam echosounder observations reveal interactions between Antarctic krill and air-breathing predators. *Marine Ecology-Progress Series* 378:199-209
- da Cunha L C, Buitenhuis E T, Le Quéré C, Giraud X, Ludwig W (2007) Potential impact of changes in river nutrient supply on global ocean biogeochemistry. *Global Biogeochemical Cycles* 21
- Dagg M J (1976) Complete carbon and nitrogen budgets for the carnivorous amphipod, *Calliopius laeviusculus* (Kroyer). *Internationale Revue der gesamten Hydrobiologie* 61:297-357
- Daponte M C, Capitanio F L, Esnal G B (2001) A mechanism for swarming in the tunicate *Salpa thompsoni* (Foxton, 1961). *Antarctic Science* 13:240-245
- Deibel D (1990) Still water sinking velocity of fecal material from the pelagic Tunicate *Doliolleta gegenbauri*. *Marine Ecology-Progress Series* 62:55-60
- Deibel D (1998) Feeding and metabolism in Appendicularia. In: Q Bone (ed) *The Biology of Pelagic Tunicates*. Oxford University Press, New York, p 340
- Dilling L, Wilson J, Steinberg D, Alldredge A (1998) Feeding by the euphausiid *Euphausia pacifica* and the copepod *Calanus pacificus* on marine snow. *Marine Ecology-Progress Series* 170:189-201
- Eppley R W (1972) Temperature and phytoplankton growth in sea. *Fishery Bulletin* 70:1063-1085

- Folt C L, Burns C W (1999) Biological drivers of zooplankton patchiness. *Trends in Ecology & Evolution* 14:300-305
- Fulton R S (1982) Predatory feeding of two marine mysids. *Marine Biology* 72:183-191
- Garcia H, Locarnini R, Boyer T, Antonov J I (2006a) World Ocean Atlas 2005, Volume 3: Dissolved oxygen, apparent oxygen utilization, and oxygen saturation. NOAA Atlas NESDIS 63, U.S. Government Printing Office, Washington, D.C.
- Garcia H, Locarnini R, Boyer T, Antonov J I (2006b) World Ocean Atlas 2005, Volume 4: Nutrients (phosphate, nitrate, silicate). NOAA Atlas NESDIS 64, U.S. Government Printing Office, Washington, D.C.
- Gaspar P, Gregoris Y, Lefevre J M (1990) A simple eddy kinetic energy model for simulations of the oceanic vertical mixing - tests at Station Papa and long-term upper ocean study site. *Journal of Geophysical Research-Oceans* 95:16179-16193
- Gent P R, McWilliams J C (1990) Isopycnal mixing in ocean circulation models. *Journal of Physical Oceanography* 20:150-155
- Hansen P J, Bjornsen P K, Hansen B W (1997) Zooplankton grazing and growth: scaling within the 2-2,000 μm body size range. *Limnology and Oceanography* 42:687-704
- Harbison G R, Gilmer R W (1976) Feeding rates of the pelagic tunicate *Pegea confederata* and two other salps. *Limnology and Oceanography* 21:517-528
- Harbison G R, McAlister V L (1979) Filter-feeding rates and particle retention efficiencies of three species of *Cyclosalpa* (Tunicata, Thaliacea). *Limnology and Oceanography* 24:875-892
- Harbison G R, McAlister V L, Gilmer R W (1986) The response of the salp, *Pegea confoederata*, to high levels of particulate material - starvation in the midst of plenty. *Limnology and Oceanography* 31:371-382
- Haywood G J, Burns C W (2003) Feeding response of *Nyctiphanes australis* (Euphausiacea) to various nanoplankton sizes and taxa. *Marine Ecology-Progress Series* 253:209-216
- Hirst A G, Kjørboe T (2002) Mortality of marine planktonic copepods: global rates and patterns. *Marine Ecology-Progress Series* 230:195-209
- Hirst A G, Roff J C, Lampitt R S (2003) A synthesis of growth rates in marine epipelagic invertebrate zooplankton. *Advances in Marine Biology* 44:1-142
- Ikeda T (1985) Metabolic rates of epipelagic marine zooplankton as a function of body mass and temperature. *Marine Biology* 85:1-11
- Jickells T D, An Z S, Andersen K K, Baker A R, Bergametti G, Brooks N, Cao J J, Boyd P W, Duce R A, Hunter K A, Kawahata H, Kubilay N, la Roche J, Liss P, Mahowald N, Prospero J M, Ridgwell A J, Tegen I, Torres R (2005) Global iron connections between desert dust, ocean biogeochemistry, and climate. *Science*:67-71
- Kalnay E, Kanamitsu M, Kistler R, Collins W, Deaven D, Gandin L, Iredell M, Saha S, White G, Woollen J, Zhu Y, Chelliah M, Ebisuzaki W, Higgins W, Janowiak J, Mo K C, Ropelewski C, Wang J, Leetmaa A, Reynolds R, Jenne R, Joseph D (1996) The NCEP/NCAR 40-year reanalysis project. *Bulletin of the American Meteorological Society* 77:437-471

- Key R, Kozyr A, Sabine C, Lee K, Wanninkhof R, Bullister J, Feely R, Millero F, Mordy C, Peng T-H (2004) A global ocean carbon climatology: results from GLODAP. *Global Biogeochemical Cycles* 18
- Kremer P (1977) Respiration and excretion by ctenophore *Mnemiopsis leidyi*. *Marine Biology* 44:43-50
- Labat J P, CuzinRoudy J (1996) Population dynamics of the krill *Meganyctiphanes norvegica* (M Sars, 1857) (Crustacea: Euphausiacea) in the Ligurian Sea (NW Mediterranean sea). Size structure, growth and mortality modelling. *Journal of Plankton Research* 18:2295-2312
- Larson R J (1992) Riding Langmuir Circulations and swimming in circles - a novel form of clustering behavior by the scyphomedusa *Linuche unguiculata*. *Marine Biology* 112:229-235
- Lebrato M, Jones D O B (2009) Mass deposition event of *Pyrosoma atlanticum* carcasses off Ivory Coast (West Africa). *Limnology and Oceanography* 54:1197-1209
- Levin S A, Segel L A (1976) Hypothesis for origin of planktonic patchiness. *Nature* 259:659-659
- Locarnini R A, Mishonov A V, Antonov J I, Boyer T P, Garcia H E (2006) World Ocean Atlas 2005, Volume 1: Temperature. NOAA Atlas NESDIS 61, U.S. Government Printing Office, Washington, D.C.
- Longhurst A R, Harrison W G (1989) The biological pump - profiles of plankton production and consumption in the upper ocean. *Progress in Oceanography* 22:47-123
- Madec G (2008) NEMO ocean engine. Note du Pole de modélisation, Institut Pierre-Simon Laplace (IPSL), France
- Madin L P (1982) Production, composition and sedimentation of salp fecal pellets in oceanic waters. *Marine Biology* 67:39-45
- Madin L P (unpublished) in Madin & Kremer 1995.
- Madin L P, Cetta C M (1984) The use of gut fluorescence to estimate grazing by oceanic salps. *Journal of Plankton Research* 6:475-492
- Madin L P, Kremer P (1995) Determination of the filter-feeding rates of salps (Tunicata, Thaliacea). *ICES Journal of Marine Science* 52:583-595
- Madin L P, Purcell J E, Miller C B (1997) Abundance and grazing effects of *Cyclosalpa bakeri* in the subarctic Pacific. *Marine Ecology-Progress Series* 157:175-183
- Mann K H, Lazier J R N (1996) Dynamics of marine ecosystems: biological-physical interactions in the oceans. Blackwell Publishing
- Matthews J B (1973) Ecological studies on deep-water pelagic community of Korsfjorden, Western Norway - population dynamics of *Meganyctiphanes norvegica* (Crustacea, Euphausiacea) in 1968 and 1969. *Sarsia*:75-90
- McClatchie S (1988) Functional response of the Euphausiid *Thysanoessa raschii* grazing on small diatoms and toxic dinoflagellates. Reports of the Steno Memorial Hospital and the Nordisk Insulin Laboratorium 46:631-646
- McClatchie S, Jaquiere P, Kawachi R, Pilditch C (1991) Grazing rates of *Nyctiphanes australis* (Euphausiacea) in the laboratory and Otago Harbor, New Zealand, measured using three independent methods. *Continental Shelf Research* 11:1-22

- McGurk M D (1986) Natural mortality of marine pelagic fish eggs and larvae - role of spatial patchiness. *Marine Ecology-Progress Series* 34:227-242
- Moriarty R (2009) Respiration rates in epipelagic macro-zooplankton: a data set. PANGAEA
- Murphy E J, Morris D J, Watkins J L, Priddle J (1988) Scales of interaction between Antarctic krill and the environment. Springer-Verlag Berlin
- Nagasawa S (1985) The digestive efficiency of the chaetognath *Sagitta crassa* Tokioka, with observations on the feeding process. *Journal of Experimental Marine Biology and Ecology* 87:271-282
- Perissinotto R, Pakhomov E A (1998) Contribution of salps to carbon flux of marginal ice zone of the Lazarev Sea, Southern Ocean. *Marine Biology* 131:25-32
- Phillips B, Kremer P, Madin L P (2009) Defecation by *Salpa thompsoni* and its contribution to vertical flux in the Southern Ocean. *Marine Biology* 156:455-467
- Ploug H, Iversen M H, Koski M, Buitenhuis E T (2008) Production, oxygen respiration rates, and sinking velocity of copepod fecal pellets: direct measurements of ballasting by opal and calcite. *Limnology and Oceanography* 53:469-476
- Purcell J E (2005) Climate effects on formation of jellyfish and ctenophore blooms: a review. *Journal of the Marine Biological Association of the United Kingdom* 85:461-476
- Purcell J E, Arai M N (2001) Interactions of pelagic cnidarians and ctenophores with fish: a review. *Hydrobiologia* 451:27-44
- Reeve M R, Syms M A, Kremer P (1989) Growth dynamics of a ctenophore (*Mnemiopsis*) in relation to variable food-supply.1. Carbon biomass, feeding, egg-production, growth and assimilation efficiency. *Journal of Plankton Research* 11:535-552
- Rovinsky A B, Adiwidjaja H, Yakhnin V Z, Menzinger M (1997) Patchiness and enhancement of productivity in plankton ecosystems due to the differential advection of predator and prey. *Oikos* 78:101-106
- Schlitzer R (2004) Export production in the equatorial and North Pacific derived from dissolved oxygen, nutrient and carbon data. *Journal of Oceanography* 60:53-62
- Siegel V (1999) Krill (Euphausiacea) demography and variability in abundance and distribution. 2nd International Symposium on Krill, Santa Cruz, California
- Stavn R H (1971) Horizontal-vertical distribution hypothesis - Langmuir circulations and Daphnia distributions. *Limnology and Oceanography* 16:453-&
- Steele J H, Henderson E W (1981) A simple plankton model. *American Naturalist* 117:676-691
- Steele J H, Henderson E W (1992) A simple model for plankton patchiness. *Journal of Plankton Research* 14:1397-1403
- Steinberg D K, Carlson C A, Bates N R, Goldthwait S A, Madin L P, Michaels A F (2000) Zooplankton vertical migration and the active transport of dissolved organic and inorganic carbon in the Sargasso Sea. *Deep-Sea Research Part I-Oceanographic Research Papers* 47:137-158
- Stoecker D K, Michaels A E, Davis L H (1987a) Grazing by the jellyfish *Aurelia aurita* on microzooplankton. *Journal of Plankton Research* 9:901-915
- Stoecker D K, Verity P G, Michaels A E, Davis L H (1987b) Feeding by larval and postlarval ctenophores on microzooplankton. *Journal of Plankton Research* 9:667-683

- Straile D (1997) Gross growth efficiencies of protozoan and metazoan zooplankton and their dependence on food concentration, predator-prey weight ratio, and taxonomic group. *Limnology and Oceanography* 42:1375-1385
- Tarling G A, Klevjer T, Fielding S, Watkins J, Atkinson A, Murphy E, Korb R, Whitehouse M, Leaper R (2009) Variability and predictability of Antarctic krill swarm structure. *Deep-Sea Research Part I Oceanographic Research Papers* 56:1994-2012
- Timmermann R, Goosse H, Madec G, Fichefet T, Ette C, Duliére V (2005) On the representation of high latitude processes in the ORCA-LIM global coupled sea ice-ocean model. *Ocean Modelling* 8:175-201
- Titelman J, Hansson L J (2006) Feeding rates of the jellyfish *Aurelia aurita* on fish larvae. *Marine Biology* 149:297-306
- Torres J J, Childress J J (1983) Relationship of oxygen consumption to swimming speed in *Euphausia pacifica*. 1. Effects of temperature and pressure. *Marine Biology* 74:79-86
- Trathan P N, Brierley A S, Brandon M A, Bone D G, Goss C, Grant S A, Murphy E J, Watkins J L (2003) Oceanographic variability and changes in Antarctic krill (*Euphausia superba*) abundance at South Georgia. *Fisheries Oceanography* 12:569-583
- Turner J T (2002) Zooplankton fecal pellets, marine snow and sinking phytoplankton blooms. *Aquatic Microbial Ecology* 27:57-102
- Uitz J, Claustre H, Morel A, Hooker S B (2006) Vertical distribution of phytoplankton communities in open ocean: an assessment based on surface chlorophyll. *Journal of Geophysical Research-Oceans* 111:23
- Vogt M, Buitenhuis E T, Vallina S, Bopp L, Le Quéré C (submitted) DMS production and its interaction with climate in a fully mechanistic global ocean DMS model.
- Watkins J L, Morris D J, Ricketts C, Priddle J (1986) Differences between swarms of Antarctic krill and some implications for sampling krill populations. *Marine Biology* 93:137-146
- Wiedenmann J, Cresswell K A, Mangel M (2009) Connecting recruitment of Antarctic krill and sea ice. *Limnology and Oceanography* 54:799-811
- Wittmann K J (1976) Modification of association and swarming in North Adriatic Mysidacea in relation to habitat and interacting spaces. In: B F Keegan, O'Ceidigh P, Boaden P J S (eds) *Biology of Benthic Organisms*. Pergamon Press, Oxford, p 605–612

5 THE EFFECT OF TEMPERATURE ON THE PHYSIOLOGICAL RATES OF HETEROTROPHIC ZOOPLANKTON: A SIZED BASED COMPARISON

5.1 ABSTRACT

To understand the effect that global warming will have on ocean biology and its interactions with the carbon cycle and climate, information is needed on how physiological process rates of heterotrophic zooplankton relate to temperature. This chapter focuses on the heterotrophic component of the zooplankton, including flagellates, dinoflagellates, ciliates, copepods, crustaceans and gelatinous macro-zooplankton. Heterotrophic zooplankton play a number of vital roles in the ocean. Small zooplankton exert an important control on primary productivity, whereas the larger zooplankton are important for the export of carbon from the surface layers to the deep sea. Zooplankton are also an important food source for higher trophic levels. Here data was gathered from the literature and presented a synthesis of heterotrophic zooplankton grazing and respiration rates. This analysis reveals that although temperature explained 10 to 40% of the variance in gross growth efficiency (GGE) for three of the six groups (flagellates, dinoflagellates, ciliates) both positive and negative relationships between GGE and temperature have been found in this analysis. Partitioning of ingestion, hereafter grazing, was similar across nearly all groups. Grazing in carbon specific units (d^{-1}) was highest in the flagellates (3.65 ± 0.17 , at 15°C , $n = 871$) and lowest in the crustacean macro-zooplankton (0.16 ± 0.006 , at 15°C , $n = 246$). The Q_{10} of grazing ranges from 1.53 in the flagellates to 2.57 in the crustacean macro-zooplankton. There was a significant inverse relationship between grazing rate and body mass across groups. Body mass explains 70% of the variance in grazing rate. The relationship between the Q_{10} of grazing rate and body mass across groups was not significant. Respiration in carbon specific units (d^{-1}) was highest in the flagellates and ciliates with $\sim 0.5 \text{ d}^{-1}$ at 25°C and lowest among the larger zooplankton with $\sim 0.05^{-1}$ at 15°C . The Q_{10} of respiration ranges from 2.04 to 2.31. There was a significant inverse relationship between respiration rate and body mass. Body mass explains 90% of the variance in respiration rate. As with the relationship between the Q_{10} of grazing and body mass, the relationship between the Q_{10} of respiration and body mass was not significant.

5.2 INTRODUCTION

Heterotrophic zooplankton, including heterotrophic flagellates, dinoflagellates, ciliates, copepods, crustacean macro-zooplankton and gelatinous macro-zooplankton, are important members of the plankton community. They utilise organic matter in two ways, to produce new biomass through growth, and to provide energy for respiration. Zooplankton graze and repack small particles into faecal pellets and their own bodies releasing dissolved organic and inorganic nutrients. Smaller zooplankton such as flagellates, dinoflagellates and ciliates are important in controlling phytoplankton blooms. Larger zooplankton such as copepods, crustacean and gelatinous macro-zooplankton are more important in export of organic carbon from the surface ocean to the deep sea. Crustacean and gelatinous zooplankton in particular contribute to the downward flux of organic material in a variety of ways; through the production of large faecal pellets that sink out of the surface waters, through the contribution of abandoned feeding apparatus, e.g. the appendicularians (Alldredge & Gotschalk 1988, Robison et al. 2005), the discarded mucus feeding nets of some species of pteropods (Hamner et al. 1975), crustacean molts (Alldredge & Gotschalk 1988), episodic mass sedimentation of gelatinous macro-zooplankton carcasses, e.g. thaliacea (Lebrato & Jones 2009), and miscellaneous detritus to marine snow (Turner 2002). Zooplankton are also important as a food source to higher trophic levels. Changes in community composition and community process rates in heterotrophic zooplankton may impact the availability of food resources for higher trophic levels, and affect the ocean carbon cycle and in turn climate.

The top 300 m of the ocean has warmed by 0.31°C since the 1950s (Levitus et al. 2000). Ocean biology and climate are intricately linked through the physico-chemical and biotic components of the ocean carbon cycle (Boyd & Doney 2002). Global warming caused by anthropogenic CO₂ will affect ocean biology and its functioning in the carbon cycle. Temperature has both a direct and indirect effect on the physiological processes of organisms. Observations of climate variability such as El Niño/Southern Oscillation, show that ocean warming leads to increased stratification, and changes in circulation patterns and deep water formation (Boyd & Doney 2002, Sarmiento et al. 2004, Behrenfeld et al. 2006, Hansen et al.

2006). In cold well mixed conditions there is a constant supply of nutrients from deep to surface waters, here light availability is the limiting factor in phytoplankton growth. Under warm and stratified conditions, nutrients limit phytoplankton growth. Increased stratification also results in changes in the availability of light and this affects primary production. The physio-chemical environment also determines community structure and succession (Richardson 2007). Changes in community structure and succession have implications for phytoplankton and may also have knock on effects of higher trophic levels and can lead to either an increase or decrease in primary production (Le Quéré et al. 2003).

The impact of ocean warming on global ocean primary production has been studied previously with models (Sarmiento et al. 2004, Behrenfeld et al. 2006). However, the impact of ocean warming on heterotrophic plankton is not known. As with primary production, observations of climate variability indicate shifts in community composition under variable climate (Beaugrand et al. 2002). Regime shifts have been documented for a number of zooplankton assemblages on a regional level, e.g. for the North Atlantic (Beaugrand et al. 2002), the northeast Pacific (Peterson & Schwing 2003) and the California Current (Lavaniegos & Ohman 2003). Periods of warm or cool episodes have been linked to changes in zooplankton assemblages, such as the decrease in the diversity of colder-temperate, sub-Arctic and Arctic copepod species and the increased diversity of warmer water southern and pseudo-oceanic temperate copepod species caused by increasing sea surface temperature and changes in circulation (Beaugrand et al. 2002). These studies are species or assemblage specific and spatially restricted. In the absence of such comprehensive data sets for other heterotrophic zooplankton, especially the smaller zooplankton, a synthesis of the physiological process rate data available for the heterotrophic zooplankton has been created. The effects of temperature on the physiological processes of gross growth efficiency (GGE), grazing and respiration in the six members of the heterotrophic zooplankton are considered. Quantification of these physiological processes and the associated temperature dependencies may give an indication of how ocean warming will affect the dynamic equilibrium of the system. It is important to determine general

patterns that would allow broad scale projections of change in heterotrophic zooplankton caused by ocean warming for the entire ocean.

5.3 METHODS

Data were gathered from published syntheses, laboratory studies and on-line data sets (see Table 5.2 for all references to data sources). All physiological process rates are expressed in biomass-specific terms (d^{-1}). There are many reported measurements of physiological process rates such as growth and respiration in the literature but few with the associated biomass estimates necessary to estimate biomass-specific rates. Mass units were standardised to carbon if they were not originally reported as such and mass-specific rates were calculated.

GGE was used to determine the proportion of ingestion, hereafter grazing, that was converted to body mass. For all groups except crustacean macro-zooplankton GGE was determined in specifically designed paired experiments (Reeve et al. 1989, Straile 1997, Bamstedt et al. 2001, Purcell & Arai 2001) where grazing and growth rates were measured and GGE is then calculated as follows:

$$GGE = \text{grazing rate} / \text{growth rate} \quad (5.1)$$

where GGE is gross growth efficiency, grazing and growth rates are mass-specific rates (d^{-1}). For the crustacean macro-zooplankton GGE was calculated from unpaired experiments for grazing and growth rates in amphipods (Dagg, 1976 and Chapter 4) which also allowed GGE to be calculated using Equation 5.1. The relationship between GGE and temperature was described using the linear function:

$$GGE = a + b \cdot T \quad (5.2)$$

where a is GGE at 0°C , b is the temperature dependence and T is temperature in $^{\circ}\text{C}$.

Only two groups of heterotrophic zooplankton, the dinoflagellates and the ciliates, had grazing rate data and the accompanying biomass data necessary to calculate mass-specific rates. Grazing rate calculated from growth rate data and GGE were used to supplement experimentally measured grazing rate in all groups apart from the dinoflagellates. For ciliates only the cold

water (1.4°C) growth rates (Levinsen et al. 1999) were converted to grazing rate as the remainder of the data for this group was experimentally determined grazing rate. Grazing rate may be calculated from growth rate using a temperature dependent GGE correction as follows:

$$\text{Grazing rate} = \text{growth rate} / a + b \cdot T \quad (5.3)$$

In the absence of a predictive relationship between GGE and temperature grazing rate was calculated from GGE and growth rate as follows (see Straile 1997):

$$\text{Grazing rate} = \text{growth rate} / \text{GGE} \quad (5.4)$$

where grazing rate and growth rate are mass specific rates (d^{-1}) and GGE is the mean GGE for the heterotrophic zooplankton in question.

Respiration rates calculated in this analysis are routine (Chapter 2), starved or unfed respiration rates. No fit was attempted between respiration rate and temperature for flagellates and ciliates as the temperature range was small in both cases, 20 to 29°C and 20 to 30°C respectively, and would lead to poorly constrained temperature dependencies. These temperature ranges are unrepresentative of the ubiquitous distribution of both groups. Sample sizes were also low; eight and eleven respectively. A mean respiration rate was calculated instead for both. No data were found for dinoflagellate mass-specific respiration.

The relationship between rates (R) of grazing and respiration and temperature (T) were log transformed and described using a linear function:

$$\ln R = c + d \cdot T \quad (5.5)$$

where c is the rate at 0°C, d is the temperature dependency and T is temperature. Grazing and respiration data were log transformed in an effort to impart normality.

Grazing is partitioned into four pools: to body mass through GGE (above), to particulate organic matter (POM) through egestion, to dissolved organic matter (DOM) through excretion, sloppy feeding and exudation, and to dissolved inorganic carbon (DIC) through respiration. No attempt to describe the relationship between these variables and temperature was attempted but

rather a synthesis, of the limited amount of data available in relation to how grazing is partitioned, has been created. The partitioning to POM and DOM was calculated using the mean of the data, weighted by number of data points per study, for each plankton group. Where DOM was reported as a fraction of respiration it was recalculated as a fraction of grazing. Unknown fractions, i.e. DIC, were calculated, by mass balance, if data existed for three of the four compartments. These four components add up to one:

$$GGE + f[POM] + f[DOM] + f[DIC] = 1 \quad (5.6)$$

where $f[]$ is the fraction of grazing in the various compartments.

Flagellate cell volume was calculated, assuming a 5 μM spherical diameter. Cell mass was then calculated using a biovolume to carbon conversion factor of 220 $\text{fg C } \mu\text{m}^{-3}$ for heterotrophic nano-flagellates (Borodkin et al. 1982). Body mass data for dinoflagellates was calculated as the mean carbon body mass from a heterotrophic dinoflagellate grazing rate data set compiled by Sailley et al. (in prep-a). Mean body mass was calculated in a similar way for ciliates; as the mean carbon body mass from a pelagic ciliate grazing rate data set compiled by Sailley et al. (in prep-b). Mean copepod body mass was estimated from Hirst & Bunker (2003). Data compiled from two macro-zooplankton data sets Hirst et al. 2003 and Moriarty, 2009 was used to calculate the mean crustacean and gelatinous body mass. All body masses were converted to units of carbon, if not already reported as such.

The relationship between grazing and respiration rate (R) and body mass (BM) was described using regression analysis on log transformed data, in order to improve predictability, as follows:

$$\ln R = e + f \cdot \ln BM \quad (5.7)$$

where e is the rate at a given temperature, f is body size dependence and BM is body mass ($\mu\text{g C}$). The relationship between temperature dependence (Q_{10} , the change in rate as a consequence of increasing the temperature by 10°C) and body mass was described using regression analysis of log transformed body mass data as follows:

$$Q_{10} = g + h \cdot \ln BM \quad (5.8)$$

where g is the rate at a given temperature, h is body size dependence and BM is body mass ($\mu\text{g C}$). In all instances the statistical significance of the relationship is calculated using a t -test.

5.4 RESULTS

A summary of the data synthesis and analysis can be found in Table 5.2 and Figure 5.1. Grazing is partitioned into four pools: body mass, POM, DOM and DIC. Only one of those pools, the proportion of grazing that is partitioned to body mass through GGE, was accompanied by sufficient temperature data to be examined as a function of temperature. A significant and predictive relationship between GGE and temperature is shown for flagellates, dinoflagellates and ciliates. Temperature explained 1 to 40% of the GGE variance in these three groups. Ciliates showed a negative relationship with temperature whereas flagellates and dinoflagellates showed a positive relationship with temperature. The relationship between GGE and temperature for copepods and crustacean macro-zooplankton was not significant ($P > 0.05$). Although the relationship is significant in the gelatinous macro-zooplankton the temperature explains less than 10% of the variance and therefore it has little predictive or explanatory value.

Table 5.1: Relationship between GGE (%) and temperature ($^{\circ}\text{C}$) for heterotrophic plankton as calculated in Equation (5.2).

Group	GGE = a + b [T]					
	a	Stdev.	b	Stdev.	r^2	P
Flagellates	0.09	0.06	0.012	0.003	0.13	0.0003
Dinoflagellates	0.001	0.06	0.016	0.003	0.24	<0.0001
Ciliates	0.68	0.05	-0.021	0.003	0.36	<0.0001
Copepods	0.35	0.11	-0.004	0.008	0.002	0.651
Crustaceans	0.27	0.08	0.003	0.007	0.004	0.629
Gelatinous	0.15	0.06	0.007	0.003	0.03	<0.05

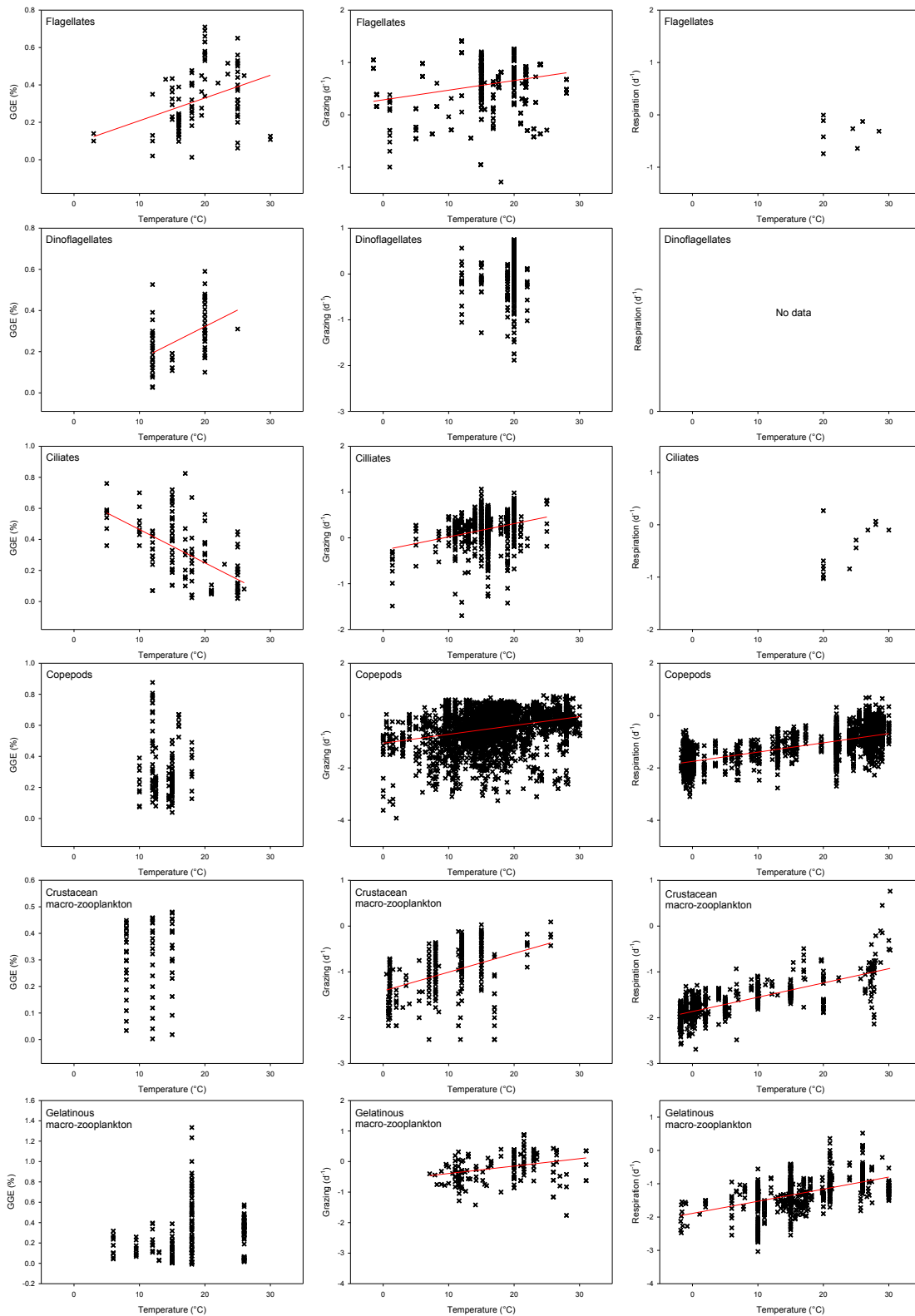


Figure 5.1: GGE (%) [left], grazing [middle] and respiration [right] rate (d^{-1}) as a function of temperature ($^{\circ}C$) for heterotrophic zooplankton. Relationship is only shown when significant and has predictive value. Where the temperature range was less than $20^{\circ}C$ no fit to grazing or respiration data was attempted.

Table 5.2: Physiological rates for heterotrophic zooplankton. Notes: n = number of data points, d = day.

Group	Flagellates		Dinoflagellates		Ciliates		Copepods		Crustacean		Gelatinous		Units
	n		n		n		n		n		n		
Grazing rate													
Grazing rate (15°C)	3.65 ¹	871	0.74 ²	347	1.46 ³	715	0.28 ⁴	2740	0.16 ⁵	246	0.58 ⁵	188	d ⁻¹
Q ₁₀	1.53		1.58		1.95		2.16		2.57		1.75		
Partitioning of grazing													
mean GGE	0.32 ⁶	104	0.29 ⁶	69	0.27 ⁶	132	0.25 ⁶	181	0.30 ⁷	56	0.29 ⁸	195	
to POM	--		--		0.21 ⁹	1	0.31 ¹⁰	272	0.26 ¹¹	4	0.28 ¹¹	4	
to DOM	--		0.19 ¹²	22	--		0.14 ¹³	93	0.11 ¹⁴	46	0.16 ¹⁴	37	
to DIC	--		--		0.63 ¹⁵	1	0.30 ¹⁹		0.33 ¹⁹		0.27 ¹⁹		
Loss rate													
Respiration rate (15°C)	0.54 ^{16, 20}	7	--		0.53 ^{17, 20}	11	0.06 ¹⁷	2962	0.04 ¹⁸	767	0.05 ¹⁸	988	d ⁻¹
Q ₁₀	--		--		--		2.26		2.05		2.31		

References: ¹ Henjes 2008; ² Sailley in prep-b; ³ Levinsen et al. 1999, Sailley in prep-a; ⁴ Hirst & Bunker 2003; ⁵ Hirst et al. 2003; ⁶ Straile 1997; ⁷ Daggs 1976; ⁸ Reeve et al. 1989, Straile 1997, Bamstedt et al. 2001, Purcell & Arai 2001; ⁹ Stoecker 1984; ¹⁰ Besiktepe & Dam 2002; ¹¹ Madin unpublished in Madin & Kremer 1995, Conover & Lalli 1974, Cosper & Reeve 1975, Nagasawa 1985, Madin & Kremer 1995, Madin et al. 1997, Dilling et al. 1998; ¹² Nagata 2000; ¹³ Kremer 1977, Copping & Lorenzen 1980, Small et al. 1983, Steinberg et al. 2000; ¹⁴ Kremer 1977, Steinberg et al. 1994; ¹⁵ Verity 1985; ¹⁶ Fenchel & Finlay 1983, Crawford et al. 1994, Crawford & Stoecker 1996; ¹⁷ Torres et al. 1982, Torres & Childress 1983, Ikeda 1985, Buskey 1998, Ikeda et al. 2001; ¹⁸ Moriarty submitted (Crawford & Stoecker). Notes: ¹⁹ calculated to complete the grazing budget, ²⁰ mean of data between 20 and 30°C.

Grazing rate was calculated using temperature corrected GGE and growth rate (Equation 5.3) for the flagellates and dinoflagellates. Mean GGE was used to convert growth rate into grazing rate (Equation 5.4) in the copepods, crustacean and gelatinous macro-zooplankton where the relationship between GGE and temperature was not statistically significant or it explained less than 10% of the variation. The grazing rates calculated with the mean GGE have the same Q_{10} as growth rate (Figure 5.1). Grazing rate at 15°C is lowest in crustacean macro-zooplankton (0.16 ± 0.006 , $n = 246$) and highest in flagellates (3.65 ± 0.17 , $n=871$; Table 5.1 and Figure 5.2). Q_{10} ranges from $1.53 (\pm 0.01, n = 871)$ in the flagellates to $2.57 (\pm 0.06, n = 246)$ in the crustacean macro-zooplankton (Figure 5.1 and Figure 5.3). The coefficients, standard deviation, correlation coefficients and significance of the grazing analysis can be found in Table 5.3.

Table 5.3: Relationship between grazing (d^{-1}) and temperature ($^{\circ}C$) for heterotrophic plankton calculated with Equation 5.5.

Group	$\ln R = c + d [T]$					
	c	Stdev.	d	Stdev.	r^2	P
Flagellates	0.66	0.09	0.04	0.005	0.07	<0.0001
Dinoflagellates	- 1.11	0.54	0.05	0.028	0.01	0.052
Ciliates	- 0.62	0.14	0.07	0.009	0.07	<0.0001
Copepods	- 2.42	0.09	0.08	0.05	0.08	<0.0001
Crustaceans	- 3.26	0.15	0.09	0.01	0.18	<0.0001
Gelatinous	- 1.46	0.27	0.06	0.01	0.08	<0.0001

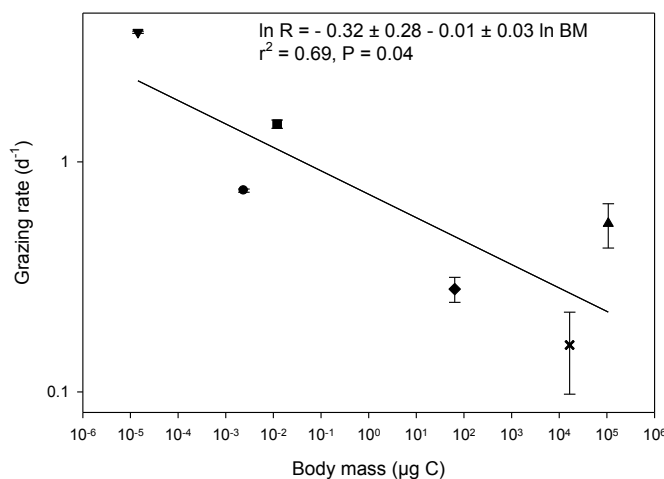


Figure 5.2: Grazing rate (d^{-1}) calculated at 15°C as a function of body mass ($\mu g C$) with standard deviation of the rate (whiskers) for heterotrophic plankton. Grazing rate is calculated at 15°C for each group of heterotrophic zooplankton. Body mass for each group is a mean value for the group. Symbols: Flagellates (▼), dinoflagellates (●), ciliates (■), copepods (◆), crustacean macro-zooplankton (x), and gelatinous macro-zooplankton (▲).

The relationship between grazing rate and body mass across groups was investigated at 15°C. An inverse relationship exists between grazing and body mass (Figure 5.2) and body mass is responsible for ~70% of the variation in grazing rate across the heterotrophic zooplankton presented in this study. The relationship between Q_{10} and body mass was investigated to see if it is possible to identify a relationship across groups. The relationship between the Q_{10} of grazing and body mass is not statistically significant.

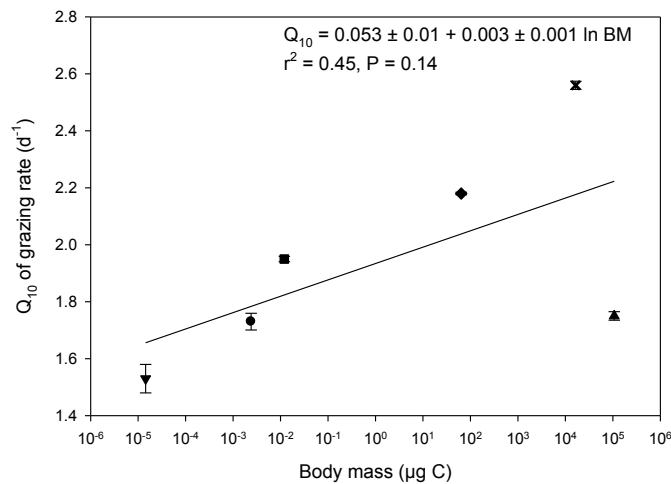


Figure 5.3: Q_{10} of grazing with standard deviation of Q_{10} (whiskers). Body mass for each group is a mean value for the group. Symbols as in Figure 5.2. Q_{10} values for copepods, crustacean macro-zooplankton and gelatinous macro-zooplankton (the three groups to the right of the figure) are a consequence of growth rate rather than grazing.

Respiration rate data were compiled for five of the six groups (Table 5.5). Copepods had the highest respiration rates ($0.06 \text{ d}^{-1} \pm 0.0005$, $n = 2962$) of the heterotrophic zooplankton considered here. Crustacean macro-zooplankton had the lowest respiration rate ($0.04 \text{ d}^{-1} \pm 0.0004$, $n = 767$). The flagellates and ciliates show very similar mean respiration rates between 20 and 30°C, 0.54 and 0.53 d^{-1} respectively. Respiration is four-fold higher in the two smaller groups than in the copepod or macro-zooplankton groups. Rates of respiration among the copepods, crustacean and gelatinous macro-zooplankton are also very similar. Q_{10} of respiration rate of crustacean macro-zooplankton was the lowest (2.05 ± 0.003 , $n = 767$) and highest in the gelatinous macro-zooplankton (2.31 ± 0.002 , $n = 988$).

Table 5.4: Relationship between respiration (d^{-1}) and temperature ($^{\circ}\text{C}$) for heterotrophic plankton calculated with Equation (5.5).

Group	$\ln R = a + b [T]$					
	c	Stdev.	d	Stdev.	r^2	P
Flagellates	--	--	--	--	--	--
Dinoflagellates	--	--	--	--	--	--
Ciliates	--	--	--	--	--	--
Copepods	- 4.0	0.03	0.08	0.001	0.55	<0.0001
Crustaceans	- 4.3	0.03	0.07	0.003	0.52	<0.0001
Gelatinous	- 4.4	0.08	0.08	0.005	0.25	<0.0001

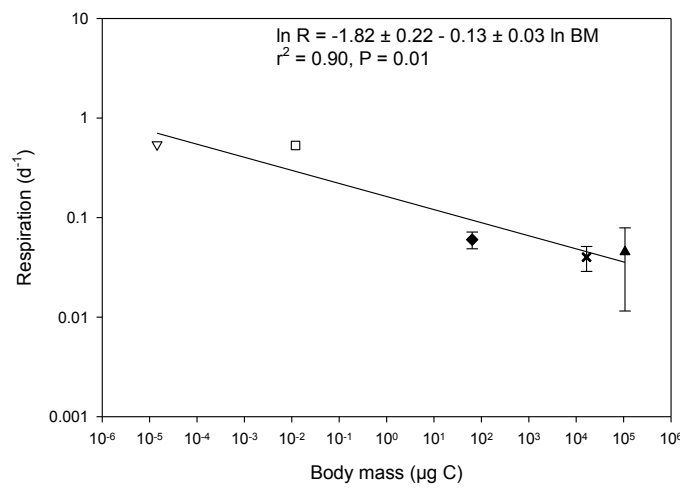


Figure 5.4: Respiration (d^{-1}) at 15°C as a function of body mass ($\mu\text{g C}$) with standard deviation (whiskers) for heterotrophic plankton. Symbols as in Figure 5.2, white symbols are flagellate and ciliate mean respiration at 25°C . There is no data on dinoflagellate respiration.

The relationship between respiration rate and body size was investigated at 15°C . A similar trend was found in respiration as in grazing for the relationship with body mass. An inverse relationship exists between respiration rate and body mass in heterotrophic zooplankton (Figure 5.1). According to these results body mass predicts 90% of the variation in respiration rate across the heterotrophic zooplankton groups presented in this study. The relationship between the Q_{10} of respiration and body mass was also examined. In this instance there were only three groups, the copepods, crustacean and gelatinous macro-zooplankton where a relationship with temperature could be established. The result was similar to that presented for the relationship between the Q_{10} of grazing. The relationship was not statistically significant.

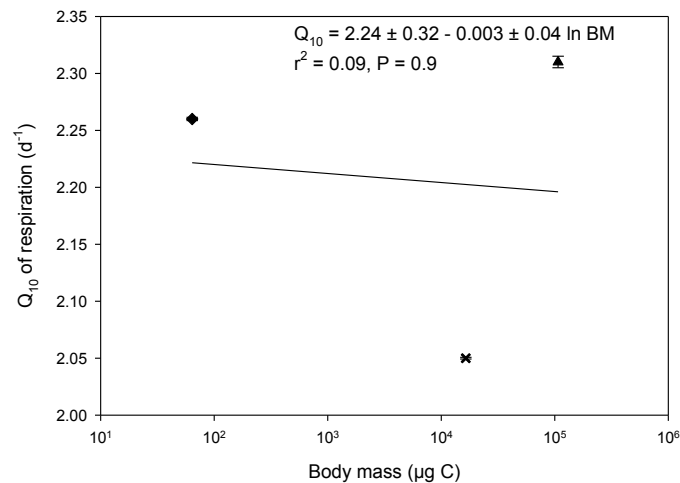


Figure 5.5: Q_{10} of respiration with standard deviation (whiskers). No data for temperature dependence of flagellate, dinoflagellate and ciliate respiration. Symbols as in Figure 5.2.

Mean GGE was similar across all groups ranging from 25 to 32% of grazing (Table 5.2). Mean GGE was highest in the flagellates, 32%, and lowest in the copepods, 25%. There was however large variation in the standard deviation which ranged up to $\pm 23\%$ in the gelatinous macro-zooplankton. Measurements of POM and DOM production were found for four of the six groups and ranged between 21 and 28% of grazing for POM and 11 and 19% of grazing for DOM. One measurement of DIC as a fraction of grazing was published for the ciliates (Verity 1985). In the remaining groups DIC as a fraction of grazing was calculated using Equation 5.6. The reported result for DIC as a fraction of grazing for ciliates, 63% was twice as high as the results calculated for the other groups which ranged between 27 and 33% of grazing. The partitioning of grazing was similar across groups with the exception of the fraction of grazing that is partitioned to DIC in the ciliates (Table 5.1).

5.5 DISCUSSION

This analysis has revealed similarities in the partitioning of grazing to body mass, through GGE, to POM, DOM and DIC across groups. There is considerable variation in partitioning of grazing to these four pools within each group (data not shown for POM, DOM and DIC). With so little data currently available on the partitioning of grazing for heterotrophic zooplankton it is difficult to attribute differences among groups to taxonomy or to refute the role of taxonomy as a determinant of the differences in the partitioning of grazing. Variations caused by differences

in methodological approach, experimental technique, difficulties inherent in measuring and calculating physiological characteristics such as ingestion, growth, egestion, sloppy feeding, and the production of DOM and DIC, may overshadow any real trend. That is not to say it is not worth carrying out a comparative analysis because of the inherent differences or errors involved but that more data is required to identify robust trends in these data sets.

Both positive and negative relationships between GGE and temperature are identified across the groups. Although the relationship between GGE and temperature was significant in four of the six groups, temperature was only a predictor of GGE in three of the six groups. Higher temperatures in oligotrophic regions of the world ocean, where food concentrations are generally low, make it difficult to separate the effect of low food concentration from the effect of temperature. As GGE is the product of net growth efficiency ($NGE = \text{growth} / [\text{growth} + \text{respiration}]$) and assimilation efficiency ($AE = [\text{growth} + \text{respiration}] / \text{ingestion}$) (after Strale 1997) the temperature dependence of GGE is derived from the temperature dependencies of ingestion, growth and respiration. While temperature may be used as a predictor of GGE there other environmental variables, such as food concentration may have a greater influence on GGE than temperature.

The relationship between mass-specific grazing rate for the six groups of heterotrophic zooplankton presented in this study were examined. The highest rates of mass-specific grazing at 15°C are found in the proto-zooplankton which includes the flagellates, dinoflagellates and ciliates. The grazing rate in gelatinous macro-zooplankton is closer to the grazing rate in dinoflagellates than either copepods or the crustacean macro-zooplankton, which are two to four fold lower than the gelatinous macro-zooplankton rate. There is little variation in Q_{10} among the groups with a range between 1.5 and 2.6. The groups with the highest grazing rate, flagellates, dinoflagellates, ciliates and the gelatinous macro-zooplankton all have Q_{10} values of less than 2 whereas the remaining two groups with the lowest grazing rates have Q_{10} values greater than 2. Although the grazing rate of the proto-zooplankton groups and the gelatinous macro-zooplankton will remain higher than the grazing rates of the other two groups, increasing

temperature will have a greater effect on copepod and crustacean macro-zooplankton, because of higher temperature dependencies.

The relationship between respiration rate and temperature for three of the six groups presented in this study were also examined. In the three larger heterotrophic zooplankton groups there was very little variation in respiration rate at 15°C. The same is true for the Q_{10} values among these groups, which range between 2.0 and 2.3. There was no temperature data for the remaining two groups of the smaller heterotrophs but it was possible to estimate mean respiration rate at 25°C for both flagellates and ciliates. The mean respiration rates for the two proto-zooplankton groups is similar $\sim 0.5 \text{ d}^{-1}$. This indicates that the respiration rates in the smaller heterotrophs is ten times greater than in the larger copepod and macro-zooplankton groups. Slightly greater effects of increasing temperature will be seen in the copepods and the gelatinous macro-zooplankton caused by their slightly higher respiration rates and Q_{10} than in the crustacean macro-zooplankton where both respiration rate and Q_{10} are lower.

The relationship between GGE, grazing rate and respiration rate with temperature have been considered. In all cases a linear function was employed to describe the relationship. Across the synthesis it is clear, even after data transformations have been applied, that some of the residuals are not normally distributed, i.e. copepods and gelatinous macro-zooplankton for the relationship between GGE and temperature, dinoflagellates, copepods, crustacean and gelatinous macro-zooplankton for the relationship between grazing rate and temperature, copepods, crustacean and gelatinous macro-zooplankton for the relationship between respiration rate and temperature. The residuals in the relationship mentioned above are not normally distributed. This indicates one of three things 1) the function that is being fit is not a good representation of the underlying processes, 2) there is not sufficient data, and/or 3) some of the data are incorrect because of measurement errors or because the organisms were not grown in optimal conditions. The last reason is likely to be predominant because even in the cases where there is a large number of data points, the errors are not normally distributed. Furthermore, the data available contains negative growth rates, which clearly shows the conditions for growth are

not optimal in some experiments. In order to directly compare physiological rates across the groups it is necessary to analyse the data for each group using a similar approach.

Mass-specific grazing rate, calculated for each group of heterotrophic zooplankton from Equation 5.5 at a temperature of 15°C, decreases with body mass across groups of heterotrophic zooplankton with an exponent of $f = -0.01$ ($P = 0.04$, from Equation 5.7, see Figure 5.2). The Q_{10} of the grazing rate shows no significant relationship with body mass ($P = 0.14$, Figure 5.3). There is a negative relationship between grazing rate and body mass although two groups, the ciliates and the gelatinous macro-zooplankton, appear out of line. The analysis shows a difference in factor of approximately two between dinoflagellate and ciliate grazing rates. Hansen et al. (1997) found a similar result between dinoflagellates and ciliates of a similar size. Gelatinous macro-zooplankton grazing rates are higher than crustacean macro-zooplankton and copepod grazing rates. This analysis also confirms previous work by Hirst et al. (2003) on growth rates of thaliacea, ctenophores and cnidarians, groups belonging to the gelatinous macro-zooplankton, showing higher grazing rates than either copepods or crustacean macro-zooplankton.

Mass-specific respiration is known to decrease with body size (Zeuten 1955). Quantitative data is presented on the decrease of respiration rate for the heterotrophic groups analysed in this study. Mass-specific respiration rate, calculated for each group of heterotrophic zooplankton from Equation 5.5 at a temperature of 15°C, decreases with body mass across groups of heterotrophic zooplankton with an exponent of $g = -0.13$ ($P < 0.01$, Equation 5.7, Figure 5.4). This is much less than the exponent of $g = -0.25$ which is being advocated in metabolic theory (West, 1997). The Q_{10} of respiration shows a negative slope with temperature but is not significant ($P < 0.9$, Figure 5.5). This result is closer to that advocated by Glazier (2005) where pelagic organisms show isometric rather ($b \sim 1$) than allometric ($b < 1$) scaling. Glazier (2006) suggests that metabolic rate is not just restricted by internal physical constraints, as advocated in the metabolic theory of ecology, but that there may be multiple constraints (Kozłowski et al. 2003a, b) or metabolic boundaries (Kooijman 2000, Chapter 2). In the case of zooplankton, Glazier (2006) suggests that their increased respiration rate is the result of having

to stay afloat, e.g. expending energy through constant swimming. High predation rates are also offered as a hypothesis for higher respiration rates (Glazier 2005).

This analysis of the temperature dependencies of mass-specific grazing and respiration rates suggest that there will be a greater increase in grazing rate in the copepods and crustacean macro-zooplankton with increasing temperature than in the smaller heterotrophs and the gelatinous macro-zooplankton. While this would lead to small increases in grazing among these groups, overall the smaller groups and the gelatinous macro-zooplankton would still have higher grazing rates. Respiration rates would also increase slightly in the larger groups. As temperature dependence data are unavailable for the smaller heterotrophic zooplankton it is impossible to assess the effects of changes in temperature on the respiration rates of these groups and how it might relate to changes in the larger groups. Both grazing and respiration rates will increase in all the heterotrophic zooplankton groups presented here as a result of ocean warming.

The greatest effects are likely to be on small heterotrophic zooplankton, particularly the flagellates and ciliates, in the low latitudes. As the increase in grazing rates in larger heterotrophs is small compared to the increase in smaller heterotrophs, even when the difference in temperature dependence is considered, the corresponding increase in faecal pellet production will also be small. The preliminary analysis thus suggests that the dynamic equilibrium of the system will shift towards smaller heterotrophic organisms as they react more to changes in temperature because of their higher grazing rates. Without information on the temperature dependency of respiration rates in the smaller heterotrophic zooplankton groups it is difficult to assess the effect of ocean warming on these groups.

So far the effect that increasing temperature will have on the foods stuffs that these heterotrophic zooplankton feed on has not been considered. From the relationships between the physiological process rates presented above temperature can only be a partial indicator of increase or decrease in these rates. Food availability and concentration, along with predation mortality, is one of the most important environmental variables that should be considered when examining physiological process rates in heterotrophic zooplankton. It was not possible to create a synthesis of this type during the course of this study. In the absence of such data broad

generalisations on the effect of ocean warming on heterotrophic zooplankton foods must be considered. Increased warming will generally lead to stratification, which will result in increased oligotrophic conditions and a subsequent decrease in the size of the phytoplankton community (Behrenfeld et al. 2006). This will favour smaller heterotrophs and will have knock on effects on higher trophic levels. If any or all of these groups, particularly the smaller heterotrophs or the gelatinous macro-zooplankton, do better in a warming ocean, e.g. there is an abundance of their preferred food type and/or they have a greater increase in grazing rate relative to the increase in respiration rate, the outcome may result in increased pressure on resources and changes in the composition, structure and, possibly, functioning of the ecosystem. Changes such as these may result in changes in the carbon cycle and may have implications for climate.

5.6 CONCLUSIONS

The global ocean is warming and increasing temperature is already be affecting marine ecosystem processes. Predictive power, in regard to changes associated with warming, in heterotrophic groups is impaired by gaps in the data and lack of knowledge on broad scale patterns that may be applied at a global level. The data compilation presented here is the first step towards predicting changes caused by global warming in heterotrophic groups. Using existing data some general relationships between physiological process rates, temperature and body size have been defined. A lack of respiration data for heterotrophic protozoans, has been identified in the data, and identification of this lack may help tailor new research to broaden our knowledge and refine the results of this analysis. The ability to predict changes in community structure, composition and functioning caused by changes in the physio-chemical environment caused by global warming will help in the identification and quantification of changes in ocean biology and the effect that it has on the carbon cycle in the ocean, and ultimately the implications that it may have for climate.

REFERENCES

- Allredge A L, Gotschalk C (1988) Insitu settling behavior of marine snow. *Limnology and Oceanography* 33:339-351

- Bamstedt U, Wild B, Martinussen M B (2001) Significance of food type for growth of ephyrae *Aurelia aurita* (Scyphozoa). *Marine Biology* 139:641-650
- Beaugrand G, Reid P C, Ibanez F, Lindley J A, Edwards M (2002) Reorganization of North Atlantic marine copepod biodiversity and climate. *Science* 296:1692-1694
- Behrenfeld M J, O'Malley R T, Siegel D A, McClain C R, Sarmiento J L, Feldman G C, Milligan A J, Falkowski P G, Letelier R M, Boss E S (2006) Climate-driven trends in contemporary ocean productivity. *Nature* 444:752-755
- Besiktepe S, Dam H G (2002) Coupling of ingestion and defecation as a function of diet in the calanoid copepod *Acartia tonsa* *Marine Ecology-Progress Series* 234:310-310
- Borodkin S O, Nalbandov Y R, Stunzhas P A (1982) Elemental chemical composition of *Aurelia aurita* marine jellyfish and their role in the cycle of chemical elements in the Black Sea. In: Sezonnnye Izmeneniya Chernomorskogo Planktona NAUKA, Moscow, p 133-139
- Boyd P W, Doney S C (2002) Modelling regional responses by marine pelagic ecosystems to global climate change. *Geophysical Research Letters* 29
- Buskey E J (1998) Energetic costs of swarming behavior for the copepod *Dioithona oculata*. *Marine Biology* 130:425-431
- Conover R J, Lalli C M (1974) Feeding and growth in *Clione limacina* (Phipps), a pteropod mollusk. 2. Assimilation, metabolism, and growth efficiency. *Journal of Experimental Marine Biology and Ecology* 16:131-154
- Copping A E, Lorenzen C J (1980) Carbon budget of a marine phytoplankton-herbivore system with C-14 as a tracer. *Limnology and Oceanography* 25:873-882
- Cosper T C, Reeve M R (1975) Digestive efficiency of chaetognath *Sagitta hispida* Conant. *Journal of Experimental Marine Biology and Ecology* 17:33-38
- Crawford D W, Rogerson A, Laybournparry J (1994) Respiration of the marine ameba *Trichosphaerium sieboldi* determined by C-14 labeling and Cartesian Diver methods. *Marine Ecology-Progress Series* 112:135-142
- Crawford D W, Stoecker D K (1996) Carbon content, dark respiration and mortality of the mixotrophic planktonic ciliate *Strombidium capitatum*. *Marine Biology* 126:415-422
- Dagg M J (1976) Complete carbon and nitrogen budgets for the carnivorous amphipod, *Calliopius laeviusculus* (Kroyer). *Internationale Revue der gesamten Hyrobiologie* 61:297-357
- Dilling L, Wilson J, Steinberg D, Alldredge A (1998) Feeding by the euphausiid *Euphausia pacifica* and the copepod *Calanus pacificus* on marine snow. *Marine Ecology-Progress Series* 170:189-201
- Fenchel T, Finlay B J (1983) Respiration rates in heterotrophic, free-living protozoa. *Microbial Ecology* 9:99-122
- Glazier D S (2005) Beyond the '3/4-power law': variation in the intra- and interspecific scaling of the metabolic rate in animals. *Biological Reviews of the Cambridge Philosophical Society*:611-662
- Glazier D S (2006) The 3/4-power law is not universal: evolution of isometric, ontogenetic metabolic scaling in pelagic animals. *Bioscience* 56:325-332

- Hamner W M, Madin L P, Alldredge A L, Gilmer R W, Hamner P P (1975) Underwater observations of gelatinous zooplankton - sampling problems, feeding biology, and behavior. *Limnology and Oceanography* 20:907-917
- Hansen J, Sato M, Ruedy R, Lo K, Lea D W, Medina-Elizade M (2006) Global temperature change. *Proceedings of the National Academy of Sciences of the United States of America* 103:14288-14293
- Hansen P J, Bjornsen P K, Hansen B W (1997) Zooplankton grazing and growth: scaling within the 2-2,000 μm body size range. *Limnology and Oceanography* 42:687-704
- Henjes J (2008) Nano-zooplankton data set. PANGAEA
- Hirst A G, Bunker A J (2003) Growth of marine planktonic copepods: global rates and patterns in relation to chlorophyll *a*, temperature, and body weight. *Limnology and Oceanography* 48:1988-2010
- Hirst A G, Roff J C, Lampitt R S (2003) A synthesis of growth rates in marine epipelagic invertebrate zooplankton. *Advances in Marine Biology* 44:1-142
- Ikeda T (1985) Metabolic rates of epipelagic marine zooplankton as a function of body mass and temperature. *Marine Biology* 85:1-11
- Ikeda T, Kanno Y, Ozaki K, Shinada A (2001) Metabolic rates of epipelagic marine copepods as a function of body mass and temperature *Marine Biology* 139:1020-1020
- Kooijman S A L M (2000) *Dynamic Energy and Mass Budgets in Biological Systems*. Cambridge University Press, Cambridge
- Kozłowski J, Konarzewski M, Gawelczyk A T (2003a) Cell size as a link between noncoding DNA and metabolic rate scaling. *Proceedings of the National Academy of Sciences of the United States of America* 100:14080-14085
- Kozłowski J, Konarzewski M, Gawelczyk A T (2003b) Intraspecific body size optimization produces interspecific allometries. In: T M Blackburn, Gaston K J (eds) *Macroecology: Concepts and Consequences*. Blackwell, Malden, Massachusetts, p 299-320
- Kremer P (1977) Respiration and excretion by ctenophore *Mnemiopsis leidyi*. *Marine Biology* 44:43-50
- Lavaniegos B E, Ohman M D (2003) Long-term changes in pelagic tunicates of the California Current. *Deep-Sea Research Part II-Topical Studies in Oceanography* 50:2473-2498
- Le Quéré C, Aumont O, Monfray P, Orr J (2003) Propagation of climatic events on ocean stratification, marine biology, and CO₂: case studies over the 1979-1999 period. *Journal of Geophysical Research-Oceans* 108
- Lebrato M, Jones D O B (2009) Mass deposition event of *Pyrosoma atlanticum* carcasses off Ivory Coast (West Africa). *Limnology and Oceanography* 54:1197-1209
- Levinsen H, Nielsen T G, Hansen B W (1999) Plankton community structure and carbon cycling on the western coast of Greenland during the stratified summer situation. II. Heterotrophic dinoflagellates and ciliates. *Aquatic Microbial Ecology* 16:217-232
- Levitus S, Antonov J I, Boyer T P, Stephens C (2000) Warming of the world ocean. *Science* 287:2225-2229
- Madin L P (unpublished) in Madin & Kremer 1995.

- Madin L P, Kremer P (1995) Determination of the filter-feeding rates of salps (Tunicata, Thaliacea). ICES Journal of Marine Science 52:583-595
- Madin L P, Purcell J E, Miller C B (1997) Abundance and grazing effects of *Cyclosalpa bakeri* in the subarctic Pacific. Marine Ecology-Progress Series 157:175-183
- Moriarty R (2009) Respiration rates in epipelagic macro-zooplankton: a data set. PANGAEA
- Nagasawa S (1985) The digestive efficiency of the chaetognath *Sagitta crassa* Tokioka, with observations on the feeding process. Journal of Experimental Marine Biology and Ecology 87:271-282
- Nagata T (2000) Production mechanisms of dissolved organic matter. In: D L Kirchman (ed) Microbial ecology of the oceans. Wiley-Liss, Inc.
- Peterson W T, Schwing F B (2003) A new climate regime in northeast pacific ecosystems. Geophysical Research Letters 30:4
- Purcell J E, Arai M N (2001) Interactions of pelagic cnidarians and ctenophores with fish: a review. Hydrobiologia 451:27-44
- Reeve M R, Syms M A, Kremer P (1989) Growth dynamics of a ctenophore (*Mnemiopsis*) in relation to variable food-supply.1. Carbon biomass, feeding, egg-production, growth and assimilation efficiency. Journal of Plankton Research 11:535-552
- Richardson A J (2007) In hot water: zooplankton and climate change. 4th International Zooplankton Production Symposium, Hiroshima, JAPAN
- Rivkin R B, Legendre L (2001) Biogenic carbon cycling in the upper ocean: effects of microbial respiration. Science 291:2398-2400
- Robison B H, Reisenbichler K R, Sherlock R E (2005) Giant larvacean houses: rapid carbon transport to the deep sea floor. Science 308:1609-1611
- Sailley S, Klass C, Wolf-Gladrow D (in prep-a) Heterotrophic dinoflagellates feeding behaviour and growth rates, an analysis based on laboratory experiments.
- Sailley S, Klass C, Wolf-Gladrow D (in prep-b) Pelagic ciliates feeding behaviour and growth rates, an analysis based on laboratory experiments.
- Sarmiento J L, Slater R, Barber R, Bopp L, Doney S C, Hirst A C, Kleypas J, Matear R, Mikolajewicz U, Monfray P, Soldatov V, Spall S A, Stouffer R (2004) Response of ocean ecosystems to climate warming. Global Biogeochemical Cycles 18
- Small L F, Fowler S W, Moore S A, Larosa J (1983) Dissolved and fecal pellet carbon and nitrogen release by zooplankton in tropical waters. Deep-Sea Research Part I-Oceanographic Research Papers 30:1199-1220
- Steinberg D K, Carlson C A, Bates N R, Goldthwait S A, Madin L P, Michaels A F (2000) Zooplankton vertical migration and the active transport of dissolved organic and inorganic carbon in the Sargasso Sea. Deep-Sea Research Part I-Oceanographic Research Papers 47:137-158
- Steinberg D K, Silver M W, Pilskaln C H, Coale S L, Paduan J B (1994) Midwater zooplankton communities on pelagic detritus (giant larvacean houses) in Monterey Bay, California. Limnology and Oceanography 39:1606-1620
- Stoecker D K (1984) Particle production by planktonic ciliates. Limnology and Oceanography 29:930-940

- Straile D (1997) Gross growth efficiencies of protozoan and metazoan zooplankton and their dependence on food concentration, predator-prey weight ratio, and taxonomic group. *Limnology and Oceanography* 42:1375-1385
- Torres J J, Childress J J (1983) Relationship of oxygen consumption to swimming speed in *Euphausia pacifica*. 1. Effects of temperature and pressure. *Marine Biology* 74:79-86
- Torres J J, Childress J J, Quetin L B (1982) A pressure-vessel for the simultaneous determination of oxygen-consumption and swimming speed in zooplankton. *Deep-Sea Research Part I-Oceanographic Research Papers* 29:631-639
- Turner J T (2002) Zooplankton fecal pellets, marine snow and sinking phytoplankton blooms. *Aquatic Microbial Ecology* 27:57-102
- Verity P G (1985) Grazing, respiration, excretion, and growth rates of tintinnids. *Limnology and Oceanography* 30:1268-1282
- Zeuten E (1955) Comparative physiology (respiration). *Annual Review Physiology*:459-482

6 CONCLUSION

6.1 INTRODUCTION

Macro-zooplankton are known as an important vehicle for the transport of carbon from the surface waters of the world ocean to the deep sea. The focus of this PhD was to investigate the role of macro-zooplankton in global biogeochemical cycles, and in particular to provide constraints on the contribution of macro-zooplankton to global export production. It was necessary to characterise macro-zooplankton physiological and ecological process rates for their inclusion in the ocean biogeochemical model PlankTOM10. This process involved the collection, synthesis and analysis of physiological and ecological process rate data and associated environmental variables and the derivation of functional relationships. The data collection, synthesis and analysis of process rates form the basis of three of the four results chapters presented here: Chapters 2, 4 and 5. The results of these chapters led to the inclusion of macro-zooplankton as a PFT in PlankTOM10. In order to validate the performance of macro-zooplankton in the model it was necessary to create a synthesis of biomass concentrations in the epipelagic zone, this data formed the basis of Chapter 3. My experience with data synthesis and analysis, familiarity with heterotrophic processes within the plankton and involvement in the Dynamic Green Ocean Group lead to my participation in the heterotrophic comparison and its inclusion as the last results chapter in my thesis (Chapter 5). This thesis has contributed to addressing many important questions, including:

1. What is the relationship between respiration rate, body mass and temperature in macro-zooplankton?
2. What is the global distribution and biomass concentration of macro-zooplankton? How does it compare with the distribution and biomass concentrations of other groups?
3. Do physiological process rates in macro-zooplankton vary depending on the group that is examined? If so is it possible to characterise macro-zooplankton as one PFT?
4. What is the contribution of macro-zooplankton to global export production?
5. What effect will global ocean warming have on heterotrophic members of the plankton?

6. What additional information is required to predict changes in heterotrophic processes associated with global ocean warming?

6.2 MAJOR FINDINGS AND CONCLUSIONS

6.2.1 CHAPTER 2

A synthesis of macro-zooplankton metabolic rates and associated body mass and temperature data was produced. Analysis of the relationship between metabolic rate, body mass and temperature on both inter- and intraspecific levels revealed strong patterns in epipelagic macro-zooplankton. The results for the relationship between metabolic rate, body mass and temperature across the entire data set support those published by Ikeda (1985). This work also supports the suggestions made in previous studies (Ikeda 1985, Larson 1985, 1986, Schneider 1992) that metabolic rate of zooplankton should be reported in terms of carbon-specific body mass, as it allows all groups within the macro-zooplankton to be compared on equal terms. This message is particularly important today as many ecosystem modellers require parameters in carbon units.

The examination of metabolic scaling with body mass in the macro-zooplankton revealed an interspecific metabolic scaling exponent of $b = 0.70$. A mean value of $b = 0.90$ with a range of 0.5 to 1.3 was identified for intra-specific metabolic scaling exponent. This adds to the evidence supporting a range of metabolic scaling exponents as advocated by Glazier (2005) as opposed to one value of $b \sim 0.75$ as advocated by West et al. (1997). The findings in relation to the inter- and intraspecific temperature dependence (Q_{10}) of metabolic rate support the theory that optimisations occurring at species level are constrained by a variety of both internal (physical and chemical) and external (ecological) factors rather than one single factor. The analysis also suggests that species within the macro-zooplankton have undergone optimisations that enable them to persist in the pelagic environment, e.g. higher resting metabolic rates, and this confers some advantages upon them. The fact that there are a number of different phyla within the macro-zooplankton means that these optimisations have arisen independently on a number of occasions and this itself suggests, as Glazier (2006) points out, that the robust

patterns within the pelagic zooplankton may have been forced to converge by the pelagic environment. For my purposes a descriptive relationship between metabolic rate, body mass and temperature, irrespective of how it has arisen, is all that is required for the parameterisation of macro-zooplankton processes so they may be included in PFT type models.

6.2.2 CHAPTER 3

A global data set for the validation of macro-zooplankton biomass in ocean biogeochemical models was created. Maps produced from abundance data give an indication of the global distribution of macro-zooplankton. At low latitudes the abundance ranges between 0 and 0.05 ind. L⁻¹. At high latitudes abundance ranges from 0 to ≤ 30 ind. L⁻¹. In general, macro-zooplankton abundance is more homogenous in the tropics with constant low levels of abundance. At high latitudes the background abundance is lower but there are patches of very high abundance. Maps of macro-zooplankton biomass concentration show a patchy distribution; concentrations ranging between 0 and ~ 1000 $\mu\text{M C}$. The median biomass of macro-zooplankton, 0.006 $\mu\text{M C}$, is low compared to those of meso- and proto-zooplankton, at 0.61 and 0.43 $\mu\text{M C}$, respectively, yet they can reach very high biomass concentrations, e.g. 973 $\mu\text{M C}$ compared to the lower biomass concentrations of meso- and proto-zooplankton, 9 and 25 $\mu\text{M C}$, respectively.

While it was possible to calculate the mean, median and maximum values of biomass concentration for macro-zooplankton, the data coverage is poor outside of the Southern Ocean. It is clear from the maps of both macro-zooplankton abundance and biomass concentration that there are notable gaps in global coverage for abundance in the Pacific Ocean, the Atlantic, particularly in the north for abundance data, and in the Indian Ocean for biomass concentrations. A fuller set of observations would allow better estimations of macro-zooplankton biomass concentrations and distribution and a more useful global validation data set.

6.2.3 CHAPTER 4

Macro-zooplankton physiological and ecological process rates have been parameterised from specially synthesised data sets and included a representation of macro-zooplankton in the

biogeochemical model PlankTOM10. The crustacean parameterisation was chosen for the standard simulation of macro-zooplankton in the model. Macro-zooplankton activity affected other PFTs, with the largest impact on PFTs of the highest trophic level represented. Macro-zooplankton exerted strong control on the biomass of meso- and proto-zooplankton. Without tuning, the standard model simulation was able to reproduce biomass for meso- and macro-zooplankton of 0.52 and 0.003 Pg C, which was close to observations. It was possible to increase the contribution of macro-zooplankton to carbon export production from 0.26 Pg C y⁻¹ in the standard model simulation to 0.57 Pg C y⁻¹ in an optimised simulation where grazing threshold, grazing rate and particulate egestion were increased. The model was unable to reproduce the patchy distribution and high biomass concentrations (> 100 µM C) observed for biomass and this had implications for their contribution to export production.

On average macro-zooplankton have very low biomass concentration globally and it was possible to reproduce this using PlankTOM10. The low level contribution of ~0.6 Pg C y⁻¹ produced by the model represent low global biomass of macro-zooplankton (0.005 Pg C). From observations of macro-zooplankton it is known that they are capable of reaching very high biomass concentrations (~ 1000 µM C) in patches. These high biomass patterns have not been reproduced using the model and therefore neither has the increased export production associated with such patches. These patches are important both in terms of the increased export production associated with them and in terms of the implications they have for the other trophic levels, for example, early termination of the spring bloom and the knock on effects for succession and export production associated with primary producers. A clear understanding of the role of macro-zooplankton in the global carbon cycle is hampered by the lack of quantitative information on the mechanisms that control patchiness in the macro-zooplankton. Although it is now possible to include macro-zooplankton in global biogeochemical models like PlankTOM10 key processes associated with their functioning in the carbon cycle are missing. Until such mechanisms can be included in models such as PlankTOM10 it will be difficult to understand whether or not macro-zooplankton play a role in ecosystem-climate feedbacks.

6.2.4 CHAPTER 5

Information relating to physiological process rates of heterotrophic zooplankton and temperature was gathered to gain understanding of the effect that global warming will have on ocean biology. It is difficult to assess the effect of increasing temperature on the heterotrophic zooplankton without information on changing food concentrations in a warming ocean. This means that only part of the picture may be presented. The analysis suggests that overall grazing rate among the heterotrophic zooplankton will increase in all groups; however grazing rates in copepods and crustacean macro-zooplankton are likely to increase faster with increasing temperature than in the other groups because of their slightly higher temperature dependencies. It was not possible to describe the relationship between respiration rate and temperature in the smaller heterotrophic zooplankton groups but rate and temperature dependence data in the larger groups suggest a slight increase. If the high grazing rates in the small heterotrophic zooplankton are anything to go by the greatest effects of increasing temperature are likely to be found in flagellates and ciliates at low latitudes.

It is important that the power to predict changes in ecosystem processes associated with increasing temperature is improved. The global ocean is warming and increasing temperature may already be affecting marine ecosystem processes. The data synthesis of heterotrophic zooplankton process rates presented here is the first step towards both the understanding and the prediction of changes in heterotrophic zooplankton groups associated with global warming. The ability to predict changes in community structure, composition and functioning caused by global warming will help in identifying, and possibly quantifying, changes in ocean biology and subsequent changes in the ocean carbon cycle. Limited data means there is uncertainty associated with the effects of increasing temperature on marine ecosystems and therefore the possible implications that it may have for climate.

6.2.5 REDEFINITION OF MACRO-ZOOPLANKTON THE PFT

The concept of PFTs and PFT modeling was introduced in Chapter 1. It is necessary at this point to redefine the definition of a PFT in the case of macro-zooplankton. Macro-zooplankton

only satisfy three of the four requirements, as defined in Chapter 1, necessary for their inclusion as a PTF. It is clear from what I have learnt about macro-zooplankton in the course of this investigation that it was incorrectly assumed that their physiological and ecological process rate parameters are different to those of other zooplankton. In addition macro-zooplankton do not have a set of environmental conditions that are distinct from those of other PFTs. If the information in Chapter 2 is considered it is clear that the physiological process rates involved in respiration are related to the body mass of the organism and to a lesser extent the temperature of the water that the organism resides in. This applies across the epipelagic zooplankton as can be seen in the data presented from Ikeda (1985) in Table 2.1. If the information presented in Table 5.2 and Figure 5.1 is considered it is clear that there are similarities in a variety of physiological process rates across different groups of zooplankton. The similarities in the partitioning of grazing across zooplankton groups shows that macro-zooplankton are not an exception when it comes to the internal and external constraints that exert control on the physiological processes involved in grazing, growth, respiration and more generally metabolism. Now that more is understood about macro-zooplankton and the other PFTs in PlankTOM10 it is perhaps time that the definition for the selection of PFTs is adjusted somewhat. An expansion of the selection criteria for PFTs may help in the selection of new PFTs.

If we consider macro-zooplankton alone there are a number of ways that the selection criteria for PFTs can be adjusted in order to reflect the characteristics of the group. Size is an obvious consideration. Although macro-zooplankton size is an important consideration it was not thought important enough to be included as a criterion for PFT selection. Alternatively, in an effort to steer away from sized based models in favour of PFT models, size was ignored when considering selection criteria. It is difficult to define macro-zooplankton in terms of size when the entire life history of a group is considered. Different stages are different sizes. It is always difficult to come up with a size definition that will suit the needs of all those working in a particular field but I think that only adult stages of species that grow to > 2 mm should be considered as macro-zooplankton. Many epipelagic zooplankton species display close to isometric scaling of metabolism and body mass as adults whereas scaling at earlier life stages

often varies with the type of growth occurring. Using adults of macro-zooplankton means there is less variability in the type of growth or metabolism occurring and thus narrowing the parameterisation window for associated physiological processes rates. Adding a size and maturity selection criteria to the PFT selection definition is useful for the parameterisation of not only the larger zooplankton groups but it will also remove elements of variation associated with size and life history stage in phytoplankton groups where elemental composition is known to change with age and size.

Another way to define macro-zooplankton is using both local and global biomass distributions along with biomass concentrations. All the PFTs in PlankTOM10 are of quantitative importance in at least one region on the global ocean. Although these regions overlap to some extent in the majority of cases each PFT has a signature distribution. This signature distribution could be used as an added selection criteria for choosing PFTs. This selection criterion builds on two of the original of the original selection criteria presented in Chapter 1. Both have been referred to above. The first is the selection criteria that is problematic for macro-zooplankton and the second is their quantitative importance in at least one region of the global ocean. As more information about the biomass distribution of various PFTs become available it will become easier to identify these signature distribution and biomass concentrations. It is currently possible to identify the signature distributions of a variety of PFTs, e.g. coccolithophores and diatoms. Thus when considering any group with an explicit role in biogeochemical cycling it is not difficult to identify their range and global biomass concentration which in some cases is known from secondary sources.

Signature distribution may also help to identify whether or not PFT groups with similar biogeochemical roles can be grouped together or whether they should be separated into one or more PFTs. For macro-zooplankton the key to the group being defined as a PFT was their role in the carbon cycle through their role in the export of carbon from the surface to the deep sea. The original set of selection criteria was devised to help in the selection of the first set of PFTs that PlankTOM10 would be developed to include. With all definitions it is necessary that they modified as new information comes to light. The selection criteria discussed in the introduction

will remain as the preliminary selection criteria, a guide, that PFTs are selected by. As with macro-zooplankton when it becomes clear that a group with an important role in biogeochemical cycling is identified but does not conform to those criteria a secondary set of criteria will be applied. Size and maturity are useful in grouping species together but as PFTs are being viewed on the gross level of biogeochemical cycling perhaps it is more helpful to look at them from a global perspective using signature distributions.

6.3 FUTURE WORK

This is the first time that macro-zooplankton have been included as a PFT in a global biogeochemical model. The collection, synthesis and analysis of macro-zooplankton process rate data has led to an increased understanding of macro-zooplankton as a group and of its component parts. The creation of validation datasets for distribution and biomass concentration have also added valuable information on macro-zooplankton. Using model analysis, the role of macro-zooplankton in marine ecosystems has been examined, and their contribution to export production has been quantified. Through this data synthesis gaps in the observations of macro-zooplankton process rates have been identified. However, the results of the model analysis carried out in the course of this investigation reveals that increasing knowledge of physiological and ecological process rates does not lead to the emergence of patchy distribution or mass sedimentation. These are important macro-zooplankton characteristics when it comes to considering the role of macro-zooplankton in the global carbon cycle. It is clear that something fundamental is missing in regard to how macro-zooplankton distribution is modelled in PFT models. The key to a fully functional macro-zooplankton group in the future will be the inclusion of the processes important in controlling patchiness. This will allow their explicit inclusion in PFT models rather than an over reliance on emergent properties, which, in this case results in no such demonstration of such properties. In addition the factors important in 'bloom/bust' events need to be further investigated in terms of both the organism life history and environmental factors associated with very high biomass concentrations.

6.3.1 RESPIRATION

There is still a long way to go before a mechanistic understanding of macro-zooplankton metabolic scaling with body mass and temperature can be reached. There are multiple lines of investigation that need to be pursued (see Glazier 2005 & Chapter 2) if a mechanistic understanding is required, which is necessary only if trying to elucidate the processes that result in the scaling relationships demonstrated between metabolism and body mass. A better understanding of the constraints and evolutionary drivers associated with life in the pelagic realm (e.g. predation, high mortality rates among juveniles and staying afloat) may help explain patterns in metabolic scaling that appear to have evolved independently again and again in a variety of different phyla. If the interest is only in a descriptive relationship between metabolic scaling and body mass and temperature, as is the case here, simple considerations such as measuring metabolic rate at a variety of different temperatures and the reporting of metabolic rate and/or mass specific-metabolic rate and the body mass of the animal(s) used in the experiment will increase the number of measurements for any one species. More relevant observations will increase statistical significance thus giving greater scientific validity to the conclusions drawn from the data.

To discover the causes of metabolic scaling with body mass and temperature a more in depth investigation is necessary. Metabolic scaling with body mass and temperature is not restricted to the zooplankton. It is a robust pattern found throughout all organisms. There are a huge range of values for metabolic scaling with both body mass and temperature. Understanding the interplay between the internal and external constraints placed on an organism is the key to understanding metabolic scaling and its relationship with body mass and temperature. Broad ranging studies of phylogeny are necessary in order to remove the effect of phylogeny and allow between species patterns in internal and external constraints to be recognised and compared, especially in those groups where little is currently understood in relation to how metabolism scales with body mass or temperature. Experimental investigations are necessary on a wide variety of organisms and rigorous statistical testing of these results is also necessary. A wide range of hypotheses must be tested as must the theoretical models developed to try and explain

metabolic scaling. If there is an over arching metabolic scaling theory, its intricacies are not yet fully understood. It is possible to elucidate the mechanisms involved in control of metabolic scaling with body mass and temperature but not without the types of studies mentioned above. Any over arching metabolic scaling theory will come through the synthesis of experimental, statistical and modelling work. It is currently unclear how internal and external constraints interplay to produce the different types of metabolic scaling that have been observed. Through the current challenging debate in the scientific literature related to metabolic scaling, the synthesis and statistical testing of metabolic scaling data and the development of theoretical models that is ongoing we are getting a little closer to understanding the fundamentals of metabolic scaling.

6.3.2 VALIDATION DATA

Further work is necessary to extend the distribution of macro-zooplankton biomass concentration measurements in the global ocean. Currently there are areas with little or no macro-zooplankton biomass concentration data (see above), including areas where coastal upwelling is associated with high productivity regimes. Much information on abundance and biomass concentration exists for macro-zooplankton, however gaining permission, extraction, standardisation and data conversion are time consuming. Fortunately funding from the European project Eur-Oceans was provided to support the collection and synthesis of pre-existing abundance and biomass data for several PFTs including macro-zooplankton. Such efforts need to be pursued. For macro-zooplankton it is now possible to access some of the data that comes from two time-series studies HOTS and BATS. Any future work on the biomass concentration and distribution of macro-zooplankton would have to incorporate this data. HOTS and BATS data is spatially limited especially when global distributions are considered, however they have high temporal resolution.

There are two ways in which macro-zooplankton biomass data sets can be expanded. The first, as mentioned above is to gather existing data. The second is to gather more in situ observations. Work has already begun on trying to access existing data sets and making them

available to the wider community through various data centres and government bodies. Members of the modelling community have communicated the importance of gathering information on biomass concentration to the wider scientific community (see Le Quéré & Pesant 2009). This will hopefully increase the amount of information collected when new measurements of macro-zooplankton biomass are made, and allow more accurate conversions from abundance to biomass. It is helpful that the modelling community and the observationists have opened lines of communication but if a fully quantitative global estimate of macro-zooplankton biomass is required then much more work is required in terms of gathering in situ observations. A concerted and global effort is necessary to gather in situ information on abundance, bio-volume, biomass, the identity of species and the chemical composition of those species. Regions where little or no information has been collected at present should be prioritised and where possible temporal resolution should be increased to all seasons. At present it is impossible to track the natural variability in the global ocean system or the effect that changes in climate are having on the distribution or biomass concentrations of macro-zooplankton. If a comprehensive, quantitative global macro-zooplankton biomass distribution is assembled then not only will the true distribution and biomass macro-zooplankton, and the variability therein, be known but it will be possible to revisit areas that have been previously sampled and examine any changes that have occurred since the last occupation. A global baseline of macro-zooplankton biomass and distribution will help to improve both the parameterisation and validation of PFT models where macro-zooplankton have been included. Access to and addition to already existing data sets is very important if a quantitative high resolution global macro-zooplankton biomass distribution is sought.

6.3.3 CHARACTERISATION OF PHYSIOLOGICAL AND ECOLOGICAL PROCESS RATES

Further work would be necessary to better constrain the temperature dependencies of both physiological and ecological process rate data. Increasing the amount of data to a point where it is continuous across biologically relevant temperatures would strengthen any functional

relationship derived from observations (see Section 6.3.1). Food concentration is another environmental variable of importance when deriving community process rates. For macro-zooplankton and other heterotrophic groups, the lack of information on food concentration in carbon terms means that two important variables, the half-saturation of grazing and the grazing threshold have not been characterised from observations. If parameterisations for any sub-group within the macro-zooplankton are preferred then it is even more important to gather additional observations so these functional relationships can be more fully described across a complete range of temperatures and food concentrations. If a full range of temperature and/or food concentration observations could be assembled, it would be possible to identify the different niches of the macro-zooplankton groups, to increase understanding of the interactions between groups within the macro-zooplankton, and to estimate the combined effect of macro-zooplankton on lower trophic levels.

Ideally more information is required on all physiological (growth, grazing, ingestion, assimilation efficiencies, gross growth efficiencies, respiration, excretion and egesting) and ecological (mortality, prey concentrations, food preferences) process rates across all zooplankton groups in a variety of environmental settings. This information may only be obtained through experiment and in the case of some of the ecological process rates, e.g. mortality, in situ observation. There are gaps in the data as can be seen in Figure 5.1 and Table 5.2. More experimental work needs to be carried out. This is clear now that the vast majority of available data for these groups has been collected and synthesised. Again there is a need for a concerted and focused effort to fill in these gaps, especially where mortality, partitioning of uptake, food preference, food concentration and temperature are concerned. This information is not only necessary to improve model parameterisation but also to increase our understanding of the dynamics that exist between lower trophic levels and the zooplankton and also the dynamics that exist within the zooplankton. A fuller knowledge of the process rates, temperature dependencies and food concentration involved will help us to design better experiments and improve model representations of the processes involved. Without information to fill these gaps it is difficult to understand how PFT modelling can move ahead in terms of zooplankton

parameterisation. The fullest representation of environmental factors and their effect on both the physiological and ecological processes involved is necessary in order to correctly represent PFTs in models such as PlankTOM10.

6.3.4 MODEL DEVELOPMENT AND FUTURE USE

The model's inability to reproduce patchiness and very high biomass concentration ($\sim 1000 \mu\text{M C}$) that can be identified from observations suggest that the current description of macro-zooplankton in PlankTOM10 does not include the processes that produce this type of distribution. A better understanding of both the physical and the biological processes involved in the creation of macro-zooplankton aggregations, swarms and blooms are necessary if this fundamental trait of macro-zooplankton is to be represented in PlankTOM10. It has been suggested that appropriate patchiness for zooplankton can be generated by non-linearities in some models and this negates the use of complex assumptions about zooplankton behaviour (Steele & Henderson 1992). Finding a model that is suitable for use at such high resolution and that is simple enough to be included in PlankTOM10 is the challenge. Even if such a model could be included it does not necessarily mean that mass sedimentation of macro-zooplankton will occur in association with these patches. The combination of patchiness, favourable environmental conditions and high growth/grazing rates in macro-zooplankton may lead to the emergence of 'bloom/bust' scenarios in the model where mass sedimentation of macro-zooplankton occurs. As this property has not emerged from PlankTOM10 more work on the triggers associated with mass sedimentation events of macro-zooplankton will also need to be investigated. The importance of patchiness and mass sedimentation events has been mentioned above but there are also other processes such as the interaction of certain groups within the macro-zooplankton with sea-ice. Inclusion of this process in the model might lead to a more heterogeneous distribution of macro-zooplankton in the Southern Ocean, particularly in regions where ice cover is important.

Now that macro-zooplankton have been parameterised and included in PlankTOM10 it is time that their role is examined in the light of both climate change and changes that are

occurring throughout the marine ecosystem. It is now possible to examine the effect that changes in temperature will have on the macro-zooplankton and the PFT ecosystem as a whole. Using PlankTOM10 the interannual variability and the sensitivity of macro-zooplankton to climate change can also be investigated. The inclusion of higher zooplankton trophic levels in PlankTOM10 means that it is possible to investigate top down effects of changes that occur at higher trophic levels, particularly increased pressure on fisheries and changes in fisheries management. It is also possible to investigate the effect that perturbations at lower trophic levels will have on macro-zooplankton. PlankTOM10 is a working model with 10 explicitly represented PFT groups. The inclusion of macro-zooplankton in the model has made interactions between PFTs more dynamic and at this level of complexity will start to add something to the debate on ecosystem-climate feedbacks and prove a useful tool in terms of an experimental platform on which hypotheses may be tested.

6.4 GENERAL REVIEW

Data collection and synthesis has been the backbone of this PhD thesis. Sourcing information and the subsequent critical evaluation of the data gathered have made this project possible. The goal of data synthesis is to produce a standardised and seamless data set that can be trusted. I think this goal has been achieved for all data sets that have been produced here. There are limitations to every data set and these have been noted throughout. It is important to know and understand the limits of the data and to build around these limitations. Macro-zooplankton data related to the physiological and ecological process rates important for PFT model parameterisation have been gathered together for the first time in the course of this PhD.

Data analysis has mainly taken the form of examining the functional relationship that exist between physiological and ecological process rates and environmental variables such as temperature and food concentration. A variety of functional relationships were tested using PlankTOM10 and development of the model equations and different parameterisations were used to explore the interactions between macro-zooplankton and the other PFTs and to dissect the processes that were occurring in the model. This approach helped to develop a

representation of a complex system lacking the co-evolution of the PFTs involved. The application of a variety of parameterisation sets has greatly increased understanding of how the model works and had aided in the improvement of the model equations. The opposite is also true, through model outcomes a better understanding of the parameterisation data and the types of functional relationships that work best when considering the interactions between PFTs.

Throughout this investigation the focus has remained concentrated where information is the strongest. Every effort has been made to make realistic and logical assumptions within the model where data and knowledge are usually the limiting factors. Throughout the addition of macro-zooplankton the PFT and the development of PlankTOM10 hypotheses and model experiments have been developed that are designed to solve some of the problems associated with adding PFT groups and understanding the effect that this has on both top-down and bottom-up processes in the ecosystem. Model experiments were also designed to help better understand the shortcomings in both the data and the model.

It is important to understand much of the data synthesised in the course of this project in a wider context. The respiration data set was the major synthesis work that took place and there was enough scope within the data set to address metabolic scaling with body mass and temperature. Various metabolic scaling exponents have been identified across biological kingdoms. Macro-zooplankton and epi-pelagic zooplankton are just one part of a bigger picture. Understanding how internal (physiological) and external (environmental) constraints act upon epi-pelagic zooplankton may help improve understanding of these constraints across different phyla and groups and help to determine the mechanisms involved in controlling metabolic scaling with body mass and temperature. When considering macro-zooplankton biomass concentration and distribution it was important to look at their distribution and concentration in the context of the concentration and distribution of the other zooplankton groups. On one level it reaffirmed differences between these groups and on another comparing all three means that visible patterns may be interpreted partially as signs of interactions between zooplankton groups. This investigation was originally centred on exploring patterns in the physiological process rates of macro-zooplankton. This investigation was then extended to search for patterns

across all zooplankton groups where data on physiological rates was available. Extending the investigation enabled the identification of some patterns that were not apparent from the macro-zooplankton data available, e.g. half saturation of grazing and grazing threshold values. Similarity in how grazing is partitioned suggests that some common constraint or constraints is/are forcing a convergence. Our knowledge of these constraints is limited by the amount of data currently available. Examining patterns found in different zooplankton groups has helped inform decisions about macro-zooplankton parameterisation when information has been lacking.

To gain an understanding of macro-zooplankton the PFT it is necessary to consider its parameterisation, its effect in the model and the relative importance of its role in carbon export. When considering macro-zooplankton as a PFT in PlankTOM10 a variety of parameterisations were tested. The crustacean parameterisation resulted in the closest match to observations. Looking within the macro-zooplankton it is clear that it is a diverse collection of phyla. This diversity might warrant the eventual breaking up of macro-zooplankton into smaller groups or redefinition of the group as mentioned above even though they all contribute to carbon export in a similar manner. The inclusion of macro-zooplankton as a PFT in PlankTOM10 means that the mortality of all lower trophic levels is now represented in a dynamic manner. This is important in the model as it removes the necessity of parameterising mortality which is an ecological process rate and difficult to measure and replaces it with a dynamic mortality from within the ecosystem representation of PlankTOM10. The addition of macro-zooplankton the PFT has increased heterogeneity in the distribution of the other zooplankton and phytoplankton groups. This means that adding one more level of complexity; a higher trophic level PFT, one that is both a gazer and a predator has resulted in more realistic distribution of phytoplankton and zooplankton biomass. PlankTOM10 has been used to explore the role of macro-zooplankton in carbon export and although the initial estimates of their contribution to carbon export are low, it is possible that with the inclusion of a model that will create greater aggregation and patchiness there will be more export will be associated with these localised patches. Until this process can be represented in PlankTOM10 it is difficult to assess the true impact that macro-zooplankton have in carbon export. Macro-zooplankton are an important addition to PlankTOM10 in terms

of how they impact upon the model ecosystem. The model has also helped in creating a better understanding of the processes that are important for carbon export by macro-zooplankton. Although their contribution to carbon export is small compared to that of meso-zooplankton they have a very high carbon turnover in terms of biomass. Small changes in biomass in macro-zooplankton may have important implications for carbon export.

It is difficult to interpret data when there are gaps. Tailoring the conclusions of the investigation to take the uncertainty into account is important especially when our knowledge of the processes involved, e.g. food selection, temperature dependence of physiological process rates and the effect of food concentration on grazing rate, is not complete. Throughout this investigation I have endeavoured to temper my conclusions in this manner. It is important however to look to the future. It is necessary to push the boundaries of what can be done even if all the necessary information is not in place. Much of the debate centred on PFT type models is concerned with proceeding to quickly without fully understanding the processes involved. It is important that that these models are developed and that the concepts involved are explored and developed even if the information necessary to parameterise and validate model results is not available. Models are tools that help us to understand processes, especially complex processes where it is difficult to determine what is happening in a system. As with limitations in the data models can help to focus attention on areas where understanding is deficient. One of the goals of this project was to find data for both the parameterisation and validation of macro-zooplankton in a PFT model. The PFT concept and model had been developed before the data had been gathered. Data analysis and the identification of functional relationships enabled both the PFT concept and the model equations to develop in parallel. Even without a full suite of data it was possible to develop the model and incorporate a working macro-zooplankton PFT into PlankTOM10.

Throughout this project the value and importance of open communication and exchange of information between groups and individuals has become apparent. The exchange of ideas and information across sections of the modelling and experimental communities has helped concept and model development. There are many groups and individuals that have helped to make

PlankTOM10 a reality. Cooperation of this kind is important and facilitates pushing the boundaries forward especially when trying to develop a working representation of a complex system. I hope that learning the value of this type of exchange will benefit my future undertakings and help in the development of new ideas and forwarding concept development and scientific understanding.

6.5 CLOSING STATEMENTS

6.5.1 MARINE ECOSYSTEM - CLIMATE FEEDBACKS

Although our understanding of marine ecosystem-climate feedbacks is rudimentary at present, further investigations in this field will be based upon strong foundations laid down over the last few years. The development of ocean biogeochemical models including explicit representations of multiple PFTs allows a quantitative exploration of the biological response to increasing levels of CO₂ in the atmosphere. Without the explicit representation of biological processes it is impossible to investigate marine ecosystem-climate feedbacks. The foundations mentioned above include the collection, synthesis and analysis of physiological and ecological process rate data that allow the explicit representation of biology in ocean biogeochemical models. They also include the development of first generation ocean biogeochemical models to include biologically mediated processes. Models with a full suite of PFTs are now being included in Earth system models. The investigation of marine-ecosystem feedbacks on timescales of one year to a hundred thousand years now begins in earnest. Now that the tools used in such investigations are in place, questions relating to the stability of the marine ecosystems and sensitivities within the marine ecosystem may be explored. It is important to gain an appreciation of the challenges that we may face in a warming world. The identification of marine ecosystem-climate feedbacks may alert us to potentially hazardous climate scenarios best avoided.

6.5.2 CHANGE

Humanity's greatest challenge lies ahead. Can we adapt our behaviour to ensure that our environment is not altered to our detriment? Whether humans survive or not life will continue

on Earth. This will not occur through some delicate balancing act of keeping the system in a manner that is comfortable for life, but through life's ability to adapt to the surrounding environment and exploit new niches. Life's capacity for change, its greatest asset, is underestimated by many. Life will persist, perhaps even as long as the Earth persists, possibly longer. As a species we are afraid of change. A changing Earth, as a result of our wanton consumption of fossil fuels, will have consequences for us all. Should we be reluctant or afraid to implement change now, our prospects become very bleak.

REFERENCES

- Glazier D S (2005) Beyond the '3/4-power law': variation in the intra- and interspecific scaling of the metabolic rate in animals. *Biological Reviews of the Cambridge Philosophical Society*:611-662
- Glazier D S (2006) The 3/4-power law is not universal: evolution of isometric, ontogenetic metabolic scaling in pelagic animals. *Bioscience* 56:325-332
- Ikeda T (1985) Metabolic rates of epipelagic marine zooplankton as a function of body mass and temperature. *Marine Biology* 85:1-11
- Larson R J (1985) Trophic ecology of gelatinous predators (Cnidaria and Ctenophora) in Saanich Inlet, Vancouver Is., B.C., Canada. University of Victoria
- Larson R J (1986) Water-content, organic content, and carbon and nitrogen composition of medusae from the Northeast Pacific. *Journal of Experimental Marine Biology and Ecology* 99:107-120
- Le Quéré C, Pesant S (2009) Plankton Functional Types in a new generation of biogeochemical models. EOS : Transactions American Geophysical Union
- Schneider G (1992) A comparison of carbon-specific respiration rates in gelatinous and nongelatinous zooplankton - a search for general rules in zooplankton metabolism. *Helgoländer Wissenschaftliche Meeresuntersuchungen* 46:377-388
- Steele J H, Henderson E W (1992) A simple model for plankton patchiness. *Journal of Plankton Research* 14:1397-1403
- West G B, Brown J H, Enquist B J (1997) A general model for the origin of allometric scaling laws in biology. *Science* 276:122-126